Cardiology Journal 2021, Vol. 28, No. 3, pp. 355–502

CARDIOLOGY JOURNAL

Impact Factor: 1.669

May 2021, Vol. 28, No. 3, pp. 355–502 www.cardiologyjournal.org

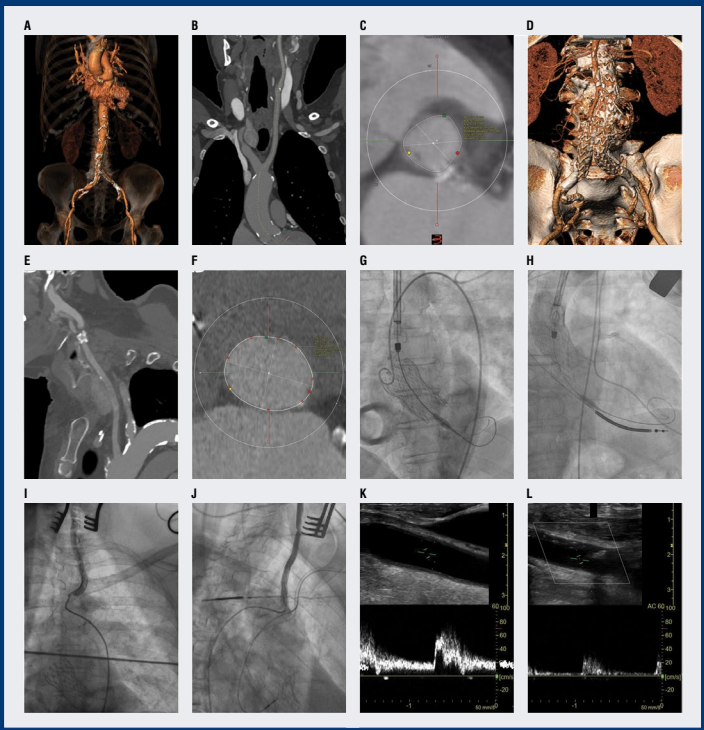

Damian Hudziak et al., see figure legend on page 490

ISSN 1897–5593
eISSN 1898–018X

VIA MEDICA

CARDIOLOGY JOURNAL

www.cardiologyjournal.org

CARDIOLOGY JOURNAL

www.cardiologyjournal.org

"Cardiology Journal", a bimonthly publication, is an official journal of the Working Groups on Cardiac Rehabilitation and Exercise Physiology, Congenital and Valvular Heart Disease, Echocardiography, Experimental Cardiology, Heart Diseases in Women, Heart Failure, Heart Rhythm, Invasive Cardiology, Noninvasive Electrocardiology and Telemedicine, Pediatric Cardiology and Resuscitation and Intensive Care of the Polish Cardiac Society.

Cardiology Journal (ISSN 1897-5593, eISSN 1898–018X) is published 6 times a year by VM Media sp. z o.o. VM Group sp.k.

Subscription rates: Paper subscription, 6 issues incl. package and postage institutional — 270 euro. The above prices are inclusive of regular postage costs. Payment should be made to: VM Media sp. z o.o. VM Group sp.k., Grupa Via Medica, Bank BGŻ Paribas SA account number: 15 1600 1303 0004 1007 1035 9021; SWIFT: PPABPLPK. Single issues, subsriptions orders and requests for sample copies should be send to e-mail: prenumerata@viamedica.pl. Electronic orders option available at: https://journals.viamedica.pl/cardiology_journal.

Editorial address: VM Media sp. z o.o. VM Group sp.k., ul. Swietokrzyska 73, 80–180 Gdansk, tel: (+48 58) 320 94 94, fax: (+48 58) 320 94 60, www.cardiologyjournal.org, e-mail: cj@viamedica.pl

Journal has an international indexation in CrossRef, EBSCO, EMBASE, FMJ, Google Scholar, Science Citation Index Expanded, Index Copernicus (169.43 points), MEDLINE, Scopus, SJR, Ulrich's Periodicals Directory, Web of Science CC and WorldCat database, Ministry of Science and Higher Education score (100 points). Current Impact Factor of "Cardiology Journal" (2019) is 1.669.

Advertising: For details on media opportunities within this journal please contact the advertising sales department ul. Swietokrzyska 73, 80–180 Gdansk, tel: (+48 58) 320 94 94, e-mail: viamedica@viamedica.pl
The Editors take no responsibility for the published advertisements.

Editorial policies and author guidelines are published on journal website: www.cardiologyjournal.org

Legal note: https://journals.viamedica.pl/cardiology_journal/about/legalNote

20-0801.003.001

CARDIOLOGY JOURNAL

www.cardiologyjournal.org

May 2021, Vol. 28, No. 3

Table of Contents

VIA MEDICA

EDITORIAL

Cardiology Journal
2021, Vol. 28, No. 3, 355–357
DOI: 10.5603/CJ.2021.0047

ISSN 1897–5593
eISSN 1898–018X

Going through or around the occlusion? All roads lead to Rome

Niccolò Ciardetti, Alessio Mattesini, Carlo Di Mario

Structural Interventional Cardiology, Department of Clinical and Experimental Medicine, Careggi University Hospital, Florence, Italy

This editorial accompanies the article on page 369

This meta-analysis approaches one of the most heavily debated aspects of the chronic total occlusion (CTO) technique. How soon should operators switch from the conventional wire escalation (WE) technique to the creation of a subintimal path. Peripheral interventionalists use the latter technique as standard in very long occlusions of the superficial femoral artery or infrapopliteal vessels but their reocclusion rate is high and stenting is used more rarely. Flow rather than lumen size appears to be the determinant of late patency in this setting.

For coronary interventions, the technique is very different and the adjunctive use of a partial or complete subintimal path remains very controversial. Progress in wire steerability within the occlusion and dedicated wires able to pierce calcified segments stepping down to softer wires in the remaining part of the procedure [1]. The same considerations can be repeated for retrograde recanalization with retrograde WE using the novel Gaia family (Asahi Intecc, Japan) of wires, often sufficient to regain the proximal end of the occlusion.

The question comes when the proximal or distal stump is ambiguous or when the length and tortuosity of the occluded segment makes safe handling of the CTO wires impossible, with high risk of wire exits. The ambiguity of the stump can occasionally be solved with intravascular ultrasound (IVUS) or pre-interventional coronary computed tomography-angiography but remains a driver to rely on the ability of a knuckled wire to follow the vessel architecture minimizing the risk of perforation [2]. The difficulty is hardly ever the ability to quickly gain ground within the occluded segment. Occasionally the knuckled wire can follow side-branches rather than the main vessel but this is not as frequent as with stiff devices such as the CrossBoss (Boston Scientific, USA). Most of the time, the problem comes at the end (proximal or distal) when reentry in the true lumen can become nearly impossible. Retrogradely, there is low pressure building up within the false lumen and the anterograde wire and balloon advanced can facilitate reentry with a traditional or modified reverse controlled anterograde retrograde tracking (CART) technique. Anterogradely, the situation is trickier. The use of a guide extension or deep intubation to reduce anterograde pressure strictly avoiding

Address for correspondence: Professor Carlo Di Mario, Department of Clinical and Experimental Medicine, Clinica Medica, Room 124, Careggi University Hospital, Largo Brambilla 3, 50139, Florence, Italy, tel/fax: +39 3486522399, e-mail: carlo.dimario@unifi.it

contrast or flush may limit the size of the distal dissection and avoid full collapse of the distal lumen but we still miss a consistent reliable method to achieve successful wire dissection reentry. The only small randomized trial in this field compared anterograde dissection and reentry (ADR) with CrossBoss/StingRay and anterograde WE (AWE) and showed a similar procedure duration but the percentage of stand-alone ADR used as primary approach remained low (77%) [3]. Large registries (RECHARGE; US Registry; UK Hybrid CTO Registry) with experienced ADR operators reported a 60–81% success rate [4–6]. Dual lumen catheters are more deliverable and may offer an alternative to StingRay but they miss the dedicated features that facilitate distal reentry with the StingRay balloon and should be considered more as a modified AWE technique with the use of parallel wires. Alternatives are scarce because IVUS guidance of distal reentry, with the exception of large less calcified vessels in the hands of very experienced IVUS operators, remains unpredictable. Pushing a wire to the distal vasculature (STAR) should be considered only a bail-out technique when all other options have failed and more of an investment procedure than a true procedural success, irrespective of the final flow achieved. In smaller vessels, for instance diagonals with ostial irretrievable dissections, mini-STAR is a viable option but this should not enter into the true CTO options.

The struggle between wire "manipulators" and wire "pushers" is more theoretical than real. The complexity of the lesion determines the technique and knuckling remains indispensable for very long calcified and tortuous occlusions. The difference is more in the time allowed to pass before switching strategy but this is also an important procedural step and the data presented in this article may favor a more liberal or more conservative use of dissection and reentry (DR) techniques based on long-term outcome.

There is evidence that the immediate outcome when techniques more complex than AWE are required is worse, with damage to collateral vessels as the main driver of adverse events for retrograde procedures and inability to protect and save branches distal to the occlusion as a driver of ADR complications [7]. The article by Zhao et al. [8] goes beyond the immediate procedural outcome to explore in 5265 patients the clinical results at 12–24 months, in terms of restenosis and adverse clinical events.

Analyzing 12 non-randomized cohort studies, the authors found that DR techniques, compared to WE, are associated with higher risk of myocardial infarction (MI), target-vessel revascularization (TVR), in-stent restenosis (ISR), and in-stent reocclusion. Cardiovascular death and in-stent thrombosis were similar in the two groups.

Patients treated with a creation of a subintimal path required a higher number of stents and a greater mean stent length, in the face of more complex CTO lesions, as shown by significantly higher J-CTO score and longer CTO length. This could be a relevant limitation, since typically DR techniques are needed when CTO lesions are severely tortuous or calcified and WE is not sufficient for complete recanalization of the occluded segment.

Fortunately, the authors went even further: they performed subgroup analyses according to different approaches (anterograde or retrograde) and different DR techniques. They distinguished between patients treated with 'extensive' DR techniques — including CTO lesions recanalized with the STAR technique, mini-STAR, contrast--guided STAR and limited antegrade subintimal tracking — and those in whom 'limited' DR techniques were used — reverse-CART and device-facilitated techniques with the CrossBoss/ /StingRay system.

Long term endpoints were different based on DR techniques used: 'extensive' DR techniques have higher risk of TVR, ISR and composite endpoint (death, MI, TVR) compared to WE (Fig. 1A), while no differences were found between 'limited' DR and WE techniques (Fig. 1B), as well as between anterograde and retrograde approaches.

It seems clear that the issue is not the presence of a subintimal path but rather of extensive and uncontrolled dissections. Unfortunately, CTO lesion complexity was not consistently reported in the two DR groups, hence, it is not known if the higher risk is carried by the extensive dissection or by the intrinsic complexity of the disease. These clinical long-term data support the results of two smaller registries (ISAR-CTO and CONSISTENT-CTO) that performed follow-up angiography in all CTO patients, completing an assessment with optical coherence tomography [9, 10]. Results were slightly different. CONSISTENT-CTO [9] performed 175 optical coherence tomography late after CTO recanalization, with patients divided nearly equally into DR techniques and no DR group. More than 90% of stent struts were covered in both groups with no features (frequency and length of uncovered strut segment) shown to be at risk for stent

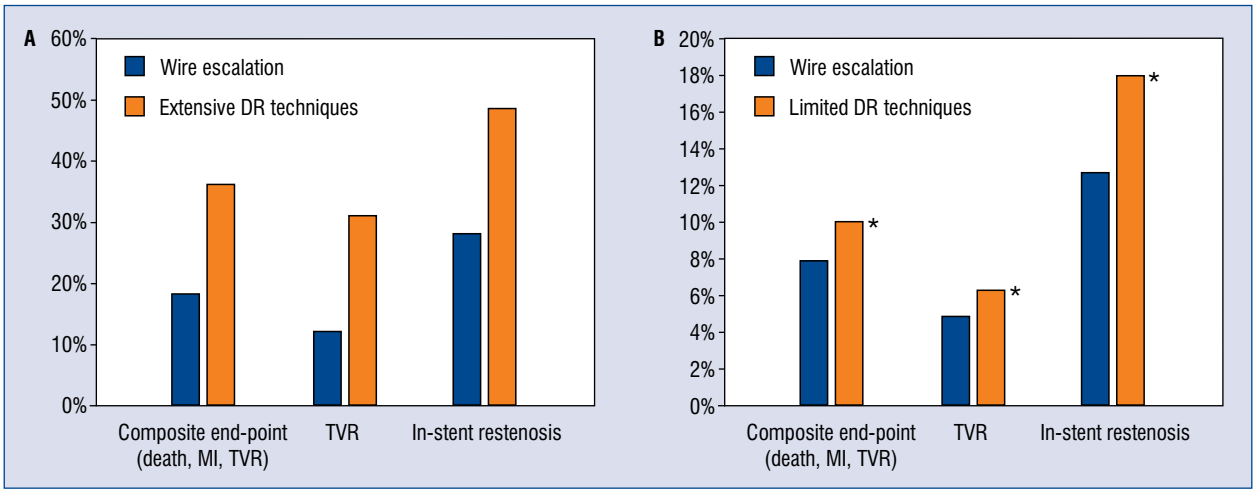

Figure 1. Long term endpoints according to the techniques used for recanalization; **A.** Wire escalation versus 'extensive' dissection and reentry (DR) techniques; **B.** Wire escalation versus 'limited' DR techniques; *Differences are not statistically significant; MI — myocardial infarction; TVR — target vessel revascularization.

thrombosis. ISAR-CTO [10], in a smaller number of patients and without the benefit of a consistent IVUS confirmation of the presence of a subintimal path during recanalization, showed a numerically higher percentage of uncovered struts and significantly more malapposed struts in the DR technique group. ISAR-CTO also showed rare cases of large aneurysms originating at the site of implantation of subintimal stents, confirming anectodical previous case reports.

After these studies and the reports summarized by Zhao et al. [8], the bitter controversies at times dominating the CTO sessions of the main interventional congresses can come to rest. Operators' experience and anatomy rather than aprioristic credos should drive individual technical decisions with no need for the CTO operators to choose one camp or the other.

Conflict of interest: None declared

References

1. Galassi AR, Werner GS, Boukhris M, et al. Percutaneous recanalisation of chronic total occlusions: 2019 consensus document from the EuroCTO Club. EuroIntervention. 2019; 15(2): 198–208, doi: 10.4244/EIJ-D-18-00826, indexed in Pubmed: 30636678.
2. Di Mario C, Mattesini A. What do you need for chronic total occlusion recanalization: swiftness or skillfulness? JACC Cardiovasc Interv. 2019; 12(6): 556–557, doi: 10.1016/j.jcin.2019.01.214, indexed in Pubmed: 30898252.
3. Karacsonyi J, Tajti P, Rangan BV, et al. Randomized comparison of a CrossBoss first versus standard wire escalation strategy for crossing coronary chronic total occlusions: the CrossBoss first trial. JACC Cardiovasc Interv. 2018; 11(3): 225–233, doi: 10.1016/j.jcin.2017.10.023, indexed in Pubmed: 29413236.
4. Maeremans J, Walsh S, Knaapen P, et al. The hybrid algorithm for treating chronic total occlusions in europe: the RECHARGE registry. J Am Coll Cardiol. 2016; 68(18): 1958–1970, doi: 10.1016/j.jacc.2016.08.034, indexed in Pubmed: 27788851.
5. Christopoulos G, Karmpaliotis D, Alaswad K, et al. Application and outcomes of a hybrid approach to chronic total occlusion percutaneous coronary intervention in a contemporary multicenter US registry. Int J Cardiol. 2015; 198: 222–228, doi: 10.1016/j.ijcard.2015.06.093.
6. Wilson WM, Walsh SJ, Yan AT, et al. Hybrid approach improves success of chronic total occlusion angioplasty. Heart. 2016; 102(18): 1486–1493, doi: 10.1136/heartjnl-2015-308891, indexed in Pubmed: 27164918.
7. Song L, Maehara A, Finn MT, et al. Intravascular ultrasound analysis of intraplaque versus subintimal tracking in percutaneous intervention for coronary chronic total occlusions and association with procedural outcomes. JACC Cardiovasc Interv. 2017; 10(10): 1011–1021, doi: 10.1016/j.jcin.2017.02.043, indexed in Pubmed: 28521919.
8. Zhao Y, Peng H, Li X, et al. The impact of dissection and re-entry versus wire escalation techniques on long-term clinical outcomes in patients with chronic total occlusion lesions following percutaneous coronary intervention: An updated meta-analysis. Cardiol J. 2021; 28(3): 369–383, doi: 10.5603/CJ.a2020.0026, indexed in Pubmed: 32104900.
9. Walsh SJ, Hanratty CG, McEntegart M, et al. Intravascular healing is not affected by approaches in contemporary CTO PCI: the CONSISTENT CTO study. JACC Cardiovasc Interv. 2020; 13(12): 1448–1457, doi: 10.1016/j.jcin.2020.03.032, indexed in Pubmed: 32553333.
10. Xhepa E, Cassese S, Rroku A, et al. Subintimal versus intraplaque recanalization of coronary chronic total occlusions: mid-term angiographic and OCT findings from the ISAR-OCT-CTO registry. JACC Cardiovasc Interv. 2019; 12(19): 1889–1898, doi: 10.1016/j.jcin.2019.04.049, indexed in Pubmed: 31521651.

VIA MEDICA

EDITORIAL

Cardiology Journal
2021, Vol. 28, No. 3, 358–359
DOI: 10.5603/CJ.2021.0048

ISSN 1897–5593
eISSN 1898–018X

Measuring the QT interval on the go

William F. McIntyre[1], Carlos A. Morillo[2]

[1]Cardiac Electrophysiology and Peri-Operative Medicine Division of Cardiology PhD Candidate, Health Research Methods, McMaster University, Hamilton, Ontario, Canada
[2]Division of Cardiology, Department of Cardiac Sciences, Libin Cardiovascular Institute of Alberta, University of Calgary, Foothills Medical Center, Calgary, Alberta, Canada

This editorial accompanies the article on page 483

Since March 2019, the coronavirus disease 2019 (COVID-19) pandemic has dominated news cycles, challenged politics and inspired scientists. Many of the early candidate drugs to help fight this deadly virus were existing anti-infective agents. Among them were azithromycin, hydroxychloroquine, lopinavir and ritonavir — drugs that are known to prolong the QT interval, and as a consequence, increase an individual's risk of sudden cardiac death. Widespread use and research with these drugs led to a larger need to monitor electrocardiograms (ECG) in these patients, ideally without bringing COVID-19 infected patients in contact with healthcare personnel and other patients [1].

In the current issue of the journal, Abellas-Sequeiros et al. [2] report an experience using a hand-held ECG-recording device to measure the QTc interval in patients with COVID-19. The authors used the KardiaMobile6L® 6-lead ECG to make recordings at varying frequencies in patients who were taking azithromycin, hydroxychloroquine, lopinavir/ritonavir, or combinations of these drugs. Over a mean follow-up of 6.2 ± 8.4 days, they observed mean QTc interval prolongations of 28 ms in patients taking two drugs and mean QTc interval prolongations of 41 ms in patients taking 3 drugs. A total of 12 of the 70 patients in their study had their therapies changed because of increases in their QTc. The authors concluded that portable ECG-recorders are a useful and reliable tool for QT interval monitoring in COVID-19 patients.

Myriad studies have now refuted the efficacy of azithromycin, hydroxychloroquine, and lopinavir/ritonavir across the spectrum of patients who have or are at risk for COVID-19 [3–6]. However, the need for convenient and reliable ways to measure the QT interval persists. Several common classes of drugs are known to prolong the QT and are frequently administered in outpatient settings (Table 1) [7]. The authors have clearly demonstrated the feasibility of using hand-held ECG technology to monitor the QT interval in ambulatory patients who have started a new drug therapy. Clinicians should consider this approach in select patients to minimize hospitalizations and to maximize convenience and compliance.

Conflict of interest: None declared

Address for correspondence: Professor Carlos A. Morillo, MD, FRCPC, FACC, FHRS, FESC, Department of Cardiac Sciences, Cumming School of Medicine Section Chief Division of Cardiology, Libin Cardiovascular Institute, University of Calgary, Zone Head Cardiology Calgary and Southeastern Alberta Region, Alberta Health Services Foothills Medical Center C823, 1403 29th Street NW Calgary, Alberta T2N 2T9, Canada, tel: 403-944-2670, e-mail: carlos.morillo@ucalgary.ca; carlos.morillo@albertahealthservices.ca

Table 1. QT-prolonging drugs that could be monitored using ambulatory hand-held electrocardiogram.

Anti-arrhythmics	Anti-migraine
Anti-biotics	Anti-malarials
Anti-depressants	Anti-protozoals
Anti-emetics	Anti-psychotic
Anti-histamines	Anti-rheumatics
Anti-fungals	Methadone

References

1. Li G, Saguner AM, An J, et al. Cardiovascular disease during the COVID-19 pandemic: Think ahead, protect hearts, reduce mortality. Cardiol J. 2020; 27(5): 616–624, doi: 10.5603/CJ.a2020.0101, indexed in Pubmed: 32789839.
2. Abellas-Sequeiros M, Lozano-Granero C, Garcia-Sebastian C, et al. Monitoring of QTc interval in patients with COVID-19. First experience with a portable ECG-recording device. Cardiol J. 2021; 28(3): 483–485, doi: 10.5603/CJ.a2021.0033, indexed in Pubmed: 33843037.
3. Horby P, Mafham M, Linsell L, et al. RECOVERY Collaborative Group. Effect of hydroxychloroquine in hospitalized patients with COVID-19. N Engl J Med. 2020; 383(21): 2030–2040, doi: 10.1056/NEJMoa2022926, indexed in Pubmed: 33031652.
4. Cavalcanti AB, Zampieri FG, Rosa RG, et al. Hydroxychloroquine with or without azithromycin in mild-to-moderate COVID-19. N Engl J Med. 2020; 383(21): 2041–2052, doi: 10.1056/NEJMoa2019014, indexed in Pubmed: 32706953.
5. Mitjà O, Corbacho-Monné M, Ubals M, et al. A Cluster-Randomized Trial of Hydroxychloroquine for Prevention of COVID-19. N Engl J Med. 2021; 384(5): 417–427, doi: 10.1056/NEJMoa2021801, indexed in Pubmed: 33289973.
6. Cao B, Wang Y, Wen D, et al. A trial of lopinavir-ritonavir in adults hospitalized with severe COVID-19. N Engl J Med. 2020; 382(19): 1787–1799, doi: 10.1056/NEJMoa2001282, indexed in Pubmed: 32187464.
7. Nachimuthu S, Assar MD, Schussler JM. Drug-induced QT interval prolongation: mechanisms and clinical management. Ther Adv Drug Saf. 2012; 3(5): 241–253, doi: 10.1177/2042098612454283, indexed in Pubmed: 25083239.

VIA MEDICA

ORIGINAL ARTICLE

Cardiology Journal
2021, Vol. 28, No. 3, 360–368
DOI: 10.5603/CJ.a2021.0034

ISSN 1897–5593
eISSN 1898–018X

Impact of the presence of heart disease, cardiovascular medications and cardiac events on outcome in COVID-19

Gonzalo Cabezón Villalba[1], Ignacio J. Amat-Santos[1, 2], Carlos Dueñas[3], Diego López Otero[2, 4], Pablo Catalá[1], Álvaro Aparisi[1], Javier López-Pais[2, 4], Carla Eugenia Cacho Antonio[4], Jordi Candela[1], Pablo Antúnez Muiños[4], José Francisco Gil[1], Teba González Ferrero[4], Marta Marcos[1], Marta Pérez-Poza[4], Gino Rojas[1], Oscar Otero García[4], Carlos Veras[1], Víctor Jiménez Ramos[4], Aitor Uribarri[1, 2], Ana Revilla[1, 2], Pablo Elpidio García-Granja[1, 2], Itzíar Gómez[1, 2], José Ramón González-Juanatey[2, 4], J. Alberto San Román[1, 2]

[1]Cardiology Department, Hospital Clínico Universitario, Valladolid, Spain
[2]Centro de Investigación Biomédica en Red — Cardiovascular (CIBER-CV), Spain
[3]Department of Infectious Diseases, Hospital Clínico Universitario, Valladolid, Spain
[4]Cardiology Department, Hospital Clínico Universitario, Santiago de Compostela, Spain

Abstract

Background: *Cardiovascular risk factors and usage of cardiovascular medication are prevalent among coronavirus disease 2019 (COVID-19) patients. Little is known about the cardiovascular implications of COVID-19. The goal herein, was to evaluate the prognostic impact of having heart disease (HD) and taking cardiovascular medications in a population diagnosed of COVID-19 who required hospitalization. Also, we studied the development of cardiovascular events during hospitalization.*

Methods: *Consecutive patients with definitive diagnosis of COVID-19 made by a positive real time-polymerase chain reaction of nasopharyngeal swabs who were admitted to the hospital from March 15 to April 14 were included in a retrospective registry. The association of HD with mortality and with mortality or respiratory failure were the primary and secondary objectives, respectively.*

Results: *A total of 859 patients were included in the present analysis. Cardiovascular risk factors were related to death, particularly diabetes mellitus (hazard ratio in the multivariate analysis: 1.810 [1.159–2.827], $p = 0.009$). A total of 113 (13.1%) patients had HD. The presence of HD identified a group of patients with higher mortality (35.4% vs. 18.2%, $p < 0.001$) but HD was not independently related to prognosis; renin–angiotensin–aldosterone system inhibitors, calcium channel blockers, diuretics and beta-blockers did not worsen prognosis. Statins were independently associated with decreased mortality (0.551 [0.329–0.921], $p = 0.023$). Cardiovascular events during hospitalization identified a group of patients with poor outcome (mortality 31.8% vs. 19.3% without cardiovascular events, $p = 0.007$).*

Conclusions: *The presence of HD is related to higher mortality. Cardiovascular medications taken before admission are not harmful, statins being protective. The development of cardiovascular events during the course of the disease is related to poor outcome.* (Cardiol J 2021; 28, 3: 360–368)

Key words: COVID-19, heart failure, statins, diabetes mellitus, cardiovascular diseases

Address for correspondence: Dr. J. Alberto San Roman, Department of Cardiology, Institute of Heart Sciences (ICICOR), Hospital Clínico Universitario, Valladolid, Spain, e-mail: asanroman@secardiologia.es

Received: 7.10.2020 Accepted: 25.02.2021

Introduction

On Thursday, December 12th, some people who had visited the Huanan Seafood Market were found to present viral pneumonia, later labeled by the World Health Organization as coronavirus disease 2019 (COVID-19). Since then, the outbreak which has changed our lives forever has infected more than 100 million people around the world carrying a mortality of approximately 2% [1]. Comorbidities, which have a clear impact on prognosis, are frequent in patients with severe COVID-19 [2–5]. Zhou et al. [6] have seen that 86% of patients who presented coronary artery disease died. In a series of 487 patients, cardiovascular diseases were more frequent in patients who died (8.2% vs. 1.6%) but only age, male gender and hypertension independently predicted death [7]. Besides, the term "cardiovascular diseases" was not defined.

Viral infections can contribute to acute coronary syndromes both by a direct effect on an atherosclerotic plaque inducing inflammation in the endothelium and smooth muscle cells, or by an indirect effect causing a hyperinflammatory stage with elevated pro-inflammatory cytokines, which may elicit plaque rupture of a coronary artery [8–11]. While some investigations have dealt with the impact of myocardial injury [12] or ischemic heart disease [13] on the outcome of patients with COVID-19, little is known about other types of heart disease (HD) like valvular disease or other cardiomyopathies.

The impact of HD and outcome has not been studied in other diseases with many similarities to COVID-19, the Middle East respiratory syndrome and the severe acute respiratory syndrome. Eventually, if patients with HD have worse outcomes than other patients, public health policies should be designed to target those patients as a priority group for vaccination against the severe acute respiratory syndrome coronavirus 2 (SARS-CoV-2).

Furthermore, the prognostic consequences of taking cardiovascular medications are undetermined. While some authors warn about the harmful effect of renin–angiotensin–aldosterone system (RAAS) blockers and advise its discontinuation to prevent poor outcome [14] others advocate maintaining these drugs until more evidence is available [15]. There is little information concerning statins.

In addition, cardiovascular events could occur during the course of the disease, such as myocardial infarction, decompensated heart failure, myocarditis and others. Nonetheless, the rate, and impact on outcome of different cardiovascular events are far from clear.

Keeping in mind this background, we have assessed the cardiovascular implications of COVID-19. Thus, the present study investigated the prognostic impact of having HD and taking cardiovascular medications in a well characterized population diagnosed of COVID-19 who required hospitalization. In addition, the development of cardiovascular events during hospitalization was also studied.

Methods

This is an observational and retrospective multicenter study with a total of 210 variables per patient gathered in a specific database from data prospectively collected from the electronic medical records. All consecutive non-selected patients with definitive diagnosis of COVID-19 made by a positive real time-polymerase chain reaction of nasopharyngeal swabs who were admitted to two tertiary hospitals from March 15 to April 14 were included. No exclusion criteria were considered. Follow-up after discharge from hospital was not performed.

A descriptive analysis of heart related characteristics of a COVID-19 population was carried out. Association of HD with mortality and the composite of mortality or respiratory failure were the primary and secondary objectives, respectively.

Data recorded at admission covered epidemiological, clinical, laboratory (complete blood count, coagulation testing including D-dimer, iron metabolism including ferritin, electrolytes, assessment of liver and renal function, C-reactive protein, erythrocyte sedimentation rate, lactate dehydrogenase, procalcitonin and creatine kinase), electrocardiogram (ECG) when available, and chest-X ray parameters. Computed tomography scan was performed when indicated by the physician in charge of the patient. Interpretation of chest imaging tests were performed by an expert radiologist. Troponin and interleukin-6 were obtained at the discretion of the physician. The study was approved by the local ethics committee.

Definitions

Ischemic heart disease comprised patients with a previous diagnostic angiography, previous myocardial infarction and patients with no anatomical confirmation but symptoms compatible and, at least, one noninvasive positive test for ischemia. Valvular heart disease was diagnosed when the patient had moderate or severe dysfunction of at least one valve. Cardiovascular events were defined as

follows: heart failure, pericarditis and myocarditis were defined according to the corresponding guidelines of the European Society of Cardiology [16–18]; acute myocardial infarction was diagnosed when the patient presented compatible chest pain, ST changes and elevation of troponin. Isolated elevation of troponin was considered as myocardial injury but not as an infarction. Atrial fibrillation was regarded as an event when it appeared during hospitalization. Respiratory failure was defined as $pO_2 < 60$ mmHg or $SatO_2 < 90\%$ without oxygen support at any moment of the patient's hospitalization. Azithromycin, hydroxychloroquine and lopinavir-ritonavir were considered drugs that may cause QT interval prolongation.

Statistical analysis

Categorical variables were reported as absolute values and percentages. Continuous variables were reported as the mean ± standard deviation or median and interquartile range. Normal distribution of quantitative variables were verified with the Kolmogorov-Smirnov test. Categorical variables were compared with the χ^2 test and the Fisher exact test. Continuous variables were compared with the Student t test or its equivalent for nonparametric tests, the Mann-Whitney U test was used for variables that were not normally distributed.

To identify factors that were predictive of mortality and the composite endpoint (mortality or respiratory failure), a logistic regression model with the maximum likelihood method was constructed by using backward stepwise selection, which included the variables that were statistically significant in the univariate analysis. No more than 1 variable per 10 outcome events was entered in the logistic model to avoid overfitting. For the final model we calculated odds ratios adjusted for each of the variables included, along with their 95% confidence intervals. Goodness of fit for each model was determined with the Hosmer-Lemeshow test and C-index.

All data were entered into a database and analyzed with version 15.0 of the Statistical Package for Social Sciences (SPSS Inc., Chicago, IL). Differences were considered statistically significant when p was < 0.05.

Results

Characteristics of the patients

A total of 859 patients made up the present study group. Main characteristics of patients are shown in Table 1. Mean age was 68 years and 49.5% were female (n = 425). Among comorbid conditions, 49.5% presented arterial hypertension, 19.3% diabetes mellitus, 40.5% dyslipidemia, 9.3% chronic obstructive pulmonary disease (COPD) and 6.9% chronic kidney disease (CKD). A total of 20.5% patients died (n = 176).

Heart disease was present in 113 (13.1%) patients (Table 2). The most frequent was ischemic HD with 71 patients; 34 patients had valvular HD and 14 cardiomyopathy; 6 patients presented more than one.

Comparison of patients with and without HD

Patients with HD were older and presented higher rates of arterial hypertension, diabetes mellitus, dyslipidemia and CKD as shown in Table 1. Regarding laboratory data, HD patients had more lymphopenia, anemia, higher values of creatinine, D-dimer and procalcitonin. Sinus rhythm was more frequent in patients without HD. Patients with HD suffered more respiratory failure and death.

Predictors of outcome

Multivariate analysis for predictors of death was performed, included in the model were all variables that were significant in the univariate analysis, namely: age, hypertension, diabetes mellitus, CKD, presence of HD, COPD, dyslipidemia, lymphocyte count $< 1000/mm^3$, D-dimer $> 500\ \mu g/L$, C-reactive protein (CRP) > 10 mg/mL and hemoglobin < 10 mg/dL. As can be seen in Table 3, age, diabetes mellitus, COPD, lymphocyte count $< 1000/mm^3$ and CRP > 10 mg/L were independently associated with mortality. HD was strongly associated with mortality, but was not an independent predictor of death.

For the composite endpoint (respiratory failure and death), variables predictive in the univariate analysis were age, hypertension, diabetes mellitus, CKD, presence of HD, lymphocyte count $< 1000/mm^3$, D-dimer $> 500\ \mu g/L$, CRP > 10 mg/mL and hemoglobin < 10 mg/dL. Independent predictors of the composite endpoint after multivariate analysis were age, diabetes mellitus, CKD, low lymphocyte count, high D-dimer, high CRP. Again, HD was not independently related to the composite endpoint.

Medications at admission and mortality

Table 4 shows the mortality rate of patients according to the medications taken at admission. Univariate and multivariate analysis of composite endpoint according to medication are depicted in Table 5. Angiotensin converting enzyme (ACE) inhibitors, angiotensin receptor blockers and

Table 1. Main characteristics of the overall population and comparison between patients with heart disease (HD) and without HD.

	Total (n = 859)	With HD (n = 113)	Without HD (n = 746)	P
Mean age	68.1	75.6	67.0	< 0.001
Female	425 (49.5%)	50 (44.2%)	375 (50.2%)	0.233
Comorbidities				
Hypertension	425 (49.5%)	86 (76.1%)	339 (45.4%)	< 0.001
Diabetes mellitus	166 (19.3%)	43 (38.1%)	123 (16.5%)	< 0.001
Chronic kidney disease	59 (6.9%)	16 (14.2%)	43 (5.8%)	< 0.001
Dyslipidemia	348 (40.5%)	79 (69.9%)	269 (36.1%)	< 0.001
Current smoker	36 (4.2%)	3 (2.7%)	33 (4.4%)	0.612
Chronic obstructive pulmonary disease	79 (9.3%)	15 (13.3%)	64 (8.7%)	0.120
Clinical picture				
Temperature > 37.5°	627 (73.0%)	81 (71.7%)	546 (73.2%)	0.753
Cough	581 (67.6%)	61 (54.0%)	520 (69.7%)	0.001
Dyspnea	402 (46.8%)	55 (48.7%)	347 (46.5%)	0.668
Diarrhea	182 (21.2%)	22 (19.5%)	160 (21.4%)	0.631
Blood analysis				
Leukocytes > 10.000/mm^3	136 (15.9%)	24 (21.6%)	112 (15.0%)	0.076
Leukocytes < 4.000/mm^3	137 (16.0%)	21 (18.9%)	116 (15.6%)	0.368
Lymphocytes < 1.000/mm^3	478 (55.6%)	76 (67.0%)	402 (53.9%)	0.010
Hemoglobin < 10 g/dL	52 (6.1%)	15 (13.4%)	37 (5.0%)	0.001
Platelets < 150.000/mm^3	210 (24.5%)	35 (31.2%)	175 (23.5%)	0.076
Aspartate aminotransferase > 40 U/L	356 (41.4%)	53 (46.9%)	303 (40.5%)	0.230
Alanine aminotransferase > 40 U/L	311 (36.2%)	41 (36.1%)	270 (36.2%)	0.991
Lactate dehydrogenase > 250 U/L	564 (65.7%)	78 (69.4%)	486 (65.2%)	0.415
D-dimer > 500 μg/L	620 (72.2%)	92 (81.1%)	528 (70.8%)	0.027
Creatinine > 1.5 mg/dL	119 (13.9%)	31 (27.7%)	88 (11.8%)	< 0.001
C-reactive protein > 10 mg/L	618 (71.9%)	83 (73.4%)	535 (71.7%)	0.711
Procalcitonin > 0.5 ng/mL	126 (14.7%)	26 (22.8%)	100 (13.6%)	0.019
Chest-X ray				
Abnormal	799 (93.0%)	104 (92.0%)	695(93.2%)	0.664
Local opacity/shadowing	421 (40.9%)	42 (37.6%)	379 (41.4%)	0.472
Diffuse/bilateral shadowing/opacity	559 (65.1%)	76 (67.0%)	483 (64.9%)	0.671
Interstitial pattern	140 (16.3%)	19 (17.2%)	121 (16.1%)	0.793
Alveolointerstitial pattern	367 (42.7%)	46 (40.6%)	321 (43.0%)	0.651
Electrocardiogram				
Sinus rhythm	760 (88.5%)	83 (73.3%)	677 (90.6%)	< 0.001
Clinical evolution				
In-hospital death	176 (20.5%)	40 (35.4%)	136 (18.2%)	< 0.001
Respiratory failure	350 (40.8%)	64 (56.4%)	286 (38.5%)	< 0.001
Mechanical ventilation	73 (8.5%)	8 (7.1%)	65 (8.7%)	0.562
Heart failure	67 (7.8%)	19 (16.8%)	48 (6.4%)	0.001

beta-blockers were not independent predictors of death. However, statins were independently associated to better prognosis after multivariate analysis.

Clinical course

During hospitalization 85 patients developed cardiovascular events (Table 6), 24 of them (28.2%) had history of HD. The development of cardio-

Table 2. Characterization of the 113 patients with heart disease.

Condition	N	Mortality
Ischemic heart disease	71 (63%)	25 (35.2%)
Previous myocardial infarction	49	17 (34.7%)
Percutaneous revascularization:	56	20 (35.7%)
One vessel	35	13 (37.1%)
Two vessels	13	4 (30.8%)
Three vessels	8	3 (37.5%)
Left anterior descending artery	36	13 (36.1%)
Surgical revascularization	4	0 (0%)
Valvular heart disease	34 (30%)	14 (41%)
Mitral regurgitation	11	5 (45%)
Mitral stenosis	0	—
Aortic regurgitation	5	1 (20%)
Aortic stenosis	12	6 (50%)
Prosthesis	5	1 (20%)
Other	5	1 (20%)
Cardiomyopathy	14 (12%)	6 (43%)
Dilated	10	4 (40%)
Hypertrophic	4	2 (50%)

Table 4. Crude mortality rate according to the medications taken at admission

	N	Mortality
Angiotensin converting enzyme inhibitors	147	36 (24.5%)
Angiotensin receptor blockers	176	49 (27.8%)
Beta-blockers	158	57 (36.1%)
Calcium antagonists	82	28 (34.1%)
Diuretics	130	51 (39.2%)
Statins	295	66 (22.4%)
Acetylsalicylic acid	131	43 (32.8%)
Antivitamin K	94	42 (44.7%)
Direct oral anticoagulants	31	18 (58.1%)

vascular events during hospitalization identified a group of patients with poor outcome (mortality 31.8% vs. 19.3% in patients without cardiovascular events, $p = 0.007$). Acute heart failure was the most frequent cardiovascular event ($n = 64$) and was associated with increased mortality (32.8% vs. 16.6%, $p > 0.001$).

Table 3. Predictors of mortality and the composite endpoint.

Variable	Univariate		Multivariate	
	OR (95% CI)	P	OR (95% CI)	P
Mortality				
Age	1.093 (1.074–1.111)	< 0.001	1.076 (1.057–1.095)	< 0.001
Hypertension	2.928 (2.052–4.179)	< 0.001		
Diabetes mellitus	2.715 (1.866–3.949)	< 0.001	1.810 (1.159–2.827)	0.009
Chronic kidney disease	4.294 (2.500–7.375)	< 0.001	1.882 (0.984–3.601)	0.056
Heart disease	2.458 (1.602–3.771)	< 0.001		
COPD	2.296 (1.402–3.759)	0.001	1.787 (1.004–3.182)	0.048
Dyslipidemia	1.675 (1.200–2.338)	0.002		
Lymphocytes < 1000/m^3	2.350 (1.638–3.371)	< 0.001	1.692 (1.111–2.577)	0.014
D-dimer > 500 μg/L	2.388 (1.522–3.747)	< 0.001		
C-reactive protein > 10 mg/L	3.383 (2.083–5.492)	< 0.001	2.786 (1.639–4.734)	< 0.001
Hemoglobin < 10 g/dL	4.000 (2.257–7.089)	< 0.001		
Mortality + respiratory failure				
Age	1.045 (1.034–1.056)	< 0.001	1.029 (1.017–1.041)	< 0.001
Hypertension	2.047 (1.556–2.692)	< 0.001		
Diabetes mellitus	2.664 (1.877–3.782)	< 0.001	2.173 (1.459–3.236)	< 0.001
Chronic kidney disease	4.114 (2.252–7.515)	< 0.001	2.617 (1.331–5.144)	0.005
Heart disease	2.230 (1.487–3.344)	< 0.001		
Lymphocytes < 1000/m^3	2.534 (1.911–3.361)	< 0.001	2.074 (1.509–2.849)	< 0.001
D-dimer > 500 μg/L	2.191 (1.582–3.035)	< 0.001	1.523 (1.061–2.186)	0.023
C-reactive protein > 10 mg/L	3.434 (2.445–4.824)	< 0.001	3.160 (2.189–4.559)	< 0.001
Hemoglobin < 10 g/dL	3.357 (1.813–6.216)	< 0.001		

CI — confidence interval; COPD — chronic obstructive pulmonary disease; OR — odds ratio

Table 5. Univariate and multivariate analysis of mortality according to medication.

Variable	Univariate		Multivariate	
	OR (95% CI)	P	OR (95% CI)	P
Age	1.093 (1.074–1.111)	< 0.001	1.079 (1.060–1.099)	< 0.001
Hypertension	2.928 (2.052–4.179)	< 0.001		
Diabetes mellitus	2.715 (1.866–3.949)	< 0.001	1.886 (1.181–3.012)	0.008
Chronic kidney disease	4.294 (2.500–7.375)	< 0.001		
Heart disease	2.458 (1.602–3.771)	< 0.001		
COPD	2.296 (1.402–3.759)	0.001	1.817 (1.005–3.287)	0.048
Dyslipidemia	1.675 (1.200–2.338)	0.002	1.651 (0.996–2.736)	0.052
Lymphocytes < 1000/m^3	2.350 (1.638–3.371)	< 0.001	1.668 (1.088–2.526)	0.019
D-dimer > 500 μg/L	2.388 (1.522–3.747)	< 0.001		
C-reactive protein > 10 mg/L	3.383 (2.083–5.492)	< 0.001	2.741 (1.610–4.666)	< 0.001
Hemoglobin < 10 g/dL	4.000 (2.257–7.089)	< 0.001	2.376 (1.145–4.931)	0.020
ACE inhibitor	1.325 (0.871–2.016)	< 0.188		
Angiotensin receptor blocker	1.691 (1.154–2.480)	0.007		
Beta-blockers	2.750 (1.880–4.023)	< 0.001		
Statins	1.156 (0.816–1.628)	0.419	0.551 (0.329–0.921)	0.023

ACE — angiotensin convertin enzyme; CI — confidence interval; COPD — chronic obstructive pulmonary disease; OR — odds ratio

Table 6. Cardiovascular events during hospital stay. Several patients had more than one event.

Cardiovascular event	N (%)	Mortality
Heart failure	64 (7.4%)	21 (33%)
Acute myocardial infarction	4 (0.4%)	0 (0%)
Pericarditis	3 (0.3%)	1 (33%)
Myocarditis	2 (0.2%)	1 (50%)
Atrial fibrillation	12 (1.4%)	3 (25%)
Ventricular tachycardia or sudden cardiac death	1 (0.1%)	1 (100%)
Other cardiovascular events	4 (0.4%)	1 (25%)
TOTAL	90 (10.5%)	

Electrocardiogram

Electrocardiogram was performed in 485 (57.9%) patients. Only 50.8% of patients admitted in March had an ECG available (308 of 606) but this percentage rose to 65.8% (166 of 252) in April. In patients with ECG performed QTc was measured in 52.8% (n = 256) and QT interval lengthening (longer than 440 ms in men and 460 ms in women) was found in 16 (6.3%) patients. Of the 353 patients without ECG, 326 (92.3%) took, at least, one medication which lengthens the QT interval and 304 (86.1%) at least two.

Discussion

This study regarding hospitalized patients with COVID-19 had the goal to examine specific cardiovascular aspects, and several findings have to be underlined: 1) cardiovascular risk factors are common in COVID-19 and entail poor prognosis, particularly diabetes mellitus; 2) the presence of HD identifies a group of patients with poor outcome; HD is not independently related to prognosis, though; 3) cardiovascular medications normally used are not harmful, and statins may be protective; 4) cardiovascular events are frequent and negatively impact on prognosis. All these assertions not only emphasize the close relationship between COVID-19 and the heart but also highlight the importance of cardiologists being part of the multidisciplinary team taking care of these patients.

Cardiovascular risk factors are frequent in COVID-19 patients. Diabetes mellitus is as frequent as 20% [12], hypertension 30% [4] and active smoking 12.6% [3]. Surprisingly, dyslipidemia was not reported in any of the series. In the current cohort, the prevalence of these risk factors is even greater. Importantly, diabetes mellitus was a very powerful predictor of death in the current series, in line with previous publications [19].

Several physiopathologic mechanisms have been proposed to explain the poor prognosis in dia-

betic patients with COVID-19, linked to increased ACE2, furin and interleukin-6 levels [20, 21].

There are multiple mechanisms proposed to explain the association between HD and poor outcome in COVID-19. Patients in the present study with HD show more anemia, higher levels of D-dimer and procalcitonin and worse renal function, which suggests that the worse clinical evolution of these patients may be related to an aggressive hyperinflammatory and prothrombotic response and to a deficient immune response as suggested by the lower levels of lymphocytes.

Despite HD, it did not constitute an independent predictor of death in the population study, the current work shows that the presence of HD identifies a high-risk population and is a marker of poor outcome in COVID-19. Therefore, intensive surveillance and precocious treatment could be beneficial in this population. Public health policies should target those patients as a priority group for the vaccination against the SARS-CoV-2.

Discontinuing cardiovascular medications taken at admission during COVID-19 has been a controversial topic. Increased ACE2 receptor expression with RAAS blockade has been documented, which theoretically would favor SARS-CoV-2 entry into the cells. Nonetheless, other animal [22] and human studies [23] could not reproduce this upregulation of the receptor during treatment with RAAS blockade. Some authors warn about the harmful effect of RAAS blockers and advise its discontinuation to prevent poor outcome [14] while others claim to maintain these drugs until more evidence is available [15, 24]. The present data show that RAAS blockers are not harmful as seen in a recent Spanish study [25]. Only a prospective randomized study in patients free of the infection would provide evidence-based answers, which seems very difficult to undertake. In this regard, the investigators of the RASTAVI trial, which is currently randomizing patients with severe aortic stenosis who have indication for a percutaneous aortic prosthesis to ramipril or not, have shown that randomization to ramipril had no impact in the incidence or severity of COVID-19 [26].

Beta-blockers and statins are widely used due to their multiple beneficial effects in cardiovascular disease. In particular, statins may improve endothelial dysfunction, decrease expression of pro-inflammatory cytokines like interleukin-6 [27] and modulate the immune response at different levels, including immune cell adhesion and migration, antigen presentation, and cytokine production [28].

The current study results suggest that keeping cardiovascular related medication during COVID-19 is not harmful. Indeed, statins were found to be protective, which could be related to their pleiotropic effects. It has to be emphasized that this refers to medications the patient is already taking at admission and the present results do not support initiating these medications during hospital stays to enhance outcome.

Acute heart failure may be present in 23% of patients in their initial presentation for COVID-19 [6]. In the current cohort, acute heart failure was the most frequent cardiovascular event and showed a significant association with mortality. Results confirm the suspicions raised by previous works [29, 30]. Bearing this in mind, we recommend an active search of heart failure for its prompt diagnosis and treatment during COVID-19. However, we are aware of the difficulty of making a differential diagnosis between heart failure and respiratory failure in this setting.

There is available evidence of the occurrence of myocarditis secondary to SARS-CoV-2, confirmed by magnetic resonance and autopsy findings of inflammatory mononuclear infiltrate in myocardial tissue [31]. In the present cohort 2 cases of myocarditis were diagnosed and both required venoarterial extracorporeal membrane oxygenation as life support therapy.

With respect to acute coronary syndromes, it has been previously demonstrated the increased incidence in other viral infections like influenza [10, 32]. Frequency of type I myocardial infarction of patients with COVID-19 is unknown. The true prevalence in this setting may be underreported given the logistical challenges associated with limited testing and cardiac catheterization laboratory availability in this scenario.

Another concern about the management of COVID-19 is to reduce as much as possible the incidence of life-threatening ventricular tachyarrhythmias. COVID-19 treatment includes the use of hydroxychloroquine and azithromycin, which have known potential to induce QT prolongation. Besides, lopinavir-ritonavir presents a possible "torsade de pointes" risk.

Despite the importance of ECG to detect lengthening of QT interval it was performed in only 56.7% of the cohort. Physicians taking care of COVID-19 patients may be unaware of arrhythmogenic capacity of commonly used medications in this disease, particularly if used in combination. As stated previously, it was herein considered that hydroxychloroquine, azithromycin and lopinavir-ritonavir prolongers of the QT interval.

Limitations of the study

Some limitations have to be recognized. The protocol did not include troponin and B-type natriuretic peptide measurements that were done at the physicians' discretion, and a putative link between these parameters and the development of cardiac complications was not explored. Being the number of patients without ECG a limitation, it reflects the real-life practice in busy hospitals struggling with a massive admission of patients but having limited capacity and resources. The conclusions made here cannot be extrapolated to outpatients given that only patients admitted to the hospital were included. Finally, although the utmost care was taken to accurately apply our database, unintended mistakes cannot be ruled out. Nonetheless, to verify reliability of the gathered data 50 patient records were reviewed by an independent observer and only 0.04% variables were found to be incorrect. Moreover, all quantitative outliers (more than mean ± 2 standard deviation) were checked by an independent observer.

Conclusions

Heart disease identifies patients with higher mortality, but it is not an independent predictor of death. Cardiovascular medications taken before admission are not harmful, statins being protective. The development of cardiovascular events is related to poor outcome.

Conflict of interest: None declared

References

1. Dong E, Du H, Gardner L. An interactive web-based dashboard to track COVID-19 in real time. Lancet Infect Dis. 2020; 20(5): 533–534, doi: 10.1016/S1473-3099(20)30120-1, indexed in Pubmed: 32087114.
2. Guan WJ, Ni ZY, Hu Y, et al. Clinical characteristics of coronavirus disease 2019 in China. N Engl J Med. 2020; 382(18): 1708–1720.
3. Huang C, Wang Y, Li X, et al. Clinical features of patients infected with 2019 novel coronavirus in Wuhan. Lancet. 2020; 395(10223): 497–506.
4. Liang WH, Guan WJ, Li CC, et al. Clinical characteristics and outcomes of hospitalised patients with COVID-19 treated in Hubei (epicentre) and outside Hubei (non-epicentre): a nationwide analysis of China. Eur Respir J. 2020; 55(6), doi: 10.1183/13993003.00562-2020, indexed in Pubmed: 32269086.
5. Wang D, Hu Bo, Hu C, et al. Clinical characteristics of 138 hospitalized patients with 2019 novel coronavirus-infected pneumonia in Wuhan, China. JAMA. 2020; 323(11): 1061–1069, doi: 10.1001/jama.2020.1585, indexed in Pubmed: 32031570.
6. Zhou F, Yu T, Du R, et al. Clinical course and risk factors for mortality of adult inpatients with COVID-19 in Wuhan, China: a retrospective cohort study. Lancet. 2020; 395(10229): 1054––1062, doi: 10.1016/S0140-6736(20)30566-3, indexed in Pubmed: 32171076.
7. Shi Yu, Yu X, Zhao H, et al. Host susceptibility to severe COVID-19 and establishment of a host risk score: findings of 487 cases outside Wuhan. Crit Care. 2020; 24(1): 108, doi: 10.1186/s13054-020-2833-7, indexed in Pubmed: 32188484.
8. Hemmat N, Ebadi A, Badalzadeh R, et al. Viral infection and atherosclerosis. Eur J Clin Microbiol Infect Dis. 2018; 37(12): 2225–2233, doi: 10.1007/s10096-018-3370-z, indexed in Pubmed: 30187247.
9. Kwok CS, Aslam S, Kontopantelis E, et al. Influenza, influenza-like symptoms and their association with cardiovascular risks: a systematic review and meta-analysis of observational studies. Int J Clin Pract. 2015; 69(9): 928–937, doi: 10.1111/ijcp.12646, indexed in Pubmed: 25940136.
10. Warren-Gash C, Smeeth L, Hayward A. Influenza as a trigger for acute myocardial infarction or death from cardiovascular disease: a systematic review. Lancet Infect Dis. 2009; 9(10): 601–610, doi: 10.1016/s1473-3099(09)70233-6.
11. Udell JA, Farkouh ME, Solomon SD, et al. Does influenza vaccination influence cardiovascular complications? Expert Rev Cardiovasc Ther. 2015; 13(6): 593–596, doi: 10.1586/14779072.2015.1044439, indexed in Pubmed: 25971953.
12. Guo T, Fan Y, Chen M, et al. Cardiovascular implications of fatal outcomes of patients with coronavirus disease 2019 (COVID-19). JAMA Cardiol. 2020; 5(7): 811–818, doi: 10.1001/jamacardio.2020.1017, indexed in Pubmed: 32219356.
13. Clerkin KJ, Fried JA, Raikhelkar J, et al. COVID-19 and cardiovascular disease. Circulation. 2020; 141(20): 1648–1655, doi: 10.1161/CIRCULATIONAHA.120.046941, indexed in Pubmed: 32200663.
14. Esler M, Esler D. Can angiotensin receptor-blocking drugs perhaps be harmful in the COVID-19 pandemic? J Hypertens. 2020; 38(5): 781–782, doi: 10.1097/HJH.0000000000002450, indexed in Pubmed: 32195824.
15. Vaduganathan M, Vardeny O, Michel T, et al. Renin-angiotensin-aldosterone system inhibitors in patients with COVID-19. N Engl J Med. 2020; 382(17): 1653–1659, doi: 10.1056/NEJMsr2005760, indexed in Pubmed: 32227760.
16. Ponikowski P, Voors A, Anker S, et al. 2016 ESC Guidelines for the diagnosis and treatment of acute and chronic heart failure. Eur Heart J. 2016; 37(27): 2129–2200, doi: 10.1093/eurheartj/ehw128.
17. Adler Y, Charron P, Imazio M, et al. ESC Scientific Document Group. 2015 ESC Guidelines for the diagnosis and management of pericardial diseases: The Task Force for the Diagnosis and Management of Pericardial Diseases of the European Society of Cardiology (ESC)Endorsed by: The European Association for Cardio-Thoracic Surgery (EACTS). Eur Heart J. 2015; 36(42): 2921–2964.
18. Caforio ALP, Pankuweit S, Arbustini E, et al. Current state of knowledge on aetiology, diagnosis, management, and therapy of myocarditis: a position statement of the European Society of Cardiology Working Group on Myocardial and Pericardial Diseases. Eur Heart J. 2013; 34(33): 2636–48, 2648a, doi: 10.1093/eurheartj/eht210, indexed in Pubmed: 23824828.
19. Huang I, Lim MA, Pranata R. Diabetes mellitus is associated with increased mortality and severity of disease in COVID-19

pneumonia — a systematic review, meta-analysis, and meta-regression. Diabetes Metab Syndr. 2020; 14(4): 395–403, doi: 10.1016/j.dsx.2020.04.018, indexed in Pubmed: 32334395.
20. Ferrario CM, Jessup J, Chappell MC, et al. Effect of angiotensin-converting enzyme inhibition and angiotensin II receptor blockers on cardiac angiotensin-converting enzyme 2. Circulation. 2005; 111(20): 2605–2610, doi: 10.1161/CIRCULATIONAHA.104.510461, indexed in Pubmed: 15897343.
21. Furuhashi M, Moniwa N, Mita T, et al. Urinary angiotensin-converting enzyme 2 in hypertensive patients may be increased by olmesartan, an angiotensin II receptor blocker. Am J Hypertens. 2015; 28(1): 15–21, doi: 10.1093/ajh/hpu086, indexed in Pubmed: 24842388.
22. Burchill LJ, Velkoska E, Dean RG, et al. Combination renin-angiotensin system blockade and angiotensin-converting enzyme 2 in experimental myocardial infarction: implications for future therapeutic directions. Clin Sci (Lond). 2012; 123(11): 649–658, doi: 10.1042/CS20120162, indexed in Pubmed: 22715807.
23. Campbell DJ, Zeitz CJ, Esler MD, et al. Evidence against a major role for angiotensin converting enzyme-related carboxypeptidase (ACE2) in angiotensin peptide metabolism in the human coronary circulation. J Hypertens. 2004; 22(10): 1971–1976, doi: 10.1097/00004872-200410000-00020, indexed in Pubmed: 15361769.
24. de Abajo FJ, Rodríguez-Martín S, Lerma V, et al. Use of renin-angiotensin-aldosterone system inhibitors and risk of COVID-19 requiring admission to hospital: a case-population study. Lancet. 2020; 395(10238): 1705–1714, doi: 10.1016/S0140-6736(20)31030-8, indexed in Pubmed: 32416785.
25. López-Otero D, López-Pais J, Cacho-Antonio C, et al. Impact of angiotensin-converting enzyme inhibitors and angiotensin receptor blockers on COVID-19 in a western population. CARDIOVID registry. Rev Esp Cardiol. 2021; 74(2): 175–182, doi: 10.1016/j.rec.2020.05.018.
26. Amat-Santos IJ, Santos-Martinez S, López-Otero D, et al. Ramipril in high-risk patients with COVID-19. J Am Coll Cardiol. 2020; 76(3): 268–276, doi: 10.1016/j.jacc.2020.05.040, indexed in Pubmed: 32470515.
27. Oesterle A, Laufs U, Liao JK. Pleiotropic effects of statins on the cardiovascular system. Circ Res. 2017; 120(1): 229–243, doi: 10.1161/CIRCRESAHA.116.308537, indexed in Pubmed: 28057795.
28. Zeiser R. Immune modulatory effects of statins. Immunology. 2018; 154(1): 69–75, doi: 10.1111/imm.12902, indexed in Pubmed: 29392731.
29. Madjid M, Safavi-Naeini P, Solomon SD, et al. Potential effects of coronaviruses on the cardiovascular system: a review. JAMA Cardiol. 2020; 5(7): 831–840, doi: 10.1001/jamacardio.2020.1286, indexed in Pubmed: 32219363.
30. Inciardi RM, Adamo M, Lupi L, et al. Characteristics and outcomes of patients hospitalized for COVID-19 and cardiac disease in Northern Italy. Eur Heart J. 2020; 41(19): 1821–1829, doi: 10.1093/eurheartj/ehaa388, indexed in Pubmed: 32383763.
31. Siripanthong B, Nazarian S, Muser D, et al. Recognizing COVID-19-related myocarditis: The possible pathophysiology and proposed guideline for diagnosis and management. Heart Rhythm. 2020; 17(9): 1463–1471, doi: 10.1016/j.hrthm.2020.05.001, indexed in Pubmed: 32387246.
32. Kwong JC, Schwartz KL, Campitelli MA, et al. Acute myocardial infarction after laboratory-confirmed influenza infection. N Engl J Med. 2018; 378(4): 345–353, doi: 10.1056/NEJMoa1702090, indexed in Pubmed: 29365305.

VIA MEDICA

ORIGINAL ARTICLE

Cardiology Journal
2021, Vol. 28, No. 3, 369–383
DOI: 10.5603/CJ.a2020.0026

ISSN 1897–5593
eISSN 1898–018X

The impact of dissection and re-entry versus wire escalation techniques on long-term clinical outcomes in patients with chronic total occlusion lesions following percutaneous coronary intervention: An updated meta-analysis

Yejing Zhao*, Hongyu Peng*, Xiaonan Li, Jinghua Liu

Department of Cardiology, Beijing Anzhen Hospital, Capital Medical University, Beijing Institute of Heart, Lung and Blood Vessel Diseases, Beijing, China

Abstract

Background: *The meta-analysis was performed to evaluate the effect of dissection and re-entry (DR) vs. wire escalation (WE) techniques on long-term clinical outcomes in patients with chronic total occlusion (CTO) lesions undergoing percutaneous coronary intervention.*

Methods: *Studies were searched in electronic databases from inception to September, 2019. Results were pooled using random effects model and fixed effects model and are presented as risk ratios (RR) with 95% confidence intervals (CI).*

Results: *Pooled analyses revealed that patients with DR techniques had overall higher complexity CTO lesions than patients with WE techniques and required a greater number of stents and a greater mean stent length. The "extensive" DR techniques may have a higher incidence of target vessel revascularization (TVR) (RR = 2.30, 95% CI: 1.77–2.98), in-stent restenosis (RR = 1.71, 95% CI: 1.30–2.23), in-stent reocclusion (RR = 1.86, 95% CI: 1.03–3.3) and death/myocardial infarction/TVR (RR = 2.10, 95% CI: 1.71–2.58), when compared with WE techniques, during the long-term follow-up. However, "limited" DR techniques result in more promising outcomes, and are comparable to conventional WE techniques.*

Conclusions: *Dissection and re-entry techniques were associated with increased risk of long-term negative clinical events, especially "extensive" DR techniques. However, "limited" DR techniques resulted in good long-term outcomes, comparable to WE techniques.* (Cardiol J 2021; 28, 3: 369–383)

Key words: chronic total occlusion, percutaneous coronary intervention, dissection and re-entry, wire escalation, meta-analysis

This article is accompanied by the editorial on page 355

Introduction

In the hybrid algorithm to chronic total occlusion (CTO) percutaneous coronary intervention (PCI), dissection and re-entry (DR) by either the antegrade or the retrograde approach has since evolved to an indispensable strategy for crossing the occlusion, and this has contributed in improving the technical success rate of CTO PCI, when compared to conventional wire escalation (WE) techniques, especially for complex lesions [1]. However, the long-term prognosis of patients with DR techniques remains controversial. Some concerns have been raised on the possible increased

Address for correspondence: Jinghua Liu, MD, PhD, Beijing Anzhen Hospital, Capital Medical University, Beijing Institute of Heart, Lung and Blood Vessel Diseases, No. 2 Anzhen Street, Chaoyang District, Beijing, China, tel: +86 010 64456541, e-mail: liujinghua@vip.sina.com

Received: 6.01.2020 Accepted: 16.02.2020

*These authors contributed equally to this work.

risk of a higher incidence of restenosis, while other concerns support the potential role of DR in the contemporary CTO PCI, when compared to a conventional true-to-true (TTT) lumen strategy [2, 3]. Furthermore, positive improvements have already been made with the development of new and better materials and equipment, such as device-based "controlled" antegrade DR (ADR) and retrograde DR (RDR) [4]. However, it remains unknown whether this can further improve the prognosis of patients. Although there has been a meta-analysis on the subject so far [5]. Moreover, many additional cohort studies have been published since. Therefore, a comprehensive updated meta-analysis is warranted. Therefore, the present meta-analysis was conducted to evaluate the impact of DR vs. WE techniques on long-term clinical outcomes in patients undergoing CTO PCI.

Methods

Search strategy

Eligible trials were identified by performing electronic searches on PubMed, Embase, Web of Science, and the Cochrane Central Register of Controlled Trials (CENTRAL) using the following search items: "chronic total occlusion" or "CTO" AND "subintimal" OR "subadventitial" OR "dissection" OR "tracking" OR "re-entry" OR "CART" OR "controlled antegrade and retrograde tracking" OR "STAR" OR "subintimal tracking and re-entry" OR "LAST" OR "limited antegrade subintimal tracking" OR "CrossBoss and Stingray" OR "Boston Scientific" OR "wire escalation" OR "intraplaque" OR "intimal" OR "true-to-true" OR "crossing". was provided in the supplementary data. The inclusion period was from the establishment of the databases to September 2019. YJZ and HYP independently performed the literature search, and any differences were resolved by discussion.

Study selection

Studies were included when the following were satisfied: (1) studies that directly compared the clinical outcomes of all-cause death, cardiac death, myocardial infarction (MI), target vessel revascularization (TVR), in-stent restenosis (ISR), in-stent occlusion (ISO) or stent thrombosis (ST), during the follow-up period, after the successful recanalization of CTO lesions. using the DR technique vs. WE technique is directly made; (2) observational studies and randomized controlled trials (RCTs) published as original articles.

Data extraction and quality assessment

Data were extracted by one reviewer (YJZ) and independently checked by another two reviewers (HYP and XNL). Any disagreements between the reviewers were resolved by discussion with a fourth investigator (JHL), and by referencing the original report. The quality of the cohort study was assessed using the Newcastle-Ottawa scale. A study was regarded as high-quality when it was awarded a total score of ≥ 6 in the Newcastle--Ottawa scale [6, 7].

Statistical analysis

For dichotomous data, the available risk estimates extracted were mostly rate ratios (RRs), while those in partial studies were hazard ratios (HRs), incidence rate ratios (IRRs), or odds ratios (ORs). When risk estimates and confidence intervals (CIs) were not provided, the RRs and CIs were calculated from the available data using the Woolf method in the Stata version 15.0 software. For continuous data, standard mean differences (SMD) and the corresponding 95% CIs were pooled to compare the continuous outcomes between the two groups [8, 9]. Heterogeneity across studies was determined using the I^2 statistic, which is a quantitative measure of inconsistency across studies. The following criteria was used: $I^2 < 50\%$: low heterogeneity; $I^2 = 50–75\%$: moderate heterogeneity and $I^2 > 75\%$: high heterogeneity. The heterogeneity was considered significant when the χ^2 test was significant ($p < 0.10$) or the I^2 was $> 50\%$ [9, 10]. The analysis was performed with random effects models at first, then further changed to the fixed effects models to calculate the RR and 95% CIs again to avoid interferences from small sample studies. The sensitivity was determined to evaluate the stability of the present results by removing each study one at a time (metaninf command). What is more, subgroup analyses stratified according to different approaches (anterograde or retrograde), different DR techniques ("limited DR" or "extensive DR") and different areas (Asia, Europe or America) were performed to explore potential sources of heterogeneity in outcomes (metan command). The "extensive DR" techniques were as follows: (1) subintimal tracking and re-entry (STAR, including mini-STAR and contrast-guided STAR); (2) limited antegrade subintimal tracking (LAST) for the antegrade approach; (3) controlled antegrade and retrograde tracking (CART) for the retrograde approach. The "limited DR" techniques were as follows: (1) reverse CART for the retrograde approach; (2) device-facilitated techniques (using the Cross-

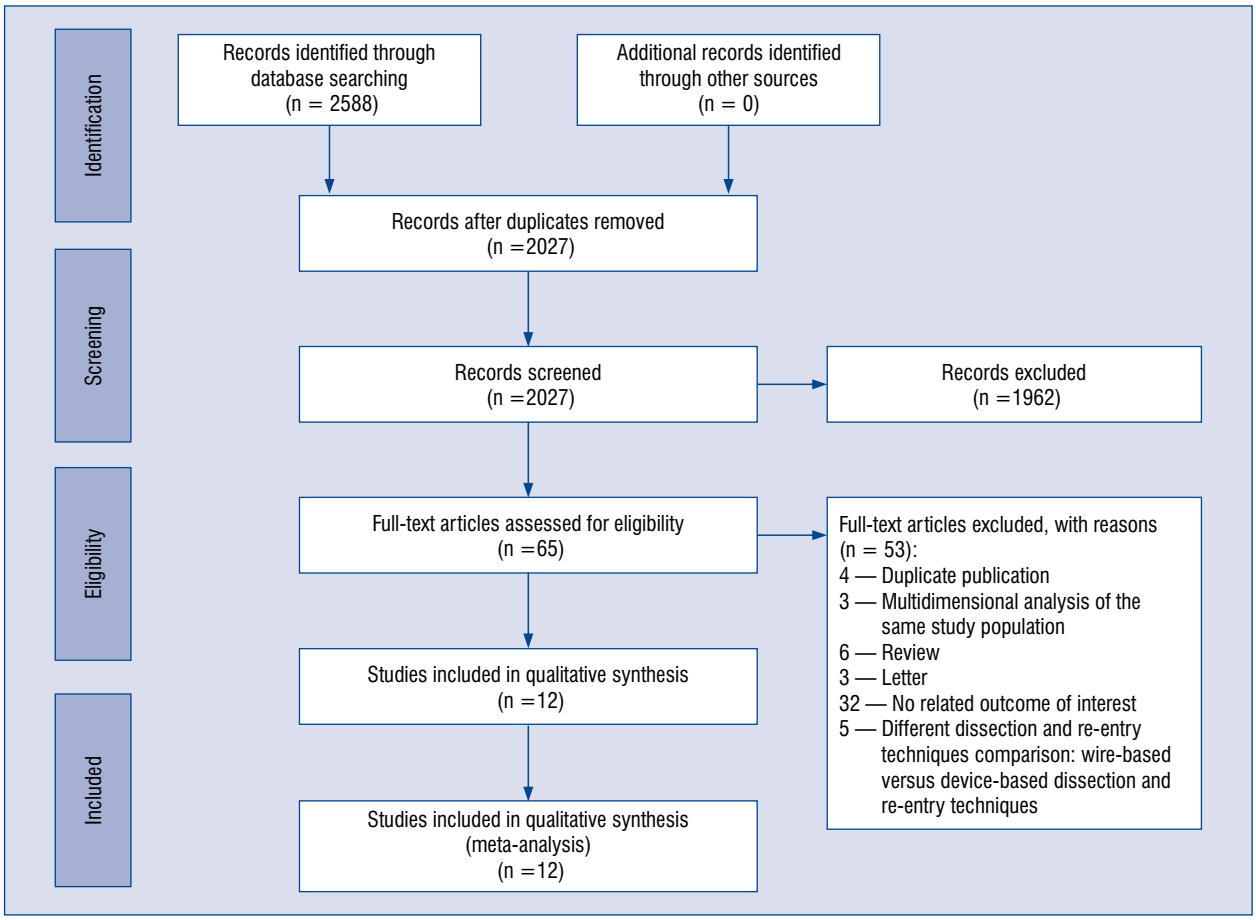

Figure 1. Flow diagram of the study selection process.

Boss/Stingray system; Boston Scientific, Marlborough, MA) [11]. For dichotomous data, publication bias was assessed by Harbord's regression asymmetry test [12]. For continuous data, publication bias was assessed by the Egger regression asymmetry test [13]. The statistical tests were two-sided, and a significance level of $p < 0.05$ was used.

Results

Literature search and quality assessment

A total of 2,588 studies were identified through the electronic searches, and 561 were excluded due to duplication. Then, 2,027 studies were also excluded after reading the titles and abstracts. The remaining 65 studies were assessed by reading the full texts. Eventually, 12 cohort studies were included in qualitative synthesis and meta-analysis [11, 14–24]. The flow diagram of the study selection process is presented in Figure 1. The characteristics of the included studies are summarized in **Supplementary Table S1**. The quality of cohort studies assessed with the Newcastle-Ottawa scale were summarized in **Supplementary Table S2**. All included studies were of high quality, as determined by a Newcastle-Ottawa scale score of ≥ 6 for cohort studies.

Long-term outcomes

Mortality

All-cause mortality. The outcome occurred in at least 76 events among the 3,166 participants from 9 cohort studies [14–19, 21, 22, 24]. The pooled RR value of all-cause mortality in the DR technique group, when compared with that in the conventional WE technique group, was 1.52 (95% CI: 0.95–2.45; Fig. 2A), and there was no heterogeneity ($I^2 = 0.0\%$, $p = 0.858$).

Cardiovascular mortality. Nine cohort studies (3,164 patients) reported this outcome [11, 14, 16–20, 22, 24], and no heterogeneity was found among these trials ($I^2 = 0.00\%$, $p = 0.637$; Fig. 2B). The results were RR = 0.97 and 95% CI: 0.52–1.81, indicating no statistical differences.

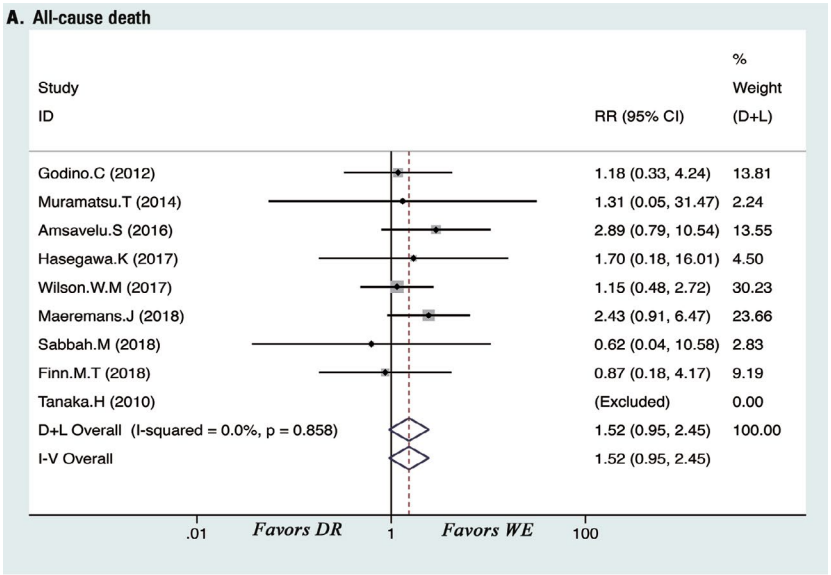
A. All-cause death
Study
ID
RR (95% CI)
% Weight (D+L)
Godino.C (2012) 1.18 (0.33, 4.24) 13.81
Muramatsu.T (2014) 1.31 (0.05, 31.47) 2.24
Amsavelu.S (2016) 2.89 (0.79, 10.54) 13.55
Hasegawa.K (2017) 1.70 (0.18, 16.01) 4.50
Wilson.W.M (2017) 1.15 (0.48, 2.72) 30.23
Maeremans.J (2018) 2.43 (0.91, 6.47) 23.66
Sabbah.M (2018) 0.62 (0.04, 10.58) 2.83
Finn.M.T (2018) 0.87 (0.18, 4.17) 9.19
Tanaka.H (2010) (Excluded) 0.00
D+L Overall (I-squared = 0.0%, p = 0.858) 1.52 (0.95, 2.45) 100.00
I-V Overall 1.52 (0.95, 2.45)
.01
Favors DR
1
Favors WE
100

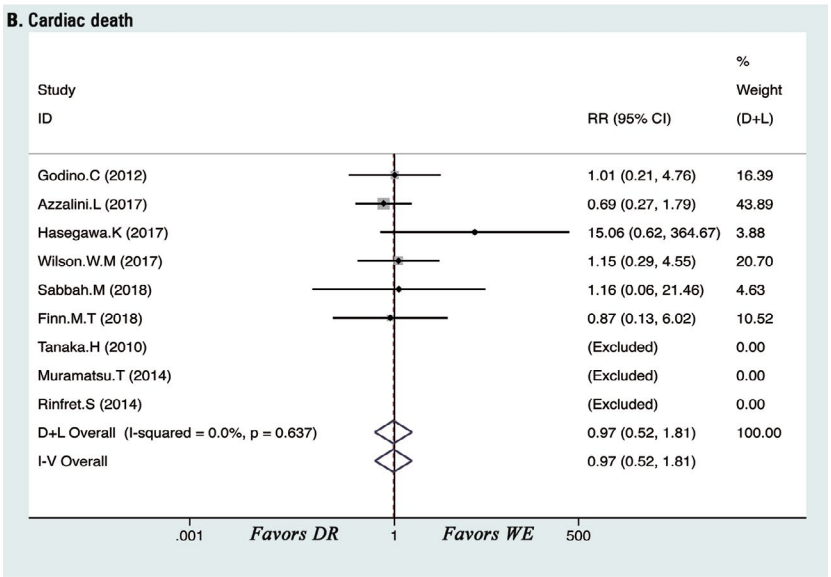
B. Cardiac death
Study
ID
RR (95% CI)
% Weight (D+L)
Godino.C (2012) 1.01 (0.21, 4.76) 16.39
Azzalini.L (2017) 0.69 (0.27, 1.79) 43.89
Hasegawa.K (2017) 15.06 (0.62, 364.67) 3.88
Wilson.W.M (2017) 1.15 (0.29, 4.55) 20.70
Sabbah.M (2018) 1.16 (0.06, 21.46) 4.63
Finn.M.T (2018) 0.87 (0.13, 6.02) 10.52
Tanaka.H (2010) (Excluded) 0.00
Muramatsu.T (2014) (Excluded) 0.00
Rinfret.S (2014) (Excluded) 0.00
D+L Overall (I-squared = 0.0%, p = 0.637) 0.97 (0.52, 1.81) 100.00
I-V Overall 0.97 (0.52, 1.81)
.001
Favors DR
1
Favors WE
500

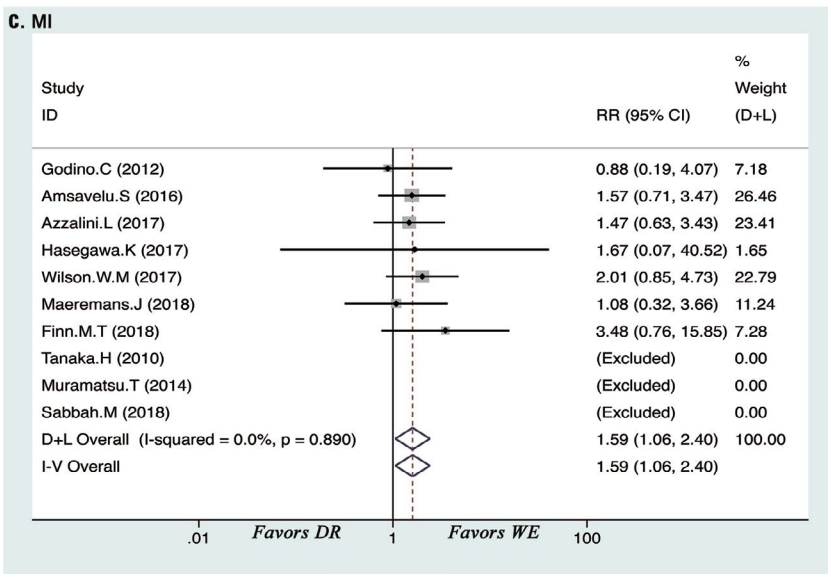
C. MI
Study
ID
RR (95% CI)
% Weight (D+L)
Godino.C (2012) 0.88 (0.19, 4.07) 7.18
Amsavelu.S (2016) 1.57 (0.71, 3.47) 26.46
Azzalini.L (2017) 1.47 (0.63, 3.43) 23.41
Hasegawa.K (2017) 1.67 (0.07, 40.52) 1.65
Wilson.W.M (2017) 2.01 (0.85, 4.73) 22.79
Maeremans.J (2018) 1.08 (0.32, 3.66) 11.24
Finn.M.T (2018) 3.48 (0.76, 15.85) 7.28
Tanaka.H (2010) (Excluded) 0.00
Muramatsu.T (2014) (Excluded) 0.00
Sabbah.M (2018) (Excluded) 0.00
D+L Overall (I-squared = 0.0%, p = 0.890) 1.59 (1.06, 2.40) 100.00
I-V Overall 1.59 (1.06, 2.40)
.01
Favors DR
1
Favors WE
100

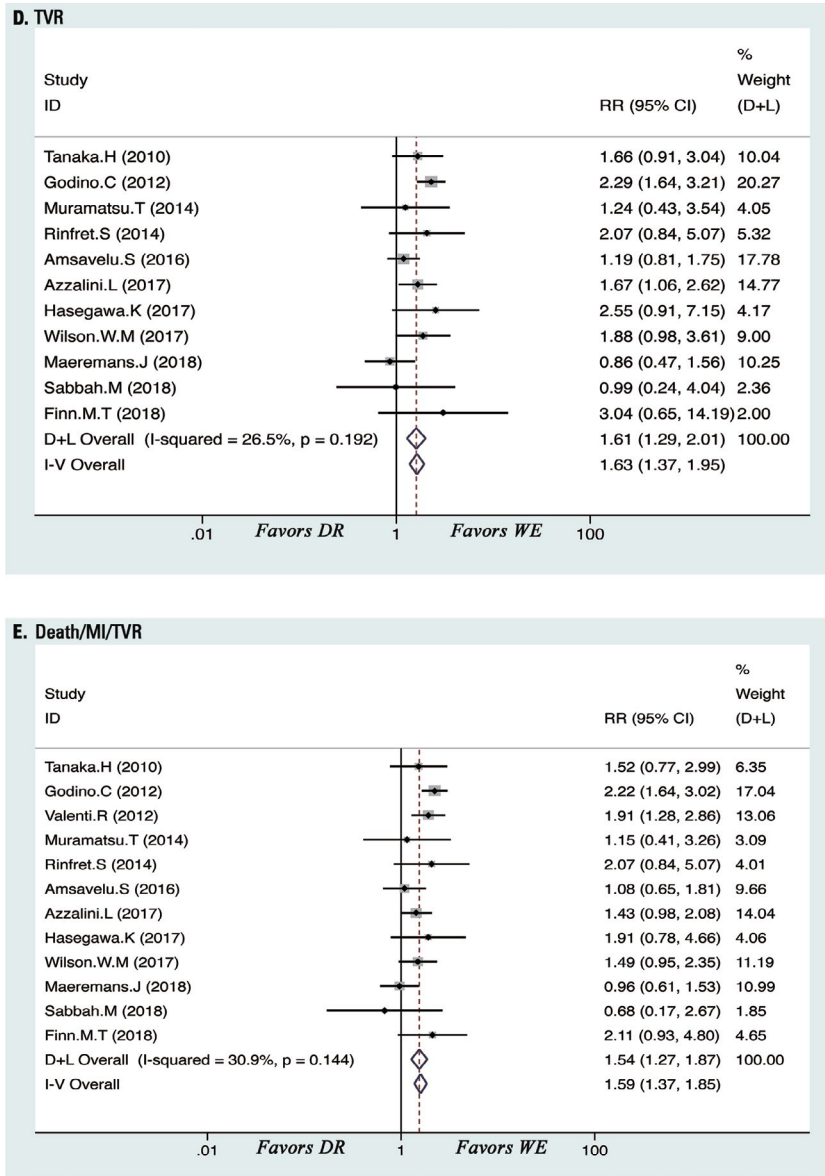

Figure 2. Forest plot for mortality, myocardial infarction (MI), target vessel revascularization (TVR) and composite outcomes (death/MI/TVR) in long-term follow-up. Forest plot demonstrates a pooled estimate of mortality during the follow-up period: **A.** All-cause mortality; **B.** Cardiovascular mortality; **C.** Myocardial infarction; **D.** Target vessel revascularization; **E.** Death/MI/TVR. The risk ratio of each study along with a pooled risk ratio with 95% confidence intervals (CI) is depicted; DR — dissection and re-entry; WE — wire escalation.

Myocardial infarction

Ten cohort studies were included for the outcome, which involved 4,090 participants and 97 events, and no heterogeneity was found for MI incidence (I^2 = 0.00%, p = 0.890; Fig. 2C) [11, 14–19, 21, 22, 24]. The pooled results indicated that DR technique in CTO PCI may have a higher incidence of MI, when compared with the conventional WE technique, during long-term follow-up (RR = 1.59, 95% CI: 1.06–2.40; Fig. 2C).

Target vessel revascularization

Eleven studies with 4,260 patients were included, and low heterogeneity was found (I^2 = = 26.50%, p = 0.192; Fig. 2D) [11, 14–22, 24]. The data revealed significant differences between the two groups with regard to TVR (RR = 1.61, 95% CI: 1.29–2.01; Fig. 2D). Compared with the conventional WE strategy, successful CTO PCI after DR crossing was associated with a higher rate of TVR in long-term follow-up.

Composite outcomes: Death/MI/TVR

The incidence of composite outcomes was 15.35% (n = 234) in the DR technique group and 13.58% (n = 480) in the WE technique group [11, 14–24]. There was a significantly higher incidence of death/MI/TVR in the DR technique group, when compared with that in the WE technique group (RR = 1.54, 95% CI: 1.27–1.87; Fig. 2E). There was a low heterogeneity among these trials (I^2 = 30.9%, p = 0.144; Fig. 2E).

In-stent restenosis, reocclusion and thrombosis

The pooled outcomes revealed that the DR technique in CTO PCI was associated with higher rates of ISR (RR = 1.62, 95% CI: 1.26–2.10; I^2 = 0.0%, p = 0.459; Fig.3A) and in-stent reocclusion (RR = = 1.90, 95% CI: 1.09–3.31; I^2 = 0.00%, p = 0.891; Fig. 3B) [16, 19, 22, 24]. As shown in Figure 3C, no significant difference in stent thrombosis was observed during follow-up after successful CTO PCI between the DR technique and WE technique (RR = 1.59, 95% CI: 0.64–3.93; I^2 = 0.00%, p = 0.733) [14, 16–19, 22, 24].

Procedural characteristics in the real world

CTO occlusion length and J-CTO score

The CTO length was significantly longer in patients with subintimal DR techniques, when compared with conventional WE crossing (SMD: 0.64, 95% CI: 0.31–0.97, p < 0.001; I^2 = 83.4%, p < 0.001; Fig. 3D) [14, 16, 17, 19, 21]. Furthermore, patients with DR techniques had an overall higher complexity of CTO lesions than patients with WE techniques, which was evidenced by the J-CTO score (SMD: 0.90, 95% CI: 0.68–1.12, p < 0.001; I^2 = 79.4%, p < 0.001; Fig. 3E) [11, 14, 17, 20, 21].

Stent length and number of stents

Stent length were recorded by 9 cohort studies [11, 14, 16–22], while the number of stents were recorded by 7 cohort studies [14, 16, 18–20, 22, 24]. CTO PCI with DR tracking required a greater number of stents (SMD: 0.57, 95% CI: 0.49–0.66, p < 0.001; I^2 = 66.0%, p < 0.001; Fig. 3G) and a greater mean stent length (SMD: 0.80, 95% CI: 0.73-0.86, p < 0.001; I^2 = 59.1%, p = 0.007; Fig. 3F), when compared to WE tracking.

Subgroup analysis for long-term outcomes

Predefined subgroup analyses were conducted across key study characteristics summarized in Table 1. Specifically, the intension was to conduct subgroup analyses by different approaches and different DR techniques to clarify whether patients with retrograde approach and "extensive/old" DR techniques were at particularly high cardiovascular risk. In the subgroup analyses by different approaches, no differences were found between the anterograde approach and retrograde approach in CTO PCI. However, there were significant statistical differences in the long-term clinical outcomes between "limited/new" DR techniques and "extensive/old" DR techniques. Subgroup analysis indicated that the use of "extensive" DR techniques was associated with higher risk of TVR (RR = 2.30, 95% CI: 1.77–2.98; Table 1), ISR (RR = 1.71, 95% CI: 1.30–2.23; Table 1), in-stent occlusion (RR = 1.86, 95% CI: 1.03–3.38; Table 1) and composite endpoints (RR = 2.10, 95% CI: 1.71–2.58; Table 1), while "limited" DR techniques did not higher the cardiovascular risk, when compared with WE techniques. Besides, considering different technologies in CTO PCI applied in different areas, subgroup analyses was conducted by different areas. The results showed that the incidence of major adverse cardiovascular events with DR techniques in studies from Europe was reported higher than that of others (Table 1).

Sensitivity analysis

In sensitivity analysis, risk estimates all slightly changed after analysis while removing a study for all outcomes, indicating the robustness of the present findings, and that no single study drove the summary effects (Fig. 4).

Publication bias

The Harbord regression test suggested no obvious publication bias for all binary outcomes, as shown in Figure 5. The Egger regression test suggested no obvious publication bias for J-CTO score, stent length, and number of stents. However, a significant publication bias for the outcome of CTO occlusion length was detected using the Egger regression test (p = 0.048, Fig. 5I). The conclusion did not change after adjustment for publication bias using the trim and fill method.

Discussion

According to available research, this is the latest and largest meta-analysis reported to date on the effect of DR techniques vs. conventional WE techniques on long-term clinical outcomes in CTO PCI, which included 5,265 participants from 12 cohort studies. With accumulating evidence, the statistical power was enhanced to provide more precise and reliable risk estimates. The most-rel-

A. In-stent restenosis

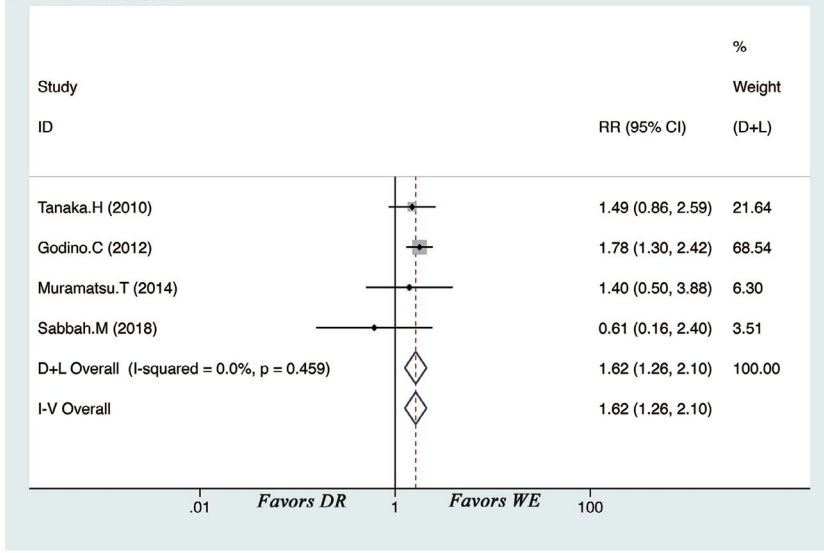

B. In-stent occlusion

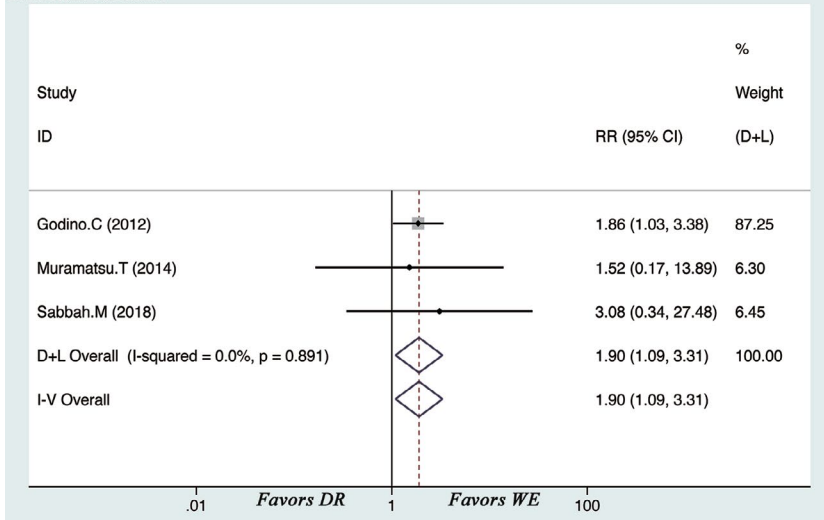

C. Stent thrombosis

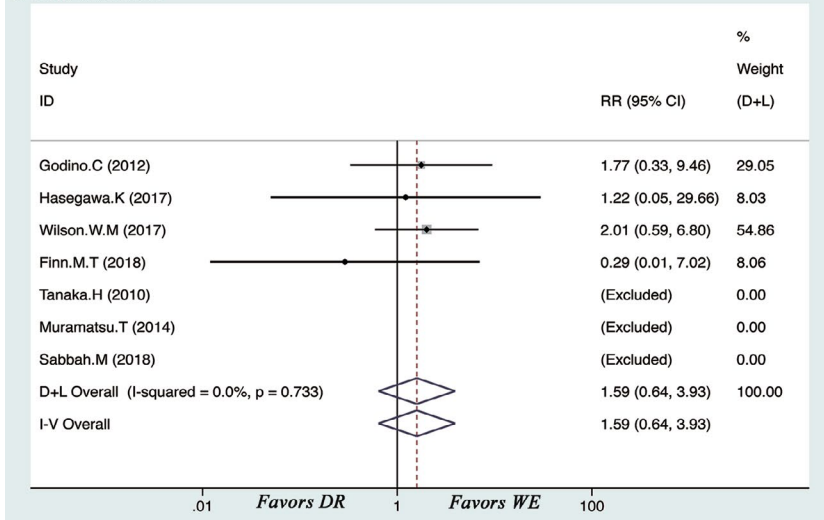

→

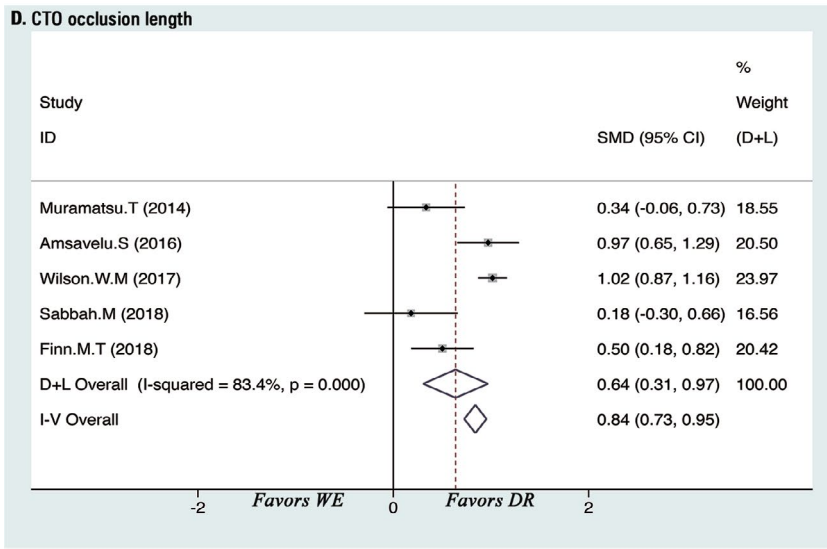
D. CTO occlusion length
Study
ID
SMD (95% CI)
%
Weight
(D+L)
Muramatsu.T (2014) 0.34 (-0.06, 0.73) 18.55
Amsavelu.S (2016) 0.97 (0.65, 1.29) 20.50
Wilson.W.M (2017) 1.02 (0.87, 1.16) 23.97
Sabbah.M (2018) 0.18 (-0.30, 0.66) 16.56
Finn.M.T (2018) 0.50 (0.18, 0.82) 20.42
D+L Overall (I-squared = 83.4%, p = 0.000) 0.64 (0.31, 0.97) 100.00
I-V Overall 0.84 (0.73, 0.95)
-2
Favors WE
0
Favors DR
2

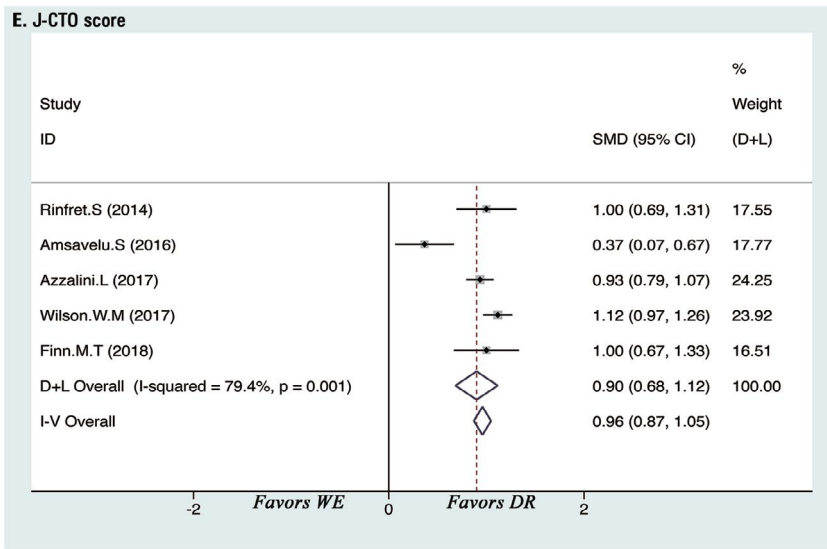
E. J-CTO score
Study
ID
SMD (95% CI)
%
Weight
(D+L)
Rinfret.S (2014) 1.00 (0.69, 1.31) 17.55
Amsavelu.S (2016) 0.37 (0.07, 0.67) 17.77
Azzalini.L (2017) 0.93 (0.79, 1.07) 24.25
Wilson.W.M (2017) 1.12 (0.97, 1.26) 23.92
Finn.M.T (2018) 1.00 (0.67, 1.33) 16.51
D+L Overall (I-squared = 79.4%, p = 0.001) 0.90 (0.68, 1.12) 100.00
I-V Overall 0.96 (0.87, 1.05)
-2
Favors WE
0
Favors DR
2

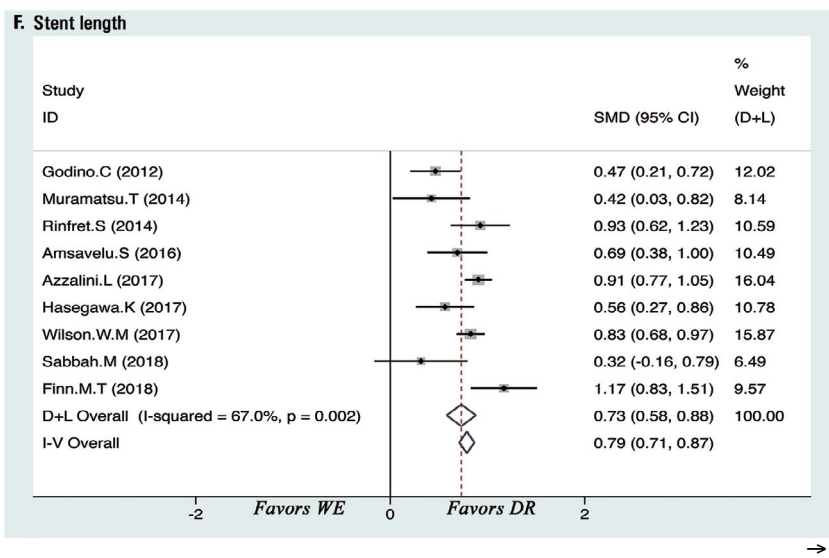
F. Stent length
Study
ID
SMD (95% CI)
%
Weight
(D+L)
Godino.C (2012) 0.47 (0.21, 0.72) 12.02
Muramatsu.T (2014) 0.42 (0.03, 0.82) 8.14
Rinfret.S (2014) 0.93 (0.62, 1.23) 10.59
Amsavelu.S (2016) 0.69 (0.38, 1.00) 10.49
Azzalini.L (2017) 0.91 (0.77, 1.05) 16.04
Hasegawa.K (2017) 0.56 (0.27, 0.86) 10.78
Wilson.W.M (2017) 0.83 (0.68, 0.97) 15.87
Sabbah.M (2018) 0.32 (-0.16, 0.79) 6.49
Finn.M.T (2018) 1.17 (0.83, 1.51) 9.57
D+L Overall (I-squared = 67.0%, p = 0.002) 0.73 (0.58, 0.88) 100.00
I-V Overall 0.79 (0.71, 0.87)
-2
Favors WE
0
Favors DR
2

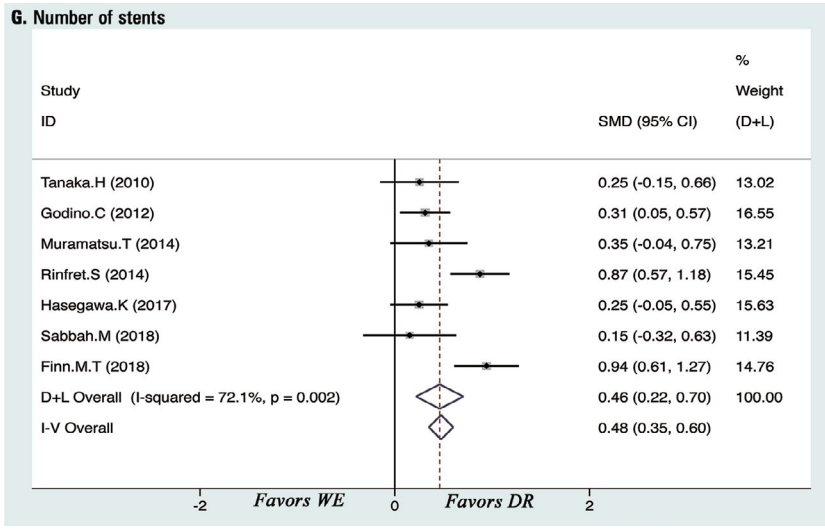

Figure 3. Forest plot for in-stent restenosis, reocclusion, thrombosis in the long-term follow-up and the procedural characteristics of patients with chronic total occlusion (CTO). Forest plot demonstrating a pooled estimate of the following outcomes during the follow-up period: **A.** In-stent restenosis; **B.** In-stent reocclusion; **C.** Stent thrombosis; **D.** CTO occlusion length; **E.** J-CTO score; **F.** Stent length; **G.** Number of stents. The risk ratio of each study along with a pooled risk ratio with 95% confidence intervals (CI) is depicted; DR — dissection and re-entry; WE — wire escalation.

evant heterogeneity moderators have been identified by subgroup analyses. The sensitivity analysis and publication bias were performed to ensure the stability of the present results. The following are the main findings of the present meta-analysis:

— The application of DR techniques in CTO PCI is associated with similar risk of mortality, but with higher risk of MI, TVR, ISR and in-stent re-occlusion, when compared with WE techniques, during clinical follow-up of 12–24 months.

— DR techniques were more applied in patients with higher complexity CTO lesions, which was evidenced by higher J-CTO score and longer CTO occlusion length. Therefore, CTO PCI with DR tracking required a greater number of stents and longer stent length, that may explain the higher incidence of long-term adverse cardiovascular events in the DR techniques group as compared with WE techniques.

— Furthermore, extensive DR techniques raises the risk of long-term clinical adverse events. However, limited DR techniques for crossing CTO was associated with similar long-term major adverse cardiovascular events, as compared to WE crossing, highlighting the growing role of more controlled subintimal crossing technique utilization in achieving high procedural success.

The recanalization of coronary occlusion lesions remains one of the major challenges in interventional cardiology. Conventional WE techniques typically use an intraplaque course for CTO crossing. DR techniques exploit the subintimal space for coronary wire passage with subsequent re-entry into the true lumen, which is needed more often to obtain success, when compared to antegrade and/or retrograde wiring strategies, especially for treating higher complexity CTO lesions. With the positive improvement and development of dedicated equipment, DR techniques have since evolved to an indispensable strategy of contemporary CTO PCI [25]. According to previous reports, the frequency of subintimal tracking ranges from 8.7% to 45.5% in the antegrade approach, and from 24.2% to 50.0% in the retrograde approach [18]. Although DR strategies have been increasingly adopted, controversial data regarding long-term clinical prognosis of DR techniques have been published in this area, prompting the investigators to conducted the present meta-analysis to evaluate the long-term clinical outcomes of DR techniques, when compared to conventional WE techniques.

The findings of the present analysis indicated that DR techniques may increase the incidence of MI, TVR and ISR in patients with successful CTO PCI, when compared to a conventional WE strategy. Both ADR and RDR involves dissection and subsequent stenting within the subintimal space. A previous intravascular ultrasound (IVUS) reported that subintimal stenting could disturb the vessel geometry, which may lead to late acquired

Table 1. Subgroup and heterogeneity analyses of pooled risk ratios for long-term outcomes.

Factors	N (studies)	Events/participants		RR (95% CI)	I^2	P[a]
		DR	WE			
MYOCARDIAL INFARCTION						
Different approaches						
Anterograde	4	15/252	14/894	1.93 (0.94–3.99)	0.0%	0.475
Retrograde	5	2/261	3/322	0.45 (0.09–2.31)	0.0%	0.728
Different DR techniques						
Extensive/Old DR techniques	3	7/195	19/957	1.79 (0.60–5.30)	32.4%	0.224
Limited/New DR techniques	6	31/1120	29/2072	1.58 (0.93–2.71)	0.0%	0.657
Location						
Asia	4	0/126	1/652	1.67 (0.07–40.52)	–	–
Europe	4	30/1120	34/1862	1.47 (0.88–2.45)	0.0%	0.758
America	2	21/167	11/163	1.86 (0.92–3.76)	0.0%	0.357
TARGET VESSEL REVASCULARIZATION						
Different approaches						
Anterograde	4	34/252	65/894	1.19 (0.83–1.70)	0.0%	0.701
Retrograde	5	34/263	49/324	1.23 (0.75–2.02)	24.6%	0.257
Different DR techniques						
Extensive/Old DR techniques	3	62/197	115/959	2.30 (1.77–2.98)	3.1%	0.356
Limited/New DR techniques	6	72/1120	106/2072	1.37 (0.97–1.94)	17.0%	0.304
Location						
Asia	4	21/132	63/647	1.62 (1.04–2.52)	0.0%	0.688
Europe	5	119/1193	142/1958	1.69 (1.19–2.40)	52.6%	0.077
America	2	41/167	33/163	1.41 (0.68–2.93)	28.5%	0.237
DEATH/MYOCARDIAL INFARCTION/TARGET VESSEL REVASCULARIZATION						
Different approaches						
Anterograde	3	18/219	61/871	1.22 (0.74–2.02)	0.0%	0.479
Retrograde	4	31/264	59/525	1.17 (0.67–2.07)	43.8%	0.149
Different DR techniques						
Extensive/Old DR techniques	4	83/229	316/1725	2.10 (1.71–2.58)	0.0%	0.658
Limited/New DR techniques	6	114/1120	168/2072	1.24 (0.97–158)	5.1%	0.384
Location						
Asia	4	20/130	74/645	1.40 (0.89–2.20)	0.0%	0.622
Europe	6	175/1227	377/2726	1.61 (1.24–2.10)	54.7%	0.051
America	2	39/167	29/163	1.40 (0.74–2.64)	45.8%	0.174
IN-STENT RESTENOSIS						
Different DR techniques						
Extensive/Old DR techniques	2	45/92	94/331	1.71 (1.30–2.23)	0.0%	0.588
Limited/New DR techniques	1	4/22	13/100	1.40 (0.50–3.88)	–	–
Location						
Asia	2	15/51	46/230	1.47 (0.91–2.39)	0.0%	0.910
Europe	2	50/382	96/804	1.29 (0.61–2.71)	80.9%	0.022
America	0	–	–	–	–	–
IN-STENT OCCLUSION						
Different DR techniques						
Extensive/Old DR techniques	1	14/63	24/201	1.86 (1.03–3.38)	–	–
Limited/New DR techniques	1	1/22	3/100	1.52 (0.17–13.89)	–	–
Location						
Asia	2	2/35	6/220	2.17 (0.46–10.29)	0.0%	0.653
Europe	1	14/63	24/201	1.86 (1.03–3.38)	–	–
America	0	–	–	–	–	–

[a]P value for heterogeneity; DR — dissection and re-entry; WE — wire escalation; IVUS — intravascular ultrasound; CTO — chronic total occlusion; PCI — percutaneous coronary intervention; RCT — randomized controlled trial; RR — risk ratio; CI — confidence interval

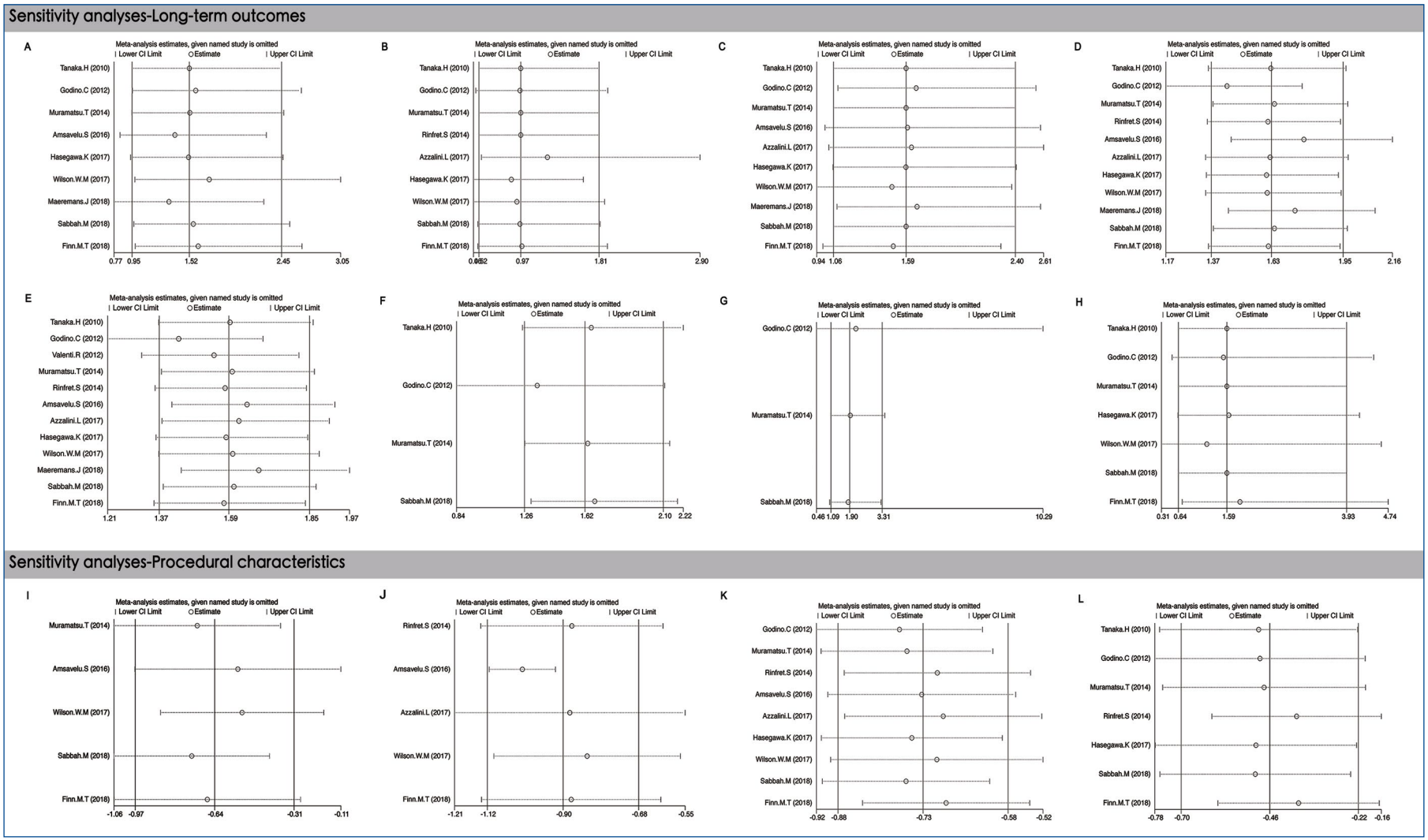

Figure 4. Sensitivity analyses of pooled rate ratios for outcomes. Sensitivity analyses for the following outcomes; **A.** All-cause mortality; **B.** Cardiac mortality; **C.** Myocardial infarction (MI); **D.** Target vessel revascularization (TVR); **E.** Death/MI/TVR; **F.** In-stent restenosis; **G.** In-stent reocclusion; **H.** Stent thrombosis; **I.** Chronic total occlusion (CTO) occlusion length; **J.** J-CTO score; **K.** Stent length; **L.** Stent numbers. The risk ratio of each study along with a pooled risk ratio with 95% confidence intervals (CI) is depicted. The vertical lines in the middle represent the total combined effect of all the studies, and the left and right vertical lines represent the upper and lower limits of 95% CI of the total combined effect. The corresponding horizontal line for each study represents the combined effect of the remaining studies after deletion of the corresponding study.

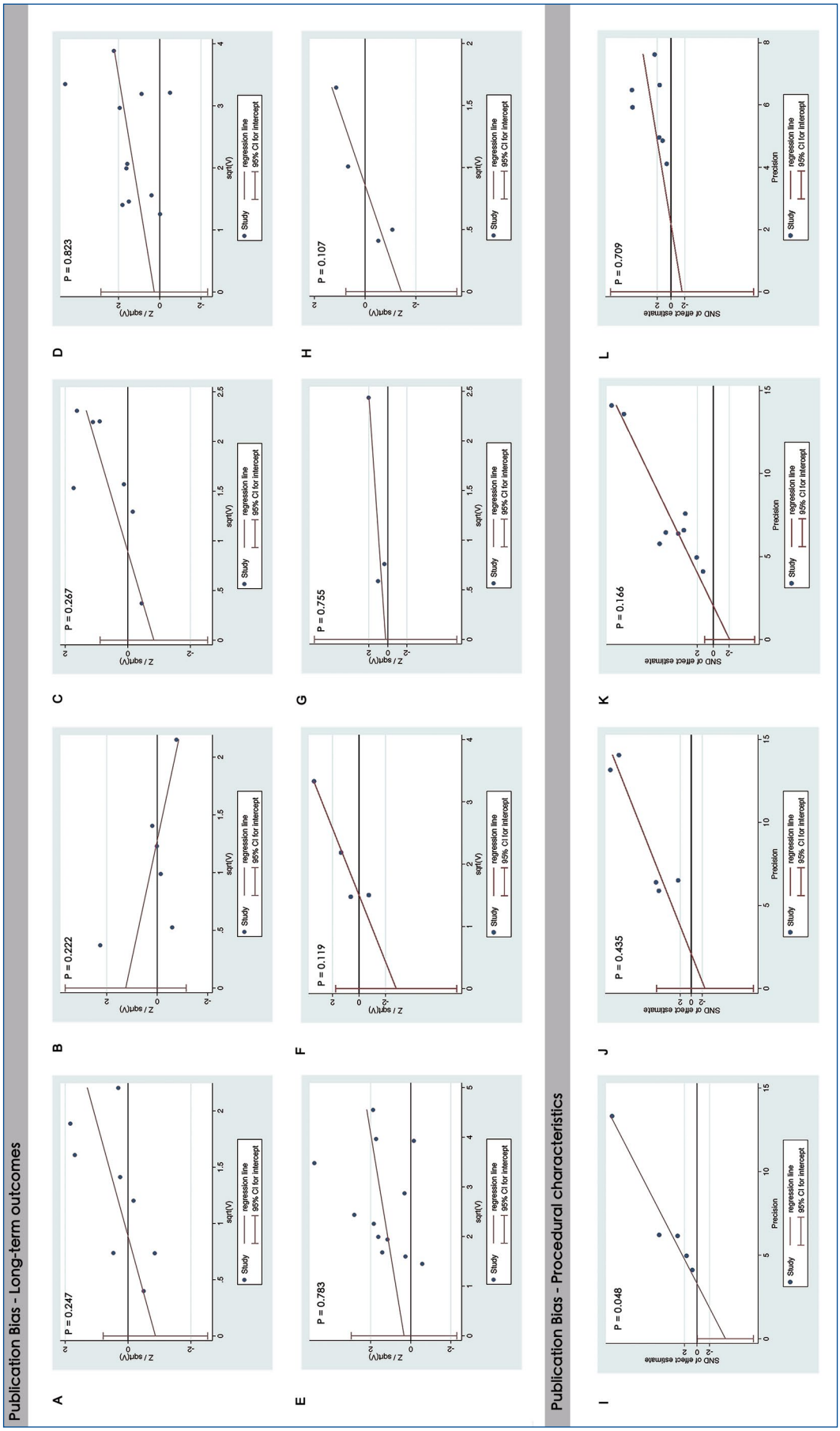

Figure 5. Publication bias plots of included studies. Publication bias of included studies for the following outcomes: **A**. All-cause mortality; **B**. Cardiac mortality; **C**. Myocardial infarction (MI); **D**. Target vessel revascularization (TVR); **E**. Death/MI/TVR; **F**. In-stent restenosis; **G**. In-stent reocclusion; **H**. Stent thrombosis; **I**. Chronic total occlusion (CTO) occlusion length; **J**. J-CTO score; **K**. Stent length; **L**. Stent numbers.

malposition and microaneurysms, stent thrombosis, and re-occlusion [26–28]. Furthermore, the present meta-analysis showed that the overall higher risks of TVR and ISR with DR techniques could also be partially explained by the greater number of stents and longer stent length after subintimal tracking in CTO PCI. The impact of total stent length on long-term clinical outcomes has been reported [29]. In brief, the main reason for the negative clinical impact was not only the subintimal wire tracking itself but also the greater number and longer stent requirement.

It was found in the present meta-analysis that early subintimal DR strategies were associated with a greater risk of adverse events, which were mainly almost two-fold higher rates of TVR and ISR, when compared with WE techniques, during clinical follow-up of 12–24 months. Since the first application of STAR in 2005, continuous improvements have been made including mini-STAR, LAST for antegrade, and the CART technique for retrograde subintimal revascularization [30–33]. These early subintimal techniques pose a higher risk of subintimal hematoma formation and extensive dissection, causing a side-branch vessel occlusion to occur, potentially limiting distal outflow, and predisposing high TVR risk. Thus, this would further result in negative clinical events. Meanwhile, the disappointing clinical outcomes were also due to the unnecessary longer stent lengths, greater numbers of stents, as well as compression of the distal lumen with consequent under sizing of stents. Nevertheless, data regarding the outcomes with modern DR techniques were much more promising, indicating that neither TVR, nor the ISR rates, were increased by modern subintimal strategies, when compared to conventional WE crossing, from the present meta-analysis. Both the "new" ADR and "new" RDR involved proper wiring techniques and available equipment to minimize the subintimal space, potentially lowering the risks for TVR or ISR. In contemporary ADR, the dedicated CrossBoss and Stingray system (Boston Scientific, Natick, MA, USA) has the advantage of creating a safe and controlled antegrade dissection in the subintimal space, and a geographically precise and predictable successful re-entry [34]. In contemporary RDR, the subintimal space within the CTO segment is created by ballooning from antegrade direction (rCART), thereby limiting the length of dissection [35]. As a result, the present data provides evidence that support the application of limited DR techniques in contemporary CTO PCI practice, even as a first-line strategy for DR.

Limitations of the study

There were some limitations in the present study. First, almost all the studies included in the present meta-analysis were observational studies, thereby making these susceptible to the effects of unidentified confounders. Thereby, RCTs should be performed in the future, in order to provide further support for the present results. Second, the intended crossing technique frequently does not frequently reflect the actual guidewire positioning, and this can be detected by IVUS [36, 37]. It has been previously reported that subintimal tracking occurs in approximately 50% of successful PCI cases, when carefully assessed by IVUS [38]. However, IVUS was utilized in only a minority of studies to differentiate the guidewire positioned in either the subintimal, or intimal. Hence, subintimal guidewire tracking is likely more common than expected in CTO-PCI practice, which may have affected the present results.

Conclusions

Dissection and re-entry techniques were applied more in patients with higher complexity CTO lesions and "extensive" DR techniques could increase the incidence of long-term negative clinical events. However, "limited" DR techniques resulted in good long-term outcomes, comparable to WE techniques, supporting the expanding use of more controlled DR techniques in contemporary CTO PCI practice. Further evidence from large RCTs is needed to define the optimal role of DR in hybrid CTO PCI.

Funding

The work was supported by the National Basic Research Program of China (973 Program) (2015CB554404) and the National Natural Science Foundation of China (81570388).

Conflict of interest: None declared

References

1. Tajti P, Karmpaliotis D, Alaswad K, et al. The Hybrid Approach to Chronic Total Occlusion Percutaneous Coronary Intervention: Update From the PROGRESS CTO Registry. JACC Cardiovasc Interv. 2018; 11(14): 1325–1335, doi: 10.1016/j.jcin.2018.02.036, indexed in Pubmed: 29706508.
2. Hall AB, Brilakis ES. Hybrid 2.0: Subintimal plaque modification for facilitation of future success in chronic total occlusion percutaneous coronary intervention. Catheter Cardiovasc Interv. 2019; 93(2): 199–201, doi: 10.1002/ccd.28088, indexed in Pubmed: 30719852.

3. Azzalini L, Carlino M, Brilakis ES, et al. Subadventitial techniques for chronic total occlusion percutaneous coronary intervention: The concept of „vessel architecture". Catheter Cardiovasc Interv. 2018; 91(4): 725–734, doi: 10.1002/ccd.27025, indexed in Pubmed: 28303648.
4. Owen M, Vishal PG, Tesfaldet MT, et al. Long-term outcomes with use of the CrossBoss and stingray coronary CTO crossing and re-entry devices. J Invasive Cardiol. 2013; 25(11): 579–585, indexed in Pubmed: 24184892.
5. Karatasakis A, Danek BA, Karacsonyi J, et al. Mid-term outcomes of chronic total occlusion percutaneous coronary intervention with subadventitial vs. intraplaque crossing: A systematic review and meta-analysis. Int J Cardiol. 2018; 253: 29–34, doi: 10.1016/j.ijcard.2017.08.044, indexed in Pubmed: 29306468.
6. Stang A. Critical evaluation of the Newcastle-Ottawa scale for the assessment of the quality of nonrandomized studies in meta-analyses. Eur J Epidemiol. 2010; 25(9): 603–605, doi: 10.1007/s10654-010-9491-z, indexed in Pubmed: 20652370.
7. Jadad AR, Moore RA, Carroll D, et al. Assessing the quality of reports of randomized clinical trials: is blinding necessary? Control Clin Trials. 1996; 17(1): 1–12, doi: 10.1016/0197-2456(95)00134-4, indexed in Pubmed: 8721797.
8. Ades AE, Lu G, Higgins JPT. The interpretation of random-effects meta-analysis in decision models. Med Decis Making. 2005; 25(6): 646–654, doi: 10.1177/0272989X05282643, indexed in Pubmed: 16282215.
9. DerSimonian R, Laird N. Meta-analysis in clinical trials revisited. Contemp Clin Trials. 2015; 45(Pt A): 139–145, doi: 10.1016/j.cct.2015.09.002, indexed in Pubmed: 26343745.
10. Borenstein M, Higgins JPT. Meta-analysis and subgroups. Prev Sci. 2013; 14(2): 134–143, doi: 10.1007/s11121-013-0377-7, indexed in Pubmed: 23479191.
11. Azzalini L, Dautov R, Brilakis ES, et al. Impact of crossing strategy on midterm outcomes following percutaneous revascularisation of coronary chronic total occlusions. EuroIntervention. 2017; 13(8): 978–985, doi: 10.4244/EIJ-D-16-01010, indexed in Pubmed: 28242587.
12. Harbord RM, Egger M, Sterne JAC. A modified test for small-study effects in meta-analyses of controlled trials with binary endpoints. Stat Med. 2006; 25(20): 3443–3457, doi: 10.1002/sim.2380, indexed in Pubmed: 16345038.
13. Seagroatt V, Stratton I. Bias in meta-analysis detected by a simple, graphical test. Test had 10% false positive rate. BMJ. 1998; 316(7129): 470; author reply 470–470; author reply 471, indexed in Pubmed: 9492688.
14. Finn MT, Doshi D, Cleman J, et al. Intravascular ultrasound analysis of intraplaque versus subintimal tracking in percutaneous intervention for coronary chronic total occlusions: One year outcomes. Catheter Cardiovasc Interv. 2019; 93(6): 1048–1056, doi: 10.1002/ccd.27958, indexed in Pubmed: 30489684.
15. Maeremans J, Avran A, Walsh S, et al. One-Year Clinical Outcomes of the Hybrid CTO Revascularization Strategy After Hospital Discharge: A Subanalysis of the Multicenter RECHARGE Registry. J Invasive Cardiol. 2018; 30(2): 62–70, indexed in Pubmed: 29138365.
16. Sabbah M, Tada T, Kadota K, et al. Clinical and angiographic outcomes of true vs. false lumen stenting of coronary chronic total occlusions: Insights from intravascular ultrasound. Catheter Cardiovasc Interv. 2019; 93(3): E120–E129, doi: 10.1002/ccd.27861, indexed in Pubmed: 30345649.
17. Wilson WM, Walsh SJ, Bagnall A, et al. One-year outcomes after successful chronic total occlusion percutaneous coronary intervention: The impact of dissection re-entry techniques. Catheter Cardiovasc Interv. 2017; 90(5): 703–712, doi: 10.1002/ccd.26980, indexed in Pubmed: 28296045.
18. Hasegawa K, Tsuchikane E, Okamura A, et al. Incidence and impact on midterm outcome of intimal versus subintimal tracking with both antegrade and retrograde approaches in patients with successful recanalisation of chronic total occlusions: J-PROCTOR 2 study. EuroIntervention. 2017; 12(15): e1868–e1873, doi: 10.4244/EIJ-D-16-00557, indexed in Pubmed: 27802928.
19. Muramatsu T, Tsuchikane E, Oikawa Y, et al. Incidence and impact on midterm outcome of controlled subintimal tracking in patients with successful recanalisation of chronic total occlusions: J-PROCTOR registry. EuroIntervention. 2014; 10(6): 681–688, doi: 10.4244/EIJV10I6A119, indexed in Pubmed: 25330501.
20. Rinfret S, Ribeiro HB, Nguyen CM, et al. Dissection and re-entry techniques and longer-term outcomes following successful percutaneous coronary intervention of chronic total occlusion. Am J Cardiol. 2014; 114(9): 1354–1360, doi: 10.1016/j.amjcard.2014.07.067, indexed in Pubmed: 25242364.
21. Amsavelu S, Christakopoulos GE, Karatasakis A, et al. Impact of crossing strategy on intermediate-term outcomes after chronic total occlusion percutaneous coronary intervention. Can J Cardiol. 2016; 32(10): 1239.e1–1239.e7, doi: 10.1016/j.cjca.2016.01.020, indexed in Pubmed: 27006316.
22. Godino C, Latib A, Economou FI, et al. Coronary chronic total occlusions: mid-term comparison of clinical outcome following the use of the guided-STAR technique and conventional anterograde approaches. Catheter Cardiovasc Interv. 2012; 79(1): 20–27, doi: 10.1002/ccd.23058, indexed in Pubmed: 21805559.
23. Valenti R, Vergara R, Migliorini A, et al. Predictors of Reocclusion After Successful Drug-Eluting Stent–Supported Percutaneous Coronary Intervention of Chronic Total Occlusion. J Am Coll Cardiol. 2013; 61(5): 545–550, doi: 10.1016/j.jacc.2012.10.036.
24. Tanaka H, Hosogi S, Fuku Y, et al. TCT-208: Angiographic and Clinical Outcomes of Retrograde Recanalization for Chronic Total Occlusions. J Am Coll Cardiol. 2010; 56(13): B48, doi: 10.1016/j.jacc.2010.08.232.
25. Brilakis ES, Grantham JA, Rinfret S, et al. A percutaneous treatment algorithm for crossing coronary chronic total occlusions. JACC Cardiovasc Interv. 2012; 5(4): 367–379, doi: 10.1016/j.jcin.2012.02.006, indexed in Pubmed: 22516392.
26. Erlich I, Strauss BH, Butany J. Stent thrombosis following the STAR technique in a complex RCA chronic total occlusion. Catheter Cardiovasc Interv. 2006; 68(5): 708–712, doi: 10.1002/ccd.20820, indexed in Pubmed: 17039512.
27. Valenti R, Vergara R, Migliorini A, et al. Predictors of reocclusion after successful drug-eluting stent-supported percutaneous coronary intervention of chronic total occlusion. J Am Coll Cardiol. 2013; 61(5): 545–550, doi: 10.1016/j.jacc.2012.10.036, indexed in Pubmed: 23273395.
28. Tsujita K, Maehara A, Mintz GS, et al. Cross-sectional and longitudinal positive remodeling after subintimal drug-eluting stent implantation: multiple late coronary aneurysms, stent fractures, and a newly formed stent gap between previously overlapped stents. JACC Cardiovasc Interv. 2009; 2(2): 156–158, doi: 10.1016/j.jcin.2008.11.008, indexed in Pubmed: 19463419.
29. Hiromasa T, Kuramitsu S, Shinozaki T, et al. Impact of total stent length after cobalt chromium everolimus-eluting stent

implantation on 3-year clinical outcomes. Catheter Cardiovasc Interv. 2017; 89(2): 207–216, doi: 10.1002/ccd.26455, indexed in Pubmed: 26910036.

30. Colombo A, Mikhail GW, Michev I, et al. Treating chronic total occlusions using subintimal tracking and reentry: the STAR technique. Catheter Cardiovasc Interv. 2005; 64(4): 407–11; discussion 412, doi: 10.1002/ccd.20307, indexed in Pubmed: 15789384.
31. Galassi AR, Tomasello SD, Costanzo L, et al. Mini-STAR as bail-out strategy for percutaneous coronary intervention of chronic total occlusion. Catheter Cardiovasc Interv. 2012; 79(1): 30–40, doi: 10.1002/ccd.22998, indexed in Pubmed: 21956876.
32. Michael TT, Mogabgab O, Alomar M, et al. Long-term outcomes of successful chronic total occlusion percutaneous coronary interventions using the antegrade and retrograde approach. J Interv Cardiol. 2014; 27(5): 465–471, doi: 10.1111/joic.12149, indexed in Pubmed: 25158049.
33. Kimura M, Katoh O, Tsuchikane E, et al. The efficacy of a bilateral approach for treating lesions with chronic total occlusions the CART (controlled antegrade and retrograde subintimal tracking) registry. JACC Cardiovasc Interv. 2009; 2(11): 1135–1141, doi: 10.1016/j.jcin.2009.09.008, indexed in Pubmed: 19926057.
34. Whitlow PL, Burke MN, Lombardi WL, et al. Use of a novel crossing and re-entry system in coronary chronic total occlusions that have failed standard crossing techniques: results of the FAST-CTOs (Facilitated Antegrade Steering Technique in Chronic Total Occlusions) trial. JACC Cardiovasc Interv. 2012; 5(4): 393–401, doi: 10.1016/j.jcin.2012.01.014, indexed in Pubmed: 22516395.
35. Tsuchikane E, Katoh O, Kimura M, et al. The first clinical experience with a novel catheter for collateral channel tracking in retrograde approach for chronic coronary total occlusions. JACC Cardiovasc Interv. 2010; 3(2): 165–171, doi: 10.1016/j.jcin.2009.10.026, indexed in Pubmed: 20170873.
36. Rathore S, Terashima M, Suzuki T. Value of intravascular ultrasound in the management of coronary chronic total occlusions. Catheter Cardiovasc Interv. 2009; 74(6): 873–878, doi: 10.1002/ccd.22065, indexed in Pubmed: 19434743.
37. Muhammad KI, Lombardi WL, Christofferson R, et al. Subintimal guidewire tracking during successful percutaneous therapy for chronic coronary total occlusions: insights from an intravascular ultrasound analysis. Catheter Cardiovasc Interv. 2012; 79(1): 43–48, doi: 10.1002/ccd.23139, indexed in Pubmed: 21542105.
38. Song L, Maehara A, Finn MT, et al. Intravascular ultrasound analysis of intraplaque versus subintimal tracking in percutaneous intervention for coronary chronic total occlusions and association with procedural outcomes. JACC Cardiovasc Interv. 2017; 10(10): 1011–1021, doi: 10.1016/j.jcin.2017.02.043, indexed in Pubmed: 28521919.

VIA MEDICA

ORIGINAL ARTICLE

Cardiology Journal
2021, Vol. 28, No. 3, 384–390
DOI: 10.5603/CJ.a2019.0019

ISSN 1897–5593
eISSN 1898–018X

Transfermoral aortic valve implantation using self-expanding New Valve Technology (NVT) Allegra bioprosthesis: A pilot prospective study

Dariusz Jagielak[1], Aleksandra Stanska[1], Andrzej Klapkowski[1], Maciej Brzezinski[1], Maciej Kowalik[1], Dariusz Ciecwierz[2], Milosz Jaguszewski[2], Marcin Fijalkowski[2]

[1]Department of Cardiac and Vascular Surgery, Medical University of Gdansk, Poland
[2]1st Department of Cardiology, Medical University of Gdansk, Poland

This paper was guest edited by Prof. Wojciech Wojakowski

Abstract

Background: *Transcatheter aortic valve implantation (TAVI) has become a standard therapeutic option for patients with severe aortic stenosis (AS) at high cardiac surgical risk. The aim of the NAUTILUS study was to investigate the safety and performance of the New Valve Technology (NVT) Allegra bioprosthesis in high-risk patients undergoing TAVI.*

Methods: *Twenty seven patients with severe, symptomatic AS at high surgical risk were prospectively enrolled, who underwent treatment using the novel self-expanding NVT Allegra bioprosthesis via transfemoral approach (TF-TAVI). The primary end-point was all-cause mortality at 30 days.*

Results: *Patients were elderly (83 years, range 75–89 years), and predominantly female (70.4%, n = 19). All patients were deemed to be at high surgical risk, with a mean logistic EuroSCORE of 12.4% (range, 2.8–31.8%). The bioprosthesis was successfully implanted in 96% of the cases (n = 25). The echocardiographic assessment confirmed good hemodynamic profile after implantation of the NVT Allegra bioprosthesis. Complications included cardiac tamponade (4%, n = 1) and the need for permanent pacemaker implantation (8%, n = 2). The analysis of procedural aspects showed a short learning effect related to the precise placement of the valve. A significant improvement in clinical symptoms were observed, and no patients died in-hospital or within 30 days of post-discharge observation.*

Conclusions: *This prospective observation shows that the NVT Allegra bioprosthesis was associated with a satisfactory safety profile and a remarkable hemodynamic performance after implantation.* (Cardiol J 2021; 28, 3: 384–390)

Key words: aortic stenosis, clinical trial, elderly population, transcatheter aortic valve implantation

Introduction

Transcatheter aortic valve implantation (TAVI) has evolved from a challenging and hazardous procedure to a minimally invasive, safe, and predictable treatment strategy. It has become a standard treatment for intermediate and high-risk patients with severe aortic stenosis (AS) [1]. Since 2002, when the first TAVI was performed [2], a large number of studies have proven its clinical utility and low rates of procedure-related complications [3]. Currently, in some countries, the annual rate of TAVIs surpassed the surgical replacement procedure [4]. Even though there are many Conformité Européenne (CE) marked devices available, there is still a strong need for further technological improvement and new valve design. In spite of the procedural success, undesirable, adverse events related to the TAVI procedure or TAVI system are still reported in up to 4% of cases [5–10]. Im-

Address for correspondence: Dariusz Jagielak, MD, PhD, Department of Cardiac and Vascular Surgery, ul. Dębinki 7, 80–241 Gdańsk, Poland, tel: +48 509487577, e-mail: darjag@gumed.edu.pl

Received: 25.07.2018 Accepted: 23.01.2019

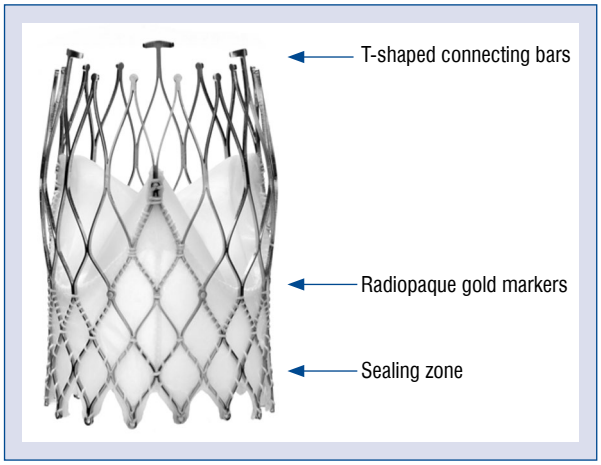

Figure 1. Design of the Allegra valve.

provement of technology may have the potential to minimize the complication rate [11].

The New Valve Technology (NVT) Allegra system is a novel self-expanding TAVI device designed to overcome some limitations of the first-generation systems, including malpositioning, paravalvular leakage (PVL), hemodynamic compromise, and necessity for pacemaker implantation. The valve is implanted in a three-step deployment process that ensures accurate final positioning (Fig. 1). The first-in-human experience showed a high rate of procedural success, satisfactory hemodynamic results, and clinical symptom improvement [12].

The purpose of this study was to assess the safety and performance of the novel NVT Allegra self-expanding aortic prosthesis using a transfemoral approach. The study provides 30-day outcomes in a high-risk patient setting, treated in a well-experienced TAVI center.

Methods

Study overview and patient population

NAUTILUS (NVT trAnsfemoral mUlticentric aorTIc valve pivotaL stUdy for Safety and effectiveness) was a single-arm clinical study conducted at 8 centers in 3 countries (Switzerland, Poland, and Brazil), designed to assess the safety and performance of the NVT Allegra TAVI System (NVT, GmbH, Hechingen, Germany).

Herein, is presented the largest single-center experience with the novel NVT Allegra system implanted in 26 patients accepted by the Heart Team to undergo transfemoral transcatheter aortic valve implantation (TF-TAVI). All patients suffered from severe, symptomatic AS and met the NAUTILUS eligibility criteria. The main inclusion criteria were: 1) age ≥ 75 years; 2) symptomatic (New York Heart Association [NYHA] class II or greater) severe degenerative native AS (mean transvalvular pressure gradient > 40 mmHg and/or aortic jet velocity > 4.0 m/s and/or aortic valve area of < 1.0 cm^2 [or aortic valve area index ≤ 0.6 cm^2/m^2]); 3) high risk for surgical aortic valve replacement with a logistic EuroSCORE ≥ 20%, or documented agreement of the Heart Team that the patient is at high risk for surgery due to frailty and/or coexisting comorbidities.

Amongst others, the protocol defined exclusion criteria comprised: 1) unicuspid or bicuspid valve disease; 2) non-calcified aortic valve disease; 3) mixed valve disease with predominant aortic regurgitation greater than 3+ or with associated severe (greater than 3+) mitral regurgitation; 4) aortic annulus size < 19 mm or > 29 mm; 5) type of femoral access, or any other anatomical conditions that prevented safe placement of an 18 French introducer sheath and manipulation of the TAVI system (e.g. severe femoral-iliac obstructive calcification or tortuosity) [13].

All patients were followed-up for 30 days. Written informed consent was obtained from each participant. The study was approved by the local ethics committee and the competent authority.

NVT Allegra system and the TAVI implantation protocol

The NVT Allegra transcatheter heart valve (Fig. 1) is a self-expanding device, designed to avoid hemodynamic compromise and to facilitate correct positioning during the subsequent steps of implantation. The valve consists of a nitinol stent frame and bovine pericardium (annular skirt and leaflets). The stent frame has a closed cell, diamond-shaped configuration. The variable cell size distribution allows for better coronary perfusion and easier access for any further percutaneous coronary interventions. Six radiopaque gold markers are incorporated into the stent frame. They indicate the distal part of the semilunar valve to facilitate correct valve positioning. The 12-mm bovine pericardial sealing skirt reduces the risk of significant PVL. The NVT Allegra valve is available in 3 sizes (23, 27 and 31 mm), with a frame height of 37.3, 41.3, and 43.0 mm, respectively, (Table 1) covering aortic annulus diameter sizes from 19 to 29 mm.

The delivery system has an 18 French cartridge and a 15 French catheter shaft. The grip uses a Squeeze-to-Release® mechanism, which prevents rotation during a stepwisely performed implanta-

Table 1. Specifications of New Valve Technology (NVT) Allegra transcatheter valve.

	NVT 23	NVT 27	NVT 31
Frame height [mm]	37.3	41.3	43.0
Inflow diameter [mm]	23.8	27.4	31.0
Outflow diameter [mm]	20.8	24.0	24.0
Tissue annulus diameter [mm]	19–22	22–25	25–29

tion. The prosthesis is released in a three-step deployment mechanism. The novel implantation technology (PermaFlow®; New Valve Technology) facilitates positioning of the Allegra valve and prevents interference with the left ventricular outflow tract. In the first step of the implantation, the middle part of the valve is released, while both ends of the device are still captured (Fig. 2). During the second step, the bottom of the valve is released (Fig. 3). The operator can assess valve position, patency of the coronaries, hemodynamic functions, and paravalvular regurgitation. The process can be re-started till this step, and the valve can thus be retrieved. In the third step, when the operator confirms the position of the prosthesis, the safety locker is released for final deployment of the NVT Allegra valve.

All procedures were performed via the open transfemoral approach for TAVI (TF-TAVI) under local or general anaesthesia. According to the protocol, pre-dilatation before valve implantation was mandatory.

Data management and statistical analysis

The data for the clinical trial was collected prospectively during hospitalization (baseline and discharge) and after 30 days in an outpatient setting by using a dedicated electronic case report form. Each patient underwent transthoracic echocardiography assessment at least three times — before the implantation, after the procedure and/or at discharge and after 1 month. Hemodynamic prosthesis performance assessment estimation included maximal velocity, mean pressure gradient, effective orifice area, and presence and grade of PVL. Results were presented as numbers of patients (percentages) or means, where applicable. Statistical analysis was performed using STATISTICA 12.0 PL (StatSoft, Krakow, Poland).

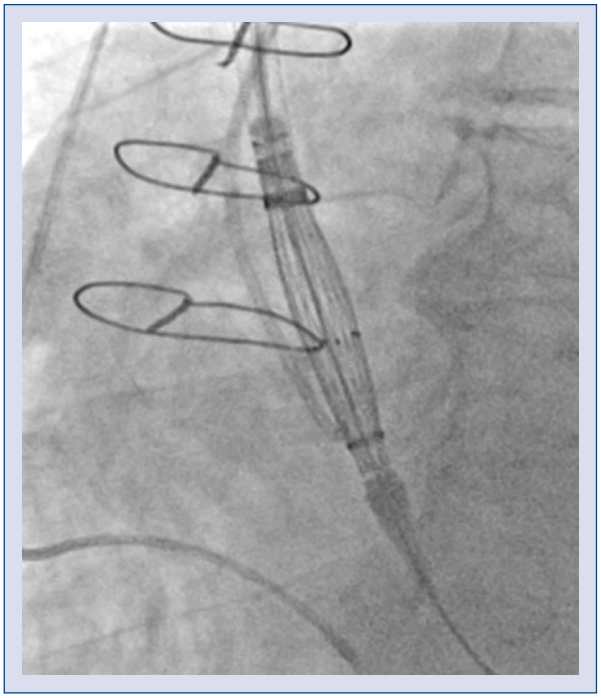

Figure 2. The Allegra valve positioning.

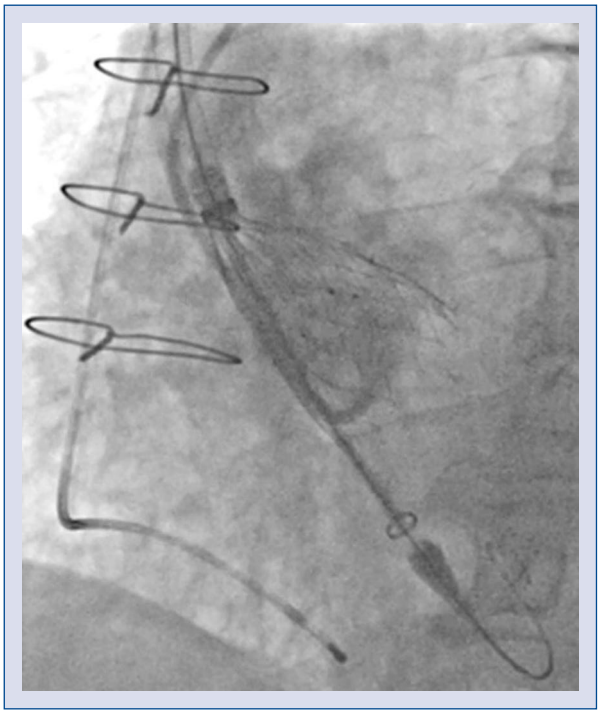

Figure 3. Releasing of the bottom of the valve.

Results

Twenty-seven patients were considered eligible for the treatment and signed the informed consent. One patient underwent isolated balloon valvuloplasty of the native aortic valve due to unexpected anatomical conditions; massive, bulky asymmetric calcification. Therefore, 26 patients

underwent attempted implantation of the NVT Allegra valve.

The patient population was elderly with a mean age of 83 years (range, 75–89 years), 70.4% were female, and the mean logistic EuroSCORE was 12.4% (range, 2.8–31.8%). Patient characteristics and parameters at baseline are presented in Table 2.

The implantation of a single functioning NVT bioprosthesis in the correct annular position was successfully completed in 25 patients. Due to the dislocation of the prosthesis into the left ventricle, 1 patient required open-heart aortic valve replacement. Flow chart of the study is presented (Fig. 4). The dislocation of the valve was caused by the combination of a relatively low degree of calcification of the annulus, and disconnection of the prosthesis from the delivery system.

Most events were considered as expected and documented in the case report form (Table 3). Two patients could not attend the clinic for a follow-up visit at 30 days and clinical data were collected by the phone. No patient died within the period of 30 days (Table 4).

The echocardiographic assessment immediately after valve implantation and before discharge showed excellent hemodynamic performance, which was maintained at 30 days (Table 5). At 30 days, the majority (84%) had only mild or less residual aortic regurgitation, while 16% moderate and 0% severe aortic regurgitation was noted (Table 6).

Table 2. Preoperative characteristics and parameters (n = 27).

Age [years]	83 (75–89)
Gender:	
Male	8 (29.6%)
Female	19 (70.4%)
Logistic EuroSCORE [%]	12.4 (2.8–31.8)
Hypertension	22 (81.5%)
Diabetes mellitus	14 (51.8%)
COPD	5 (18.5%)
Coronary artery stenosis (> 50%)	2 (7.4%)
Previous myocardial infarction	7 (25.9%)
Previous coronary surgery	4 (14.8%)
Previous coronary angioplasty	12 (44.4%)
Previous stroke or TIA	1 (3.7%)
Creatinine clearance (< 60 mL/min)	7 (25.9%)
NYHA:	
I	–
II	3 (11.1%)
III	23 (85.2%)
IV	1 (3.7%)
Conduction disorders (LBBB, RBBB, AVB)	2 (7.4%)
Pre-existing permanent pacemaker	3 (11.1%)
Aortic valve insufficiency (≥ mild)	11 (40.7%)
Mitral valve insufficiency (≥ mild)	18 (66.7%)

AVB — atrio-ventricular block; COPD — chronic obstructive pulmonary disease; LBBB — left bundle branch block; NYHA — New York Heart Association functional class; RBBB — right bundle branch block; TIA — transient ischemic attack

Discussion

This is the largest single-center study of the novel transcatheter self-expanding NVT Allegra bioprosthesis transfemoral system. The main purpose of the NAUTILUS study was to assess safety and performance of the NVT Allegra valve. The new valve had a favorable post-deployment hemodynamic profile, with low post-procedural transvalvular gradients. No cardiac death or cerebrovascular incidents, as well as a very low permanent pacemaker implantation rate was recorded at 30 days. These results suggest that the novel valve has a good safety and efficacy profile and could be used in patients with severe symptomatic AS.

Given the dynamic development of the procedure and different product refinements, the field of transcatheter heart valve systems is currently highly competitive, with a wide spectrum of various CE-marked devices. However, TAVI is still associated with a risk of severe complications,

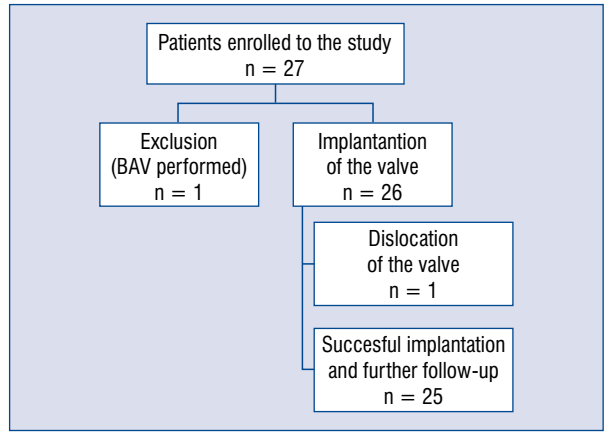

Figure 4. Flow chart of the study; BAV — balloon aortic valvuloplasty.

which may occur in up to 5% of procedures [1]. The contemporary TAVI system design should provide easy positioning, and an option to retrieve

Table 3. Procedural characteristics (n = 27).

Procedural success (one prosthesis implanted)	25 (92.6%)
Failed study valve implantation:	2 (7.4%)
Valve-in-valve	0 (0%)
Conversion to other TAVI	0 (0%)
Conversion to surgical AVR	1 (3.7%)
Unexpected anatomical conditions	1 (3.7%)
Attempted valve retrieval:	
Successful retrieval	2 (7.4%)
Failed retrieval	0 (0%)
Fluoroscopy time [min]	17.6 (7–60)
Volume of contrast [mL]	107 (60–290)
Valve size (n = 27):	
23 mm	0 (0%)
27 mm	15 (55.6%)
31 mm	11 (40.7%)
Need for post-dilatation	0 (0%)

AVR — aortic valve replacement; TAVI — transcatheter aortic valve implantation

Table 4. Prevalence of clinical outcomes and adverse events (n = 25).

All-cause mortality	0 (0%)
Permanent pacemaker implantation due to atrio-ventricular block	2 (8%)
Sepsis	1 (4%)
Any stroke	0 (0%)
Pericardium drainage due to late cardiac tamponade	1 (4%)
Renal failure	0 (0%)
Respiratory failure	1 (4%)
Major vascular complication	0 (0%)
Minor vascular complication	0 (0%)
Acute myocardial infarction	0 (0%)
Minor bleeding (sheath failure)	1 (4%)

the device when the position of the valve is compromised. A reduced rate of complications related to the malposition of the prosthesis such as PVL, pacemaker implantation or overlie of coronary ostia is essential for improving long-term results.

In this study, a high rate of procedural success was demonstrated with the Allegra NVT bioprosthesis (96%). One of the greatest advantages of this new system is the ability to reposition and retrieve the device in cases of malposition or a suboptimal result. In the present cohort, the device had to be retrieved in 2 patients. The retrieving maneuvers and second deployment were easily controlled without complications. The Allegra system has features allowing for very precise positioning. The presence of radiopaque markers in the delivery system as well as at the transition between the annular skirt and the bottom of the leaflets, markedly facilitates the procedure by enabling direct and clear visualization of the optimal implantation height and limits of the sealing skirt.

The overall risk of permanent atrio-ventricular conduction disturbances following TAVI procedures varies, but remains around 17% [14]. In comparison to balloon expandable valves, the self-expandable (nitinol-based) TAVI valve prostheses have a slightly higher rate of postprocedural atrio-ventricular conduction block, requiring pacemaker implantation (28%) [15, 16]. In this study, only 8% of patients required pacemaker implantation, and incomparison to other self-expandable valve prostheses, this is a very promising result. This may be related to a high valve implantation facilitated by refined deployment technology and valve design.

Table 6. The prevalence of paravalvular leakage (PVL) on discharge day and 30-days follow-up (FU).

PVL	Discharge (n = 25)	30-days FU (n = 23)
None	3 (12%)	3 (13%)
Mild	18 (72%)	16 (69.6%)
Moderate	4 (16%)	4 (17,4%)
Severe	0 (0%)	0 (0%)

Table 5. Echocardiographic aortic valve function from baseline until 30 days of patients successfully treated with the study prosthesis.

	Baseline (n = 27)	Discharge (n = 25)	30-days (n = 23)
Peak gradient [mmHg]	87 (58–138)	16.9 (8–42)	15.9 (8–27)
Mean gradient [mmHg]	56.8 (35–91)	9.4 (4–21)	9 (4–16)
Peak aortic velocity [m/s]	4.6 (4–6)	2 (1–3)	2 (1–3)
Effective orifice area [cm^2]	0.63 (0–1)	1.4 (1–2)	1.5 (1–2)

The releasing mechanism of the Allegra allows for a stable and stepwise delivery of the valve, which starts to function early in the deployment process, preventing hemodynamic collapse.

Despite the supra-annular design, the Allegra valve has a reduced frame height to facilitate manipulation and deployment. Short TAVI systems with supra-annular construction are advantageous for the percutaneous treatment of degenerated surgical bioprostheses [11, 12]. However, patients with non-native aortic valve stenosis were excluded from the study.

The durability of transcatheter aortic valve bioprostheses still remains unknown. The first TAVI procedures were performed in the early 2000s, and the age and clinical profile of that early group of patients make a clear evaluation of TAVI durability very difficult. Patients with either serious co-morbidities and/or are elderly have restricted prediction of life expectancy. Transferring TAVI to lower-risk, younger patients with longer life expectancy increases the requirements regarding freedom from structural valve deterioration. Randomized trials in this group of patients are already under way [13]. The novel Allegra system tested in the present study incorporates a feature that aims to improve a long-term bioprosthesis functional life. The upper portion of its nitinol frame, to which the commissures of the valve leaflets are attached, has increased compliance and is able to partially flex, accommodating the forces generated across the cardiac cycle, reducing the mechanical stress on the leaflets. Reduction of the stress on the biological part of the valve (i.e. pericardial leaflets) would result in enhanced valve durability. Obviously, such an effect cannot be evaluated in the 30-day results presented in the current study and requires longer observation periods.

Moderate-aortic regurgitation occurred in 16% of patients at 30 days, which is proportional to other self-expandable-valve-studies [4]. Moreover, it is noteworthy that there was no severe PVL in the present setting. Altogether, it is not possible to rule out whether these events are inherent to valve design or complications that can be minimized as experience with the prosthesis grows and the learning curve levels out. Nevertheless, the results presented are promising, particularly when compared to other TAVI devices in similar clinical scenarios.

Stroke and other cerebrovascular events (CVE) remain common complications following TAVI, ranging between 1.5% and 4% [17–19]. The incidence of CVEs is highly related to a higher mortality rate and longer hospital stay [19, 20]. In the current subset, not a single procedure was complicated with cerebrovascular incidents in the 30-day follow-up period. Compared to other studies, this is an outstanding result, confirming safety of the procedure and prosthesis itself. It requires further observation, nevertheless, the first month is usually the most vulnerable period for CVE incidence.

Surgical cut-down was used as vascular access in all cases. There were no vascular complications. The valve has good transition and controllability, but estimation of iliofemoral anatomy is crucial in prevention of vascular events.

The Allegra system is intuitive and easy to use. The learning curve regarding the precision of placement of the device is short.

Limitations of the study

The present study has some important shortcomings. It is a single-arm study of relatively small sample size, which *per se* precludes any in-depth comparison against a control group or detailed analyses related to uncommonly-occurring events. Furthermore, the evaluation was focused on the short-term safety and effectiveness, and no inferences can be drawn regarding long-term outcomes after implantation of the device.

Conclusions

This prospective study shows a satisfactory safety and performance profile of NVT Allegra bioprosthesis. This novel valve prosthesis has an excellent hemodynamic performance and low rate of pacemaker implantations. The analysis of procedural aspects showed a favorable learning curve related to precision of placement of the prosthesis.

References

1. Aldalati O, MacCarthy P, Dworakowski R. Trans-catheter aortic valve implantation: Contemporary practice and the future. Cardiol J. 2017; 24(2): 206–215, doi: 10.5603/CJ.a2017.0022, indexed in Pubmed: 28248406.
2. Cribier A, Eltchaninoff H, Bash A, et al. Percutaneous transcatheter implantation of an aortic valve prosthesis for calcific aortic stenosis: first human case description. Circulation. 2002; 106(24): 3006–3008, indexed in Pubmed: 12473543.
3. Giordana F, D'Ascenzo F, Nijhoff F, et al. Meta-analysis of predictors of all-cause mortality after transcatheter aortic valve implantation. Am J Cardiol. 2014; 114(9): 1447–1455, doi: 10.1016/j.amjcard.2014.07.081, indexed in Pubmed: 25217456.
4. Eggebrecht H, Mehta RH. Transcatheter aortic valve implantation (TAVI) in Germany 2008-2014: on its way to standard therapy for aortic valve stenosis in the elderly? EuroIntervention. 2016; 11(9): 1029–1033, doi: 10.4244/EIJY15M09_11, indexed in Pubmed: 26384006.

5. Urena M, Webb JG, Eltchaninoff H, et al. Late cardiac death in patients undergoing transcatheter aortic valve replacement: incidence and predictors of advanced heart failure and sudden cardiac death. J Am Coll Cardiol. 2015; 65(5): 437–448, doi: 10.1016/j.jacc.2014.11.027, indexed in Pubmed: 25660921.
6. Ribeiro HB, Nombela-Franco L, Muñoz-García AJ, et al. Predictors and impact of myocardial injury after transcatheter aortic valve replacement: a multicenter registry. J Am Coll Cardiol. 2015; 66(19): 2075–2088, doi: 10.1016/j.jacc.2015.08.881, indexed in Pubmed: 26541917.
7. Gensas CS, Caixeta A, Siqueira D, et al. Predictors of permanent pacemaker requirement after transcatheter aortic valve implantation: insights from a Brazilian registry. Int J Cardiol. 2014; 175(2): 248–252, doi: 10.1016/j.ijcard.2014.05.020, indexed in Pubmed: 24880480.
8. Wenaweser P, Stortecky S, Heg D, et al. Short-term clinical outcomes among patients undergoing transcatheter aortic valve implantation in Switzerland: the Swiss TAVI registry. EuroIntervention. 2014; 10(8): 982–989, doi: 10.4244/EIJV10I8A166, indexed in Pubmed: 24694729.
9. Ribeiro HB, Webb JG, Makkar RR, et al. Predictive factors, management, and clinical outcomes of coronary obstruction following transcatheter aortic valve implantation: insights from a large multicenter registry. J Am Coll Cardiol. 2013; 62(17): 1552–1562, doi: 10.1016/j.jacc.2013.07.040, indexed in Pubmed: 23954337.
10. Athappan G, Patvardhan E, Tuzcu EM, et al. Incidence, predictors, and outcomes of aortic regurgitation after transcatheter aortic valve replacement: meta-analysis and systematic review of literature. J Am Coll Cardiol. 2013; 61(15): 1585–1595, doi: 10.1016/j.jacc.2013.01.047, indexed in Pubmed: 23500308.
11. Tchetche D, Van Mieghem NM. New-generation TAVI devices: description and specifications. EuroIntervention. 2014; 10 Suppl U: U90–U9U100, doi: 10.4244/EIJV10SUA13, indexed in Pubmed: 25256338.
12. Wenaweser P, Stortecky S, Schütz T, et al. Transcatheter aortic valve implantation with the NVT Allegra transcatheter heart valve system: first-in-human experience with a novel self-expanding transcatheter heart valve. EuroIntervention. 2016; 12(1): 71–77, doi: 10.4244/EIJV12I1A13, indexed in Pubmed: 27173865.
13. Leon MB, Piazza N, Nikolsky E, et al. Standardized endpoint definitions for Transcatheter Aortic Valve Implantation clinical trials: a consensus report from the Valve Academic Research Consortium. J Am Coll Cardiol. 2011; 57(3): 253–269, doi: 10.1016/j.jacc.2010.12.005, indexed in Pubmed: 21216553.
14. Siontis GCM, Jüni P, Pilgrim T, et al. Predictors of permanent pacemaker implantation in patients with severe aortic stenosis undergoing TAVR: a meta-analysis. J Am Coll Cardiol. 2014; 64(2): 129–140, doi: 10.1016/j.jacc.2014.04.033, indexed in Pubmed: 25011716.
15. Hayashida K, Morice MC, Chevalier B, et al. Sex-related differences in clinical presentation and outcome of transcatheter aortic valve implantation for severe aortic stenosis. J Am Coll Cardiol. 2012; 59(6): 566–571, doi: 10.1016/j.jacc.2011.10.877, indexed in Pubmed: 22300690.
16. Khawaja MZ, Rajani R, Cook A, et al. Permanent pacemaker insertion after CoreValve transcatheter aortic valve implantation: incidence and contributing factors (the UK CoreValve Collaborative). Circulation. 2011; 123(9): 951–960, doi: 10.1161/CIRCULATIONAHA.109.927152, indexed in Pubmed: 21339482.
17. Eggebrecht H, Schmermund A, Voigtländer T, et al. Risk of stroke after transcatheter aortic valve implantation (TAVI): a meta-analysis of 10,037 published patients. EuroIntervention. 2012; 8(1): 129–138, doi: 10.4244/EIJV8I1A20, indexed in Pubmed: 22391581.
18. Chieffo A, Buchanan GL, Van Mieghem NM, et al. Transcatheter aortic valve implantation with the Edwards SAPIEN versus the Medtronic CoreValve Revalving system devices: a multicenter collaborative study: the PRAGMATIC Plus Initiative (Pooled-RotterdAm-Milano-Toulouse In Collaboration). J Am Coll Cardiol. 2013; 61(8): 830–836, doi: 10.1016/j.jacc.2012.11.050, indexed in Pubmed: 23333140.
19. Tchetche D, Farah B, Misuraca L, et al. Cerebrovascular events post-transcatheter aortic valve replacement in a large cohort of patients: a FRANCE-2 registry substudy. JACC Cardiovasc Interv. 2014; 7(10): 1138–1145, doi: 10.1016/j.jcin.2014.04.018, indexed in Pubmed: 25240554.
20. Stortecky S, Windecker S, Pilgrim T, et al. Cerebrovascular accidents complicating transcatheter aortic valve implantation: frequency, timing and impact on outcomes. EuroIntervention. 2012; 8(1): 62–70, doi: 10.4244/EIJV8I1A11, indexed in Pubmed: 22580250.

VIA MEDICA

ORIGINAL ARTICLE

Cardiology Journal
2021, Vol. 28, No. 3, 391–401
DOI: 10.5603/CJ.a2020.0138

ISSN 1897–5593
eISSN 1898–018X

Iron status, catabolic/anabolic balance, and skeletal muscle performance in men with heart failure with reduced ejection fraction

Michał Tkaczyszyn[1, 2], Marcin Drozd[1, 2], Kinga Węgrzynowska-Teodorczyk[3, 4], Joanna Bojarczuk[4], Jacek Majda[5], Waldemar Banasiak[4], Piotr Ponikowski[2, 6], Ewa A. Jankowska[1, 2]

[1]Laboratory for Applied Research on Cardiovascular System, Department of Heart Diseases, Wroclaw Medical University, Wroclaw, Poland
[2]Department of Heart Diseases, Center for Heart Diseases, University Hospital, Wroclaw, Poland
[3]Faculty of Physiotherapy, University School of Physical Education of Wroclaw, Poland
[4]Cardiology Department, Center for Heart Diseases, Military Hospital, Wroclaw, Poland
[5]Department of Laboratory Diagnostics, Military Hospital, Wroclaw, Poland
[6]Department of Heart Diseases, Wroclaw Medical University, Wroclaw, Poland

Abstract

Background: *Metabolic derangements related to tissue energetics constitute an important pathophysiological feature of heart failure. We investigated whether iron deficiency and catabolic/anabolic imbalance contribute to decreased skeletal muscle performance in men with heart failure with reduced ejection fraction (HFrEF), and whether these pathologies are related to each other.*

Methods: *We comprehensively examined 23 men with stable HFrEF (median age [interquartile range]: 63 [59–66] years; left ventricular ejection fraction: 28 [25–35]%; New York Heart Association class I/II/III: 17/43/39%). We analyzed clinical characteristics, iron status, hormones, strength and fatigability of forearm flexors and quadriceps (surface electromyography), and exercise capacity (6-minute walking test).*

Results: *None of the patients had anemia whereas 8 were iron-deficient. Flexor carpi radialis fatigability correlated with lower reticulocyte hemoglobin content (CHR, $p < 0.05$), and there was a trend towards greater fatigability in patients with higher body mass index and lower serum ferritin (both $p < 0.1$). Flexor carpi ulnaris fatigability correlated with lower serum iron and CHR (both $p < 0.05$). Vastus medialis fatigability was related to lower free and bioavailable testosterone (FT and BT, respectively, both $p < 0.05$), and 6-minute walking test distance was shorter in patients with higher cortisol/FT and cortisol/BT ratio (both $p < 0.05$). Lower ferritin and transferrin saturation correlated with lower percentage of FT and BT. Men with HFrEF and iron deficiency had higher total testosterone, but lower percentage of FT and BT.*

Conclusions: *Iron deficiency correlates with lower bioactive testosterone in men with HFrEF. These two pathologies can both contribute to decreased skeletal muscle performance in such patients.* (Cardiol J 2021; 28, 3: 391–401)

Key words: heart failure, anabolic hormones, iron status, skeletal muscles, exercise capacity

Address for correspondence: Michał Tkaczyszyn, MD, Laboratory for Applied Research on Cardiovascular System, Department of Heart Diseases, Wroclaw Medical University and Department of Heart Diseases, University Hospital, ul. Borowska 213, 50–556 Wrocław, Poland, tel: +48 71 733 11 12, e-mail: michal.tkaczyszyn@umed.wroc.pl

Received: 16.06.2020 Accepted: 13.10.2020

Introduction

Metabolic derangements associated with abnormal energy generation, utilization, and storage, and hormonal disorders promoting and modulating these processes, constitute an important pathophysiological feature of heart failure (HF) [1–7]. Disordered energy metabolism contributes to the progression of myocardial dysfunction and abnormalities seen in other tissues (such us skeletal muscles), and these processes promote each other in the mechanism of a vicious circle [1, 3, 8]. Being closely associated with abnormal tissue energetics, both iron deficiency (ID) and catabolic/anabolic imbalance negatively impact symptoms, exercise capacity, and outcomes in patients with HF [9, 10].

In this study we investigated whether metabolic derangements associated with abnormal mitochondrial energy metabolism, namely ID and catabolic/anabolic imbalance, contribute to decreased skeletal muscle performance in men with HF with reduced ejection fraction (HFrEF). Additionally, we evaluated whether these two pathologies (ID and hormonal abnormalities) are related to each other.

Methods

Patients

We decided to prospectively recruit only male patients due to the significant hormonal differences (influencing the functioning of skeletal muscles) in men and women. Study participants were recruited among male patients of a tertiary referral cardiology department and related outpatient clinic dedicated to HF patients. In all participants we analyzed clinical characteristics and evaluated iron status, anabolic and catabolic hormones, skeletal muscle performance, and sub-maximal exercise capacity. Detailed inclusion and exclusion criteria are presented below.

Inclusion criteria were as follows:

- male sex, age > 18 years;
- left ventricular ejection fraction (LVEF) ≤ 40% as assessed in latest echocardiography;
- an established diagnosis of HF (according to the criteria of the European Society of Cardiology [11]);
- clinical stability with no hospitalizations (either planned or unplanned) within the last 30 days;
- written informed consent for participation in the study.

Exclusion criteria were as follows:

- acute coronary syndrome, coronary revascularization, or major surgery within 90 days preceding the study;
- malignancy (cancer) diagnosed within the previous 5 years;
- cognitive impairment or inability to perform all procedures related to the study;
- current or previous therapy with erythropoiesis-stimulating agents, intravenous iron, or hormonal therapy (except for finasteride administered for benign prostatic hyperplasia);
- muscular, neurological, or orthopedic disorders impairing muscle performance and/or physical fitness.

The protocol was approved by the Bioethics Committee of Wroclaw Medical University, and all subjects gave written informed consent for participation in the study. The study was conducted in accordance with the Helsinki Declaration.

Hematology, iron status, hormonal measurements, and other laboratory tests

In all participants venous blood samples were taken in the morning (8–10 a.m. — important for credible hormonal measurements) following an overnight fast. The majority of laboratory tests were made from fresh venous blood. Some parameters were measured from frozen serum/plasma (after centrifugation the cryotubes were stored at –70°C) after collecting the material for all study participants (at the end of the study). All laboratory tests were performed in one laboratory: the central hospital laboratory of the Military Hospital, Wroclaw, Poland.

Hematological measurements were made in fresh venous blood anticoagulated with ethylene diamine tetra-acetic acid. Hemoglobin concentration, red cell indices, and reticulocytes were measured using the ADVIA 2120 hematology system (Siemens). Anemia was defined according to the World Health Organization (WHO): hemoglobin concentration < 13 g/dL in men [12].

Serum ferritin was measured using an electrochemiluminescence immunoassay (ECLIA) with a Cobas e601 module (Roche Diagnostics). Serum iron and unsaturated iron binding capacity (UIBC) were assessed using the colorimetric method with the Konelab Prime 60i system (Thermo Scientific). Total iron-binding capacity (TIBC) was automatically calculated using serum iron and UIBC. Transferrin saturation (TSAT) was calculated as the ratio of serum iron (μg/dL) and TIBC (μg/dL) multiplied

by 100 and expressed as a percentage. ID was defined (according to HF guidelines) as serum ferritin < 100 μg/L or serum ferritin 100–299 μg/L in combination with TSAT < 20% [11]. Serum soluble transferrin receptor (sTfR, mg/L) was measured using immunonephelometry with the BN II System (Siemens). Additionally, the following parameters obtained from automated blood count (ADVIA 2120 hematology system) were considered indirect indices of iron status: reticulocyte hemoglobin content (CHR, pg) and the percentage of hypochromic red cells (PHRC, %) [9].

The plasma level of N-terminal pro-B type natriuretic peptide (NT-proBNP, pg/mL) was measured using a chemiluminescence immunoassay with the Dimension ExL system (Siemens). The serum level of high-sensitivity C-reactive protein (hs-CRP, mg/L) was assessed using immunonephelometry with the BN II System (Siemens). One missing hs-CRP value was imputed with an available non-hs-CRP value of 5.53 mg/L. The estimated glomerular filtration rate (eGFR, mL/min/1.73 m^2) was calculated using the Modification of Diet in Renal Disease equation [13].

For the assessment of catabolic/anabolic balance the following hormones were measured in morning venous blood: total testosterone (TT, nmol/L), estradiol (pg/mL), insulin-like growth factor-1 (IGF-1, ng/mL), and dehydroepiandrosterone sulfate (DHEAS, μg/dL). Based on albumin and sex hormone-binding globulin (SHBG) concentrations, we used an online calculator (http://www.issam.ch/freetesto.htm) to estimate the fraction of free testosterone (FT, this fraction has the most potent biological activity) and bioavailable testosterone (BT = FT + albumin-bound testosterone; BT fraction is available for peripheral tissues) [10, 14]. FT and BT were expressed in nmol/L and as the percentage of TT pool (%FT and %BT, respectively). We also measured morning cortisol (nmol/L), and the following ratios were calculated to evaluate the catabolic/anabolic balance in examined men with HFrEF: cortisol/TT, cortisol/BT, cortisol/FT, cortisol/IGF-1, and cortisol/DHEAS [5]. TT, estradiol, DHEAS, and SHBG were measured using ECLIA with a Cobas e411 module (Roche Diagnostics), and cortisol was measured with ECLIA using a Cobas e601 module (Roche Diagnostics). IGF-1 was measured using chemiluminescence immunoassay with a Liaison XL analyzer (DiaSorin).

Skeletal muscle strength and fatigability

For the assessment of skeletal muscle performance, we measured handgrip and quadriceps strength, and the fatigability of forearm flexors and the quadriceps. Handgrip strength (N) of a dominant upper extremity was measured using the electronic dynamometer (Noraxon), and after the training the average from three maximal voluntary contractions was used for further analyses. Right leg quadriceps strength was evaluated by measuring quadriceps torque using an armchair with an isometric dynamometer. The torque was measured in a sitting position with 90° flexion of the knee joint. The parameter was calculated for the maximal isometric knee extension maneuver. After the initial training, the measurements were repeated three times and the average value was used in further analyses.

Non-invasive surface electromyography (sEMG) was applied to objectively evaluate muscle fatigability in different muscle regions: forearm flexors (flexor carpi radialis and flexor carpi ulnaris) and quadriceps (vastus lateralis and vastus medialis) [15]. Rectus femoris muscle signal was not analyzed due to the overlapping myoelectric signal from the vastii [16]. For the purposes of current study, we used a four-channel sEMG station MyoTrace 400 (Noraxon) combined with a dedicated electronic handgrip dynamometer (or used with the aforementioned armchair to evaluate the quadriceps). The crude sEMG signal was processed using dedicated research software: MyoResearch XP (Noraxon). Briefly, during a 10-second isometric exercise at 50% of predetermined maximal handgrip/quadriceps contraction, the sEMG was recorded in four predefined regions, and after signal processing the decrease in frequency (of the total power range, Hz) between the first and the last second was calculated as an index of muscle fatigability (greater decrease in frequency indicates more tired muscle). Handgrip and quadriceps contraction curves in N and Nm, respectively, were displayed "live" on a large monitor to help the patient to precisely follow the required 50% of the maximum.

Sub-maximal exercise capacity

Standard 6-minute walking test (6MWT) was performed to assess sub-maximal exercise capacity. Patients were walking at a comfortable (self-set but as brisk as possible) pace along a marked 30 m hospital corridor to cover the longest possible distance during 6 minutes. In case of any significant symptoms (e.g. dyspnea), the patient was allowed to slow down or even stop and rest.

Statistical analyses

Continuous variables were expressed as a median with lower and upper quartile (interquar-

tile range). Categorized variables were expressed as a number and percentage. The intergroup differences between subjects with vs. without ID were tested using the Mann-Whitney U-test for unpaired samples or χ^2 test, where appropriate.

In the first part of the statistical analyses we investigated the relationships between muscle function and metabolic derangements. We calculated Spearman's rank correlation coefficients (r) to establish the relationships between HFrEF symptoms (New York Heart Association [NYHA] class), handgrip strength, quadriceps torque, indices of muscle fatigability, and 6MWT distance and the following: (1) clinical parameters (age, body mass index [BMI], LVEF, key laboratory parameters), (2) hematological parameters, (3) iron parameters, and (4) indices of catabolic/anabolic balance. Further, we calculated Spearman's rank correlation coefficients to investigate the relationships between iron and hormonal parameters.

Hormonal parameters in patients with vs. without concomitant ID as well as 6MWT distance according to NYHA class (I to III), hs-CRP (≥ 2 vs. < 2 mg/L), and cortisol/testosterone ratio (≥ vs. < median) were compared using the Kruskal-Wallis H test.

A p-value of < 0.05 was considered statistically significant. Statistical analyses were performed using STATISTICA 13.3 data analysis software (TIBCO Software).

Results

Baseline characteristics of the examined men with HFrEF

The baseline characteristics of the examined patients according to the presence of ID are presented in Table 1. Although none of patients was anemic according to WHO criteria, 8 patients were iron-deficient. All subjects were taking evidence-based HFrEF pharmacotherapy, and 22 of them had either an implantable cardioverter-defibrillator or cardiac resynchronization therapy.

Metabolic derangements, skeletal muscle performance, and exercise capacity

The relationships between clinical variables, iron status, hormonal parameters, skeletal muscle performance, and exercise capacity are presented in Table 2. In the examined men with HFrEF lower quadriceps strength correlated with higher sTfR and PHRC, but these associations were not valid for handgrip strength. Flexor carpi radialis fatigability was greater in patients with lower CHR, and there was a trend towards greater fatigability in subjects with higher BMI and lower serum ferritin. Analogously, flexor carpi ulnaris fatigability correlated with lower serum iron and lower CHR, and there was a trend towards greater fatigability with decreasing hemoglobin. Vastus medialis fatigability was inversely correlated with FT and BT. 6MWT distance was greater in patients with lower NYHA class as well as in those with lower hs-CRP, cortisol/BT ratio, and cortisol/FT ratio (Fig. 1, Table 2).

Iron status versus catabolic/anabolic balance in men with HFrEF

The associations between iron parameters and measured hormones are presented in Table 3. Serum ferritin was related to %FT, %BT, and estradiol, and TSAT correlated with %FT and %BT (all $p < 0.05$). Indirect measures of ID (PHRC and CHR) were not related to hormonal parameters. Although male patients with ID compared with those without ID had higher TT, both %FT and %BT were significantly lower in iron-deficient subjects (Fig. 2). SHBG was higher in men with HFrEF with vs. without ID (median 72 vs. 46 nmol/L, $p = 0.01$), but these two groups had comparable albumin concentrations ($p = 0.9$).

Discussion

The current study provides additional evidence that metabolic derangements related to disordered tissue energetics, namely ID and catabolic/anabolic imbalance, can contribute to decreased skeletal muscle performance in non-anemic men with stable HFrEF.

The complex and multifaceted skeletal and respiratory myopathy constitutes an important element of HF pathophysiology [17, 18], and muscle dysfunction contributes to the symptomatology of HF [8]. Importantly, the key role in limiting HF patients' sub-maximal and maximal exercise performance is attributed to increased skeletal muscle fatigability, which has already been demonstrated for HF as long as three decades ago [18–23]. There is evidence that early and extensive skeletal muscle fatigue in HF results from intrinsic pathology of this tissue rather than insufficient perfusion, decreased cardiac reserve, or abnormal neural signaling [19, 20, 23, 24]. Although skeletal myopathy constitutes an important pathophysiological feature of HF, the precise mechanisms underlying muscular changes are not fully understood. In our study we have demonstrated that ID and catabolic/

Table 1. Baseline characteristics of examined men (n = 23) with heart failure with reduced ejection fraction (HFrEF) according to the presence of iron deficiency.

Variables	All patients (n = 23)	Iron deficiency (+) (n = 8)	Iron deficiency (–) (n = 15)
Clinical parameters			
Age [years]	63 (59–66)	64 (60–66)	62 (56–65)
Body mass index [kg/m^2]	29.7 (27.2–34.7)	28.7 (25.9–29.7)	32.3 (27.2–35.2)
New York Heart Association class I/II/III	4/10/9 (17/43/39%)	1/3/4 (13/38/50%)	3/7/5 (20/47/33%)
Ischemic heart failure etiology	13 (56%)	5 (63%)	8 (53%)
Left ventricular ejection fraction [%]	28 (25–35)	27 (23–33)	30 (25–37)
High-sensitivity CRP[$] [mg/L]	1.59 (1.01–3.2)	1.43 (1.04–2.09)	1.73 (0.87–3.45)
Plasma NT-proBNP [pg/mL]	**1312 (454–2414)**	**2404 (1141–4764)**	**960 (257–1511)**[b]
eGFR [mL/min/1.73 m^2]	76 (59–93)	74 (57–83)	86 (69–93)
Hematological parameters and indices of iron status			
Hemoglobin [g/dL]	15.6 (14.1–16.1)	15.8 (14.8–16.5)	15.2 (14.1–16.1)
Reticulocytes [%]	7 (6–9)	8 (7–9)	7 (6–9)
Serum iron [μg/dL]	**101 (89–134)**	**93 (69–108)**	**126 (94–141)**[b]
Serum ferritin [μg/L]	**129 (96–336)**	**77 (55–98)**	**288 (129–383)**[d]
Serum soluble transferrin receptor [mg/L]	1.33 (1.09–1.84)	1.55 (1.36–2.05)	1.17 (0.95–1.54)[a]
Transferrin saturation [%]	**28 (20–35)**	**20 (18–28)**	**34 (28–37)**[c]
Reticulocyte hemoglobin content [pg]	33 (32–34)	33 (30–33)	33 (32–34)
Percentage of hypochromic red cells [%]	0.4 (0.2–0.9)	0.8 (0.4–1.6)	0.4 (0.1–0.6)
Hormones			
Total testosterone [nmol/L]	**18 (13–26)**	**26 (20–29)**	**16 (9–19)**[c]
Free testosterone [%]	**1.5 (1.3–1.9)**	**1.3 (1.1–1.4)**	**1.7 (1.5–2.1)**[b]
Bioavailable testosterone [%]	**37 (31–42)**	**32 (24–34)**	**40 (35–49)**[b]
Estradiol [pg/mL]	**24 (18–36)**	**38 (29–46)**	**21 (16–27)**[c]
Insulin-like growth factor 1 [ng/mL]	194 (158–212)	193 (190–207)	196 (157–213)
Dehydroepiandrosterone sulfate [μg/dL]	102 (72–149)	97 (64–211)	139 (72–149)
Cortisol [nmol/L]	388 (317–464)	402 (284–442)	388 (323–482)
Major comorbidities			
Arterial hypertension	15 (65%)	5 (63%)	10 (67%)
Chronic obstructive pulmonary disease	1 (4%)	1 (13%)	0 (0%)
Atrial fibrillation	15 (65)	6 (75%)	9 (60%)
Diabetes or prediabetes	10 (43%)	3 (38%)	7 (47%)
Skeletal muscle strength and sub-maximal exercise capacity			
Handgrip strength [N]	367 (334–399)	368 (337–402)	367 (334–399)
Right quadriceps torque [Nm]	84 (69–91)	87 (67–99)	79 (69–91)
6-minute walking test distance [m]	423 (395–495)	438 (401–520)	415 (385–495)

[$]One missing high-sensitivity (hs) CRP value was imputed with available non-hs-CRP value of 5.53 mg/L. CRP — C-reactive protein; NT-proBNP — N-terminal pro-B-type natriuretic peptide; eGFR — estimated glomerular filtration rate. Data are presented as median (with an interquartile range) or number (with percentage), where appropriate. Handgrip strength was measured for dominant upper extremity. Statistical significance legend for the comparisons between patients with vs. without iron deficiency: [a]$p < 0.1$ (trend), [b]$p < 0.05$, [c]$p < 0.01$, [d]$p < 0.001$. For details — see the 'Methods' section.

/anabolic imbalance can contribute to decreased skeletal muscle performance in men with HFrEF. It should be acknowledged that efficient energy metabolism of skeletal muscle tissue critically depends on the proper regulation of mitochondrial functioning, which is precisely orchestrated by undisturbed iron and hormonal status [25, 26]. Indeed, mammalian skeletal muscles are important

Table 2. The relationships between heart failure symptoms, skeletal muscle performance, sub-maximal exercise capacity, and iron status and catabolic/anabolic balance in men with heart failure with reduced ejection fraction.

Variables, units	NYHA class, 1 class	Handgrip strength[#] [N]	Flexor carpi radialis fatigability[$#] [Hz]	Flexor carpi ulnaris fatigability[$#] [Hz]	Quadriceps torque[#] [Nm]	Vastus lateralis fatigability[$#] [Hz]	Vastus medialis fatigability[$#] [Hz]	Six–minute walking test distance [m]
Clinical parameters								
Age [years]	–	–	–	–	–	–	–	–
Body mass index [kg/m^2]	–	–	0.36[a]	–	–	–	–	–
NYHA class, 1 class	–	–	–	0.38[a]	–	–	–	**–0.65[d]**
Left ventricular ejection fraction [%]	–0.35[a]	–	–	–	–	–	–	–
High-sensitivity CRP[$] [mg/L]	–	–	**–0.45[b]**	–	–	0.40[a]	–	**–0.50[b]**
Plasma NT–proBNP [pg/mL]	–	–	–	–	–	–	–	–
eGFR [mL/min/1.73 m^2]	–	–	–	–	–	–	–	–
Hematological parameters and indices of iron status								
Hemoglobin [g/dL]	–	–	–	–0.37[a]	–	–	–	–
Reticulocytes [%]	–	–	–	–	–	–	–	–
Serum iron [μg/dL]	–0.40[a]	–	–	**–0.47[b]**	–	–	–	–
Serum ferritin [μg/L]	–	–	–0.37[a]	–	–	–	–	–
Serum soluble transferrin receptor [mg/L]	–	–	–	–	**–0.42[b]**	–	–	–
Transferrin saturation [%]	–0.37[a]	–	–	–	–	–	–	–
Reticulocyte hemoglobin content [pg]	–0.39[a]	–	**–0.42[b]**	**–0.62[c]**	–	–	–	–
Percentage of hypochromic red cells [%]	–	–	–	–	**–0.53[b]**	–	–	–
Hormones and indices of catabolic/anabolic balance								
Total testosterone [nmol/L]	–	–	–	–	–	–	–	–
Free testosterone [nmol/L]	–	–	–	–	–	–	**–0.49[b]**	0.38[a]
Free testosterone [%]	–	0.36[a]	–	–	–	–	–	–
Bioavailable testosterone [nmol/L]	–	–	–	–	–	–	**–0.45[b]**	0.36[a]
Bioavailable testosterone [%]	–	–	–	–	–	–	–	–
Estradiol [pg/mL]	–	–	–	–	–	–	–	–
IGF-1 [ng/mL]	**0.43[b]**	–	–	–	–0.37[a]	–	–	–
DHEAS [μg/dL]	–	–	–	–	–	–	–	–
Cortisol [nmol/L]	–	–	–	–	–	–	–	–
Cortisol/IGF-1 ratio [nmol/μg]	–	–	–	–	–	–	–	–
Cortisol/total testosterone ratio	–	–	–	–	–	–	–	–
Cortisol/DHEAS ratio [nmol/10*μg]	–	–	–	–	–	–	–	–
Cortisol/bioavailable testosterone ratio	0.39[a]	–0.36[a]	–	–	–	–	–	**–0.45[b]**
Cortisol/free testosterone ratio	0.38[a]	–	–	–	–	–	–	**–0.44[b]**

Data are presented as Spearman's rank correlation coefficients (coefficients with p-value of > 0.1 are not presented). Statistical significance legend: [a]p < 0.1 (trend), [b]p < 0.05, [c]p < 0.01, [d]p < 0.001. NYHA — New York Heart Association; CRP — C-reactive protein; NT-proBNP — N-terminal pro-B-type natriuretic peptide; eGFR — estimated glomerular filtration rate; IGF-1 — insulin-like growth factor 1; DHEAS — dehydroepiandrosterone sulfate. [$]Muscle fatigability (in 4 different muscle regions) refers to the decrease in the frequency (of the total power range, Hz) of a processed electromyography signal between 1 and 10 second of an isometric exercise (greater decrease indicates more tired muscle region). [#]Dominant upper extremity and right lower extremity were tested. For details (including surface electromyography methodology) — see the 'Methods' section.

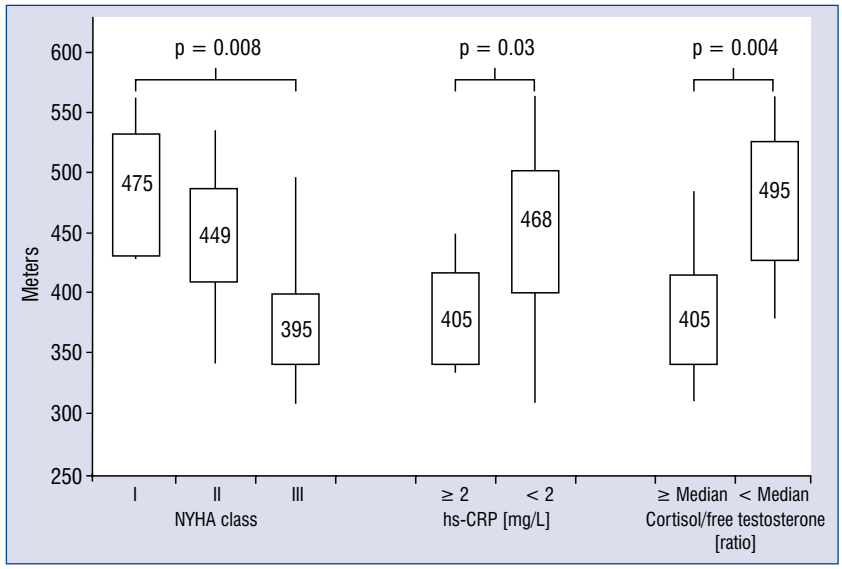

Figure 1. Six-minute walking test distance (box plots with median [number], interquartile range [box], and minimum/maximum [whiskers]) in men with heart failure with reduced ejection fraction according to New York Heart Association (NYHA) functional class, high-sensitivity C-reactive protein (hs-CRP), and the median of cortisol/free testosterone ratio (1478). P-values for the Kruskal-Wallis test are presented. For details — see the 'Methods' section.

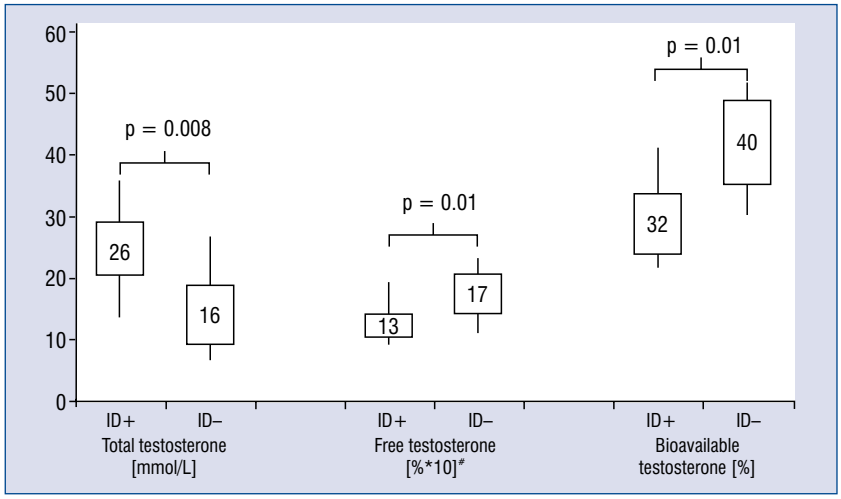

Figure 2. Total testosterone concentration with free and bioavailable testosterone fraction (box plots with median [number], interquartile range [box], and minimum/maximum [whiskers]) in examined men with heart failure with reduced ejection fraction according to the presence (ID+) or absence of iron deficiency (ID–). #Note that free testosterone values were multiplied by 10 to include this parameter in one figure with total and bioavailable testosterone (divide by 10 for normal values in percent). P-values for the Kruskal-Wallis test are presented. For details — see the 'Methods' section.

target tissues for circulating steroid hormones, in which they exert their direct anabolic properties [27, 28]. Undisturbed iron status is also necessary for the optimal functioning of mitochondria, and therefore it warrants cellular energy maintenance [29]. Importantly, iron determines tissue oxidative capacity, which is a major determinant of endurance and energetic efficacy during sub-maximal physical efforts [30].

Our results demonstrating the relationships between skeletal muscle performance and particular metabolic derangements are consistent

Table 3. The relationships between iron status, anabolic hormones, and measures of catabolic/anabolic balance in men with heart failure with reduced ejection fraction.

Variables [Units]	Hemoglobin [g/dL]	Reticulocytes [%]	Serum iron [μg/dL]	Serum ferritin [μg/L]	Soluble transferrin receptor [mg/L]	Transferrin saturation [%]	Reticulocyte hemoglobin content [pg]	Percentage of hypochromic red cells [%]
Total testosterone [nmol/L]	0.41[a]	–	–	–0.39[a]	–	–	–	–
Free testosterone [nmol/L]	0.41[a]	–	–	–	–	–	–	–
Free testosterone [%]	–	–	–	**0.49**[b]	–	**0.43**[b]	–	–
Bioavailable testosterone [nmol/L]	**0.49**[b]	–	–	–	–	–	–	–
Bioavailable testosterone [%]	–	–	–	**0.51**[b]	–	**0.45**[b]	–	–
Estradiol [pg/mL]	**0.47**[b]	–	–	**–0.47**[b]	0.36[a]	–	–	–
IGF-1 [ng/mL]	–	–	–	–	**0.48**[b]	–	–	0.41[a]
DHEAS [μg/dL]	–	–	–	–	–	–	–	–
Cortisol [nmol/L]	–	0.38[a]	–	–	–	–	–	–

Data are presented as Spearman's rank correlation coefficients (coefficients with p-value of > 0.1 are not presented). Statistical significance legend: [a]p < 0.1 (trend), [b]p < 0.05. IGF-1 — insulin-like growth factor 1; DHEAS — dehydroepiandrosterone sulfate. For details — see the 'Methods' section.

with previous studies conducted in this field. For example, Melenovsky et al. [31] demonstrated in an exercise phosphorus-31 magnetic resonance spectroscopy experiment that HF patients with ID had lower muscle strength, greater exertional muscle acidosis, and earlier metabolic shift to anaerobic metabolism. It is worth mentioning that we demonstrated in a previous study [32] that low serum ferritin correlates with inspiratory muscle weakness in men with HFrEF. Skeletal muscle dysfunction related to ID and catabolic/anabolic imbalance is a potential explanation why patients with ID or depleted anabolic drive have lower exercise capacity than subjects without these derangements [25, 26, 32–34]. It was previously demonstrated that intravenous iron therapy improves exercise capacity in patients with HFrEF and ID irrespective of anemia [35], and there is limited evidence that testosterone therapy may have similar beneficial effects [36]. In this context, the results of a small, randomized, double-blind, controlled study regarding iron isomaltoside in symptomatic HF should be acknowledged [37]. The authors demonstrated that intravenous iron repletion improves skeletal muscle energetics in both anemic and non-anemic subjects as assessed using phosphorus magnetic resonance spectroscopy [37]. Our study provides additional evidence regarding the consideration of HF as a "metabolic disease" [38, 39]. In our study, however, the distance covered in a 6MWT was related to catabolic/anabolic balance and inflammation, but the relationship with ID did not reach statistical significance. The latter was probably due to the relatively small number of examined patients. Importantly, we are able to partially compare clinical status, hemoglobin, and anabolic hormones of male patients from this study with our historical cohort of 205 men with stable, chronic HFrEF (LVEF ≤ 40%) recruited in 2001–2005 for another research project [33]. Although male HF patients from 2001–2005 had comparable age, NYHA class distribution, LVEF, NT-proBNP, and TT ($p > 0.05$ for all comparisons of mean ± standard deviation between the previous and this study), the current group of men with HFrEF had higher DHEAS (130 ± 98 vs. 88 ± 77 μg/dL, $p = 0.02$), IGF-1 (197 ± 52 vs. 134 ± 66 ng/mL, $p < 0.001$) and hemoglobin (15.3 ± 1.3 vs. 14.3 ± 1.5 g/dL, $p = 0.002$) as compared with the historical cohort [33]. The aforementioned data suggest that even clinically comparable groups of HF patients may subtly differ in particular hormonal parameters.

In this study we have also demonstrated the relationships between iron parameters and bioac-

tive testosterone. Although men with HFrEF and concomitant ID had higher TT compared with those without ID (and also higher SHBG, but not albumin), they presented with lower free and bioavailable fractions of this hormone. It should be acknowledged that the relationships between ID and hormonal status of men with HFrEF have not been studied so far, including large biomarker HF programs such as BIOSTAT-CHF [40]. The potential explanation of why depleted anabolic drive correlates with ID is related to impaired intestinal absorption and malnutrition [40]. There is clinical and experimental evidence that dysregulated catabolic/anabolic balance characterizing advanced HF promotes several maladaptive mechanisms within the gastrointestinal system, including intestinal hypoperfusion, edema, and anorexia [41–43]. The aforementioned pathomechanisms are responsible for disordered absorption of several microelements and further malnutrition, the pathologies of which are frequently observed in patients with HF [44, 45]. Decreased absorption of iron is considered one of the key mechanisms explaining how patients with HF develop ID, apart from accumulation of iron in the mononuclear phagocyte system [46]. Although the relationships between catabolic/anabolic balance and ID have not been studied in HF so far, we have some data on neuroendocrine signaling and iron status in this population. In one cross-sectional study regarding more than 700 patients with chronic HF, low TSAT was related to increased sympathetic activation, as reflected by higher circulating stress hormone norepinephrine [47]. Both increased sympathetic drive and catabolic/anabolic imbalance are involved in the complex pathomechanism of progressive catabolic state occurring in HF, and they both contribute to cardiac cachexia [48]. It remains unclear whether these unfavorable trajectories are further promoted or only accompanied by concomitant ID. It is worth noting that in experimental animals testosterone mediates systemic iron status through inhibition of the transcription of hepatic hepcidin — the key iron regulator [49, 50]. Further studies are required to determine independent effects of ID and catabolic/anabolic imbalance on skeletal muscle performance and exercise capacity in men with HFrEF.

Limitations of the study

We enrolled relatively a small number of subjects with HFrEF, and further studies in larger populations are needed not only to confirm the aforementioned relationships (metabolic derangements — skeletal muscle function; iron status — hormones), but also to evaluate independent effects of disordered iron homeostasis and catabolic/anabolic imbalance on skeletal muscle performance. Additionally, we examined only men with HFrEF, and there are no data presented regarding either female patients or subjects with the two remaining strata of LVEF (HF with preserved and mid-range ejection fraction). Finally, in the current study there was no control group, and the presented relationships should be re-evaluated in an age-matched group of healthy men without any cardiovascular disease.

Conclusions

In this preliminary study we have demonstrated that metabolic derangements related to energy generation and utilization, namely ID and catabolic/anabolic imbalance, can contribute to decreased skeletal muscle performance in men with HFrEF. Additionally, we have shown that there is a relationship between ID and reduced bioactive testosterone in these patients.

Funding

This project was funded by a National Science Center (Poland) grant allocated on the basis of the decision number DEC-2013/09/N/NZ5/00811.

Conflict of interest: Wroclaw Medical University received an unrestricted grant from Vifor Pharma. P.P. and E.A.J. report personal fees from Vifor Pharma. P.P. and E.A.J. have been co-PIs in the AFFIRM-AHF trial sponsored by Vifor Pharma. The other authors have nothing to disclose.

References

1. Neubauer S. The failing heart--an engine out of fuel. N Engl J Med. 2007; 356(11): 1140–1151, doi: 10.1056/NEJMra063052, indexed in Pubmed: 17360992.
2. Ingwall JS. Energy metabolism in heart failure and remodelling. Cardiovasc Res. 2009; 81(3): 412–419, doi: 10.1093/cvr/cvn301, indexed in Pubmed: 18987051.
3. Mettauer B, Zoll J, Garnier A, et al. Heart failure: a model of cardiac and skeletal muscle energetic failure. Pflugers Arch. 2006; 452(6): 653–666, doi: 10.1007/s00424-006-0072-7, indexed in Pubmed: 16767467.
4. Bayeva M, Gheorghiade M, Ardehali H. Mitochondria as a therapeutic target in heart failure. J Am Coll Cardiol. 2013; 61(6): 599–610, doi: 10.1016/j.jacc.2012.08.1021, indexed in Pubmed: 23219298.
5. Anker SD, Chua TP, Ponikowski P, et al. Hormonal changes and catabolic/anabolic imbalance in chronic heart failure and their importance for cardiac cachexia. Circulation. 1997; 96(2): 526–534, doi: 10.1161/01.cir.96.2.526, indexed in Pubmed: 9244221.

6. Anker SD, Clark AL, Kemp M, et al. Tumor necrosis factor and steroid metabolism in chronic heart failure: possible relation to muscle wasting. J Am Coll Cardiol. 1997; 30(4): 997–1001, doi: 10.1016/s0735-1097(97)00262-3, indexed in Pubmed: 9316530.
7. Jankowska EA, Biel B, Majda J, et al. Anabolic deficiency in men with chronic heart failure: prevalence and detrimental impact on survival. Circulation. 2006; 114(17): 1829–1837, doi: 10.1161/CIRCULATIONAHA.106.649426, indexed in Pubmed: 17030678.
8. Coats AJ, Clark AL, Piepoli M, et al. Symptoms and quality of life in heart failure: the muscle hypothesis. Br Heart J. 1994; 72(2 Suppl): S36–S39, doi: 10.1136/hrt.72.2_suppl.s36, indexed in Pubmed: 7946756.
9. Jankowska EA, von Haehling S, Anker SD, et al. Iron deficiency and heart failure: diagnostic dilemmas and therapeutic perspectives. Eur Heart J. 2013; 34(11): 816–829, doi: 10.1093/eurheartj/ehs224, indexed in Pubmed: 23100285.
10. Jankowska EA, Tkaczyszyn M, Kalicińska E, et al. Testosterone deficiency in men with heart failure: pathophysiology and its clinical, prognostic and therapeutic implications. Kardiol Pol. 2014; 72(5): 403–409, doi: 10.5603/KP.a2014.0025, indexed in Pubmed: 24526551.
11. Ponikowski P, Voors AA, Anker SD, et al. 2016 ESC Guidelines for the diagnosis and treatment of acute and chronic heart failure: The Task Force for the diagnosis and treatment of acute and chronic heart failure of the European Society of Cardiology (ESC). Developed with the special contribution of the Heart Failure Association (HFA) of the ESC. Eur J Heart Fail. 2016; 18(8): 891–975, doi: 10.1002/ejhf.592, indexed in Pubmed: 27207191.
12. Blanc B, Finch CA, Hallberg L, et al. Nutritional anaemias. Report of a WHO scientific group. WHO Tech Rep Ser. 1968; 405: 1–40.
13. Levey AS, Bosch JP, Lewis JB, et al. A more accurate method to estimate glomerular filtration rate from serum creatinine: a new prediction equation. Modification of Diet in Renal Disease Study Group. Ann Intern Med. 1999; 130(6): 461–470, doi: 10.7326/0003-4819-130-6-199903160-00002, indexed in Pubmed: 10075613.
14. Vermeulen A, Verdonck L, Kaufman JM. A critical evaluation of simple methods for the estimation of free testosterone in serum. J Clin Endocrinol Metab. 1999; 84(10): 3666–3672, doi: 10.1210/jcem.84.10.6079, indexed in Pubmed: 10523012.
15. Węgrzynowska-Teodorczyk K, Siennicka A, Josiak K, et al. Evaluation of Skeletal Muscle Function and Effects of Early Rehabilitation during Acute Heart Failure: Rationale and Study Design. Biomed Res Int. 2018; 2018: 6982897, doi: 10.1155/2018/6982897, indexed in Pubmed: 29721510.
16. Byrne CA, Lyons GM, Donnelly AE, et al. Rectus femoris surface myoelectric signal cross-talk during static contractions. J Electromyogr Kinesiol. 2005; 15(6): 564–575, doi: 10.1016/j.jelekin.2005.03.002, indexed in Pubmed: 15946862.
17. Zizola C, Schulze PC. Metabolic and structural impairment of skeletal muscle in heart failure. Heart Fail Rev. 2013; 18(5): 623–630, doi: 10.1007/s10741-012-9353-8, indexed in Pubmed: 23065040.
18. Clark AL, Poole-Wilson PA, Coats AJ. Exercise limitation in chronic heart failure: central role of the periphery. J Am Coll Cardiol. 1996; 28(5): 1092–1102, doi: 10.1016/S0735-1097(96)00323-3, indexed in Pubmed: 8890800.
19. Wilson JR, Mancini DM, Simson M. Detection of skeletal muscle fatigue in patients with heart failure using electromyography. Am J Cardiol. 1992; 70(4): 488–493, doi: 10.1016/0002-9149(92)91195-a, indexed in Pubmed: 1642187.
20. Buller NP, Jones D, Poole-Wilson PA. Direct measurement of skeletal muscle fatigue in patients with chronic heart failure. Br Heart J. 1991; 65(1): 20–24, doi: 10.1136/hrt.65.1.20, indexed in Pubmed: 1993126.
21. Harridge SD, Magnusson G, Gordon A. Skeletal muscle contractile characteristics and fatigue resistance in patients with chronic heart failure. Eur Heart J. 1996; 17(6): 896–901, doi: 10.1093/oxfordjournals.eurheartj.a014971, indexed in Pubmed: 8781829.
22. Dunnigan A, Staley NA, Smith SA, et al. Cardiac and skeletal muscle abnormalities in cardiomyopathy: comparison of patients with ventricular tachycardia or congestive heart failure. J Am Coll Cardiol. 1987; 10(3): 608–618, doi: 10.1016/s0735-1097(87)80204-8, indexed in Pubmed: 3624667.
23. Minotti JR, Pillay P, Chang L, et al. Neurophysiological assessment of skeletal muscle fatigue in patients with congestive heart failure. Circulation. 1992; 86(3): 903–908, doi: 10.1161/01.cir.86.3.903, indexed in Pubmed: 1516203.
24. Minotti JR, Christoph I, Oka R, et al. Impaired skeletal muscle function in patients with congestive heart failure. Relationship to systemic exercise performance. J Clin Invest. 1991; 88(6): 2077––2082, doi: 10.1172/JCI115537, indexed in Pubmed: 1752965.
25. Josiak K, Jankowska EA, Piepoli MF, et al. Skeletal myopathy in patients with chronic heart failure: significance of anabolic-androgenic hormones. J Cachexia Sarcopenia Muscle. 2014; 5(4): 287–296, doi: 10.1007/s13539-014-0152-z, indexed in Pubmed: 25081949.
26. Stugiewicz M, Tkaczyszyn M, Kasztura M, et al. The influence of iron deficiency on the functioning of skeletal muscles: experimental evidence and clinical implications. Eur J Heart Fail. 2016; 18(7): 762–773, doi: 10.1002/ejhf.467, indexed in Pubmed: 26800032.
27. Herbst KL, Bhasin S. Testosterone action on skeletal muscle. Curr Opin Clin Nutr Metab Care. 2004; 7(3): 271–277, doi: 10.1097/00075197-200405000-00006, indexed in Pubmed: 15075918.
28. Sato K, Iemitsu M, Aizawa K, et al. Testosterone and DHEA activate the glucose metabolism-related signaling pathway in skeletal muscle. Am J Physiol Endocrinol Metab. 2008; 294(5): E961–E968, doi: 10.1152/ajpendo.00678.2007, indexed in Pubmed: 18349113.
29. Beard JL. Iron biology in immune function, muscle metabolism and neuronal functioning. J Nutr. 2001; 131(2S-2): 568S–579S; discussion 580S, doi: 10.1093/jn/131.2.568S, indexed in Pubmed: 11160590.
30. Haas JD, Brownlie T. Iron deficiency and reduced work capacity: a critical review of the research to determine a causal relationship. J Nutr. 2001; 131(2S-2): 676S–688S; discussion 688S, doi: 10.1093/jn/131.2.676S, indexed in Pubmed: 11160598.
31. Melenovsky V, Hlavata K, Sedivy P, et al. Skeletal Muscle Abnormalities and Iron Deficiency in Chronic Heart Failure. Circ Heart Fail. 2018; 11(9): e004800, doi: 10.1161/CIRCHEARTFAILURE.117.004800, indexed in Pubmed: 30354361.
32. Tkaczyszyn M, Drozd M, Węgrzynowska-Teodorczyk K, et al. Depleted iron stores are associated with inspiratory muscle weakness independently of skeletal muscle mass in men with systolic chronic heart failure. J Cachexia Sarcopenia Muscle. 2018; 9(3): 547–556, doi: 10.1002/jcsm.12282, indexed in Pubmed: 29573220.

33. Jankowska EA, Filippatos G, Ponikowska B, et al. Reduction in circulating testosterone relates to exercise capacity in men with chronic heart failure. J Card Fail. 2009; 15(5): 442–450, doi: 10.1016/j.cardfail.2008.12.011, indexed in Pubmed: 19477405.
34. Dziegala M, Josiak K, Kasztura M, et al. Iron deficiency as energetic insult to skeletal muscle in chronic diseases. J Cachexia Sarcopenia Muscle. 2018; 9(5): 802–815, doi: 10.1002/jcsm.12314, indexed in Pubmed: 30178922.
35. Anker SD, Comin Colet J, Filippatos G, et al. FAIR-HF Trial Investigators. Ferric carboxymaltose in patients with heart failure and iron deficiency. N Engl J Med. 2009; 361(25): 2436–2448, doi: 10.1056/NEJMoa0908355, indexed in Pubmed: 19920054.
36. Toma M, McAlister FA, Coglianese EE, et al. Testosterone supplementation in heart failure: a meta-analysis. Circ Heart Fail. 2012; 5(3): 315–321, doi: 10.1161/CIRCHEARTFAILURE.111.965632, indexed in Pubmed: 22511747.
37. Charles-Edwards G, Amaral N, Sleigh A, et al. Effect of iron isomaltoside on skeletal muscle energetics in patients with chronic heart failure and iron deficiency. Circulation. 2019; 139(21): 2386–2398, doi: 10.1161/CIRCULATIONAHA.118.038516, indexed in Pubmed: 30776909.
38. Doehner W, Frenneaux M, Anker SD. Metabolic impairment in heart failure: the myocardial and systemic perspective. J Am Coll Cardiol. 2014; 64(13): 1388–1400, doi: 10.1016/j.jacc.2014.04.083, indexed in Pubmed: 25257642.
39. Anker SD, Rauchhaus M. Heart failure as a metabolic problem. Eur J Heart Fail. 1999; 1(2): 127–131, doi: 10.1016/s1388-9842(99)00006-9, indexed in Pubmed: 10937921.
40. van der Wal HH, Grote Beverborg N, Dickstein K, et al. Iron deficiency in worsening heart failure is associated with reduced estimated protein intake, fluid retention, inflammation, and antiplatelet use. Eur Heart J. 2019; 40(44): 3616–3625, doi: 10.1093//eurheartj/ehz680, indexed in Pubmed: 31556953.
41. Murphy L, Gray A, Joyce E. Anabolism to catabolism: serologic clues to nutritional status in heart failure. Curr Heart Fail Rep. 2019; 16(5): 189–200, doi: 10.1007/s11897-019-00437-y, indexed in Pubmed: 31606846.
42. Sandek A, Bauditz J, Swidsinski A, et al. Altered intestinal function in patients with chronic heart failure. J Am Coll Cardiol. 2007; 50(16): 1561–1569, doi: 10.1016/j.jacc.2007.07.016, indexed in Pubmed: 17936155.
43. Sandek A, Rauchhaus M, Anker SD, et al. The emerging role of the gut in chronic heart failure. Curr Opin Clin Nutr Metab Care. 2008; 11(5): 632–639, doi: 10.1097/MCO.0b013e32830a4c6e, indexed in Pubmed: 18685461.
44. Rahman A, Jafry S, Jeejeebhoy K, et al. Malnutrition and cachexia in heart failure. JPEN J Parenter Enteral Nutr. 2016; 40(4): 475–486, doi: 10.1177/0148607114566854, indexed in Pubmed: 25634161.
45. Sciatti E, Lombardi C, Ravera A, et al. Nutritional deficiency in patients with heart failure. Nutrients. 2016; 8(7): 442, doi: 10.3390/nu8070442, indexed in Pubmed: 27455314.
46. van Veldhuisen DJ, Anker SD, Ponikowski P, et al. Anemia and iron deficiency in heart failure: mechanisms and therapeutic approaches. Nat Rev Cardiol. 2011; 8(9): 485–493, doi: 10.1038/nrcardio.2011.77, indexed in Pubmed: 21629210.
47. Moliner P, Enjuanes C, Tajes M, et al. Association between norepinephrine levels and abnormal iron status in patients with chronic heart failure: is iron deficiency more than a comorbidity? J Am Heart Assoc. 2019; 8(4): e010887, doi: 10.1161//JAHA.118.010887, indexed in Pubmed: 30760082.
48. Anker SD, Sharma R. The syndrome of cardiac cachexia. Int J Cardiol. 2002; 85(1): 51–66.
49. Guo W, Bachman E, Li M, et al. Testosterone administration inhibits hepcidin transcription and is associated with increased iron incorporation into red blood cells. Aging Cell. 2013; 12(2): 280–291.
50. Latour C, Kautz L, Besson-Fournier C, et al. Testosterone perturbs systemic iron balance through activation of epidermal growth factor receptor signaling in the liver and repression of hepcidin. Hepatology. 2014; 59(2): 683–694, doi: 10.1002/hep.26648, indexed in Pubmed: 23907767.

VIA MEDICA

ORIGINAL ARTICLE

Cardiology Journal
2021, Vol. 28, No. 3, 402–410
DOI: 10.5603/CJ.a2021.0009

ISSN 1897–5593
eISSN 1898–018X

Improvement in quality of life with sacubitril/ /valsartan in cardiac resynchronization non-responders: The RESINA (RESynchronization plus an Inhibitor of Neprilysin/Angiotensin) registry

José Manuel Rubio Campal[1], Hugo del Castillo[2], Belén Arroyo Rivera[1], Carmen de Juan Bitriá[2], Mikel Taibo Urquia[1], Pepa Sánchez Borque[1], Ángel Miracle Blanco[1], Loreto Bravo Calero[1], David Martí Sánchez[2], José Tuñón Fernández[1]

[1]Fundación Jiménez Díaz-Quirónsalud, Madrid, Spain
[2]Hospital Central de la Defensa, Madrid, Spain

Abstract

Background: *Clinical management of cardiac resynchronization therapy (CRT) non-responders is difficult, and their prognosis is poor. The aim of the present study was to evaluate whether treatment with sacubitril/valsartan can improve quality of life (QoL) parameters in these patients.*

Methods: *Thirty five non-responders to CRT were included (75 ± 7 years, 28% females, mean left ventricular ejection fraction 28 ± 8%, 54% non-ischemic cardiomyopathy) with maximally optimized drug therapy and New York Heart Association class II–III. They were all on angiotensin-converting enzyme inhibitors or angiotensin II receptor blockers and were switched to sacubitril/valsartan. One week before and 6 months after initiation of the therapy they completed both the Minnesota Living with Heart Failure (MLWHF) and the 12-item Kansas City Cardiomyopathy Questionnaires (KCCQ-12). The primary outcome was the effect of sacubitril/valsartan on the physical, clinical, social and emotional QoL parameters and number of hospitalizations.*

Results: *The mean total scores of both questionnaires improved from baseline to the follow-up visit at 6-months (KCCQ-12 40 ± 10 to 47 ± 10; $p < 0.001$; MLWHF 40 ± 15 to 29 ± 15; $p < 0.001$). The best results were seen in the KCCQ-12 total symptom domains (77% improvement), the MLWHF physical domain (81% improvement), and the MLWHF emotional domain (71% improvement). Two patients died during follow-up. The mean number of hospitalizations reduced significantly (1 ± 0.6 vs. 0.5 ± 0.8; $p = 0.003$)*

Conclusions: *In CRT non-responders, sacubitril/valsartan significantly improved overall QoL, physical limitations and emotional domains and reduced the number of hospitalizations.* (Cardiol J 2021; 28, 3: 402–410)

Key words: resynchronization, sacubitril/valsartan, quality of life

Address for correspondence: José Manuel Rubio Campal, MD, PhD, FESC, Unidad de Arritmias, Servicio de Cardiología, Fundación Jiménez Díaz–Quirónsalud, Avda. Reyes Católicos, 2, 28040 Madrid, Spain, tel: +34-91-5441636, fax: +34-91-5499402, e-mail: jmrubio@fjd.es

Received: 9.10.2020 Accepted: 15.01.2021

Introduction

Cardiac resynchronization therapy (CRT) is the therapeutic option of choice for patients with heart failure (HF) and conduction disorders [1, 2], but 30% to 40% of them are considered non-responders and have a poor quality of life (QoL). The reasons are diverse: type of cardiomyopathy, previous non-left bundle branch block morphology, comorbidity factors, suboptimal left ventricular (LV) lead position or inadequate pacing optimization [3, 4]. Management of these patients is difficult, and they are a particularly high-risk HF group with < 50% survival at 5 years [5]. The presence of significantly limited QoL is becoming increasingly relevant for health care stakeholders, as HF is one of the main causes of poor QoL.

Sacubitril/valsartan is a new angiotensin receptor neprilysin inhibitor (ARNI), and are a class I recommendation for patients with chronic HF, reduced LV ejection fraction (LVEF) and New York Heart Association (NYHA) class II–IV instead of angiotensin-converting enzyme inhibitors (ACEIs) or angiotensin II receptor blockers (ARBs) in conjunction with other standard HF treatments [2]. Data on the clinical benefit of sacubitril/valsartan in patients with CRT are scarce, because very few patients with these devices have been included in trials (usually less than 20%) [6, 7], although some sub-group analyses have demonstrated that they experience similar clinical beneficial effects to those of patients without CRT. The aim of the current study was to determine whether administering sacubitril/valsartan instead or an ACEI/ARB in non-responders to CRT could result in a beneficial effect on morbidity and QoL.

Methods

Patients with CRT were included (CRT-D defibrillator or CRT-P pacing only) who were referred to the cardiology HF/arrhythmia outpatient clinics from the Fundación Jiménez Díaz (FJD; Madrid, Spain) and the Hospital Central de la Defensa (HCD; Madrid, Spain). They needed to fulfill the following criteria before enrollment: 1) age > 18 years; 2) recipient of a CRT device for > 6 and < 36 months for standard indications; 3) optimized medical therapy since implantation, including ACEI/ARB; 4) naïve to sacubitril-valsartan; 5) presence of sinus rhythm, or atrial fibrillation (AF) with spontaneous or induced complete atrioventricular block; 6) at least > 95% LV stimulation; 7) unchanged or worsened clinical status by CRT, according to the HF composite end point described by Packer [8], in the absence of a reversible cause. Exclusion criteria were: 1) systolic blood pressure (SBP) < 100 mmHg; 2) estimated glomerular filtration rate (eGFR) < 30 mL/m/1.73 m^2 or chronic renal dialysis; 3) serum potassium levels > 5.2 mmol/L; 4) severe anemia (hemoglobin < 9 mg/dL) or thyroid disease; 5) life-expectancy < 1 year because of concomitant, non-cardiovascular disorders; 6) history of stroke, myocardial infarction, or unstable angina pectoris within the prior 3 months; 7) presence of correctible valvular disease; 8) subject unable to attend follow-up at the study site or unable, for physical or mental reasons, to comply with the trial procedures, or to sign the informed consent; 9) subject participates in another research project.

As in the PARADIGM-HF trial, all patients taking ACEI/ARB were considered for participation, but they were required to take a stable dose of a beta-blocker (BB) and an ACEI/ARB dose equivalent to at least 10 mg of enalapril daily for a minimum of 4 weeks prior to screening [6]. After inclusion, ACEI/ARB was suspended and sacubitril/valsartan was initiated after 36 hours, at an initial dose of 24/26 mg. All the patients continued with the same BB, mineralocorticoid receptor antagonist (MRA) or diuretic dose unless they experienced symptoms due to sustained SBP < 90 mmHg. After 1 month, the sacubitril/valsartan dose was titrated according to the initial response of the patient, tolerability of the drug and patient characteristics, always trying to achieve the highest doses.

One week prior to inclusion in the study, all patients filled in two QoL questionnaires: Minnesota Living with Heart failure (MLWHF) [9] and 12-item Kansas City Cardiomyopathy Questionnaire (KCCQ-12) [10], to establish their clinical status before enrollment. The MLWHF is a self-administered disease-specific questionnaire comprising 21 items answered on a 6-point Likert scale, representing different degrees of impact of HF on QoL, from 0 (none) to 5 (very much) [11]. It provides a total score (range 0–105, from best to worse), as well as scores for two dimensions, physical (range 0–40) and emotional (range 0–25). The other 8 items are only considered for the calculation of the total score. The KCCQ-12 quantifies 8 domains of patients' HF-related health status: Physical Limitation (3 items); Swelling frequency (1 item); Fatigue frequency (1 item); Dyspnea frequency (1 item); Dyspnea — sleeping upright (1 item); Enjoyment of life (1 item); Rest of life as is now (1 item); Social limitation (3 items). Item

responses are coded sequentially (1, 2, 3, etc.) from worst to best status. For analysis, five domains are calculated: Physical limitation, Symptoms, Life status, Social limitation, and an Overall summary score. Both questionnaires have been translated into Spanish and have been validated [12, 13].

Clinical and demographic data were obtained for every patient: sex; age; presence of cardiovascular risk factors (diabetes mellitus, hypertension, and smoking) and chronic obstructive pulmonary disease; time from CRT implantation to study inclusion; type of cardiomyopathy (ischemic, non-ischemic); type of CRT device; and drugs used. The following data were also collected before inclusion and after 6 months: eGFR; potassium levels; hemoglobin levels; and NYHA class. A baseline echocardiographic study was performed in all patients, including end-diastolic LV diameter (mm), end-diastolic right ventricular diameter (mm), LVEF, and left atrium (LA) size (mm) measurements. Patients were divided according the type of CRT device.

The primary outcome was any change from baseline to the 6-month follow-up visit in all the items and total domains analyzed from both the KCCQ-12 and the MLWHF questionnaires. The secondary end point was to compare the number of hospitalizations (> 24-h before discharge)/ /Emergency Department consultations (< 24-h before discharge) because of HF 6 months before the inclusion and at 6-month follow-up. All patients provided written informed consent. The study protocol was approved by the hospital's Institutional Review Board. The study complied with the tenets of the Declaration of Helsinki.

Statistical analysis

Continuous values were expressed as mean ± standard deviation and nominal variables as counts and percentages. Median values with the corresponding interquartile range (IQR) were computed for non-normally distributed variables. A two-tailed t-test was used for comparison of normally-distributed variables, and the non-parametric Kruskal-Wallis test for values that were not normally distributed. For comparisons of categorical data, two-tailed χ^2 statistics with the Yates correction or the Fisherexact test were used, as applicable. Mean values were calculated from patient scores of both questionnaires for all domains. Values were obtained at baseline and after a 6-month follow-up period. The principal efficacy analysis was the change in mean total scores and individual domains between baseline and the follow-up visit at 6 months. In the MLWHF total score, patients were divided into cohorts on the basis of change as follows: worse ($\Delta \geq +6$ points), similar, ($\Delta < +6$ and < -6 points), better ($\Delta \geq -6$ points). Similar cohorts were made for the specific domains (Physical, Emotional, Rest) but with a difference of 2 points in each of them. Similarly, in the 12-KCCQ overall summary score, patients were divided into cohorts on the basis of change as follows: worse ($\Delta \geq -4$ points), similar ($\Delta < -4$ and < 4 points), better ($\Delta \geq +4$ points). Similar cohorts were made for the four specific domains but with a difference of 1 point in each of them. Missing values were not accounted for in the primary analysis. A value of $p < 0.05$ was considered to indicate a statistically significant difference. All analyses were done using IBM® SPSS® Statistics version 20.0.0 (Armonk, NY, USA).

Results

Tables 1 and 2 show the clinical characteristics of the patients by CRT type. 35 patients were included (mean age 75 ± 7 years, 28% females). Patients with CRT-P were significantly older compared with those with CRT-D (78 ± 6 vs. 73 ± 8 years; $p = 0.029$), and with a higher mean LVEF (32 ± 5 vs. 25 ± 9, respectively; $p = 0.005$). Mean time from CRT device implantation to inclusion in the study was 23 ± 17 months.

After initiation of sacubitril/valsartan, 6 (20%) patients experienced persistent SBP < 90 mmHg, but only one of them did not definitively tolerate the drug. In the remaining 5 patients the BB and/or diuretic dose was adjusted, and the drug was maintained at the 24/26 mg dose. Although the highest doses of sacubitril/valsartan were intended, after 6 months 46% of patients remained on the same dose and 50% used the 49/51 mg dose. There was only a slight but significant deterioration in eGFR (58 ± 16 to 54 ± 17 mL/min/1.73 m^2; $p < 0.001$) after administration of the drug. Two patients died because of refractory HF before completing the 6-month follow-up. Two patients needed outpatient treatment with levosimendan, also maintaining the lower dose of sacubitril/valsartan.

The mean number of hospitalizations/Emergency Department consultations reduced significantly after the 6-month follow-up (1 ± 0.6 to 0.5 ± 0.8 ($p < 0.001$). Although there was a slight increase in LVEF after the 6-month follow-up, it was not statistically significant (27 ± 8 vs. 28 ± 8; $p = 0.09$).

Table 1. Clinical characteristics of patients included.

	All	CRT-P	CRT-D	P
Number	35	15	20	
Age	75 ± 7	78 ± 6	73 ± 8	0.029
Female sex	10 (28%)	9 (60%)	1 (5%)	< 0.001
Diabetes	14 (40%)	7 (47%)	7 (35%)	0.363
Hypertension	30 (86%)	11 (73%)	19 (95%)	0.093
Dyslipidemia	24 (69%)	7 (47%)	17 (85%)	0.020
Former smoker	9 (23%)	1 (7%)	8 (35%)	0.055
BMI [kg/m^2]	26 ± 4	25 ± 4	27 ± 3	0.154
Ischemic disease	16 (46%)	1 (7%)	15 (75%)	< 0.001
Non-ischemic	19 (54%)	14 (93%)	5 (25%)	< 0.001
Beta-blockers	34 (97%)	14 (93%)	20 (100%)	0.429
Diuretics	35 (100%)	15 (100%)	20 (100%)	–
MRA	12 (34%)	1 (7%)	11 (55%)	0.003
Amiodarone	11 (31%)	3 (20%)	8 (40%)	0.187
Digoxin	2 (6%)	1 (7%)	1 (5%)	0.681
SGTL2	10 (28%)	5 (33%)	5 (25%)	0.433
Atrial fibrillation	12 (34%)	6 (40%)	6 (30%)	0.397
NYHA class II	29 (83%)	14 (93%)	15 (75%)	0.167
NYHA class III	6 (17%)	1 (7%)	5 (25%)	0.167
eGFR	57 ± 16	53 ± 15	60 ± 17	0.224
Potassium [mmol/mL]	4.4 ± 0.3	4.4 ± 0.3	4.5 ± 0.3	0.564
Hemoglobin [mg/dL]	13 ± 1.4	13 ± 1.3	13 ± 1.4	0.843
SBP [mm Hg]	120 ± 12	120 ± 14	120 ± 11	0.939

CRT-P — cardiac resynchronization therapy pacing only; CRT-D — cardiac resynchronization therapy with defibrillator; BMI — body mass index; eGFR — estimated glomerular filtration rate; MRA — mineralocorticoid receptor antagonist; SGTL2 — inhibitors of sodium-glucose contansporter-2; NYHA — New York Heart Association; SBP — systolic blood pressure

Table 2. Echocardiographic parameters and QRS width of patients included.

	All	CRT-P	CRT-D	P
Number	35	15	20	
LA [mm]	45 ± 9	45 ± 6	46 ± 10	0.628
LVEDD [mm]	57 ± 7	55 ± 5	58 ± 7	0.116
RVEDD [mm]	41 ± 5	40 ± 6	41 ± 4	0.383
LVEF [mm]	28 ± 8	32 ± 5	25 ± 9	0.005
QRS width pre-CRT [ms]	150 ± 30	144 ± 30	155 ± 30	0.310
QRS width with CRT [ms]	136 ± 12	132 ± 13	140 ± 11	0.090

CRT-P — cardiac resynchronization therapy pacing only; CRT-D — cardiac resynchronization therapy with defibrillator; LA — left atrium; LVEDD — left ventricular end-diastolic diameter; RVEDD — right ventricular end-diastolic diameter; LVEF — left ventricular ejection fraction

Changes in QoL questionnaires

The KCCQ-12 baseline total physical limitation domain was worse in the CRT-P group, without any significant differences in the baseline of the remaining scores (Table 3). After the 6-month follow-up visit, 31 patients filled in both questionnaires (2 patients died because of refractory HF and 2 patients were lost to follow-up).

Table 4 show the status after the 6-month follow-up visit for the different scores analyzed. The best results were obtained in the KCCQ-12 total physical limitation and total symptom domains

Table 3. Baseline quality of life domains of patients included

Baseline QoL domains	CRT-P	CRT-D	P
KCCQ-12 Total physical limitation	8 ± 2	10 ± 3	0.04
KCCQ-12 Total symptoms	16 ± 4	17 ± 4	0.531
KCCQ-12 Life status	5 ± 2	6 ± 2	0.089
KCCQ-12 Social limitations	9 ± 3	10 ± 4	0.310
KCCQ-12 Overall summary	37 ± 9	42 ± 11	0.185
MLWHF Physical	21 ± 6	18 ± 7	0.222
MLWHF Emotional	12 ± 5	10 ± 5	0.248
MLWHF Total	41 ± 14	40 ± 17	0.825

CRT-P — cardiac resynchronization therapy pacing only; CRT-D — cardiac resynchronization therapy with defibrillator; QoL — quality of life; KCCQ-12 — Kansas City Cardiomyopathy Questionnaire; MLWHF — Minnesota Living with Heart Failure

Table 4. Clinical situation after 6-month treatment with sacubitril/valsartan.

Domains at follow-up	Result					
	CRT-P (n = 14)			CRT-D (n = 17)		
	Better	Similar	Worse	Better	Similar	Worse
KCCQ-12 Total physical limitation	10 (72%)	3 (21%)	1 (7%)	12 (71%)	5 (29%)	0 (0%)
KCCQ-12 Total symptoms	10 (72%)	4 (28%)	0 (0%)	14 (82%)	2 (12%)	1 (6%)
KCCQ-12 Life status	7 (50%)	6 (43%)	1 (7%)	8 (47%)	7 (41%)	2 (12%)
KCCQ-12 Social limitations	6 (44%)	5 (35%)	3 (21%)	6 (35%)	7 (41%)	4 (24%)
KCCQ-12 Overall summary	10 (72%)	1 (7%)	3 (21%)	10 (59%)	5 (29%)	2 (12%)
MLWHF Physical	12 (86%)	1 (7%)	1 (7%)	13 (77%)	3 (17%)	1 (6%)
MLWHF Emotional	10 (72%)	3 (21%)	1 (7%)	12 (71%)	5 (29%)5	0 (0%)
MLWHF Total	12 (86%)	2 (14%)	0 (0%)	14 (83%)	3 (17%)	0 (0%)

CRT-P — cardiac resynchronization therapy pacing only; CRT-D — cardiac resynchronization therapy with defibrillator; KCCQ-12 — Kansas City Cardiomyopathy Questionnaire; MLWHF — Minnesota Living with Heart Failure; Better, Similar, Worse, Improvement, similar status, worse in each of the specific quality of life domains

(72% were better in both) and also in the MLWHF physical and emotional domains (81% and 71% were better, respectively). In the KCCQ-12 overall summary score, 65% of patients were better, 19% similar and 16% worse. When the emotional and social domains were analyzed, in the KCCQ-12 life status domain, 48% of the patients were better, 42% similar and 10% worse. In the KCCQ-12 social limitation domain, 39% were better, 39% similar and 22% worse. In the MLWHF emotional domain, 71% were better, 26% similar and only 3% worse. No significant differences between CRT-D and CRT-P patients in all the domains analyzed were demonstrated. Table 5, Figures 1 and 2 show the mean value of all the scores at baseline and at 6-month follow-up, demonstrating a significant improvement in all domains except for the KCCQ-12 Social limitations.

Discussion

Quality of life has been defined by the World Health Organization (WHO) as a broad-ranging concept affecting physical health, psychological state and social relationships [14]. Moreover, achieving a better QoL in patients with HF is important regardless of the device or drug used, because a decrease in mortality or morbidity is not always accompanied by better QoL. BBs do not significantly improve QoL [15], and ACEI/ARBs have demonstrated mixed results [16], although many trials were conducted without using actual HF-specific QoL questionnaires like the ones used in the present study. On the other hand, sacubitril/valsartan is one of the few HF therapies that have demonstrated a significant improvement in morbidity and mortality as well as in physical and social activity limitations [17, 18].

Table 5. Mean ± standard deviation values of different quality of life domains pre and after 6-month treatment with sacubitril/valsartan (S/V).

Quality of life domains	Pre S/V	Post S/V	P
KCCQ-12 Total physical limitation	9 ± 2	11 ± 3	< 0.001
KCCQ-12 Total symptoms	16 ± 4	19 ± 5	0.001
KCCQ-12 Life status	6 ± 2	7 ± 2	0.009
KCCQ-12 Social limitations	9 ± 3	10 ± 3	0.228
KCCQ-12 Overall summary	40 ± 10	47 ± 10	0.001
MLWHF Physical	19 ± 7	13 ± 6	< 0.001
MLWHF Emotional	11 ± 5	8 ± 6	< 0.001
MLWHF Total	40 ± 15	29 ± 15	< 0.001

KCCQ-12 — Kansas City Cardiomyopathy Questionnaire; MLWHF — Minnesota Living with Heart Failure

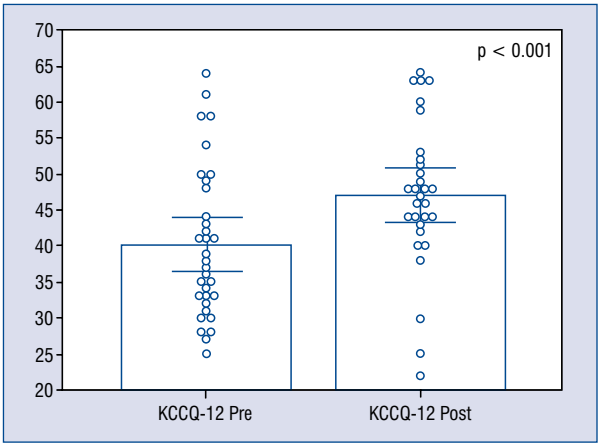

Figure 1. Kansas City Cardiomyopathy Questionnaire (KCCQ-12) overall summary scores at baseline and after 6-months of treatment with sacubitril/valsartan.

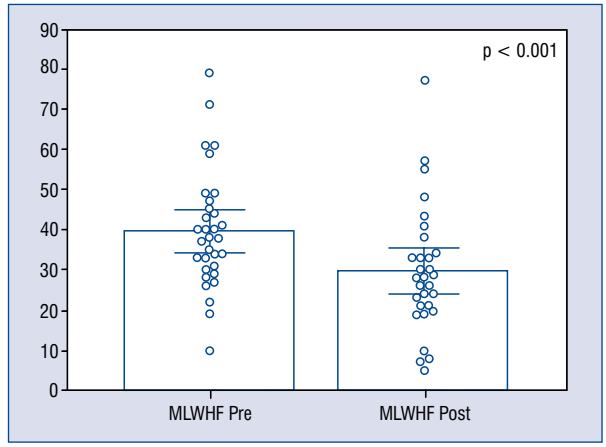

Figure 2. Minnesota Living with Heart Failure (MLWHF) total scores at baseline and after 6-months of treatment with sacubitril/valsartan.

This is the first study to provide evidence that adding sacubitril/valsartan to CRT non-responders is associated with an improvement in most HF--specific QoL domains. More specifically, there was a significant improvement in physical activities and symptoms, which were the maximum limitations of patients at baseline. Also, the improvement in the social and emotional domains was very relevant. This is important for all patients, but particularly for those with chronic HF, as most of them feel that they have a chronic disease with a poor prognosis and generally have a poor QoL. The general answer when adding sacubitril/valsartan is that patients say they "feel better now", and this resulted in a better status in emotional QoL domains.

For the analysis, we decided to differentiate between CRT-D and CRT-P devices because CRT-P patients were older, more frequently female and with non-ischemic cardiomyopathy, but the results in QoL improvement were similar in both groups, demonstrating a good effect of the drug regardless of the CRT type and patient characteristics [19].

One important fact in the present study is that the mean age was 75 ± 7 years, much higher than in other large, randomized trials with sacubitril/valsartan (64 ± 11 and 63 ± 11 years in the PARADIGM-HF [6] and PRIME [20] trials, respectively). This is important because before this study, it was assumed that some baseline physical limitations of the patients could be related more to age or muscular or neurological disorders rather than to HF symptoms, but surprisingly, most of them experienced a better physical situation, something that could be related to the better perception in

their QoL emotional domains. Depression and anxiety are not systematically studied in patients with HF, but they are very important components of QoL [21, 22]. Dereli et al. [23] have demonstrated a significant positive effect of sacubitril/valsartan on different depression and anxiety parameters in patients with HF and a reduced LVEF. In this study, 43% of the patients had clinically significant depressive symptoms at baseline, and 38% of them also had moderate to severe anxiety, and these was related to poor QoL scores regardless of functional status. Carels [24] have also reported a stronger relationship between QoL and functional capacity rather than cardiac function in HF patients and an improvement in functional capacity leading to better QoL.

Results herein are similar to other studies with sacubitril/valsartan. Chandra et al. [17] reported a significant improvement in nearly all KCCQ-12 physical and social activities compared with enalapril, with the largest responses in household chores and sexual relations, but also with a significantly 5-point or greater improvement in the combined physical and social activity mean scores. Also, at baseline, patients with the greatest limitations attributable to HF in physical and social activities were older, more likely to be women, and more likely to have a worse NYHA class. In addition, the authors reported a reduced likelihood of cardiovascular death, all-cause mortality, and HF hospitalizations. One important limitation as pointed out by the authors of this study is that the patients did not complete their baseline KCCQ-12 until randomization, and so we decided to conduct the baseline study 1 week prior to inclusion, to know the real situation of the patients before using the drug. In a study by Lewis et al. [18], the authors also reported a significant improvement in the different KCCQ-12 scores and KCCQ-12 overall summary scores in patients treated with sacubitril/valsartan compared with those treated with enalapril, with consistency in most domains, and this persisted during the follow-up that lasted over 8 months.

It was decided to set the follow-up visit at 6 months, to be sure that the initial effect of the drug was maintained in the long-term, although in most of the studies with sacubitril/valsartan the different positive effects can be seen in the first 2 months. In the PIONEER-HF [7], the authors reported an early separation of the event curves for clinically relevant end points. Examining the end points of cardiovascular death or hospitalization for HF, they observed an early effect of sacubitril/valsartan with the initiation of in-hospital treatment for 8 weeks, something consistent with the efficacy of the drug in chronic HF patients in other studies.

Limitations of the study

The present study has some limitations. Firstly, although the results are the first to point out the benefit of sacubitril/valsartan in CRT non-responder patients, the population was relatively small, so the findings should be further corroborated in a larger study. Another important limitation of the current study is that although the highest doses of sacubitril/valsartan were intended, 46% of the patients remained on the same initial dose, 51% had the 49/52 mg dose, and no patients received the highest dose. Mean baseline SBP of the patients was 120 ± 12 mmHg, similar to other studies, but as pointed out before, our patients were significantly older and had a longer HF history, perhaps reflecting a real-life situation. Taking in account these characteristics, we decided to be cautious when achieving the highest doses to avoid renal failure or significant hypotension. The incidence of hypotension was 20%, similar to other studies, and only 1 patient decided to discontinue the drug definitively. Several studies with sacubitril/valsartan have demonstrated that achieving the highest dose is difficult, and usually only half of the patients are on the highest drug dose [25]. In the PARADIGM-HF trial [6], 42% had a reduced dose, and in the PIONEER trial [26] only 55% of the patients had the highest dose. In a real-life study by Du et al. [27], at the 6-month follow-up visit 27% of patients had the highest dose, 41% the mean dose and 32% the lowest dose. In elderly patients, dose reduction or discontinuation of the drug has been associated with hypotension and/or onset of renal failure. In spite of this, Vardeny et al. [28] have demonstrated that although drug reduction identified patients at higher risk of a major cardiovascular event, the benefit for patients on lower doses of sacubitril/valsartan compared with those on lower doses of enalapril was similar to that of patients who remained on target doses for both drugs. All these data suggest that patients taking doses lower than the target doses of the drug would still derive greater benefit from sacubitril/valsartan when compared with enalapril [29].

Conclusions

In non-responder patients to CRT despite optimal medical treatment, sacubitril/valsartan significantly improved overall QoL, physical limitation and emotional scores and reduced the number of

hospitalizations. New controlled studies are needed to validate these results and to extend this benefit to more patients.

Conflict of interest: None declared

References

1. Brignole M, Auricchio A, Baron-Esquivias G, et al. 2013 ESC Guidelines on cardiac pacing and cardiac resynchronization therapy: the Task Force on cardiac pacing and resynchronization therapy of the European Society of Cardiology (ESC). Developed in collaboration with the European Heart Rhythm Association (EHRA). Eur Heart J. 2013; 34(29): 2281–2329, doi: 10.1093/eurheartj/eht150, indexed in Pubmed: 23801822.
2. Ponikowski P, Voors A, Anker S, et al. 2016 ESC Guidelines for the diagnosis and treatment of acute and chronic heart failure: The Task Force for the diagnosis and treatment of acute and chronic heart failure of the European Society of Cardiology (ESC)Developed with the special contribution of the Heart Failure Association (HFA) of the ESC. Eur Heart J. 2016; 37(27): 2129–2200, doi: 10.1093/eurheartj/ehw128.
3. Naqvi SY, Jawaid A, Goldenberg I, et al. Non-response to cardiac resynchronization therapy. Curr Heart Fail Rep. 2018; 15(5): 315–321, doi: 10.1007/s11897-018-0407-7, indexed in Pubmed: 30097910.
4. Leong DP, Höke U, Delgado V, et al. Predictors of long-term benefit of cardiac resynchronization therapy in patients with right bundle branch block. Eur Heart J. 2012; 33(15): 1934–1941, doi: 10.1093/eurheartj/ehr470, indexed in Pubmed: 22270539.
5. Daubert C, Behar N, Martins RP, et al. Avoiding non-responders to cardiac resynchronization therapy: a practical guide. Eur Heart J. 2017; 38(19): 1463–1472, doi: 10.1093/eurheartj/ehw270, indexed in Pubmed: 27371720.
6. Packer M, McMurray JJV, Desai AS, et al. Angiotensin receptor neprilysin inhibition compared with enalapril on the risk of clinical progression in surviving patients with heart failure. Circulation. 2015; 131(1): 54–61, doi: 10.1161/CIRCULATIONAHA.114.013748, indexed in Pubmed: 25403646.
7. Morrow D, Velazquez E, DeVore A, et al. Clinical outcomes in patients with acute decompensated heart failure randomly assigned to sacubitril/valsartan or enalapril in the PIONEER-HF trial. Circulation. 2019; 139(19): 2285–2288, doi: 10.1161/circulationaha.118.039331.
8. Packer M. Proposal for a new clinical end point to evaluate the efficacy of drugs and devices in the treatment of chronic heart failure. J Card Fail. 2001; 7(2): 176–182, doi: 10.1054/jcaf.2001.25652, indexed in Pubmed: 11420770.
9. Rector T, Kubo S, Cohn J. Validity of the minnesota living with heart failure questionnaire as a measure of therapeutic response to enalapril or placebo. Am J Cardiol. 1993; 71(12): 1106–1107, doi: 10.1016/0002-9149(93)90582-w.
10. Spertus JA, Jones PG. Development and validation of a short version of the kansas city cardiomyopathy questionnaire. Circ Cardiovasc Qual Outcomes. 2015; 8(5): 469–476, doi: 10.1161/CIRCOUTCOMES.115.001958, indexed in Pubmed: 26307129.
11. Rector TS, Cohn JN. Assessment of patient outcome with the Minnesota Living with Heart Failure questionnaire: reliability and validity during a randomized, double-blind, placebo-controlled trial of pimobendan. Pimobendan Multicenter Research Group. Am Heart J. 1992; 124(4): 1017–1025, doi: 10.1016/0002-8703(92)90986-6, indexed in Pubmed: 1529875.
12. Garin O, Soriano N, Ribera A, et al. [Validation of the Spanish version of the Minnesota Living with Heart Failure Questionnaire]. Rev Esp Cardiol. 2008; 61(3): 251–259, indexed in Pubmed: 18361898.
13. Comín-Colet J, Garin O, Lupón J, et al. Validation of the Spanish version of the Kansas city cardiomyopathy questionnaire. Rev Esp Cardiol. 2011; 64(1): 51–58, doi: 10.1016/j.recesp.2010.10.003, indexed in Pubmed: 21194819.
14. Sijtsma K, Emons WHM, Bouwmeester S, et al. Nonparametric IRT analysis of Quality-of-Life Scales and its application to the World Health Organization Quality-of-Life Scale (WHOQOL-Bref). Qual Life Res. 2008; 17(2): 275–290, doi: 10.1007/s11136-007-9281-6, indexed in Pubmed: 18246447.
15. Tate CW, Robertson AD, Zolty R, et al. Quality of life and prognosis in heart failure: results of the Beta-Blocker Evaluation of Survival Trial (BEST). J Card Fail. 2007; 13(9): 732–737, doi: 10.1016/j.cardfail.2007.07.001, indexed in Pubmed: 17996821.
16. Rector TS, Carson PE, Anand IS, et al. Assessment of long-term effects of irbesartan on heart failure with preserved ejection fraction as measured by the minnesota living with heart failure questionnaire in the irbesartan in heart failure with preserved systolic function (I-PRESERVE) trial. Circ Heart Fail. 2012; 5(2): 217–225, doi: 10.1161/CIRCHEARTFAILURE.111.964221, indexed in Pubmed: 22267751.
17. Chandra A, Lewis EF, Claggett BL, et al. Effects of sacubitril/valsartan on physical and social activity limitations in patients with heart failure: a secondary analysis of the PARADIGM-HF trial. JAMA Cardiol. 2018; 3(6): 498–505, doi: 10.1001/jamacardio.2018.0398, indexed in Pubmed: 29617523.
18. Lewis EF, Claggett BL, McMurray JJV, et al. Health-related quality of life outcomes in PARADIGM-HF. Circ Heart Fail. 2017; 10(8), doi: 10.1161/CIRCHEARTFAILURE.116.003430, indexed in Pubmed: 28784687.
19. Ruschitzka F. The challenge of nonresponders to cardiac resynchronization therapy: lessons learned from oncology. Heart Rhythm. 2012; 9(8 Suppl): S14–S17, doi: 10.1016/j.hrthm.2012.04.024, indexed in Pubmed: 22521933.
20. Kang DH, Park SJ, Shin SH, et al. Angiotensin receptor neprilysin inhibitor for functional mitral regurgitation. Circulation. 2019; 139(11): 1354–1365, doi: 10.1161/CIRCULATIONAHA.118.037077, indexed in Pubmed: 30586756.
21. Kitko L, McIlvennan CK, Bidwell JT, et al. American Heart Association Council on Cardiovascular and Stroke Nursing; Council on Quality of Care and Outcomes Research; Council on Clinical Cardiology; and Council on Lifestyle and Cardiometabolic Health. Family Caregiving for Individuals With Heart Failure: A Scientific Statement From the American Heart Association. Circulation. 2020; 141(22): e864–e878, doi: 10.1161/CIR.0000000000000768, indexed in Pubmed: 32349542.
22. White-Williams C, Rossi LP, Bittner VA, et al. American Heart Association Council on Cardiovascular and Stroke Nursing; Council on Clinical Cardiology; and Council on Epidemiology and Prevention. Addressing Social Determinants of Health in the Care of Patients With Heart Failure: A Scientific Statement From the American Heart Association. Circulation. 2020; 141(22): e841–e863, doi: 10.1161/CIR.0000000000000767, indexed in Pubmed: 32349541.
23. Dereli S, Kılınçel O, Çerik İB, et al. Impact of sacubitril/valsartan treatment on depression and anxiety in heart failure with re-

duced ejection fraction. Acta Cardiol. 2020; 75(8): 774–782, doi: 10.1080/00015385.2020.1730577, indexed in Pubmed: 32186467.
24. Carels RA. The association between disease severity, functional status, depression and daily quality of life in congestive heart failure patients. Qual Life Res. 2004; 13(1): 63–72, doi: 10.1023/B:QURE.0000015301.58054.51, indexed in Pubmed: 15058788.
25. Vicent L, Esteban-Fernández A, Gómez-Bueno M, et al. Sacubitril/valsartan in daily clinical practice: data from a prospective registry. J Cardiovasc Pharmacol. 2019; 73(2): 118–124, doi: 10.1097/FJC.0000000000000641, indexed in Pubmed: 30540687.
26. Velazquez E, Morrow D, DeVore A, et al. Angiotensin–neprilysin inhibition in acute decompensated heart failure. N Engl J Med. 2019; 380(6): 539–548, doi: 10.1056/nejmoa1812851.
27. Du AX, Westerhout CM, McAlister FA, et al. Titration and tolerability of sacubitril/valsartan for patients with heart failure in clinical practice. J Cardiovasc Pharmacol. 2019; 73(3): 149–154, doi: 10.1097/FJC.0000000000000643, indexed in Pubmed: 30540684.
28. Vardeny O, Claggett B, Packer M, et al. Prospective Comparison of ARNI with ACEI to Determine Impact on Global Mortality and Morbidity in Heart Failure (PARADIGM-HF) Investigators. Efficacy of sacubitril/valsartan vs. enalapril at lower than target doses in heart failure with reduced ejection fraction: the PARADIGM-HF trial. Eur J Heart Fail. 2016; 18(10): 1228–1234, doi: 10.1002/ejhf.580, indexed in Pubmed: 27283779.
29. Senni M, McMurray JJV, Wachter R, et al. Initiating sacubitril/valsartan (LCZ696) in heart failure: results of TITRATION, a double-blind, randomized comparison of two uptitration regimens. Eur J Heart Fail. 2016; 18(9): 1193–1202, doi: 10.1002/ejhf.548, indexed in Pubmed: 27170530.

VIA MEDICA

ORIGINAL ARTICLE

Cardiology Journal
2021, Vol. 28, No. 3, 411–415
DOI: 10.5603/CJ.a2019.0055

ISSN 1897–5593
eISSN 1898–018X

Clinical significance of myocardial involvement in acute idiopathic pericarditis

Aviv Mager, David Berger, Hadas Ofek, Yoav Hammer, Ilana Kedmi, Ran Kornowski

Department of Cardiology, Rabin Medical Center – Beilinson Hospital, affiliated to Sackler Faculty of Medicine, Tel Aviv University, Tel Aviv, Israel

Abstract

Background: *Acute idiopathic pericarditis (AIP) is frequently accompanied by myocardial involvement (AIPM). Although in acute myocarditis, the myocardial inflammation can lead to life-threatening complications, the outcome of patients with AIPM has been described as good. It remains unclear if a good prognosis of patients with AIPM reflects mild myocardial involvement or good medical management.*

Methods: *A retrospective analysis of life-threatening complications and life-saving interventions in a cohort of 248 consecutive patients admitted to a single medical center between 2006 and 2017 with AIP (n = 169) or AIPM (n = 79). Major adverse cardiac events (MACE) included cardiac tamponade, cardiogenic shock, ventricular tachycardia, pericardiocentesis, pericardiectomy, large pericardial effusion and death.*

Results: *Patients with AIPM were younger than patients with AIP ($p < 0.001$), and more often had left ventricular dysfunction (31.6% vs. 1.2%, $p < 0.001$) and less often had large pericardial effusion (1.3% vs. 13.6%, $p = 0.002$), and MACE (5.1% vs. 14.8%, $p = 0.014$). Cardiac tamponade occurred in 5.3% of the patients with AIP as opposed to 1.3% of the patients with AIPM ($p = 0.176$). Severe left ventricular dysfunction with cardiogenic shock occurred exclusively among patients with AIPM but the rate was low (2.5%). Life-saving interventions were used in both groups at comparable rates (2.5% vs. 5.3%, $p = 0.510$). There were no in-hospital deaths.*

Conclusions: *Myocardial involvement in acute pericarditis is associated with a low rate of severe left ventricular dysfunction and cardiogenic shock and a reduced rate of large pericardial effusion, resulting in a lower rate of MACE. Life-saving interventions were used at comparable rates in patients with and without myocardial involvement having excellent survival rates.* (Cardiol J 2021; 28, 3: 411–415)

Key words: acute idiopathic pericarditis, myocardial involvement, left ventricular dysfunction, tamponade, intervention, outcome

Introduction

Myocardial involvement has been reported in 14.6% to 60.9% of patients with acute pericarditis [1–9]. The severity of the myocardial involvement, referred to by some authors as concomitant myocarditis [1], may vary from minimal elevation of a myocardial biomarker level with or without mild left ventricular (LV) dysfunction to severe LV dysfunction and ultimately hemodynamic compromise. Although the natural history, characteristics, and outcomes of acute idiopathic pericarditis (AIP) and of acute myocarditis have been studied extensively [1, 10–13], the data for acute pericarditis with myocardial involvement (AIPM) are limited [2–6]. In acute myocarditis, myocardial inflammation can lead to life-threatening complications, including severe LV dysfunction, heart failure, cardiogenic

Address for correspondence: Aviv Mager, MD, Department of Cardiology, Rabin Medical Center – Beilinson Hospital, Petach Tikva 4941492, Israel, tel: +972-506844228, fax: +972-39376428, e-mail: a11v12@gmail.com

Received: 24.02.2019 Accepted: 28.05.2019

shock, ventricular tachycardia and atrioventricular block [10–13]. Recently, an in-hospital rate of death or heart transplant of 3.2% has been reported [13]. The long-term outcome of patients with acute pericarditis has been described as good, with and without myocardial involvement [3]. However, little is known about the rate of acute phase complications, and it remains unclear whether a good prognosis of patients with AIPM is related to a low rate of severe complications or use of life-saving interventions. Moreover, the finding that the outcome of patients with AIPM is not poorer than patients with acute pericarditis without myocardial involvement is intriguing. The purpose of this study was to examine why myocardial involvement in acute pericarditis is not associated with worse outcomes although it can lead to LV dysfunction. For this purpose, outcomes of patients with acute idiopathic pericarditis were compared with and without myocardial involvement admitted to the documented hospital over an 11-year period and possible differences were examined in acute phase complications and the use of life-saving interventions.

Methods

The computerized database of the medical center was searched for patients hospitalized between March 1, 2006 and March 1, 2017 with a first episode of AIP or AIPM in whom the diagnosis complied with current guidelines [1]. Patient electronic medical files were retrospectively reviewed for data on mortality, clinical, laboratory and imaging parameters, major adverse cardiac events (MACE), life-saving interventions, and findings on follow-up.

The diagnosis of AIP was based on the presence of at least two of the following criteria: typical chest pain, friction rub, new or worsening pericardial effusion, and typical electrocardiographic changes [1]. Patients in whom a specific etiology for the pericarditis was identified (for example, rheumatoid arthritis, systemic lupus erythematosus, familial Mediterranean fever, tuberculosis, post-myocardial injury syndrome, chronic renal failure, purulent pericarditis, and acute or recent myocardial infarction) were excluded from the study. Patients with active malignancy, pregnant patients, and patients referred from other hospitals were also excluded.

The criteria for the diagnosis of AIPM were the presence of diagnostic criteria for AIP and elevation of cardiac troponin T (cTnT) level in the presence of a normal serum creatinine level, or an elevated creatine phosphokinase level in the presence of an elevated serum creatinine level.

The size of the pericardial effusion was assessed by echocardiography and categorized semi-quantitatively as small, moderate, or large. LV global function and regional wall motion abnormalities were assessed using either echocardiography or cardiac magnetic resonance angiography. Impaired LV function was defined as an abnormal global systolic function or wall motion abnormality. LV systolic function was semi-quantitatively categorized as normal, mildly, moderately or severely decreased. Peak white blood cell count on the first day of admission, peak body temperature, and peak C-reactive protein level were recorded. Exclusion of significant coronary artery disease was done in all patients with myocardial involvement except those at very low risk, using coronary angiography or computed tomographic coronary angiography. The idiopathic nature of the disease was proved by lack of evidence for a specific etiology during hospital stay and on follow-up. Pericardial fluid was analyzed in all the patients when obtained.

The following were categorized as MACE: cardiac tamponade, non-obstructive cardiogenic shock, ventricular tachycardia, large symptomatic pericardial effusion, atrioventricular block and death. The following were recorded as life-saving interventions: pericardiocenthesis or surgical evacuation of pericardial fluid for treatment of cardiac tamponade, cardioversion for sustained ventricular tachycardia, use of intra-aortic balloon counter-pulsation device, use of extracorporeal mechanical oxygenator, and intensive intravenous catecholamine administration with intraarterial pressure monitoring for cardiogenic shock.

The study was approved by the local institutional ethics committee.

Statistical analysis

Categorical variables are described as numbers and percentages. Continuous variables were evaluated for normal distribution using histograms and Q-Q plots and are reported as median and interquartile range. Categorical variables were compared between groups using the χ^2 test or the Fisher exact test. Continuous variables were compared using the Kruskal-Wallis test and the Mann-Whitney test. A p value of < 0.05 was considered significant. All statistical tests were performed using SPSS version 21.

Results

The study group included 248 patients (76% male) aged 18–89 years (median, 47 years). Myocardial involvement was found in 79 of them (32%) and they were categorized as AIPM. Patient baseline characteristics by group are depicted in Table 1. Compared to the AIP group, the AIPM group was characterized by younger age, lower rate of moderate and large pericardial effusion, higher proportion of LV dysfunction and lower white blood cell count and they were less often given glucocorticoid therapy.

Table 2 shows the rates of in-hospital complications and of use of life-saving interventions. Patients with AIPM had a lower frequency of large symptomatic pericardial effusion. MACE was observed in 30 (12.1%) of the 248 patients. The frequency of MACE was lower in patients with AIPM than in patients with AIP. Severe LV dysfunction and cardiogenic shock occurred only in patients with AIPM but the difference was not statistically significant.

There were no in-hospital deaths. However, life-saving interventions were used in 11 (4.4%) patients: 10 patients underwent evacuation of the pericardial fluid for cardiac tamponade (9 had pericardiocentesis, 1 had surgical evacuation) and 2 patients with cardiogenic shock needed mechanical hemodynamic support (1 extracorporeal oxygenator, 1 intra-aortic balloon counter-pulsation device. One of these patients needed both pericardiocentesis and mechanical support.) Among the

Table 1. Baseline characteristics by group.

	AIP (n = 169)	AIPM (n = 79)	P
Age:			< 0.001
25	39.0	26.0	
50	53.0	35.0	
75	66.0	45.0	
Male gender	124 (73.4)	65 (82.3)	0.150
Pericardial effusion:	118 (69.8)	46 (58.2)	0.084
None	49 (29.3)	33 (41.8)	0.060
Small	53 (31.7)	35 (44.3)	0.064
Moderate	45 (36.9)	10 (14.9)	0.020
Large	22 (14.9)	1 (1.3)	0.002
Moderate or larger	67 (39.6)	11 (13.9)	< 0.001
Biomarker elevation	0 (0.0)	79 (100.0)	<0.001
LV dysfunction	2 (11.8)	25 (31.6)	< 0.001
CRP:			0.098
25	0.0	3.7	
50	11.3	7.15	
75	17.2	16.7	
WBC:			0.005
25	9090	6575	
50	11300	8515	
75	13350	12775	
Prednisone	53 (31.4)	6 (7.6)	< 0.001

Data on age, C-reactive protein (CRP) and white blood cell count (WBC) are medians and percentile 25 and 75 values. All other data are presented as number (percentage). AIP — acute idiopathic pericarditis; AIPM — acute idiopathic pericarditis with myocardial involvement; LV — left ventricular

Table 2. Complications and life-saving interventions by group.

	AIP (n = 169)	AIPM (n = 79)	P
Large symptomatic pericardial effusion	22 (14.9)	1 (1.3)	0.002
Severe LV dysfunction	0 (0)	2 (2.5)	0.102
Cardiogenic shock	0 (0.0)	2 (2.5)	0.102
Tamponade	9 (5.3)	1 (1.3)	0.176
Pericardial fluid evacuation	10 (5.9)	1 (1.3)	0.182
VT/NSVT	0 (0.0)	0 (0.0)	> 0.999
Syncope	2 (1.2)	1 (1.3)	> 0.999
In-hospital death	0 (0%)	0 (0%)	> 0.999
Major adverse cardiac events	26 (15.4)	4 (5.1)	0.002
Life-saving interventions	9 (5.3)	2 (2.5)	0.510

Data are presented as number (percentage). AIP — acute idiopathic pericarditis; AIPM — acute idiopathic pericarditis with myocardial involvement; LV — left ventricular; VT — ventricular tachycardia; NSVT — non-sustained ventricular tachycardia

patients with AIPM, 25 had impaired LV function and thus, met the criteria for perimyocarditis [3]. There was no difference in the rate of life saving interventions in this group, 8%, and the group of patients with AIP (5.3%, p = 0.637). Pericardial fluid analysis did not reveal a specific etiology in any of the patients.

Discussion

The results of this retrospective analysis of consecutive patients with acute idiopathic pericarditis show, for the first time, that acute pericarditis with myocardial involvement is characterized by lower rates of large pericardial effusion and MACE. Severe LV dysfunction and cardiogenic shock may develop in patients with AIPM, necessitating life-threatening interventions. However, the rate is low and does not significantly increase the rate of MACE. The rates of use of life-saving interventions in patients with and without myocardial involvement are comparable, resulting in a good survival rate for both groups.

Data in the literature regarding the in-hospital course of patients with myocardial involvement are very limited [3–5]. A good survival rate in the present relatively large cohort of patients is in agreement with results of previous reports [4, 5]. However, previous reports provided only limited information on life-threatening complications and use of life-saving interventions in patients with myocardial involvement. As the current findings show, life-threatening complications occurred in both groups at comparable rates. Because both cardiac tamponade and cardiogenic shock are associated with high mortality rates if untreated, the good outcomes of the present patients with acute pericarditis, with and without myocardial involvement, reflects the success of life-saving interventions rather than a benign natural history.

Although severe LV dysfunction and cardiogenic shock occurred exclusively among patients with AIPM, the proportion of patients with AIPM in need of life-saving interventions in hospital was not higher than in AIP patients. This was explained by the low frequency of this complication, together with a very low rate of cardiac tamponade and need for evacuation of pericardial fluid in the patients with AIPM. The difference in the rate of cardiac tamponade between patients with AIP and AIPM was not statistically significant. However, the significantly lower rates of large and moderate pericardial effusion among patients with AIPM indicate that patients with AIPM are at lower risk of cardiac tamponade. Thus, the lower rate of cardiac tamponade in the present patients with AIPM was probably a true finding.

The absence of atrioventricular block in the present patients was not surprising, as this complication was found to rarely occur in inflammatory cardiac syndromes [3]. Previous reports have demonstrated that myocardial involvement affects younger patients [2, 3, 5]. The younger age of the current patients with AIPM is in agreement with these findings. Interestingly, younger age is typical to acute myocarditis as well [14], supporting the hypothesis that the myocardial involvement in acute pericarditis reflects concomitant myocarditis.

Unlike most previous reports, only patients with idiopathic syndromes were included herein. All patients lived in the same geographic region and acquired the disease during the same period of time. Thus, it is unlikely that our results were biased by shifts in the viral spectrum [15], environmental or genetic factors.

A larger proportion of the patients with AIP received prednisone therapy. Although prednisone therapy is believed to favorably affect the hospital course, MACE occurred more frequently among the patients with AIP. Thus, the less frequent use of prednisone in the current patients with AIPM did not account for the lower rate of MACE in this group.

Conclusions

Myocardial involvement in patients with acute idiopathic pericarditis is associated with a low rate of severe LV dysfunction and a decreased rate of large pericardial effusion as compared to patients without myocardial involvement. These result in comparable rates of life-threatening complications and of the use of life-saving interventions in patients with acute pericarditis with and without myocardial involvement. Thus, a good prognosis of patients with AIPM despite the occurrence of severe LV dysfunction is explained at least in part by the successful use of life-saving interventions. Because severe LV dysfunction may occasionally occur in AIPM, assessment of LV function and adequate monitoring in these patients are necessary. More research is necessary to clarify whether myocardial involvement is a complication of acute pericarditis or represents a different variant of inflammatory cardiac syndrome characterized by concomitant pericarditis and myocarditis.

Conflict of interest: None declared

References

1. Adler Y, Charron P, Imazio M, et al. 2015 ESC Guidelines for the diagnosis and management of pericardial diseases: The Task Force for the Diagnosis and Management of Pericardial Diseases of the European Society of Cardiology (ESC)Endorsed by: The European Association for Cardio-Thoracic Surgery (EACTS). Eur Heart J. 2015; 36(42): 2921–2964, doi: 10.1093/eurheartj/ehv318, indexed in Pubmed: 26320112.
2. Imazio M, Cecchi E, Demichelis B, et al. Myopericarditis versus viral or idiopathic acute pericarditis. Heart. 2008; 94(4): 498–501, doi: 10.1136/hrt.2006.104067, indexed in Pubmed: 17575329.
3. Imazio M, Brucato A, Barbieri A, et al. Good prognosis for pericarditis with and without myocardial involvement: results from a multicenter, prospective cohort study. Circulation. 2013; 128(1): 42–49, doi: 10.1161/CIRCULATIONAHA.113.001531, indexed in Pubmed: 23709669.
4. Buiatti A, Merlo M, Pinamonti B, et al. Clinical presentation and long-term follow-up of perimyocarditis. J Cardiovasc Med (Hagerstown). 2013; 14(3): 235–241, doi: 10.2459/JCM.0b013e328351da6e, indexed in Pubmed: 22644404.
5. Leitman M, Tyomkin V, Peleg E, et al. FACC, FESC. Left ventricular function in acute inflammatory peri-myocardial diseases - new insights and long-term follow-up. Cardiovasc Ultrasound. 2012; 10: 42–48, doi: 10.1186/1476-7120-10-42, indexed in Pubmed: 23121688.
6. Imazio M, Trinchero R. Myopericarditis: Etiology, management, and prognosis. Int J Cardiol. 2008; 127(1): 17–26, doi: 10.1016/j.ijcard.2007.10.053, indexed in Pubmed: 18221804.
7. Imazio M, Demichelis B, Cecchi E, et al. Cardiac troponin I in acute pericarditis. J Am Coll Cardiol. 2003; 42(12): 2144–2148, indexed in Pubmed: 14680742.
8. Bonnefoy E, Godon P, Kirkorian G, et al. Serum cardiac troponin I and ST-segment elevation in patients with acute pericarditis. Eur Heart J. 2000; 21(10): 832–836, doi: 10.1053/euhj.1999.1907, indexed in Pubmed: 10781355.
9. Gamaza-Chulián S, León-Jiménez J, Recuerda-Núñez M, et al. Cardiac troponin-T in acute pericarditis. J Cardiovasc Med (Hagerstown). 2014; 15(1): 68–72, doi: 10.2459/JCM.0b013e3283641161, indexed in Pubmed: 23846679.
10. Imazio M, Gaita F, LeWinter M. Evaluation and treatment of pericarditis. JAMA. 2015; 314(14): 1498–1506, doi: 10.1001/jama.2015.12763.
11. Caforio ALP, Pankuweit S, Arbustini E, et al. European Society of Cardiology Working Group on Myocardial and Pericardial Diseases. Current state of knowledge on aetiology, diagnosis, management, and therapy of myocarditis: a position statement of the European Society of Cardiology Working Group on Myocardial and Pericardial Diseases. Eur Heart J. 2013; 34(33): 2636–2648, doi: 10.1093/eurheartj/eht210, indexed in Pubmed: 23824828.
12. Sagar S, Liu PP, Cooper LT. Myocarditis. Lancet. 2012; 379(9817): 738–747, doi: 10.1016/S0140-6736(11)60648-X, indexed in Pubmed: 22185868.
13. Ammirati E, Cipriani M, Moro C, et al. Registro Lombardo delle Miocarditi. Clinical Presentation and Outcome in a Contemporary Cohort of Patients With Acute Myocarditis. Circulation. 2018; 138(11): 1088–1099, doi: 10.1161/CIRCULATIONAHA.118.035319, indexed in Pubmed: 29764898.
14. Kytö V, Sipilä J, Rautava P. The effects of gender and age on occurrence of clinically suspected myocarditis in adulthood. Heart. 2013; 99(22): 1681–1684, doi: 10.1136/heartjnl-2013-304449, indexed in Pubmed: 24064227.
15. Shauer A, Gotsman I, Keren A, et al. Acute viral myocarditis: current concepts in diagnosis and treatment. Isr Med Assoc J. 2013; 15(3): 180–185, indexed in Pubmed: 23662385.

VIA MEDICA

ORIGINAL ARTICLE

Cardiology Journal
2021, Vol. 28, No. 3, 416–422
DOI: 10.5603/CJ.a2019.0086

ISSN 1897–5593
eISSN 1898–018X

Evaluation of the InterTAK Diagnostic Score in differentiating Takotsubo syndrome from acute coronary syndrome. A single center experience

Judyta Samul-Jastrzębska, Marek Roik, Dominik Wretowski, Andrzej Łabyk, Antonina Ślubowska, Anna Bizoń, Marzanna Paczyńska, Katarzyna Kurnicka, Piotr Pruszczyk, Michał Ciurzyński

Department of Internal Medicine and Cardiology, Medical University of Warsaw, Poland

Abstract

Background: *The aim of this study was to evaluate the usefulness of a novel clinical score — the InterTAK Diagnostic Score in differentiating Takotsubo syndrome (TTS) from acute coronary syndrome (ACS).*

Methods: *Medical records of 40 consecutive patients with ACS and 20 patients with TTS were managed and retrospectively analyzed at the documented center. Each patient was evaluated using the InterTAK Diagnostic Score. To illustrate the diagnostic ability of the score, a receiver operating characteristic (ROC) curve was performed.*

Results: *Takotsube syndrome patients were more often female compared to the ACS group (70% vs. 27.5%, $p = 0.002$), an emotional trigger was more prevalent among the TTS group (65% vs. 7.5%, $p < 0.001$). The area under the curve (AUC) for the score was 0.885 (95% confidence interval [CI] 0.78–0.97). Using a cut-off value of 45 points, the sum of sensitivity and specificity was the highest. However, when patients with a score of ≥ 50 were diagnosed as TTS, 85% were diagnosed correctly. When patients with score ≤ 31 were diagnosed as ACS, 92% were diagnosed correctly.*

Conclusions: *The InterTAK Diagnostic Score might help in differentiating TTS from ACSs with high sensitivity and specificity. This finding requires further investigation to confirm its clinical utility.*
(Cardiol J 2021; 28, 3: 416–422)

Key words: Takotsubo syndrome, broken heart syndrome, acute coronary syndrome, clinical score

Introduction

Takotsubo syndrome (TTS), also known as "broken heart syndrome" or "stress cardiomyopathy" is an acute heart failure condition characterized by a temporary wall motion abnormality of the left ventricle (LV) (hypokinesia, akinesia or dyskinesia) with no significant coronary artery obstruction responsible for ischemia [1–4]. Its clinical presentation is similar to acute coronary syndrome (ACS). These two conditions share similar symptoms at presentation (chest pain, dyspnea), electrocardiogram (ECG) abnormalities, elevated cardiac biomarkers and comparable in-hospital mortality [1, 5–10]. The final differential diagnosis requires invasive procedures such as coronary angiography and left ventriculography [2]. The International Takotsubo Diagnostic Criteria (InterTAK Diagnostic Criteria) can be found in the Expert Consensus Document published in "European Heart Journal"

Address for correspondence: Judyta Samul-Jastrzębska, MD, Department of Internal Medicine and Cardiology, Medical University of Warsaw, ul. Lindleya 4, 02–005 Warszawa, Poland, tel: +48 22 502 11 44, fax: +48 22 502 21 42, e-mail: judyta.samul@gmail.com

Received: 14.03.2019 Accepted: 19.08.2019

[1, 2]. Since TTS was first reported in Japan in 1980s, it has been increasingly recognized all over the world and some investigators suggest that TTS could represent 1–3% of all patients with ACS and 5–6% of female presenting with suspected ST-segment elevation myocardial infarction (STEMI) [6, 11]. According recent data about 90% of TTS patients are women and around 80% are older than 50 years [12–16]. Recently, in order to differentiate TTS and ACS in the acute stage, before coronary angiography, the InterTAK Diagnostic Score was created [17]. It considers 7 clinical parameters and could be easily used in the emergency room. Authors of the Score postulate its high sensitivity and specificity. The maximum number of points to get is 100. According to the creators, in the population they studied (TTS vs. ACS ratio 1:2), obtaining ≥ 50 points allows to diagnose TTS with 95% accuracy. In turn to diagnose ACS with the same accuracy, ≤ 31 points should be obtained.

It is important to emphasize, that the model used by InterTAK Diagnostic Score creators, does not reflect the true prevalence of TTS. The predicted probability of TTS depends on its prevalence in clinical practice. Thus, in real-life, correction must be made.

The aim of our study was to evaluate the usefulness of the InterTAK Diagnostic Score in differentiating TTS from ACS among patients hospitalized in reference cardiological department.

Methods

We analyzed retrospectively the medical records of 20 consecutive patients with TTS and 40 patients with ACS hospitalized in our department between 10 October 2014 and 2 October 2018. TTS was defined based on modified Mayo Clinic Diagnostic Criteria [5, 11]: 1) a transient wall motion abnormality in the LV beyond a single epicardial coronary artery distribution; 2) the absence of obstructive coronary artery disease or angiographic evidence of acute plaque rupture, which can explain the wall motion abnormality; 3) new electrocardiographic abnormalities or elevation in cardiac troponin values; and 4) the absence of myocarditis. We considered the history of possible emotional or physical trigger. Patients with pacemaker rhythm were excluded from the study. Each patient was assigned points based on the InterTAK Diagnostic Score, which considers the following criteria: female sex (25 points), emotional (24 points) or physical trigger (13 points), absence of ST-segment depression (12 points), psychiatric disorders (11 points), neurologic disorders (9 points) and QTc prolongation (6 points) (Table 1). As a control group, cohort of patients with ACS, including patients with STEMI, non-STEMI, or unstable angina, was selected. ACS was diagnosed follow European Society of Cardiology recommendations [18, 19]. Data of patient's clinical profile were collected. This included: demographics, vital signs, cardiovascular risk factors, comorbidities, laboratory markers, results of electrocardiography, echocardiography and coronary angiography. High sensitive troponin T was assayed at admission and measured using an automated quantitative electrochemiluminescence immunoassay (Roche Elecsys, Mannheim, Germany).

Table 1. InterTAK Diagnostic Score.

Criteria	Points
Female sex	25
Emotional trigger	24
Physical trigger	13
Absence of ST-segment depression	12
Psychiatric disorders	11
Neurologic disorders	9
QTc prolongation	6

Statistical analysis

The categorical variables were summarized with the frequency of occurrence in each group as well as its percentage. The continuous variables were summarized with mean value and standard deviation. The differences between groups were assessed with the Fisher exact test for categorical variables and with the Student t-test for continuous ones. Assessment of each variable included in the InterTAK scale was performed with univariate logistic regression. Optimal cut-off value for our cohort in the InterTAK scale was selected based on analysis of reciver-operator curve (ROC). All tests were two-sided and the differences were considered statistically significant if the p-values were < 0.05. No correction was applied for multiple statistical testing. All analyses were done in the R language environment (version 3.5.1).

Results

Medical records of 20 TTS and 40 ACS consecutive patients were analyzed. Baseline characteristics of these two cohorts are shown in Table 2. TTS patients were more often female compared

Table 2. Baseline Takotsubo syndrome (TTS) and acute coronary syndrome (ACS) patient characteristics.

Parameter	TTS, n = 20 (100%)	ACS, n = 40 (100%)	P
Female sex	14 (70%)	11 (27.5%)	0.002
Age [years]	72.4 ± 12.99	72.9 ± 14.31	0.893
Triggering factors and symptoms of admission:			
Emotional trigger	13 (65%)	3 (7.5%)	0.000
Physical trigger	7 (35%)	9 (22.5%)	0.360
Chest pain	11 (55%)	22 (55%)	1.000
Dyspnea	6 (30%)	14 (35%)	0.777
Vital signs:			
Heart rate [bpm]	79.76 ± 18.91	77.12 ± 19.20	0.635
Systolic BP [mmHg]	131.80 ± 22.06	129.85 ± 24.05	0.778
Diastolic BP [mmHg]	69.87 ± 9.43	72.53 ± 13.39	0.415
Laboratory tests:			
hs-TnT [ng/mL]	0.21 (0.090–0.460)	0.15 (0.070–0.427)	0.500
CRP [mg/L]	23.38 (4.28–57.20)	7.48 (1.91–42.95)	0.546
WBC [$10^3/\mu L$]	9.12 (7.25–11.25)	9.35 (7.03–11.19)	0.753
ECG on admission:			
Sinus rhythm	18 (90%)	33 (82.5%)	0.704
Atrial fibrillation	2 (10%)	6 (15%)	0.707
ST elevation	3 (15%)	15 (37.5%)	0.084
ST depression	3 (15%)	8 (20%)	0.736
Left bundle branch block	1 (5%)	1 (5%)	1.000
QTc prolongation*	2 (10%)	0 (0%)	0.999
TTE parameters:			
Ejection fraction [%]	40.9 ± 11.32	46.52 ± 12.52	0.087
LVDd [mm]	43.5 ± 6.79	46.37 ± 6.06	0.122
LA [mm]	36.05 ± 5.45	37.87 ± 5.30	0.230
Types of TTS:			
Apical type	15 (75%)		
Midventricular type	5 (25%)		
Basal type	0		
Focal type	0		
Type of ACS:			
STEMI		13 (32.5%)	
NSTEMI		26 (65%)	
Unstable angina		1 (2.5%)	
Co-morbidities:			
Hypertension	11 (55%)	30 (75%)	0.146
Diabetes mellitus	4 (20%)	16 (40%)	0.154
Hypercholesterolemia	10 (50%)	23 (57.5%)	0.596
COPD or asthma	1 (5%)	6 (15%)	0.407
Smoking	4 (20%)	18 (45%)	0.088
Cancer	4 (20%)	3 (7.5%)	0.208
Neurologic disorders	1 (5%)	7 (17.5%)	0.249
Psychiatric disorders	4 (20%)	7 (17.5%)	1.000

Data are shown as number (percentage), mean ± standard deviation or median (interquartile range). *QTc ≥ 440 ms and ≥ 460 ms for male and female sex, respectively. BP — blood pressure; COPD — chronic obstructive pulmonary disease; CRP — C-reactvie protein; ECG — electrocardiogram; hs-TnT — high sensitive troponin T; LA — left atrium diameter; LVDd — left ventricular end-diastolic dimension; NSTEMI — non-ST-segment elevation myocardial infarction; QTc — QT interval corrected for heart rate; STEMI — ST-segment elevation myocardial infarction; TTE — transthoracic echocardiogram; WBC — white blood cell count

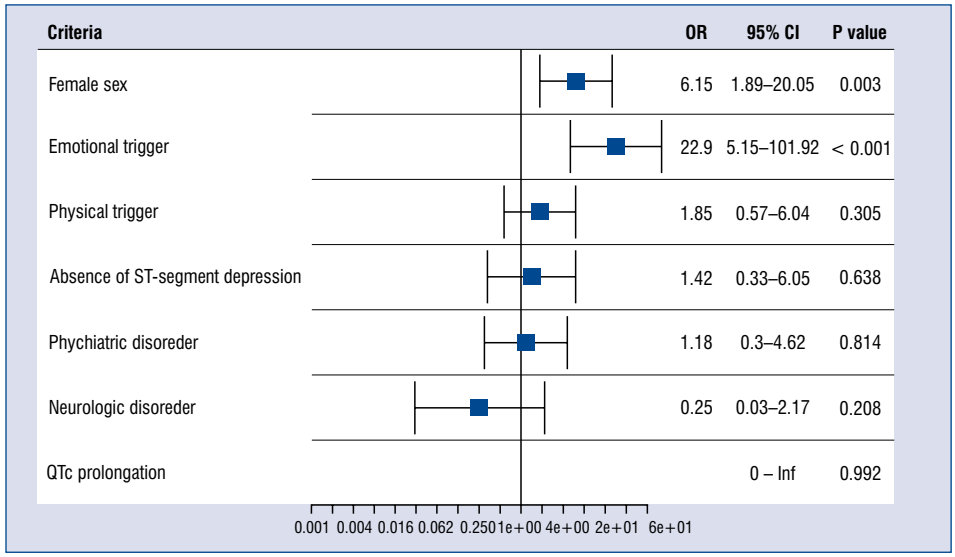

Figure 1. Clinical predictors for the diagnosis of Takotsubo syndrome — variables included in the InterTAK scale. Univariate logistic regression analysis; CI — confidence interval; Inf — infinity; OR — odds ratio.

to ACS group (70% in TTS vs. 27.5% in ACS, $p = 0.002$) and the emotional trigger was more prevalent in this group (65% vs. 7.5%, $p < 0.001$). No significant differences were found in the frequency of physical trigger. The mean value of heart rate and blood pressure at the time of admission were similar in both groups. There were no significant differences between TTS and ACS patients in mean serum troponin levels, C-reactive protein levels and white blood cell count. The analysis of electrocardiogram did not reveal any differences between groups. QTc prolongation was observed in only 2 patients with TTS.

In echocardiography examination no differences were found between the mean value of ejection fraction, LV end-diastolic diameter as well as left atrium diameter in the long axis view.

The incidence of hypertension, diabetes mellitus, hypercholesterolemia, smoking, chronic obstructive pulmonary disease, neoplasm were the same in both groups.

In univariate logistic regression each assessment was performed with each variable included in the InterTAK scale. Assessment of each variable can be seen in Figure 1.

The area under the curve (AUC) for the score was 0.885 (95% confidence interval [CI] 0.78–0.97), using a cut off value of 45 points the score of sensitivity was 75% and specificity 95% for TTS (Fig. 2). When patients with a score of ≥ 50 were diagnosed as TTS, 85% were diagnosed correctly. When patients with score ≤ 31 were diagnosed as ACS, 92% of patients were diagnosed correctly. The relation between InterTAK score values and predicted probability of TTS in the cohort analyzed is shown in Figure 3.

Discussion

Takotsubo syndrome patients have morbidity and mortality rates that are comparable to those of ACS [5, 20–22]. TTS has long been considered a benign disorder. However, in recent years it has been revealed that TTS can be associated with life threatening complications including cardiogenic shock and ventricular arrhythmias [2, 23]. Gili et al. [24] analyzed data from 2,098 TTS patients. Cardiac arrest occurred in 5.9% of them. Although TTS was first described more than 30 years ago, there are still no simple clinical criteria to allow distinguishing TTS from ACS. The most common TTS symptoms are acute chest pain, dyspnea and syncope. Moreover, new electrocardiography changes, elevation of cardiac biomarkers and LV wall motion abnormalities can be observed. Therefore, initially it is difficult to differentiate TTS patients from ACS patients. The first diagnostic criteria for TTS was introduced in 2003 by Abe et al. [25]. Since then, many documents struggling to address this issue have been created. One of the latest is the InterTAK Diagnostic Score, developed by investigators from Switzerland [17]. The InterTAK Diagnostic Score is comprised of 7 clinical parameters that can be easily obtained

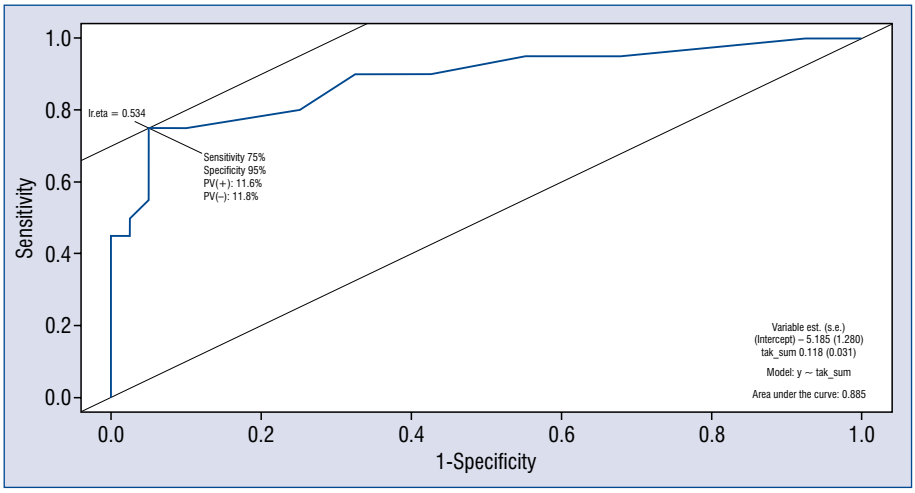

Figure 2. Receiver operating characteristic curve demonstrating area under curve and cut-off point; PV(+) — positive predictive value; PV(–) — negative predictive value.

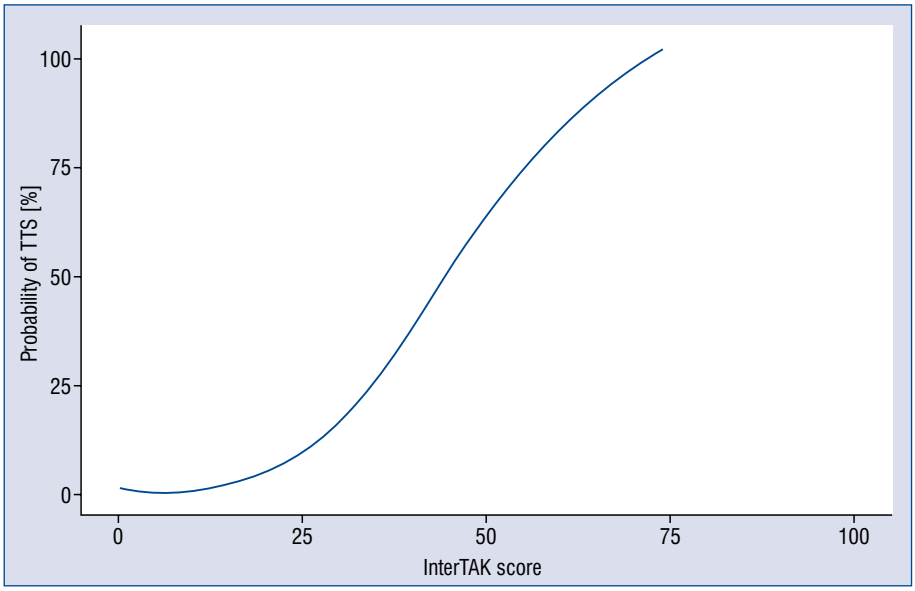

Figure 3. Relation between InterTAK score values and predicted probability of Takotsubo syndrome (TTS) in derivation cohort in the Department of Internal Medicine and Cardiology Medical University of Warsaw.

in an emergency department and do not require an imaging modality. This Score found its place in the algorithm for TTS in the International Expert Consensus Document on Takotsubo Syndrome from 2018. According to an Expert Committee, the InterTAK Diagnostic Score should be considered in symptomatic patients with no ST-segment elevation [1, 2]. In the present study, the usefulness of the InterTAK Diagnostic Score in differentiating TTS from ACS was evaluated among patients hospitalized in the Medical University of Warsaw Clinic in Poland. The score boasts high sensitivity and specificity — these results seem to confirm this thesis. In clinical practice, TTS is not a common condition. The study group size was limited and, due to this fact, calculations were hence affected. TTS mainly affects women in post-menopausal age. Women older than 55 years have an almost 5-fold increase in risk of developing TTS compared to those younger than 55 years [13, 14]. In the current study, 70% of TTS patients were women with a mean age of 72.4 ± 12.99 years. Psychological triggers represent a range of traumatic emotions [20]. However, emotional triggers are not always

negative, as positive emotional events can also provoke TTS. This entity has been described as the "happy heart syndrome" [26]. In the present TTS patients, all psychological triggers were negative and were present in 65% of the group. This however, did not achieve statistical significance for most of the parameters analyzed, but for the female sex and emotional triggers the p-value was < 0.05. These are the two criteria which gained the most points scored in the InterTAK Diagnostic Score.

The AUC for the score was 0.885, which confirms good accuracy of the test. For a cut-off value of 45 points the sum of sensitivity and specificity of the test for the group analyzed was the highest, which is close to the result obtained by investigators from Zurich: AUC = 0.971 (95% CI 0.96–0.98) in a derivation cohort and AUC = 0.901 (95% CI 0.87–0.93) in an independent validation cohort [17]. It is worth mentioning that, when using the InterTAK Score in clinical practice, the real prevalence of TTS must be considered. The current study was based on the model of the one presented by Swiss investigators, and does not reflect a true prevalence of TTS. According to the authors, correction for this bias revealed that a given score value relates to a lower corresponding probability of TTS, but still holds a very strong association of high values with the diagnosis of TTS [17]. According to the International Expert Consensus from 2018, the value of 70 score points or more in clinical practice indicates a high probability for the presence of TTS [2]. Patients with low probability should undergo coronary angiography, while in patients with high score transthoracic echocardiography should be considered.

Limitations of the study

Some of the study limitations were mentioned in the discussion above. First, this study reported a single-center experience. Second, the present study involved retrospective data for score validation. It is obvious that a prospective approach would be more promising. Moreover, the prevalence of TTS in patients admitted to the documented department was low, which affected the sample size. This may explain the lack of statistical significance for some of the parameters analyzed which are included in the InterTAK score and limit generalizability of the present data.

Conclusions

The InterTAK Diagnostic Score might help differentiating TTS from ACSs with high sensitivity and specificity and could be a useful tool for clinicians in the initial decision-making process This finding requires further investigation to confirm its clinical utility.

Conflict of interest: None declared

References

1. Ghadri JR, Wittstein IS, Prasad A, et al. International Expert Consensus Document on Takotsubo Syndrome (Part I): Clinical Characteristics, Diagnostic Criteria, and Pathophysiology. Eur Heart J. 2018; 39(22): 2032–2046, doi: 10.1093/eurheartj/ehy076, indexed in Pubmed: 29850871.
2. Ghadri JR, Wittstein IS, Prasad A, et al. International Expert Consensus Document on Takotsubo Syndrome (Part II): Diagnostic Workup, Outcome, and Management. Eur Heart J. 2018; 39(22): 2047–2062, doi: 10.1093/eurheartj/ehy077, indexed in Pubmed: 29850820.
3. Ghadri JR, Cammann VL, Napp LC, et al. International Takotsubo (InterTAK) Registry. Differences in the Clinical Profile and Outcomes of Typical and Atypical Takotsubo Syndrome: Data From the International Takotsubo Registry. JAMA Cardiol. 2016; 1(3): 335–340, doi: 10.1001/jamacardio.2016.0225, indexed in Pubmed: 27438117.
4. Sharkey SW, Lesser JR, Maron MS, et al. Why not just call it tako-tsubo cardiomyopathy: a discussion of nomenclature. J Am Coll Cardiol. 2011; 57(13): 1496–1497, doi: 10.1016/j.jacc.2010.11.029, indexed in Pubmed: 21435521.
5. Templin C, Ghadri JR, Diekmann J, et al. Clinical Features and Outcomes of Takotsubo (Stress) Cardiomyopathy. N Engl J Med. 2015; 373(10): 929–938, doi: 10.1056/NEJMoa1406761, indexed in Pubmed: 26332547.
6. Kato K, Lyon AR, Ghadri JR, et al. Takotsubo syndrome: aetiology, presentation and treatment. Heart. 2017; 103(18): 1461–1469, doi: 10.1136/heartjnl-2016-309783, indexed in Pubmed: 28839096.
7. Di Vece D, Citro R, Cammann VL, et al. Outcomes Associated With Cardiogenic Shock in Takotsubo Syndrome. Circulation. 2019; 139(3): 413–415, doi: 10.1161/CIRCULATIONAHA.118.036164, indexed in Pubmed: 30586690.
8. Frangieh AH, Obeid S, Ghadri JR, et al. InterTAK Collaborators. ECG Criteria to Differentiate Between Takotsubo (Stress) Cardiomyopathy and Myocardial Infarction. J Am Heart Assoc. 2016; 5(6), doi: 10.1161/JAHA.116.003418, indexed in Pubmed: 27412903.
9. Opolski G, Pawlak MM, Roik MF, et al. Clinical presentation, treatment, and long-term outcomes in patients with takotsubo cardiomyopathy. Experience of a single cardiology center. Pol Arch Med Wewn. 2010; 120(6): 231–236, indexed in Pubmed: 20567207.
10. Pawlak M, Roik M, Kochanowski J, et al. Comparison of on-admission ST-segment elevation tako-tsubo patients and myocardial infarction women: in-hospital course and long-term follow-up. Kardiol Pol. 2012; 70(3): 233–240, indexed in Pubmed: 22430401.
11. Prasad A, Lerman A, Rihal CS. Apical ballooning syndrome (Tako-Tsubo or stress cardiomyopathy): a mimic of acute myocardial infarction. Am Heart J. 2008; 155(3): 408–417, doi: 10.1016/j.ahj.2007.11.008, indexed in Pubmed: 18294473.

12. Deshmukh A, Kumar G, Pant S, et al. Prevalence of Takotsubo cardiomyopathy in the United States. Am Heart J. 2012; 164(1): 66–71. e1, doi: 10.1016/j.ahj.2012.03.020, indexed in Pubmed: 22795284.
13. Schneider B, Athanasiadis A, Stöllberger C, et al. Gender differences in the manifestation of tako-tsubo cardiomyopathy. Int J Cardiol. 2013; 166(3): 584–588, doi: 10.1016/j.ijcard.2011.11.027, indexed in Pubmed: 22192296.
14. Roshanzamir S, Showkathali R. Takotsubo cardiomyopathy a short review. Curr Cardiol Rev. 2013; 9(3): 191–196, indexed in Pubmed: 23642025.
15. Dias A, Núñez Gil IJ, Santoro F, et al. Takotsubo syndrome: State-of-the-art review by an expert panel - Part 1. Cardiovasc Revasc Med. 2019; 20(1): 70–79, doi: 10.1016/j.carrev.2018.11.015, indexed in Pubmed: 30528096.
16. Kochanowski J, Piatkowski R, Budnik M, et al. Biventricular takotsubo cardiomyopathy in an elderly woman with uncontrolled type 2 diabetes: the biphasic echocardiographic and clinical pattern. Acta Diabetol. 2016; 53(6): 1061–1063, doi: 10.1007/s00592-016-0916-3, indexed in Pubmed: 27665438.
17. Ghadri JR, Cammann VL, Jurisic S, et al. A novel clinical score (InterTAK Diagnostic Score) to differentiate takotsubo syndrome from acute coronary syndrome: results from the International Takotsubo Registry. Eur J Heart Fail. 2017; 19(8): 1036–1042, doi: 10.1002/ejhf.683, indexed in Pubmed: 27928880.
18. Ibanez B, James S, Agewall S, et al. ESC Scientific Document Group. 2017 ESC Guidelines for the management of acute myocardial infarction in patients presenting with ST-segment elevation: The Task Force for the management of acute myocardial infarction in patients presenting with ST-segment elevation of the European Society of Cardiology (ESC). Eur Heart J. 2018; 39(2): 119–177, doi: 10.1093/eurheartj/ehx393, indexed in Pubmed: 28886621.
19. Roffi M, Patrono C, Collet JP, et al. 2015 ESC Guidelines for the management of acute coronary syndromes in patients presenting without persistent ST-segment elevation: Task Force for the Management of Acute Coronary Syndromes in Patients Presenting without Persistent ST-Segment Elevation of the European Society of Cardiology (ESC). Eur Heart J. 2016; 37(3): 267–315, doi: 10.1093/eurheartj/ehv320, indexed in Pubmed: 26320110.
20. Sharkey SW, Windenburg DC, Lesser JR, et al. Natural history and expansive clinical profile of stress (tako-tsubo) cardiomyopathy. J Am Coll Cardiol. 2010; 55(4): 333–341, doi: 10.1016/j.jacc.2009.08.057, indexed in Pubmed: 20117439.
21. Ghadri JR, Kato K, Cammann VL, et al. Long-Term Prognosis of Patients With Takotsubo Syndrome. J Am Coll Cardiol. 2018; 72(8): 874–882, doi: 10.1016/j.jacc.2018.06.016, indexed in Pubmed: 30115226.
22. Dias A, Núñez Gil IJ, Santoro F, et al. Takotsubo syndrome: State-of-the-art review by an expert panel - Part 2. Cardiovasc Revasc Med. 2019; 20(2): 153–166, doi: 10.1016/j.carrev.2018.11.016, indexed in Pubmed: 30581088.
23. Di Vece D, Citro R, Templin C, et al. Outcomes Associated With Cardiogenic Shock in Takotsubo Syndrome. Circulation. 2019; 139(3): 413–415, doi: 10.1161/CIRCULATIONAHA.118.036164, indexed in Pubmed: 30586690.
24. Gili S, Cammann VL, Schlossbauer SA, et al. Cardiac arrest in takotsubo syndrome: results from the InterTAK Registry. Eur Heart J. 2019; 40(26): 2142–2151, doi: 10.1093/eurheartj/ehz170, indexed in Pubmed: 31098611.
25. Abe Y, Kondo M, Matsuoka R, et al. Assessment of clinical features in transient left ventricular apical ballooning. J Am Coll Cardiol. 2003; 41(5): 737–742, doi: 10.1016/s0735-1097(02)02925-x, indexed in Pubmed: 12628715.
26. Ghadri JR, Sarcon A, Diekmann J, et al. InterTAK Co-investigators:. Happy heart syndrome: role of positive emotional stress in takotsubo syndrome. Eur Heart J. 2016; 37(37): 2823–2829, doi: 10.1093/eurheartj/ehv757, indexed in Pubmed: 26935270.

VIA MEDICA

ORIGINAL ARTICLE

Cardiology Journal
2021, Vol. 28, No. 3, 423–430
DOI: 10.5603/CJ.a2019.0088

ISSN 1897–5593
eISSN 1898–018X

Predictors of pacing-dependency in patients with cardiovascular implantable electronic devices

Wolfram Grimm[1], Kathrin Grimm[1], Brandon Greene[2], Mariana Parahuleva[1]

[1]Department of Cardiology, University Hospital of Marburg and Gießen, Philipps-University Marburg, Marburg, Germany
[2]Institute for Medical Bioinformatics and Biostatistics, Philipps-University Marburg, Marburg, Germany

Abstract

Background: *Data on the prevalence and predictors for the development of pacing-dependency in patients with cardiovascular implantable electronic devices (CIEDs) are sparse.*

Methods: *Pacing-dependency defined as an absence of intrinsic rhythm of ≥ 30 bpm was determined in 802 consecutive patients with CIEDs who visited the documented pacemaker or implantable cardioverter-defibrillator outpatient clinic for routine follow-up.*

Results: *A total of 131 (16%) patients were found to be pacing-dependent 67 ± 70 months after CIED implant. Multivariate analysis revealed a significant association between pacing-dependency and the following clinical variables: second or third-degree atrioventricular (AV) block at implant (OR = 19.9; 95% CI: 10.9–38.5, p < 0.01), atrial fibrillation at implant (OR = 2.15; 95% CI: 1.16–4.05, p = 0.02), left ventricular ejection fraction (LVEF) ≤ 30% (OR = 2.06; 95% CI: 1.03–4.15, p = 0.04), B-type natriuretic peptide (BNP) > 150 pg/mL (OR = 2.12; 95% CI: 1.16–3.97, p = 0.02), chronic kidney disease (OR = 1.86; 95% CI: 1.08–3.26, p = 0.03), and follow-up duration after implantation > 5 years (OR = 3.29; 95% CI: 1.96–5.64, p < 0.01). None of the remaining clinical variables including age, gender, diabetes mellitus, underlying heart disease, prior cardiac surgery or medication during follow-up including beta-blockers and amiodarone predicted pacing-dependency.*

Conclusions: *Pacing-dependency is associated with second or third-degree AV-block at implant, atrial fibrillation before implant, low LVEF, elevated BNP, chronic kidney disease and follow-up duration after implant.* (Cardiol J 2021; 28, 3: 423–430)

Key words: pacing-dependency, permanent pacemaker, implantable cardioverter-defibrillator

Introduction

Knowledge of pacing-dependency following implantation of cardiovascular implantable electronic devices (CIEDs) is very important in various clinical settings including elective generator change, potential electromagnetic interference and management of suspected lead or generator malfunction [1, 2]. Although several million permanent pacemakers and implantable cardioverter-defibrillators (ICDs) with bradycardia pacing capability have been implanted 60 years after the first pacemaker implantation in 1958, few studies have investigated the prevalence of pacing dependency and clinical predictors for the development of pacing dependency [3–17]. Thus, the aim herein was to determine prevalence and predictors of pacing dependency in a well-defined cohort of 802 patients with pacemakers or ICDs at the documented clinic.

Address for correspondence: Wolfram Grimm, MD, Department of Cardiology, Philipps-University Marburg, Baldingerstraße, 35033 Marburg, Germany, tel: +49-6421-586-9748, fax: +49-6421-586-8954, e-mail: grimmwk.rauschenberg@t-online.de

Received: 1.04.2019 Accepted: 26.08.2019

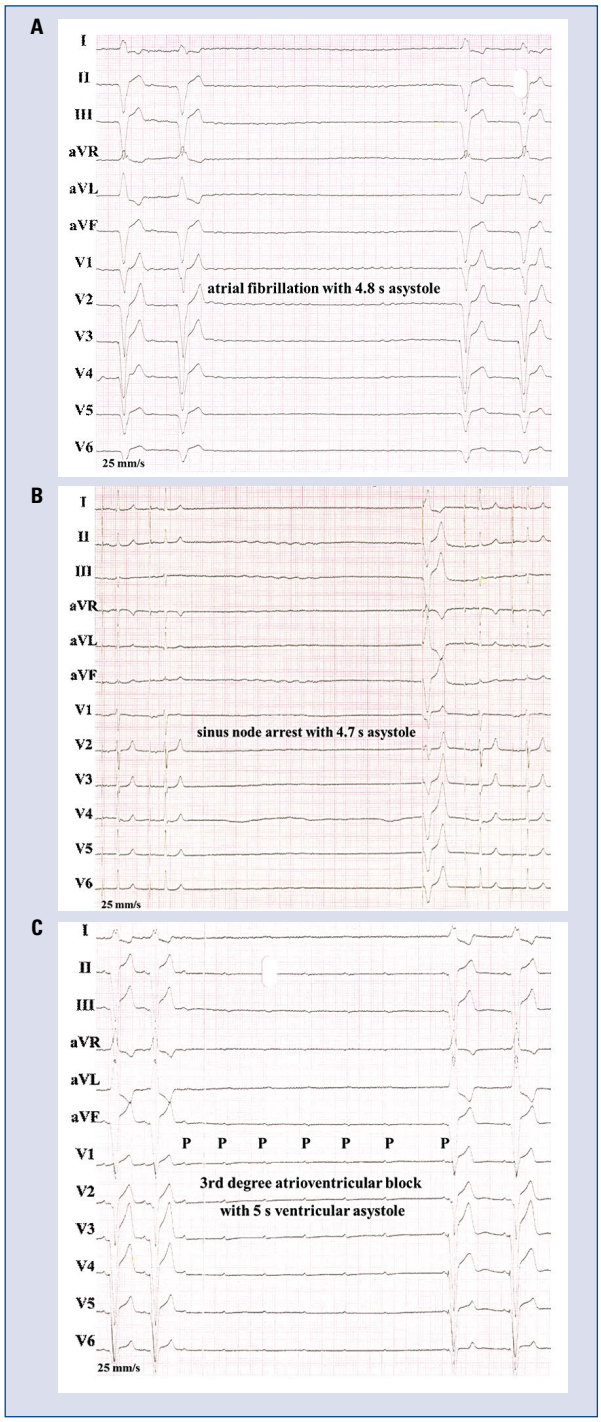

Figure 1. Electrocardiogram recordings with a paper speed of 25 mm/s showing typical examples of ventricular asystole following transient inhibition of pacing; **A.** Ventricular asystole due to third degree atrioventricular block (AVB) without ventricular escape rhythm in a patient with permanent atrial fibrillation; **B.** Ventricular asystole due to sinus arrest without escape rhythm in a patient with sinus node disease; **C.** Ventricular asystole due to third degree AVB without ventricular escape rhythm in a patient with second degree AVB type Mobitz at the time of pacemaker implant.

Methods

Study population

After written informed consent had been obtained, pacing dependency was determined prospectively in 802 consecutive patients who came to the pacemaker and ICD outpatient clinic for routine follow-up between January 2018 and December 2018 and in whom a permanent pacemaker or ICD had been implanted for at least 6 months by this institution. Pacing dependency was defined as an absence of intrinsic rhythm ≥ 30 bpm after lowering the pacing rate to 30 bpm for at least 10 s or after transient inhibition of pacing therapy (Fig. 1). A high-degree atrioventricular (AV) block at implant was defined as second degree AV block type Mobitz or third-degree AV block. Chronic kidney disease (CKD) of at least stage 3 was diagnosed in the presence of at least two estimated glomerular filtration rates (eGFR) using the Modification of Diet in Renal Disease formula below 60 mL/min per 1.73 m^2 with an interval of at least 3 months. The study protocol was reviewed and approved by the ethics committee of the Philipps-University of Marburg.

Statistical analysis

Results are expressed as mean ± standard deviation (SD) for continuous variables with normal distribution and median values with interquartile range (IQR) for continuous variables without normal distribution. Univariate comparisons of clinical characteristics between patients with and without pacing dependency were performed using the Student t-test or the Mann-Whitney U test for continuous variables, categorical values were compared using χ^2 and the Fisher exact tests, where appropriate. Logistic regression analysis was used to generate a multivariate model including all potential predictors of pacing dependency listed in Table 1 in order to investigate which factors showed independent effects on the risk of developing pacemaker dependency after adjustment for confounding by other factors including the presence or absence of ICD therapy as well as cardiac resynchronization therapy (CRT). All probability values reported are two-sided, and a probability value of $p < 0.05$ was considered to indicate statistical significance. R-software version 3.5.0 (www.R-project.org) was used for statistical analyses.

Results

Clinical characteristics

The clinical characteristics of 802 study patients are summarized in Table 1 and included 563

Table 1. Clinical characteristics of 802 patients with and without pacing dependency.

Clinical variable	All patients	Pacing-dependency		P
	N = 802	Yes (n = 131)	No (n = 671)	
Age [years]	74 ± 13	75 ± 12	74 ± 13	0.23
Male gender	521 (65%)	89 (68%)	432 (64%)	0.50
Body mass index [kg/m^2]	28 ± 12	28 ± 5	28 ± 13	0.86
Arterial hypertension	622 (78%)	105 (80%)	517 (77%)	0.27
Diabetes mellitus	143 (18%)	19 (15%)	124 (18%)	0.43
Atrial fibrillation before implant	242 (30%)	38 (29%)	205 (31%)	0.78
Left bundle branch block at implant	141 (18%)	25 (19%)	116 (17%)	0.62
Chronic kidney disease	330 (41%)	70 (53%)	260 (39%)	< 0.01
Heart failure severity				
Left ventricular ejection fraction ≤ 30%	179 (22%)	41 (31%)	138 (21%)	< 0.01
NYHA functional class III or IV	320 (40%)	74 (56%)	246 (37%)	< 0.01
B-type natriuretic peptide >150 pg/mL[a]	408 (57%)	77 (71%)	331 (54%)	< 0.01
Underlying cardiac disease				0.07
Coronary artery disease	313 (39%)	45 (34%)	268 (40%)	
Nonischemic dilated cardiomyopathy	119 (15%)	26 (20%)	93 (14%)	
Hypertensive heart disease	180 (22%)	35 (31%)	145 (22%)	
Valvular heart disease	101 (13%)	17 (15%)	84 (13%)	
Other cardiac diseases[b]	13 (2%)	4 (4%)	9 (1%)	
No structural heart disease	76 (9%)	4 (4%)	72 (11%)	
Previous cardiac surgery				
Aortocoronary bypass grafting	95 (12%)	17 (13%)	78 (12%)	0.77
Surgical aortic valve replacement	29 (4%)	4 (3%)	25 (4%)	0.90
Mitral valve reconstruction or replacement	15 (2%)	1 (1%)	14 (2%)	0.50
Transcatheter aortic valve replacement	43 (5%)	9 (7%)	34 (5%)	0.53
Cardiovascular implantable electronic device				
Antibradycardia pacemaker	563 (70%)	103 (79%)	460 (69%)	0.02
Implantable cardioverter-defibrillator	239 (30%)	28 (21%)	211 (31%)	0.02
Cardiac resynchronization therapy device	93 (12%)	20 (15%)	73 (11%)	0.07
Median amount of ventricular pacing (IQR)	30% (1–99)	100% (99–100)	12% (1–82)	< 0.01
Indication for CIED implantation				< 0.01
Sick sinus syndrome	196 (24%)	12 (9%)	184 (27%)	
Second or third-degree AV block	247 (31%)	95 (73%)	152 (23%)	
Atrial fibrillation with bradycardia	125 (16%)	14(11%)	111 (17%)	
Carotid sinus syndrome	2 (0.2%)	0 (0%)	2 (0.3%)	
Prophylactic[c]	232 (29%)	10 (7%)	222 (33%)	
Implant duration > 5 years	**330 (41%)**	**74 (56%)**	256 (38%)	**< 0.01**
Medication				
Beta-blockers	539 (67%)	85 (65%)	454 (68%)	0.14
Amiodarone	44 (5%)	7 (5%)	37 (6%)	0.94
Digitalis	68 (8%)	9 (7%)	59 (9%)	0.58
ACEI	419 (52%)	77 (59%)	342 (51%)	0.12
Angiotensin receptor blockers	171 (21%)	25 (19%)	146 (22%)	0.57
Diuretics	549 (68%)	100 (76%)	449 (67%)	0.04
Aldosterone antagonists	226 (28%)	28 (21%)	198 (30%)	0.07
Angiotensin-neprilysin inhibitor	25 (3%)	1 (1%)	24 (4%)	0.16

Plus-minus values are given as mean ± standard deviation; ACEI — angiotensin converting enzyme inhibitors; AV — atrioventricular; CIED — cardiovascular implantable electronic device; IQR — interquartile range; NYHA — New York Heart Association
[a]B-type natriuretic peptide was available in only 702 of 802 patients (88%)
[b]Other cardiac diseases include hypertrophic cardiomyopathy, cardiac sarcoidosis, cardiac amyloidosis, and tricuspid valve replacement
[c]Implantable cardioverter-defibrillator without symptomatic bradyarrhythmia at implant

(70%) patients with a permanent pacemaker and 239 (30%) patients with an ICD. Mean duration between device implant and follow-up visit was 67 ± 70 months with a minimum implant duration of 6 months. The majority of patients were male (65%). Mean age at device implant was 74 ± 13 years. Indication for pacemaker implantation was a high-degree AV block in 247 (31%) patients, sick sinus syndrome in 196 (24%) patients, carotid sinus syndrome in 2 (0.2%) patients, and atrial fibrillation with bradycardia in 125 (16%) patients. CRT devices were implanted in 93 of 802 study patients (12%) including CRT pacemakers in 25 of 563 pacemaker patients (4%) and CRT defibrillators in 68 of 239 (28%) patients with an ICD.

Prevalence and predictors of pacing dependency

A total of 131 of 802 study patients (16%) were found to be pacing dependent at follow-up 67 ± 70 months after the device implant. Pacing dependency at follow-up was found significantly more often in patients with New York Heart Association (NYHA) heart failure class 3 or 4, elevated B-type natriuretic peptide (BNP) > 150 pg/mL, decreased left ventricular ejection fraction (LVEF) ≤ 30%, CKD, high degree AV block at implant, left bundle branch block on electrocardiogram at implant, and implant duration > 5 years (Table 1). Multivariate logistic regression analysis revealed a significant association between pacing dependency and the following 6 clinical variables: second or third-degree AV block at implant (odds ratio [OR] = 19.9; 95% confidence interval [CI]: 10.9–38.5, p < 0.01), atrial fibrillation at implant (OR = 2.15; 95% CI: 1.16–4.05, p = 0.02), LVEF ≤ 30% (OR = 2.06; 95% CI: 1.03–4.15, p = 0.04), BNP > 150 pg/mL (OR = 2.12; 95% CI: 1.16–3.97, p = 0.02), CKD (OR = 1.86; 95% CI = 1.08–3.26, p = 0.03), and follow-up duration > 5 years (OR = 3.29; 95% CI: 1.96–5.64, p < 0.01) (Table 2). None of the remaining clinical variables including age, gender, body mass index, arterial hypertension, diabetes mellitus, underlying heart disease, prior cardiac surgery, transcatheter aortic valve replacement or medication during follow-up including beta-blockers and amiodarone predicted pacing dependency.

Subgroup analysis of 563 patients with permanent pacemaker

The results for the subgroup of 563 patients with permanent pacemaker without cardioverter defibrillator back-up are summarized in Table 3. Pacing dependency at follow-up was found significantly more often in patients with NYHA heart failure class 3 or 4, elevated BNP > 150 pg/mL, decreased LVEF ≤ 30%, CKD, second or third-degree AV block at implant, and implant duration > 5 years.

Subgroup analysis of 239 patients with ICD

The results for the subgroup of 239 patients with ICD are summarized in Table 4. Pacing dependency at follow-up was found significantly more often in patients with NYHA heart failure class 3 or 4, elevated BNP > 150 pg/mL, decreased LVEF ≤ 30%, CKD, non-ischemic dilated cardiomyopathy, amiodarone therapy, and implant duration > 5 years. In addition, left bundle branch block at implant, which was treated with a CRT defibrillator in 68 patients with ICD, was also associated with a higher prevalence of pacing dependency at follow-up (Table 4).

Discussion

The main finding of the present study is a 16% prevalence of pacing dependency at 67 months mean follow-up, which was associated with second or third-degree AV-block at implant, atrial fibrillation before implant, low LVEF, elevated BNP, CKD and implant duration. Although it is generally accepted that pacing dependency means absence of a sufficient intrinsic rhythm resulting in bradycardia-related symptoms during inhibition of pacing, the definition of pacing dependency is still controversial [12–14]. Similar to previous studies [5–7, 10], the current study defined pacing dependency as absence of an intrinsic rhythm of at least 30 bpm during pacemaker inhibition or ventricular pacing at a rate of lower than 30 bpm, whereas other investigators used an upper rate cutoff for the intrinsic rhythm of 40 bpm [4, 8, 9, 11] or 50 bpm [3] to define pacing dependency. The observed prevalence of pacing dependency of 16% in the present study is similar to the prevalence of 22% in a relatively large Canadian Trial of Physiologic Pacing (CTOPP), in which a pacemaker dependency test was performed in 2244 patients [4]. Of note, the prevalence of pacing dependency varies in the literature between 2% in the study of Lekalowski et al. [6] and 63% in the study of Merin et al. [8] as summarized in Table 5. The discrepancy between these studies may, in part, be explained by differences in study patients as well as different definitions used for pacing dependency. Whereas the current study enrolled consecutive patients who came for routine device follow-up visits at

Table 2. Results of the multivariate analysis for pacing dependency in 802 study patients.

Clinical variable	OR (95% CI)[a]	P[a]
Left ventricular ejection fraction ≤ 30%	2.06 (1.03–4.15)	0.04
B-type natriuretic peptide > 150 pg/mL	2.12 (1.16–3.97)	0.02
Second- or third-degree AV block at implant	19.9 (10.9– 8.5)	< 0.01
Atrial fibrillation before implant	2.15 (1.16–4.05)	0.02
Chronic kidney disease	1.86 (1.08–3.26)	0.03
Implant duration > 5 years	3.29 (1.96–5.64)	< 0.01

[a]After adjustment for potential confounding clinical variables as summarized in Table 1 including medication, implantable cardioverter defibrillator therapy and cardiac resynchronization therapy; AV — atrioventricular; CI — confidence interval; OR — odds ratio

Table 3. Subgroup analysis of 563 patients with permanent pacemaker.

Clinical variable	All patients	Pacemaker dependency		P
	N = 563	Yes (n = 103)	No (n = 460)	
Age [years]	76 ± 12	77 ± 12	76 ± 12	0.57
Male gender	336 (60%)	68 (66%)	268 (58%)	0.18
Atrial fibrillation before implant	194 (34%)	30 (29%)	164 (36%)	0.25
Left bundle branch block at implant	71 (13%)	11 (11%)	60 (13%)	0.51
Chronic kidney disease	230 (41%)	55 (53%)	175 (38%)	< 0.01
Heart failure severity				
Left ventricular ejection fraction ≤ 30%	60 (11%)	18 (17%)	42 (9%)	0.02
NYHA functional class III or IV	195 (35%)	53 (51%)	142 (31%)	< 0.01
B-type natriuretic peptide > 150 pg/mL[a]	264 (54%)	56 (68%)	208 (51%)	< 0.01
Underlying cardiac disease				0.05
Coronary artery disease	201 (36%)	37 (37%)	164 (36%)	
Nonischemic dilated cardiomyopathy	26 (5%)	8 (8%)	18 (4%)	
Hypertensive heart disease	169 (30%)	35 (34%)	134 (29%)	
Valvular heart disease	88 (16%)	16 (16%)	72 (16%)	
Other cardiac diseases[b]	5 (1%)	3 (3%)	2 (0.4%)	
No structural heart disease	74 (13%)	4 (4%)	70 (15%)	
Previous cardiac surgery				
Aortocoronary bypass grafting	55 (10%)	11 (11%)	44 (10%)	0.87
Surgical aortic valve replacement	20 (4%)	4 (4%)	16 (3%)	0.84
Mitral valve reconstruction or replacement	12 (2%)	1 (1%)	11 (2%)	0.37
Transcatheter aortic valve replacement	41 (7%)	8 (8%)	33 (7%)	0.83
Indication for pacemaker implantation				< 0.01
Sick sinus syndrome	190 (34%)	12 (12%)	178 (39%)	
Second or third-degree AV block	227 (40%)	79 (77%)	148 (32%)	
Atrial fibrillation with bradycardia	119 (21%)	12 (12%)	107 (23%)	
Carotid sinus syndrome	2 (0.4%)	0 (0%)	2 (0.4%)	
Cardiac resynchronisation[b]	25 (4%)	0 (0%)	25 (5%)	
Implant duration > 5 years	**222 (39%)**	**59 (57%)**	**163 (35%)**	**< 0.01**
Medication				
Beta-blockers	331 (59%)	59 (57%)	272 (59%)	0.47
Amiodarone	18 (3%)	0 (0%)	18 (4%)	0.08
Digitalis	46 (8%)	5 (5%)	41 (9%)	0.25
ACEI	278 (43%)	58 (56%)	220 (48%)	0.15
Angiotensin receptor blockers	114 (20%)	18 (17%)	96 (21%)	0.52
Diuretics	362 (64%)	73 (71%)	289 (63%)	0.12
Aldosterone antagonists	89 (16%)	12 (12%)	77 (17%)	0.26
Angiotensin-neprilysin inhibitor	9 (2%)	1 (1%)	8 (2%)	0.89

[a]B-type natriuretic peptide was available only in 467 of 539 patients (66%); [b]Patients with heart failure and left bundle branch block; abbreviations as in Table 1.

Table 4. Subgroup analysis of 239 patients with implantable cardioverter-defibrillator.

Clinical variable	All patients	Pacemaker dependency		P
	N = 239	Yes (n = 28)	No (n = 211)	
Age [years]	68 ± 12	68 ± 12	68 ± 12	0.93
Male gender	185 (77%)	21 (75%)	164 (78%)	0.81
Atrial fibrillation before implant	48 (20%)	8 (29%)	40 (19%)	0.41
Left bundle branch block at implant	70 (29%)	14 (50%)	56 (25%)	0.02
Chronic kidney disease	100 (42%)	15 (54%)	85 (40%)	0.18
Heart failure severity				
Left ventricular ejection fraction ≤ 30%	119 (50%)	23 (82%)	96 (45%)	< 0.01
NYHA functional class III or IV	125 (52%)	21 (75%)	104 (49%)	0.01
B-type natriuretic peptide > 150 pg/mL[a]	144 (61%)	21 (78%)	123 (59%)	< 0.01
Underlying cardiac disease				0.03
Coronary artery disease	112 (47%)	8 (29%)	104 (49%)	
Nonischemic dilated cardiomyopathy	93 (39%)	18 (64%)	75 (36%)	
Hypertensive heart disease	11 (5%)	0 (0%)	11 (5%)	
Valvular heart disease	13 (5%)	1 (4%)	12 (6%)	
Other cardiac diseases[b]	8 (3%)	1 (4%)	7 (3%)	
No structural heart disease	2 (1%)	0 (0%)	2 (1%)	
Previous cardiac surgery				
Aortocoronary bypass grafting	40 (17%)	6 (21%)	34 (16%)	0.66
Surgical aortic valve replacement	9 (4%)	0 (0%)	9 (4%)	0.27
Mitral valve reconstruction or replacement	3 (1%)	0 (0%)	3 (1%)	1.00
Transcatheter aortic-valve replacement	2 (1%)	1 (4%)	1 (0.5%)	0.56
Indication for antibradycardia pacing at ICD implant				< 0.01
Sick sinus syndrome	6 (3%)	0 (0%)	6 (3%)	
Second or third-degree AV block	20 (8%)	16 (57%)	4 (2%)	
Atrial fibrillation with bradycardia	6 (3%)	2 (7%)	4 (2%)	
Cardiac resynchronization therapy[b]	68 (28%)	20 (71%)	48 (23%)	
Implant duration > 5 years	**108 (45%)**	**15 (54%)**	**93 (44%)**	**0.03**
Medication				
Beta-blockers	208 (87%)	26 (93%)	182 (86%)	0.49
Amiodarone	26 (11%)	7 (25%)	19 (9%)	0.03
Digitalis	22 (9%)	4 (14%)	18 (9%)	0.52
ACEI	141 (59%)	19 (68%)	122 (58%)	0.31
Angiotensin receptor blockers	57 (24%)	7 (25%)	50 (24%)	0.88
Diuretics	187 (78%)	27 (96%)	160 (76%)	0.03
Aldosterone antagonists	137 (57%)	16 (57%)	121 (57%)	0.98
Angiotensin-neprilysin inhibitor	16 (7%)	0 (0%)	16 (8%)	0.27

[a]B-type natriuretic peptide was available in 235 of 239 patients (98%); [b]Patients with heart failure and left bundle branch block; abbreviations as in Table 1.

the pacemaker and ICD outpatient department, Nagatamo et al. [5] excluded patients with an intrinsic rate of < 30 bpm at implant which likely contributed to a low prevalence of pacing dependency of 4% in the study by Nagatamo et al. [5]. In contrast to the study by Nagatamo et al. [5] and the present study, Merin et al. [8] found a high prevalence of pacing dependency of 63% during follow-up. This discrepancy is likely to be due to the fact that the majority of patients in the study of Merin et al. [8] received a permanent pacemaker for third degree AV block without

Table 5. Prevalence of pacing-dependency in studies with at least 50 patients.

Author	Year	Patients	ICD	Cardiac surgery	Follow-up [months]	Pacing-dependency	Intrinsic rhythm [bpm][a]
Glikson et al. [3]	1997	86	0%	100%	41 (median)	51 (59%)	< 50
Tang et al. [4]	2001	2244	0%	NA	2 to 8	484 (22%)	< 40
Nagatomo et al. [5]	2004	518	0%	NA	44 ± 32	23 (4%)	< 30
Lelakowski et al. [6]	2007	3638	0%	NA	58 ± 22	76 (2%)	< 30
Onalan et al. [7]	2008	102	0%	100%	48 (mean)	21 (23%)	< 30
Merin et al. [8]	2009	58	0%	100%	72 ± 32	37 (63%)	< 40
Raza et al. [9]	2011	90	0%	100%	67 ± 50	36 (40%)	< 40
Rene et al. [10]	2013	98	0%	100%	43 ± 41	44 (45%)	< 30
Sood et al. [11]	2013	1058	100%	NA	50 ± 41	142 (13%)	< 40[b]
Present study	2019	802	30%	30%	67 ± 70	131 (16%)	< 30

[a]Intrinsic rhythm used to define pacemaker dependency; [b]Intrinsic rhythm < 40 bpm or < 50 bpm with symptoms; NA — data not available

sufficient ventricular escape rhythm following cardiac surgery [8].

The most important predictor of pacing dependency during follow-up in the current study was the presence second degree AV block type Mobitz or third-degree AV block at the time of pacemaker implant. This is consistent with the findings of most previous studies in patients with and without cardiac surgery prior to pacemaker implant [3, 5–8, 15–17]. Several previous investigators also found an association between pacing dependency during follow-up and body mass index [7], age [11], male gender [11], and a history of coronary artery disease [16]. Whereas none of these variables predicted pacing dependency in the present study, a significant association was found between pacing dependency and heart failure severity as indexed by a low LVEF ≤ 30% and an elevated BNP level. Furthermore, amiodarone use was associated with pacing dependency in the subgroup of patients with ICD in the current study. This is consistent with the results of Sood et al. [11], who also found a significant association between pacing dependency and amiodarone use in a large cohort of 1058 patients with ICD. The results of the present study support the hypothesis that patients with heart failure and high degree AV block at implant will probably be paced more frequently in the ventricle and may therefore benefit from physiological pacing [4]. Although CKD is a generally accepted important comorbidity in patients with heart disease of any etiology with regard to overall survival, the association between CKD and pacing dependency has not been investigated in previous studies [2–17]. Multivariate analysis in the current study revealed a twofold risk for pacing dependency in patients with CKD compared to patients without CKD.

Limitations of the study

There are several limitations of the present study. First, clinical patient data and implant data were collected retrospectively, although pacing dependency was determined prospectively between January 2018 and December 2018 at the documented pacemaker and ICD outpatient department. Secondly, pacing dependency was determined during a brief period of time at a single outpatient visit. It is well known that pacing dependency can occur transiently. Therefore, repeated pacing dependency tests and longer monitoring time may have revealed patients, in whom pacing dependency may have resolved or may have occurred at other times.

Conclusions

In conclusion, pacing dependency after CIED implantation depends on the pacing indication and is much more common in patients with high-degree AV-block at implant compared to patients with sick sinus syndrome. In addition, pacing dependency is associated with more advanced heart failure, CKD and follow-up duration after implant. Since pacing dependent patients who suffer from heart failure will need frequent ventricular pacing, physiological pacing should be considered in these patients.

Conflict of interest: None declared

References

1. Brignole M, Auricchio A, Baron-Esquivias G, et al. ESC Committee for Practice Guidelines (CPG), Document Reviewers. 2013 ESC Guidelines on cardiac pacing and cardiac resynchronization therapy: the Task Force on cardiac pacing and resynchronization therapy of the European Society of Cardiology (ESC). Developed in collaboration with the European Heart Rhythm Association (EHRA). Eur Heart J. 2013; 34(29): 2281–2329, doi: 10.1093/eurheartj/eht150, indexed in Pubmed: 23801822.
2. Steyers CM. 3rd, khera R, bhave P. Pacemaker dependency after cardiac surgery: a systematic review of current evidence. PLoS One. 2015; 10: e0140340.
3. Glikson M, Dearani JA, Hyberger LK, et al. Indications, effectiveness, and long-term dependency in permanent pacing after cardiac surgery. Am J Cardiol. 1997; 80(10): 1309–1313, doi: 10.1016/s0002-9149(97)00671-1, indexed in Pubmed: 9388104.
4. Tang AS, Roberts RS, Kerr C, et al. Relationship between pacemaker dependency and the effect of pacing mode on cardiovascular outcomes. Circulation. 2001; 103(25): 3081–3085, doi: 10.1161/01.cir.103.25.3081, indexed in Pubmed: 11425772.
5. Nagatomo T, Abe H, Kikuchi K, et al. New onset of pacemaker dependency after permanent pacemaker implantation. Pacing Clin Electrophysiol. 2004; 27(4): 475–479, doi: 10.1111/j.1540-8159.2004.00466.x, indexed in Pubmed: 15078400.
6. Lelakowski J, Majewski J, Bednarek J, et al. Pacemaker dependency after pacemaker implantation. Cardiol J. 2007; 14(1): 83–86, indexed in Pubmed: 18651439.
7. Onalan O, Crystal A, Lashevsky I, et al. Determinants of pacemaker dependency after coronary and/or mitral or aortic valve surgery with long-term follow-up. Am J Cardiol. 2008; 101(2): 203–208, doi: 10.1016/j.amjcard.2007.07.062, indexed in Pubmed: 18178407.
8. Merin O, Ilan M, Oren A, et al. Permanent pacemaker implantation following cardiac surgery: indications and long-term follow-up. Pacing Clin Electrophysiol. 2009; 32(1): 7–12, doi: 10.1111/j.1540-8159.2009.02170.x, indexed in Pubmed: 19140907.
9. Raza SS, Li JM, John R, et al. Long-term mortality and pacing outcomes of patients with permanent pacemaker implantation after cardiac surgery. Pacing Clin Electrophysiol. 2011; 34(3): 331–338, doi: 10.1111/j.1540-8159.2010.02972.x, indexed in Pubmed: 21208223.
10. Rene AG, Sastry A, Horowitz JM, et al. Recovery of atrioventricular conduction after pacemaker placement following cardiac valvular surgery. J Cardiovasc Electrophysiol. 2013; 24(12): 1383––1387, doi: 10.1111/jce.12260, indexed in Pubmed: 24028584.
11. Sood N, Crespo E, Friedman M, et al. Predictors of pacemaker dependence and pacemaker dependence as a predictor of mortality in patients with implantable cardioverter defibrillator. Pacing Clin Electrophysiol. 2013; 36(8): 945–951, doi: 10.1111/pace.12164, indexed in Pubmed: 23668483.
12. Korantzopoulos P, Letsas KP, Grekas G, et al. Pacemaker dependency after implantation of electrophysiological devices. Europace. 2009; 11(9): 1151–1155, doi: 10.1093/europace/eup195, indexed in Pubmed: 19617204.
13. Levine PA. Pacemaker dependency after pacemaker implantation. Cardiol J. 2007; 14(3): 318–320, indexed in Pubmed: 18651480.
14. Majewski JP, Lelakowski J. Pacemaker dependency: how should it be defined? Europace. 2018; 20(10): 1708, doi: 10.1093/europace/euy010, indexed in Pubmed: 29518191.
15. Feldman S, Glikson M, Kaplinsky E. Pacemaker dependency after coronary artery bypass. Pacing Clin Electrophysiol. 1992; 15(11 Pt 2): 2037–2040, doi: 10.1111/j.1540-8159.1992.tb03017.x, indexed in Pubmed: 1279595.
16. Mar PL, Angus CR, Kabra R, et al. Perioperative predictors of permanent pacing and long-term dependence following tricuspid valve surgery: a multicentre analysis. Europace. 2017; 19(12): 1988–1993, doi: 10.1093/europace/euw391, indexed in Pubmed: 28073887.
17. Kaplan RM, Yadlapati A, Cantey EP, et al. Conduction recovery following pacemaker implantation after transcatheter aortic valve replacement. Pacing Clin Electrophysiol. 2019; 42(2): 146–152, doi: 10.1111/pace.13579, indexed in Pubmed: 30548869.

VIA MEDICA

ORIGINAL ARTICLE

Cardiology Journal
2021, Vol. 28, No. 3, 431–438
DOI: 10.5603/CJ.a2019.0089

ISSN 1897–5593
eISSN 1898–018X

Genetic and environmental factors on heart rate, mean arterial pressure and carotid intima–media thickness: A longitudinal twin study

Adam D. Tarnoki[1, 2]*, Laszlo Szalontai[1]*, Corrado Fagnani[3]*, David L. Tarnoki[1, 2], Pierleone Lucatelli[4], Pal Maurovich-Horvat[5], Adam L. Jermendy[5], Attila Kovacs[5], Andrea Agnes Molnar[5], Erika Godor[1], Bence Fejer[1], Anita Hernyes[1], Carlo Cirelli[4], Fabrizio Fanelli[4], Filippo Farina[6], Claudio Baracchini[6], Giorgio Meneghetti[6], Anna V. Gyarmathy[7], Gyorgy Jermendy[8], Bela Merkely[5], Giacomo Pucci[9, 10], Giuseppe Schillaci[9], Maria A. Stazi[3], Emanuela Medda[3]

[1]Medical Imaging Center, Semmelweis University, Budapest, Hungary; [2]Hungarian Twin Registry, Budapest, Hungary; [3]Italian Twin Registry, Center for Behavioural Sciences and Mental Health, Istituto Superiore di Sanità, Rome, Italy; [4]Vascular and Interventional Radiology Unit, Department of Radiological, Oncological and Anatomo-Pathological Sciences, Sapienza University of Rome, Italy; [5]MTA-SE Cardiovascular Imaging Research Group, Heart and Vascular Center, Semmelweis University, Budapest, Hungary; [6]Department of Neurosciences, University of Padua School of Medicine, Padua, Italy; [7]Johns Hopkins Bloomberg School of Public Health, Baltimore, MD, USA; [8]Third Department of Internal Medicine, Bajcsy Zsilinszky Hospital, Budapest, Hungary; [9]Università di Perugia, Unità di Medicina Interna, Ospedale "S. Maria", Terni, Italy; [10]Struttura Complessa di Medicina Interna, Azienda Ospedaliero-Universitaria di Terni, Italy

Abstract

Background: *Heart rate (HR), mean arterial pressure (MAP) and carotid intima–media thickness (cIMT) are moderately heritable cardiovascular traits, but the environmental effects on the longitudinal change of their heritability have never been investigated.*

Methods: *368 Italian and Hungarian twins (107 monozygotic, 77 dizygotic) underwent oscillometric measurement and B-mode sonography of bilateral carotid arteries in 2009/2010 and 2014. Within-individual/cross-study wave, cross-twin/within-study wave and cross-twin/cross-study wave correlations were estimated, and bivariate Cholesky models were fitted to decompose the total variance at each wave and covariance between study waves into additive genetic, shared and unique environmental components.*

Results: *For each trait, a moderate longitudinal stability was observed, with within-individual/cross-wave correlations of 0.42 (95% CI: 0.33–0.51) for HR, 0.34 (95% CI: 0.24–0.43) for MAP, and 0.23 (95% CI: 0.12–0.33) for cIMT. Cross-twin/cross-wave correlations in monozygotic pairs were all significant and substantially higher than the corresponding dizygotic correlations. Genetic continuity was the main source of longitudinal stability, with across-time genetic correlations of 0.52 (95% CI: 0.29–0.71) for HR, 0.56 (95% CI: 0.31–0.81) for MAP, and 0.36 (95% CI: 0.07–0.64) for cIMT. Overlapping genetic factors explained respectively 57%, 77%, and 68% of the longitudinal covariance of the HR, MAP and cIMT traits.*

Conclusions: *Genetic factors have a substantial role in the longitudinal change of HR, MAP and cIMT; however, the influence of unique environmental factors remains relevant. Further studies should better elucidate whether epigenetic mechanisms have a role in influencing the stability of the investigated traits over time.* (Cardiol J 2021; 28, 3: 431–438)

Key words: cardiovascular arterial stiffness, epigenetics, genetics

Address for correspondence: Laszlo Szalontai, MD, Medical Imaging Center, Semmelweis University, 78/A Ulloi street, Budapest 1082, Hungary, tel: +36-30-6401183, fax: +36-1-2780368, e-mail: laszlo.szalontai.med@gmail.com

Received: 6.12.2018 Accepted: 3.05.2019

**These authors contributed equally to this work; †This author passed away during manuscript preparation.*

Introduction

Each year, cardiovascular disease (CVD) causes 3.9 million deaths, accounting for almost half of all deaths in Europe [1].

Some of the most commonly used non-invasive methods to assess CVD risk include cardiovascular measures such as heart rate (HR), mean arterial pressure (MAP), and carotid intima–media thickness (cIMT). A considerable number of epidemiological studies have reported a strong association between elevated HR and cardiovascular risk, and this association appears to be independent of other major risk factors for atherosclerosis [2]. These studies suggest that HR does not merely predict outcome, but that elevated heart rate may be a true cardiovascular risk factor [3].

Mean arterial pressure is a steady component of the blood pressure (BP) curve. The two main determining factors of MAP are cardiac output and peripheral vascular resistance, which are regulated by a network of interacting physiological pathways involving extracellular fluid volume homeostasis, cardiac contractility and vascular tone through renal, neural and endocrine systems [4]. cIMT is a marker of subclinical atherosclerosis normally increasing with age and generally related to the male gender. Approximately 20% to 30% of cerebral strokes are thought to be the result of ischemia from extracranial carotid stenosis due to atherosclerosis [5]. While HR, BP, and cIMT have been linked to environmental factors, cross-sectional twin and family studies have also shown a strong genetic component [6–12]. However, being complex traits, environmental factors are likely to play an important role in the longitudinal modification of the genetic influence but, the timespan over which these changes take effect is unclear [13, 14].

The environmental effects on the longitudinal change of HR, MAP and cIMT heritability have never been investigated. Significant changes in associations with genetic components over a considerably long timespan (for example, 5 years) would suggest higher importance of gene environment interaction. The aim of this longitudinal twin study was to investigate genetic and environmental influences on the stability of HR, MAP, and cIMT as CVD defining traits to provide an insight into whether environmental interventions might have a substantial beneficial effect.

Methods

Patients

In 2009/2010, 662 twins previously enrolled in the Italian and Hungarian Twin Registries were recruited in the "International twin study on atherosclerotic traits" (Wave 1) [8]. Of these, 368 participated in a second study wave (2014), with 294 (44.4%) not participating in the follow-up investigation. Attrition is explained in part by death of participants after Wave 1, health reasons, loss to follow-up due to a change of address, and the fact that only complete twin pairs could be enrolled in the study. All patients were Caucasian ethnicity. No significant differences in zygosity as well as in several baseline characteristics (such as educational level, systolic BP (SBP) and diastolic BP (DBP), smoking habits, diabetes, hypertension and cardiac disease and MAP) were found between those who took part in Wave 2 and those who were not followed up. However, participants who were followed up were significantly older, drank more coffee or alcohol, had higher body mass index (BMI) and showed lower HR at baseline compared to those who were not followed up. The Italian twins were residents of Rome, Padua, Perugia or Terni, while Hungarian twins lived in Budapest or in the province. Exclusion criteria at both visits were being pregnant at the time of the visit, prior CVDs or surgeries that might interfere with the investigated phenotypes, and acute infection occurring 2 weeks prior to their visit. Twins were examined, and data were collected at the local university hospitals. All participants signed an informed consent form in acceptance of entering the study. This observational study was approved by the Ethics Committee of the Istituto Superiore di Sanità as part of the Italian Twin Registry research activities, and the study was performed in accordance with the declaration of Helsinki.

Ethics approval and consent to participate

The study was approved by the Ethics Committee Semmelweis University TUKEB 29/2009, and the committee's reference number is ETT TUKEB 58401/2012/EKU (828/PI/12).

Data collection and measures

Heart rate, MAP, systolic aortic BP (SBPao), cIMT, and BMI were recorded by oscillometric measurement, B-mode sonography of bilateral carotid arteries and bioelectrical impedance analysis (OMRON) in 2009 and in 2014, using the same devices. Prior to measurements, participants were requested to refrain from smoking for at least 3 h, from eating for at least 1 h, and from drinking alcohol or coffee for at least 12 h. Subjects were asked not to speak during the measurements. The HR and MAP measurements were obtained after at least

10 min of resting in supine position using a previously validated [15], brachial cuff-based oscillometric device (Tensiomed Arteriograph, Medexpert Ltd., Budapest, Hungary). Mean arterial pressure was calculated as DBP + 1/3 (SBP – DBP). B-mode ultrasound was performed using high-resolution color-coded duplex sonography scanners (Esaote MyLab70 in Rome, Italy; Sonoscape S8 in Perugia, Italy; Toshiba Aplio XG in Padua, Italy; Esaote MyLab60 in Terni, Italy; Philips iU22 in Hungary) with high-frequency (12 MHz) linear probes. Carotid arteries were examined by the same reader bilaterally from the supraclavicular fossa to the submandibular angle, including common carotid artery (CCA), carotid bulb, and origin of both internal and external carotid arteries (ICA and ECA). Intima–media thickness was defined according to the Mannheim consensus [16]. IMT was measured 2 to 3 cm before the carotid bifurcation on the far wall. In cases of the presence of a carotid plaque, an area nearby without plaque was measured. Afterwards, cIMT was measured by semiautomated software online or offline in the saved images, or by calipers. Information on risk factors, chronic diseases, medications, and any other clinically relevant condition were collected by self-reported questionnaires. Twin zygosity was assessed by a self-reported questionnaire, filled out by each twin, regarding physical differences and similarities during childhood [17, 18].

Statistical analysis

Descriptive statistics (percentage distributions and mean values with their corresponding standard deviations) were produced for the overall sample and by zygosity at Wave 1 and Wave 2. Since monozygotic (MZ) twins are genetically identical and dizygotic (DZ) twins who share, on average, 50% of the genes, and both MZ and DZ twins are exposed to the same environment especially during childhood, a higher correlation of the examined traits in MZ than in DZ pairs suggests a contribution of genetic factors to the trait expression. The role of genetic and environmental factors in the expression of each trait was inferred by a comparison of "crosstwin/within-wave" correlations (i.e. between twin 1 and twin 2 at a given wave) between MZ and DZ pairs. Longitudinal phenotypic correlation ("within-individual/cross-wave" correlation, i.e. between Wave 1 and Wave 2 for twins as individuals) was calculated to investigate the stability of each trait over time. "Cross-twin/cross-wave" correlation (i.e. between twin 1 at a given wave and twin 2 at a different wave) was calculated in order to assess the stability of genetic and environmental effects across the two visits; greater values of such correlation for MZ compared to DZ pairs are interpreted as a genetic stability between Wave 1 and Wave 2. Bivariate Cholesky decomposition was performed for each trait to estimate genetic and environmental contributions to the variance at each wave and to the covariance between waves under the full and best model. The χ^2 test was used to select the best fitting model according to parsimonious criteria [19]. The contribution to variance and covariance can be decomposed in three main effects: (i) additive genetic component (A), due to additive effects of alleles at each contributing genetic locus; (ii) shared environmental component (C), attributable to environmental events common to both members of a twin pair; (iii) unique environmental component (E), which results from environmental exposures not shared by members of a twin pair, including measurement errors. Genetic and environmental variance and covariance components were expressed as percentages of the total observed variance/covariance. Therefore, the standardized genetic variance component, called heritability, was defined as the proportion of variance of a single trait (at a given wave) attributable to genetic influences. Furthermore, the standardized genetic covariance, called bivariate heritability, was defined as the proportion of phenotypic correlation (between waves) explained by common genetic influences at Wave 1 and Wave 2. Finally, genetic and environmental correlations were estimated to assess the extent to which the same genes and environments affected the traits across visits. All estimated parameters were adjusted by age, gender, country, BMI at baseline and, when necessary, by SBPao at baseline based on the Framingham Heart Study [20]. Descriptive statistics were obtained using the STATA Software, release 13. In addition, correlation estimation and bivariate Cholesky decomposition were performed using the Mx software [21].

Results

A total of 214 MZ twins and 154 DZ twins were included in the analysis (Table 1): 59.8% of the sample was recruited in Italy and about one-third of the twins were male (34.8%). The mean age at first visit was 51.9 years (range 19–73). No significant differences between zygosity groups for HR, MAP and cIMT were found. Within-pair similarity in MZ twin pairs was greater than that observed in DZ pairs for all the traits (Table 2). Phenotypic

Table 1. Demographic, clinical characteristics and measures by zygosity and time.

	Monozygotic twins		Dizygotic twins	
	Wave 1 (2009/10)	Wave 2 (2014)	Wave 1 (2009/10)	Wave 2 (2014)
Subjects, number	214	214	154	154
Age [years]	51.45 ± 13.25	56.11 ± 13.40	52.45 ± 12.19	57.12 ± 12.26
Gender, male	35.5%	–	33.8%	–
Country:				
Hungary	46.7%	–	31.2%	–
Italy	53.3%	–	68.8%	–
Smoke:				
Never smoker	59.7%	59.5%	50.0%	48.3%
Former smoker — Current smoker	40.3%	40.5%	50.0%	51.7%
Body mass index [kg/m^2]	26.20 ± 4.45	26.55 ± 4.50	26.86 ± 4.59	27.06 ± 4.86
Heart rate	69.91 ± 11.27	67.14 ± 9.80	69.27 ± 9.66	65.25 ± 8.77
Mean arterial pressure [mmHg]	94.24 ± 12.53	93.12 ± 11.48	92.97 ± 12.20	93.50 ± 13.05
Carotid intima–media thickness [mm]	0.71 ± 0.25	0.69 ± 0.19	0.71 ± 0.20	0.74 ± 0.22
Hyperlipidemia	71.1%	65.2%	69.5%	66.2%
Brachial systolic blood pressure [mmHg]	128.58 ± 17.26	126.39 ± 16.68	127.13 ± 16.63	126.66 ± 17.35
Brachial diastolic blood pressure [mmHg]	77.01 ± 11.29	76.52 ± 9.96	76.44 ± 9.99	76.82 ± 11.81

Data are expressed as mean ± standard deviation or percentage (%).

Table 2. Intraclass and cross-twin/cross-time correlations by zygosity.

		Phenotypic correlation (95% CI)	Correlations (95% CI)	
			Monozygotic	Dizygotic
HR*				
Visit 1–Visit 2	Within-individual/cross-time correlation	0.42 (0.33–0.51)		
Visit 1	Cross-twin/within-time correlation		0.47 (0.33–0.59)	0.27 (–0.02–0.49)
Visit 2	Cross-twin/within-time correlation		0.44 (0.28–0.57)	0.30 (0.06–0.50)
Visit 1–Visit 2	Cross-twin/cross-time correlation		0.24 (0.11–0.35)	0.16 (–0.05–0.33)
MAP*				
Visit 1–Visit 2	Within-individual/cross-time correlation	0.34 (0.24–0.43)		
Visit 1	Cross-twin/within-time correlation		0.44 (0.27–0.57)	0.37 (0.17–0.54)
Visit 2	Cross-twin/within-time correlation		0.50 (0.33–0.64)	0.10 (–0.10–0.28)
Visit 1–Visit 2	Cross-twin/cross-time correlation		0.27 (0.14–0.39)	0.11 (–0.05–0.26)
CCA IMT**				
Visit 1–Visit 2	Within-individual/cross-time correlation	0.23 (0.12–0.33)		
Visit 1	Cross-twin/within-time correlation		0.32 (0.23–0.46)	0.13 (–0.01–0.37)
Visit 2	Cross-twin/within-time correlation		0.59 (0.48–0.65)	0.24 (0.04–0.42)
Visit 1–Visit 2	Cross-twin/cross-time correlation		0.15 (0.02–0.27)	0.09 (–0.09–0.17)

HR — heart rate; MAP — mean arterial pressure; CCA — common carotid artery; IMT — intima–media thickness; SBPao — aortic systolic blood pressure; BMI — body mass index; *Covariates included in the model: age, gender, country, body mass index; **Covariates included in the model: age, gender, country, SBPao, body mass index; 95% CI — 95% confidence intervals

correlations between the first and second visits for HR, MAP and cIMT were 0.42, 0.34, and 0.23, respectively. Cross-twin/cross-wave correlations were higher in MZ twin pairs (range 0.15–0.27) than in DZ pairs (range 0.09–0.16). The highest difference between MZ and DZ twin correlations was observed for MAP (MZ: 0.27 and DZ: 0.11). Under the best model (AE), the variability of HR and MAP at first and second visits was explained, in similar proportions, by genetic (A from 0.48 to 0.45) and unique environmental influences (E from 0.52 to 0.55; Table 3). Unique environmental influences on cIMT expression decreased between the first visit (E = 0.68) and the second visit (E = 0.42), whereas genetic effects increased from 0.32 to 0.58 between the two visits. For longitudinal changes in HR, proportions of covariance were explained by genetic and environmental influences were A = 0.57 and E = 0.43, respectively. Genetic factors involved in MAP and cIMT expression accounted for, respectively, 77% and 68% of the longitudinal covariance of the traits; the contribution of nonshared exposures to the stability of the traits over time was quite modest (E = 0.23 and 0.32). Familial environmental influences did not contribute significantly to the longitudinal stability and change of HR, MAP and cIMT; indeed, the exclusion of C component had no effect in the model fit of any of the three phenotypes ($p > 0.05$). Many of the same genes were involved in the expression of the observed traits over time (genetic correlation, rg: HR = 0.52, MAP = 0.56 and cIMT = 0.36), while different unique environmental factors acted across visits (environmental correlation, re: HR = = 0.34, MAP = 0.15 and cIMT = 0.14).

Table 3. Standardized parameter estimates under the best-fitting models.

	Standardized variance/covariance components (95% CI)		Model fit indices[#]			Correlations (95% CI)	
	A	E	χ^2	Δdf	P	Genetic correlation, rg	Environmental correlation, re
HR*							
Visit 1	0.48 (0.34–0.59)	0.52 (0.41–0.66)					
Visit 2	0.45 (0.31–0.57)	0.55 (0.43–0.69)					
Visit 1/Visit 2	0.57 (0.32–0.78)	0.43 (0.22–0.68)	0.49	3	0.92	0.52 (0.29–0.71)	0.34 (0.17–0.48)
MAP*							
Visit 1	0.47 (0.33–0.59)	0.53 (0.41–0.67)					
Visit 2	0.46 (0.28–0.60)	0.54 (0.40–0.72)					
Visit 1/Visit 2	0.77 (0.45–1.00)	0.23 (0–0.55)	2.84	3	0.42	0.56 (0.31–0.81)	0.15 (0–0.32)
CCA IMT**							
Visit 1	0.32 (0.17–0.46)	0.68 (0.54–0.83)					
Visit 2	0.58 (0.44–0.69)	0.42 (0.31–0.56)					
Visit 1/Visit 2	0.68 (0.18–1.00)	0.32 (0–0.82)	0	3	1.00	0.36 (0.07–0.64)	0.14 (0–0.31)

A — additive genetic variance; E — unshared environmental variance; CI — confidence intervals; CCA — common carotid artery; HR — heart rate; MAP — mean arterial pressure; IMT — intima–media thickness; [#]Full model was ACE; χ^2 = (–2log-likelihood sub-model)–(–2log-likelihood full model); Δdf = (df sub-model)–(df full model); *Covariates included in the model: age, gender, country, body mass index; **Covariates included in the model: age, gender, country, aortic systolic blood pressure, body mass index

Discussion

In this study, substantial influences of genetic background on phenotypic correlations of all studied phenotypes were revealed over time. Moreover, data herein, highlighted that shared, primarily familial, environmental influences do not contribute significantly to the longitudinal stability and change of HR, MAP, and cIMT.

Heart rate

Stress and depression are among the main factors raising HR [22]. Environmental factors associated with higher HR can be divided in two groups. The first one includes lifestyle choices such as alcohol consumption [23], smoking [24], absence of exercise, and higher BMI [25]. The second one refers to occupation related exposure

such as exposure to particulate matter, several chemical components, electromagnetic fields, vibrating tools, psychosocial stress, long working hours, and fatigue [26]. A large body of evidence ranging from epidemiologic to genome-wide linkage studies, suggests that in addition to the effect of environmental factors on HR, some features of HR and HR variability (HRV) can be transmitted over generations because of the influence of genetic factors. The Framingham Heart Study in 2002 and the Examination of the "unified database for human genome mapping" provided evidence for distinct HRV quantitative trait loci on chromosomes 15 and 2 [27]. There were interesting candidate genes related to the autonomic nervous system and HRV around the region of interest on chromosome 2 [27]. A recent GWAS cohort by Eppinga et al. [28] identified 46 novel loci associated with resting HR and hypothesized that either the genetic variants exerted their effects via HR on mortality directly, or the genetic variants shared an underlying biology, both increasing HR and mortality risk. The present study provided further evidence on the role of genetic influence on HR by finding that the overall effect of the known environmental factors accounted for 52% to 55% of the variance. This is in accordance with a previous Danish study that demonstrated lower heritability (23% to 27%) while adjusting for age, gender, BMI, diabetes, hypertension, pulmonary function, smoking, physical activity and zygosity [6]. The current study also indicated that these known genetic and environmental factors had a modest but stable effect over time. Phenotypic correlation between the first and second visits for HR showed a moderate stability of the trait across time. This may suggest that environment played a non-significant effect on genetic expression through gene-environment interaction over a 5-year period.

Mean arterial pressure

Factors that increase MAP include high BMI, age, short sleep time and/or sleep apnea syndrome, high sodium intake, smoking [29, 30], stress, and clinically related diseases such as diabetes and chronic kidney disease [31]. Studies have shown that environmental influences explain 30–50% of the variance in MAP [32, 33]. Cultural heritability, comprising a constellation of factors such as lifestyle and dietary habits, might explain an additional 10% [32, 33]. A 2016 study showed that the majority of patients diagnosed with hypertension had high dietary sodium intake and low physical activity with high BMI and abdominal obesity [34]. Furthermore, a study by Małyszko et al. [35] found high prevalence and profound vitamin D deficiency in heart failure patients. Genetic heritability is estimated to account for about 40% of BP variance (ranging from 31% to 68%, depending on the study) [32, 33]. Some residual proportion of variance (estimated at about 10%) remains unknown. However, the genetic determinants are probably highly heterogeneous, which poses exceptional challenges to identification of the underlying genes. Burello et al. [36] described 43 single-nucleotide polymorphisms (SNP) variants, in a recent GWAS study, with each SNP affecting SBP and DBP by 1.0 and 0.5 mmHg, respectively. In 2017 one of the largest GWAS research studies to this date, that used the 1000 Genomes Project-based imputation in 150,134 European ancestry individuals reported 8 loci of the genome not previously connected to BP regulation and increasing the number of genes to 48 as candidates for priority follow-up [37]. Epigenetic changes, such as DNA methylation, histone modification and non-coding RNAs, have been increasingly recognized as important players in BP regulation and may justify a further part of missing heritability [36]. However, to this end, the longitudinal role of these effects on BP heritability remained unclear. In recent twin studies, MAP heritability ranged between 46% and 47%, which is in line with the magnitude of the previous heritability results of BP traits [8]. Based on the phenotypic correlation between the two study waves, the present study found a low to moderate longitudinal stability of MAP, with cross-twin/ /cross-wave correlations giving a first indication of genetic and environmental influences on the detected stability. In the current study, the higher correlation observed in MZ twin pairs compared to DZ pairs suggests that genes mainly contribute to the stability of the trait over time.

Carotid IMT

Age and BMI are the most influential environmental factors on cIMT increase, followed by pulse pressure, gender (higher cIMT values in men, although gender difference is partly attributable to differences in carotid lumen diameter), waist-hip ratio, total cholesterol, low-density lipoprotein cholesterol, triglycerides, number of pack-years of smoking, and lumen diameter of the carotid artery [38]. The ARYA Study showed a linear trend with increased cIMT after adjusting the total pack-years of smoking for age and gender [38]. cIMT increases gradually and significantly with the number of cardiovascular risk factors mentioned above. In contrast, high-density

lipoprotein cholesterol level is inversely associated with cIMT [39]. The Italian working group previously showed a genetic contribution ranging from 41% to 65% across the different carotid segments [9]. In a recent study Cecelja et al. [40] no association was found between longitudinal progression (5 years) of carotid artery pulse pressure and cIMT or carotid dilation and cIMT. This suggests that both pulse pressure and dilation are heritable but independent of IMT. Based on the present results, phenotypic correlation between the two waves suggests a moderate, significant longitudinal stability of cIMT. Moreover, the current data highlighted that shared environment (primarily familial exposures shared by both twins, such as dietary habits in childhood, parental socioeconomic status, etc.) did not contribute significantly to the longitudinal stability and change of cIMT, while unique environment had a substantial influence.

Limitations of the study

The present study has two limitations. First, the study was carried out in samples from different countries with different prevalence of hypertension, hypercholesterolemia, genetic background and other risk factors. However, this allowed us to study a more diverse sample. Second, preventive interventions or treatments might have affected the findings. However, conducting a sensitivity analysis excluding twins that changed treatment profile (i.e. not treated at baseline and treated at second wave or vice versa), the results were similar, suggesting that treatment likely had a negligible effect on the genetic component.

Conclusions

The current study of a relatively large twin cohort had the strength of being conducted by the same researchers and devices in all subjects in both study waves, using a standardized measurement procedure. This study revealed substantial influences of genetic background on longitudinal stability of all studied phenotypes over time. Moreover, data herein highlighted that shared, primarily familial, environmental influences do not contribute significantly to longitudinal stability and change of HR, MAP and cIMT. The present findings suggest that unique environmental, epigenetic changes may have a lower but considerable role in the expression of these CVD defining traits over a 5-year period due to genetic stability.

Funding: Balassi Institute, Hungarian Scholarship Office and Italian Cultural Institute, Medexpert Ltd., Semmelweis University Directorate of International Relations and University of Padua, EFSD New Horizons Programme. The position of Giacomo Pucci as an Adjunct Assistant Professor at the University of Perugia was funded by a grant from the Fondazione Cassa di Risparmio di Terni e Narni.

Conflict of interest: None declared

References

1. World Health Organization 2017. http://www.euro.who.int/en/healthtopics/ noncommunicable-diseases/cardiovascular-diseases/data-and-statistics(Accessed on 15 October, 2017).
2. Perret-Guillaume C, Joly L, Benetos A. Heart rate as a risk factor for cardiovascular disease. Prog Cardiovasc Dis. 2009; 52(1): 6–10, doi: 10.1016/j.pcad.2009.05.003, indexed in Pubmed: 19615487.
3. Zheng L, Sun Z, Li J, et al. Pulse pressure and mean arterial pressure in relation to ischemic stroke among patients with uncontrolled hypertension in rural areas of China. Stroke. 2008; 39(7): 1932–1937, doi: 10.1161/STROKEAHA.107.510677, indexed in Pubmed: 18451345.
4. Mayet J, Hughes A. Cardiac and vascular pathophysiology in hypertension. Heart. 2003; 89(9): 1104–1109, doi: 10.1136/heart.89.9.1104, indexed in Pubmed: 12923045.
5. Executive Committee for the Asymptomatic Carotid Atherosclerosis Study. Endarterectomy for asymptomatic carotid artery stenosis. JAMA. 1995; 273(18): 1421–1428, indexed in Pubmed: 7723155.
6. Jensen MT, Wod M, Galatius S, et al. Heritability of resting heart rate and association with mortality in middle-aged and elderly twins. Heart. 2017; pii: heartjnl-2016-310986.
7. Osztovits J, Horváth T, Littvay L, et al. Effects of genetic vs. environmental factors on cardiovascular autonomic function: a twin study. Diabet Med. 2011; 28(10): 1241–1248, doi: 10.1111/j.1464-5491.2011.03363.x, indexed in Pubmed: 21679234.
8. Tarnoki AD, Tarnoki DL, Stazi MA, et al. Heritability of central blood pressure and arterial stiffness: a twin study. J Hypertens. 2012; 30(8): 1564–1571, doi: 10.1097/HJH.0b013e32835527ae, indexed in Pubmed: 22688268.
9. Medda E, Fagnani C, Schillaci G, et al. Heritability of arterial stiffness and carotid intima-media thickness: an Italian twin study. Nutr Metab Cardiovasc Dis. 2014; 24(5): 511–517, doi: 10.1016/j.numecd.2013.10.031, indexed in Pubmed: 24582685.
10. Zhao J, Cheema FA, Bremner JD, et al. Heritability of carotid intima-media thickness: a twin study. Atherosclerosis. 2008; 197(2): 814–820, doi: 10.1016/j.atherosclerosis.2007.07.030, indexed in Pubmed: 17825306.
11. Jermendy G, Littvay L, Steinbach R, et al. [Heritability of the risk factors characteristic for the metabolic syndrome: a twin study]. Orv Hetil. 2011; 152(32): 1265–1271, doi: 10.1556/OH.2011.29165, indexed in Pubmed: 21803723.
12. Albarwani S, Muñoz ML, Voruganti VS, et al. Heritability of ambulatory and beat-to-beat office blood pressure in large multigenerational Arab pedigrees: the 'Oman Family study'. Twin Res Hum Genet. 2012; 15(6): 753–758, doi: 10.1017/thg.2012.59, indexed in Pubmed: 22967944.
13. Egger G, Liang G, Aparicio A, et al. Epigenetics in human disease and prospects for epigenetic therapy. Nature. 2004;

429(6990): 457–463, doi: 10.1038/nature02625, indexed in Pubmed: 15164071.
14. Weinhold B. Epigenetics: the science of change. Environ Health Perspect. 2006; 114(3): A160–A167, doi: 10.1289/ehp.114-a160, indexed in Pubmed: 16507447.
15. Horváth IG, Németh A, Lenkey Z, et al. Invasive validation of a new oscillometric device (Arteriograph) for measuring augmentation index, central blood pressure and aortic pulse wave velocity. J Hypertens. 2010; 28(10): 2068–2075, doi: 10.1097/HJH.0b013e32833c8a1a, indexed in Pubmed: 20651604.
16. Touboul PJ, Hennerici MG, Meairs S, et al. Mannheim carotid intima-media thickness consensus (2004-2006). An update on behalf of the Advisory Board of the 3rd and 4th Watching the Risk Symposium, 13th and 15th European Stroke Conferences, Mannheim, Germany, 2004, and Brussels, Belgium, 2006. Cerebrovasc Dis. 2007; 23(1): 75–80, doi: 10.1159/000097034, indexed in Pubmed: 17108679.
17. Kyvik KO, Green A, Beck-Nielsen H. The new Danish Twin Register: establishment and analysis of twinning rates. Int J Epidemiol. 1995; 24(3): 589–596, doi: 10.1093/ije/24.3.589, indexed in Pubmed: 7672901.
18. Heath AC, Nyholt DR, Neuman R, et al. Zygosity diagnosis in the absence of genotypic data: an approach using latent class analysis. Twin Res. 2003; 6(1): 22–26, indexed in Pubmed: 12626225.
19. Neale M, Cardon LR. Methodology for genetic studies of twins and families. Kluwer Academic Publishers, Dordrecht 1992.
20. Brown WM, Beck SR, Lange EM, et al. Framingham Heart Study. Age-stratified heritability estimation in the Framingham Heart Study families. BMC Genet. 2003; 4 Suppl 1: S32, doi: 10.1186/1471-2156-4-S1-S32, indexed in Pubmed: 14975100.
21. Neale MC, Boker SM, Xie G, et al. Mx: statistical modeling (7th edition), Ed. Richmond, VA: Department of Psychiatry, Virginia Commonwealth University. 2006.
22. Parati G, Mancia G, Rienzo M, et al. Cardiovascular variability is/is not an index of autonomic control of circulation. J App Physiol. 2006; 101(2): 690–691, doi: 10.1152/japplphysiol.00584.2006.
23. Albanese M, Neofytou M, Ouarrak T, et al. Evaluation of heart rate measurements in clinical studies: a prospective cohort study in patients with heart disease. Eur J Clin Pharmacol. 2016; 72(7): 789–795, doi: 10.1007/s00228-016-2046-9, indexed in Pubmed: 27023464.
24. Filipovský J, Ducimetière P, Safar ME. Prognostic significance of exercise blood pressure and heart rate in middle-aged men. Hypertension. 1992; 20(3): 333–339, doi: 10.1161/01.hyp.20.3.333, indexed in Pubmed: 1387630.
25. Palatini P, Casiglia E, Pauletto P, et al. Relationship of tachycardia with high blood pressure and metabolic abnormalities: a study with mixture analysis in three populations. Hypertension. 1997; 30(5): 1267–1273, doi: 10.1161/01.hyp.30.5.1267, indexed in Pubmed: 9369286.
26. Moser M, Lehofer M, Sedminek A, et al. Heart rate variability as a prognostic tool in cardiology. A contribution to the problem from a theoretical point of view. Circulation. 1994; 90(2): 1078–1082, doi: 10.1161/01.cir.90.2.1078, indexed in Pubmed: 8044922.
27. Palatini P, Thijs L, Staessen JA, et al. Systolic Hypertension in Europe (Syst-Eur) Trial Investigators. Predictive value of clinic and ambulatory heart rate for mortality in elderly subjects with systolic hypertension. Arch Intern Med. 2002; 162(20): 2313–2321, doi: 10.1001/archinte.162.20.2313, indexed in Pubmed: 12418945.
28. Eppinga RN, Hagemeijer Y, Burgess S, et al. Identification of genomic loci associated with resting heart rate and shared genetic predictors with all-cause mortality. Nat Genet. 2016; 48(12): 1557–1563, doi: 10.1038/ng.3708, indexed in Pubmed: 27798624.
29. Ma Y, He FJ, MacGregor GA. High salt intake: independent risk factor for obesity? Hypertension. 2015; 66(4): 843–849, doi: 10.1161/HYPERTENSIONAHA.115.05948, indexed in Pubmed: 26238447.
30. Phillips CL, O'Driscoll DM. Hypertension and obstructive sleep apnea. Nat Sci Sleep. 2013; 5: 43–52, doi: 10.2147/NSS.S34841, indexed in Pubmed: 23750107.
31. Cabrera CP, Ng FuL, Warren HR, et al. Exploring hypertension genome-wide association studies findings and impact on pathophysiology, pathways, and pharmacogenetics. Wiley Interdiscip Rev Syst Biol Med. 2015; 7(2): 73–90, doi: 10.1002/wsbm.1290, indexed in Pubmed: 25655479.
32. Rossi GP, Ceolotto G, Caroccia B, et al. Genetic screening in arterial hypertension. Nat Rev Endocrinol. 2017; 13(5): 289–298, doi: 10.1038/nrendo.2016.196, indexed in Pubmed: 28059156.
33. Padmanabhan S, Newton-Cheh C, Dominiczak AF. Genetic basis of blood pressure and hypertension. Trends Genet. 2012; 28(8): 397–408, doi: 10.1016/j.tig.2012.04.001, indexed in Pubmed: 22622230.
34. Jarosz M, Wolańska D, Stolińska H, et al. Nutrition and lifestyle in patients pharmacologically treated due to hypertensionally treated due to hypertension. Cardiol J. 2016; 23(5): 491–496, doi: 10.5603/CJ.a2016.0049, indexed in Pubmed: 27439369.
35. Małyszko J, Tomaszuk-Kazberuk A, Dobrzycki K, et al. Vitamin D deficiency and anemia is highly prevalent and dependent on the etiology of heart failure: A pilot study. Cardiol J. 2019 [Epub ahead of print], doi: 10.5603/CJ.a2019.0003, indexed in Pubmed: 30697681.
36. Burrello J, Monticone S, Buffolo F, et al. Is There a Role for Genomics in the Management of Hypertension? Int J Mol Sci. 2017; 18(6), doi: 10.3390/ijms18061131, indexed in Pubmed: 28587112.
37. Wain LV, Vaez A, Jansen R, et al. Novel blood pressure locus and gene discovery using genome-wide association study and expression data sets from blood and the kidney. Hypertension. 2017 [Epub ahead of print], doi: 10.1161/HYPERTENSIONAHA.117.09438, indexed in Pubmed: 28739976.
38. Oren A, Vos LE, Uiterwaal CS, et al. Cardiovascular risk factors and increased carotid intima-media thickness in healthy young adults: the Atherosclerosis Risk in Young Adults (ARYA) Study. Arch Intern Med. 2003; 163(15): 1787–1792, doi: 10.1001/archinte.163.15.1787, indexed in Pubmed: 12912713.
39. Sacco RL, Blanton SH, Slifer S, et al. Heritability and linkage analysis for carotid intima-media thickness: the family study of stroke risk and carotid atherosclerosis. Stroke. 2009; 40(7): 2307–2312, doi: 10.1161/STROKEAHA.109.554121, indexed in Pubmed: 19498180.
40. Cecelja M, Jiang B, Keehn L, et al. Arterial stiffening is a heritable trait associated with arterial dilation but not wall thickening: a longitudinal study in the twins UK cohort. Eur Heart J. 2018; 39(24): 2282–2288, doi: 10.1093/eurheartj/ehy165, indexed in Pubmed: 29590330.

VIA MEDICA

ORIGINAL ARTICLE

Cardiology Journal
2021, Vol. 28, No. 3, 439–445
DOI: 10.5603/CJ.a2019.0092

ISSN 1897–5593
eISSN 1898–018X

How should we teach cardiopulmonary resuscitation? Randomized multi-center study

Burak Katipoglu[1], Marcin Andrzej Madziala[2], Togay Evrin[1], Pawel Gawlowski[3], Agnieszka Szarpak[4], Agata Dabrowska[5], Szymon Bialka[6], Jerzy Robert Ladny[7], Lukasz Szarpak[2], Anna Konert[4], Jacek Smereka[3]

[1]Department of Emergency Medicine, Ufuk University Medical Faculty, Dr. Ridvan Ege Education and Research Hospital, Cankaya, Ankara, Turkey
[2]Medical Simulation Center, Lazarski University, Warsaw, Poland
[3]Department of Emergency Medical Service, Wroclaw Medical University, Wroclaw, Poland
[4]Lazarski University, Warsaw, Poland
[5]Department of Rescue Medical Service, Poznan University of Medical Sciences, Poznan, Poland
[6]Department of Anesthesiology and Intensive Care, Medical University of Silesia, Katowice, Poland
[7]Department of Emergency Medicine and Disaster, Medical University Bialystok, Poland

Abstract

Background: *A 2017 update of the resuscitation guideline indicated the use of cardiopulmonary resuscitation (CPR) feedback devices as a resuscitation teaching method. The aim of the study was to compare the influence of two techniques of CPR teaching on the quality of resuscitation performed by medical students.*

Methods: *The study was designed as a prospective, randomized, simulation study and involved 115 first year students of medicine. The participants underwent a basic life support (BLS) course based on the American Heart Association guidelines, with the first group (experimental group) performing chest compressions to observe, in real-time, chest compression parameters indicated by software included in the simulator, and the second group (control group) performing compressions without this possibility. After a 10-minute resuscitation, the participants had a 30-minute break and then a 2-minute cycle of CPR. One month after the training, study participants performed CPR, without the possibility of observing real-time measurements regarding quality of chest compression.*

Results: *One month after the training, depth of chest compressions in the experimental and control group was 50 mm (IQR 46–54) vs. 39 mm (IQR 35–42; $p = 0.001$), compression rate 116 CPM (IQR 102–125) vs. 124 CPM (IQR 116–134; $p = 0.034$), chest relaxation 86% (IQR 68–89) vs. 74% (IQR 47–80; $p = 0.031$) respectively.*

Conclusions: *Observing real-time chest compression quality parameters during BLS training may improve the quality of chest compression one month after the training including correct hand positioning, compressions depth and rate compliance.* (Cardiol J 2021; 28, 3: 439–445)

Key words: basic life support, learning, medial simulation, quality, chest compression

Introduction

Out-of-hospital cardiac arrest is a global health problem, with survival varying greatly between communities. Sudden cardiac arrest (SCA) is one of the leading causes of death in Europe. Depending how SCA is defined, 55–113 per 100,000 inhabitants per year or 350,000–700,000 individuals each year are affected in Europe [1, 2]. On initial heart-rhythm analysis, 25–50% of SCA victims have ventricular fibrillation (VF), a percentage that has declined over the last 20 years [3, 4]. However,

Address for correspondence: Marcin Andrzej Madziala, PhD, Medical Simulation Center, Lazarski University, ul. Świeradowska 43, 02–662 Warszawa, Poland, tel: +48 519 160 829, e-mail: rat.poz@wp.pl

Received: 29.05.2019 Accepted: 20.08.2019

regardless of the rhythm initiating cardiac arrest, the key is to implement resuscitation procedures as soon as possible [5].

The guidelines of the European Resuscitation Council (ERC) as well as the American Heart Association (AHA) indicate the need for high quality chest compression as an element closely correlated with the efficiency of cardiopulmonary resuscitation (CPR). Both the ERC and AHA guidelines provide a detailed description of how chest compression should be performed.

One of the key elements of the recent emphasis has been on minimizing chest compression interruptions [6]. According to Ewy et al. [7] the most optimal form of chest compression is continuous compression, which generates higher perfusion pressure than resuscitation based on 30 compressions to 2 rescue breaths. To this purpose, it may be essential to perform airway management with an endotracheal tube or supraglottic airway device and initiate asynchronous resuscitation, so that chest compression interruptions, necessary for ventilation with a face mask and a self-inflating bag, are minimized [8–10]. Further parameters indicated by the guidelines include the depth and the rate of compressions as well as the correctness of chest relaxation after each compression. However, regardless of whether resuscitation is based on European or American guidelines, as numerous studies indicate, the quality of chest compressions performed even by medical staff is insufficient [8, 11–14].

The 2017 update of the resuscitation guideline indicated the use of CPR feedback devices [15] as a resuscitation teaching method. Numerous studies indicate that chest compression using these devices is superior to standard resuscitation [16–18]. However, because of the relatively high cost of these devices they are encountered sporadically during real-life resuscitation activities as well as during training courses. It is therefore crucial to seek new methods of teaching both basic and advanced resuscitation procedures which will improve the performance of chest compressions.

The aim of the study was to compare the influence of two techniques of CPR teaching on the quality of resuscitation performed by medical students.

Methods

Study design

The study was designed as a prospective, randomized, simulation study. The study protocol was approved by the Institutional Review Board (IRB) of the Polish Society of Disaster Medicine (Approval no.: 24.11.2017.IRB). Following IRB approval and written informed consent, 115 first year students of medicine took part in the study.

Study protocol

To simulate a patient with cardiac arrest requiring CPR, Resusci Anne® QCPR (Laerdal, Stavanger, Norway) was used, which was placed on a flat surface in a brightly lit room.

Before starting the study, the participants were divided into two groups and ResearchRandomizer (randomizer.org) was used for this purpose. In both groups a 5 minutes standardized training on how to perform CPR of an adult was performed prior to the study. Both groups then underwent a basic life support (BLS) course based on the AHA guidelines, with the first group (experimental group) performed chest compressions to observe, in real-time, chest compressions parameters indicated by software included in the simulator, and the second group (control group) performed compressions without the possibility of observing simulator indications. After a 10-minute resuscitation, the participants had a 30-minute break and then a 2-minute cycle of CPR based on a scheme of 30 compressions: 2 rescue breaths. The first group performed compressions on the basis of simulator indications, while the second group did not.

The next phase of the study was conducted 1 month after training. At that time study participants in the same groups performed CPR, this time both experimental and control groups were not able to observe real-time measurements regarding quality of chest compression.

Measurements

During the study, parameters of chest compression were analyzed, including total compression score, calculated by simulator software on the basis of parameters of chest compression. Additionally, compression depth, compression depth compliance, compression rate per minute (CPM), compression rate compliance, full release as well as correctness of chest position during compression were evaluated. As reference values for depth and rates of chest compressions, the values recommended by the AHA were used, this states that the optimal depth of adult chest compressions is between 50 and 60 mm and the optimal rate of compressions should be between 100 and 120 CPM [19]. All chest compression parameters were recorded by dedicated software included in the SkillReporter (Laerdal, Stavanger, Norway).

Table 1. Chest compression (CC) data.

Parameter	Control group Manual CC (n = 56)	Experimental group The device feedback (n = 55)	P
Before practical training			
Total compression score [%]	70 (43–82)	69 (41–80)	NS
Compression depth [mm]	39 (37–42)	39 (36–42)	NS
Compression depth compliance [%]	68 (54–74)	69 (52–75)	NS
Compression rate [per min]	128 (116–131)	124 (114–130)	NS
Compression rate compliance [%]	70 (51–83)	71 (50–84)	NS
Full release [%]	76 (53–85)	77 (55–84)	NS
Correct hand position [%]	83 (71–90)	83 (70–92)	NS
After training			
Total compression score [%]	74 (51–85)	93 (87–100)	**0.001**
Compression depth [mm]	40 (39–44)	51 (48–57)	**< 0.001**
Compression depth compliance [%]	68 (60–89)	96 (90–100)	**0.001**
Compression rate [per min]	124 (110–128)	110 (103–121)	**0.019**
Compression rate compliance [%]	78 (54–88)	97 (92–100)	**0.001**
Full release [%]	76 (53–90)	91 (81–97)	**0.037**
Correct hand position [%]	83 (76–94)	96 (92–100)	**0.007**
One month after training			
Total compression score [%]	74 (50–79)	90 (84–100)	**< 0.001**
Compression depth [mm]	39 (35–42)	50 (46–54)	**0.001**
Compression depth compliance [%]	64 (50–71)	94 (90–100)	**< 0.001**
Compression rate [per min]	124 (116–134)	116 (102–125)	**0.034**
Compression rate compliance [%]	72 (53–74)	97 (89–100)	**0.001**
Full release [%]	74 (47–80)	86 (68–89)	**0.031**
Correct hand position [%]	80 (70–91)	94 (81–100)	**0.017**

NS — not statistically significant

Statistical analysis

Data were analyzed with the use of Statistica software v.13.3EN (TIBCO., Tulsa, OK). The results are shown as medians and interquartile ranges (IQR). The occurrence of normal distribution was confirmed by the Kolmogorov-Smirnov test. Analysis of variance (ANOVA) post hoc tests with the Bonferroni correction for metric data were used for univariate analysis to compare the two study groups. The Kruskal-Wallis test was used to compare non-normally distributed data. Multivariate ANOVA was also applied. The results were considered significant at the level of $p < 0.05$.

Results

One hundred and fifteen students in their first year of medical studies were enrolled in the study, however, in the initial phase of the study 4 persons decided not to participate in the study. Randomization took place for 111 participants.

A detailed summary of data obtained in the study is presented in Table 1. The initial chest quality assessment performed before the training did not show statistically significant differences between the experimental group and the control group.

After training, study participants had access to a monitor indicating the quality of chest compression and a statistically significant better total compression score was obtained in comparison with non-real time monitoring of chest compression ($p = 0.001$). The depth of chest compression in the experimental and control group showed statistically significant differences (51 mm [IQR 48–57] vs. 40 mm [IQR 39–44]; $p < 0.001$) respectively. Chest compression rate for the experimental group was 110 (IQR 103–121) CPM, and for the control group 124 (IQR 110–128 CPM; $p = 0.019$). Resuscitation

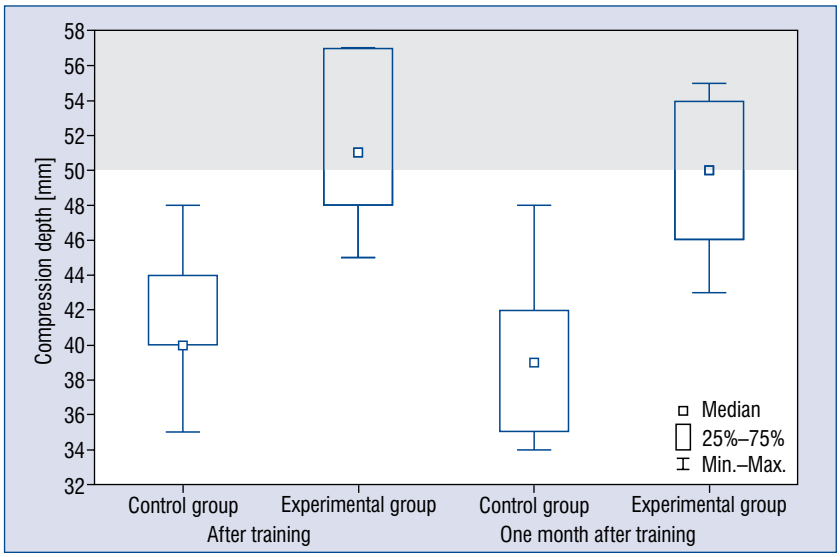

Figure 1. Median compression depth.

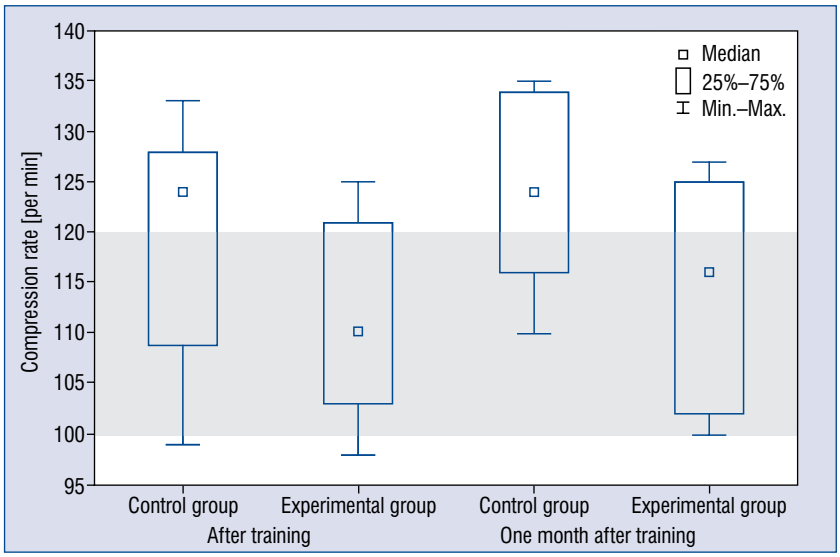

Figure 2. Median compression rate.

with a possibility to observe chest compression parameters was associated with better chest relaxation and better hand positioning (Table 1).

In the second phase of the study (1 month after the training) the depth of chest compressions in the experimental and control group was different and was 50 mm (IQR 46–54) *vs.* 39 mm (IQR 35–42; p = 0.001; Fig. 1). The chest compression rate achieved was 116 CPM (IQR 102–125) for the experimental group and 124 CPM (IQR 116–134; p = 0.034; Fig. 2) for the control group. The correctness of chest relaxation in the experimental group was 86% (IQR 68–89) and a statistically significant higher measure than in the control group — 74% (IQR 47–80; p = 0.031; Fig. 3).

The correct hand positioning, as well as compression depth compliance, compression rate compliance, and total compression score were significantly better statistically than in the experimental group in comparison with the control group ($p < 0.05$ for all parameters).

Discussion

The present study showed the validity of using systems which indicate the quality of chest

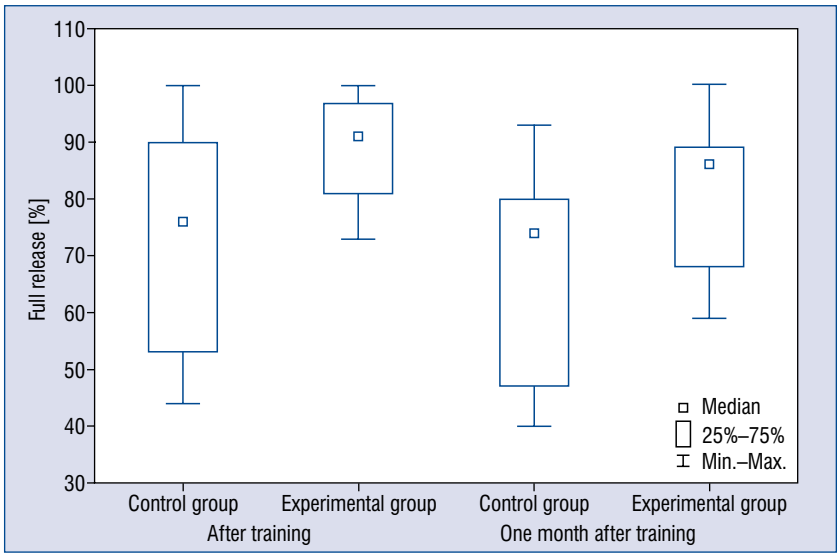

Figure 3. Median full release.

compression during teaching of basic resuscitation procedures because the correction in real time of the chest quality performed significantly improves overall quality of chest compression. Evaluation of chest compression quality with and without chest compression indicating software showed that subjects adjust to chest compression parameters in real time, and had significantly better results for all analyzed parameters compared to the group that could not observe the quality of their resuscitation.

The depth of chest compressions performed by the experimental group (with the possibility to assess the quality of compression in real time) was 51 mm, while in the case of groups without this possibility — 40 mm ($p < 0.001$). According to ERC and AHA guidelines, the depth of chest compression in adults should be between 50 and 60 mm [20]. Numerous studies indicate an improvement in the quality of chest compressions when using CPR feedback devices, including TrueCPR, PocketCPR, CPRMeter or EasyCPR [21–23].

Another parameter indicated in the resuscitation guidelines as important for the quality of chest compression is the rate of chest compressions, which should be between 100 and 120 CPM [24]. In this post-training study, the rate of chest compressions was 124 CPM for the control group and 110 CPM for the experimental group. During the evaluation phase of the study, 1 month after the training, the rates were 124 vs. 116 CPM, respectively. Jäntti et al. [25] as well as other authors' studies [13, 26, 27] also indicate that manual chest compression is performed too rapidly. As Solevåg and Schmölzer [28] had indicated a rate higher than 120/min is also more fatiguing, which affects chest compression quality. On the other hand, Zou et al. [29] studies indicate that the optimal rate of chest compression is 120/min. Studies published by Lee et al. [30] also indicate 120 CPM as the optimal chest compression rate, while noting that higher compression rates can reduce chest relaxation. Similar conclusions can also be drawn from studies by Smereka et al. [8], as well as from studies by other authors [31–33].

Another equally important parameter is the correctness of chest relaxation. It is the compression of the chest to the appropriate depth and then allowing it to return to its normal shape before compression determines the appropriate difference in pressure in the chest to generate organ perfusion [5]. In a study conducted both immediately after the training and a month after the training, a higher percentage of correctly performed relaxation was obtained by participants from the experimental group who had the opportunity to observe the parameters of chest compression in real time during the training.

The use of a system that indicates, in real time, the quality of resuscitation during basic life support learning has allowed participants to improve chest compression parameters and could therefore have a real impact on a patient's chances of survival. An important conclusion from the results is that those who have learned resuscitation using monitoring software perform higher quality chest compressions 1 month subsequent to training. This

may indicate a higher level of familiarity with this important skill of chest compression.

Limitations of the study

A limitation in this study is the use of medical simulation in the research process, however, this fact was intended and dictated by the fact that only during medical simulation was it possible to conduct such a study without potential harm to the patient [34]. An advantage of the study, in turn, is its randomized multi-center design, a relatively large study group, as well as undertaking an evaluation of chest compression skills not only immediately after training, but also 1 month after training.

Conclusions

Observing real-time chest compression quality parameters during BLS training may improve the quality of chest compression 1 month after training including correct hand positioning, compression depth and rate compliance.

Acknowledgements

The authors want to thank all participants for their participation in this study.

Funding

Study supported by the ERC Research Net, and the Polish Society of Disaster Medicine.

Conflict of interest: None declared

References

1. Gräsner JT, Bossaert L. Epidemiology and management of cardiac arrest: what registries are revealing. Best Pract Res Clin Anaesthesiol. 2013; 27(3): 293–306, doi: 10.1016/j.bpa.2013.07.008, indexed in Pubmed: 24054508.
2. Berdowski J, Berg RA, Tijssen JGP, et al. Global incidences of out-of-hospital cardiac arrest and survival rates: Systematic review of 67 prospective studies. Resuscitation. 2010; 81(11): 1479–1487, doi: 10.1016/j.resuscitation.2010.08.006, indexed in Pubmed: 20828914.
3. Jagosz A, Bursy D, Sobon A, et al. In-hospital sudden cardiac arrest protocol analysis. Kardiol Pol. 2018; 76(2): 376–380, doi: 10.5603/KP.a2017.0209, indexed in Pubmed: 29131292.
4. Vaillancourt C, Verma A, Trickett J, et al. Evaluating the effectiveness of dispatch-assisted cardiopulmonary resuscitation instructions. Acad Emerg Med. 2007; 14(10): 877–883, doi: 10.1197/j.aem.2007.06.021, indexed in Pubmed: 17761545.
5. Smereka J, Szarpak L, Rodríguez-Núñez A, et al. A randomized comparison of three chest compression techniques and associated hemodynamic effect during infant CPR: A randomized manikin study. Am J Emerg Med. 2017; 35(10): 1420–1425, doi: 10.1016/j.ajem.2017.04.024, indexed in Pubmed: 28433454.
6. Smereka J, Madziala M, Szarpak L. Comparison of two infant chest compression techniques during simulated newborn cardiopulmonary resuscitation performed by a single rescuer: a randomized, crossover multicenter trial. Cardiol J. 2018 [Epub ahead of print], doi: 10.5603/CJ.a2018.0090, indexed in Pubmed: 30155866.
7. Ewy GA, Zuercher M, Hilwig RW, et al. Improved neurological outcome with continuous chest compressions compared with 30:2 compressions-to-ventilations cardiopulmonary resuscitation in a realistic swine model of out-of-hospital cardiac arrest. Circulation. 2007; 116(22): 2525–2530, doi: 10.1161/CIRCULATIONAHA.107.711820, indexed in Pubmed: 17998457.
8. Smereka J, Iskrzycki Ł, Makomaska-Szaroszyk E, et al. The effect of chest compression frequency on the quality of resuscitation by lifeguards. A prospective randomized crossover multicenter simulation trial. Cardiol J. 2018 [Epub ahead of print], doi: 10.5603/CJ.a2018.0121, indexed in Pubmed: 30338845.
9. Czekjalo M. Are we prepared to use bag-mask-ventilation during continuous chest compression? Disaster and Emergency Medicine Journal. 2018; 3(4): 148–149, doi: 10.5603/demj.2018.0030.
10. Majer J, Madziala A, Dabrowska A, et al. The place of TrueCPR feedback device in cardiopulmonary resuscitation. Should we use it? A randomized pilot study. Disaster and Emergency Medicine Journal. 2018; 3(4): 131–136, doi: 10.5603/demj.2018.0028.
11. Jorge-Soto C, Abilleira-González M, Otero-Agra M, et al. Schoolteachers as candidates to be basic life support trainers: A simulation trial. Cardiol J. 2018 [Epub ahead of print], doi: 10.5603/CJ.a2018.0073, indexed in Pubmed: 30009374.
12. Wieczorek W, Smereka J, Szarpak L, et al. Which position for resuscitation should we take? A randomized crossover manikin study. Am J Emerg Med. 2018; 36(5): 899–900, doi: 10.1016/j.ajem.2017.09.043, indexed in Pubmed: 29100786.
13. Szarpak L, Filipiak KJ, Ładny JR, et al. Should nurses use mechanical chest compression devices during CPR? Am J Emerg Med. 2016; 34(10): 2044–2045, doi: 10.1016/j.ajem.2016.07.057, indexed in Pubmed: 27528048.
14. Szarpak L, Truszewski Z, Czyzewski L, et al. CPR using the lifeline ARM mechanical chest compression device: a randomized, crossover, manikin trial. Am J Emerg Med. 2017; 35(1): 96–100, doi: 10.1016/j.ajem.2016.10.012, indexed in Pubmed: 27756513.
15. Kleinman ME, Goldberger ZD, Rea T, et al. 2017 American Heart Association Focused Update on Adult Basic Life Support and Cardiopulmonary Resuscitation Quality: An Update to the American Heart Association Guidelines for Cardiopulmonary Resuscitation and Emergency Cardiovascular Care. Circulation. 2018; 137(1): e7–ee13, doi: 10.1161/CIR.0000000000000539, indexed in Pubmed: 29114008.
16. Wieczorek W, Smereka J, Ladny JR, et al. The impact of a CPRezy™ feedback device on the quality of chest compressions performed by nurses. Am J Emerg Med. 2018; 36(7): 1318–1319, doi: 10.1016/j.ajem.2017.11.061, indexed in Pubmed: 29196113.
17. Kurowski A, Szarpak Ł, Bogdański Ł, et al. Comparison of the effectiveness of cardiopulmonary resuscitation with standard manual chest compressions and the use of TrueCPR and PocketCPR feedback devices. Kardiol Pol. 2015; 73(10): 924–930, doi: 10.5603/KP.a2015.0084, indexed in Pubmed: 25985725.
18. Oh JeH, Kim CW. The use of the PocketCPR application in basic life support training. Am J Emerg Med. 2017; 35(1): 189–190, doi: 10.1016/j.ajem.2016.10.082, indexed in Pubmed: 27839843.
19. Kleinman ME, Brennan EE, Goldberger ZD, et al. Part 5: Adult Basic Life Support and Cardiopulmonary Resuscitation Quality:

2015 American Heart Association Guidelines Update for Cardiopulmonary Resuscitation and Emergency Cardiovascular Care. Circulation. 2015; 132(18 Suppl 2): S414–S435, doi: 10.1161/CIR.0000000000000259, indexed in Pubmed: 26472993.

20. Monsieurs KG, Nolan JP, Bossaert LL, et al. ERC Guidelines 2015 Writing Group. European Resuscitation Council Guidelines for Resuscitation 2015: Section 1. Executive summary. Resuscitation. 2015; 95: 1–80, doi: 10.1016/j.resuscitation.2015.07.038, indexed in Pubmed: 26477410.
21. Truszewski Z, Szarpak L, Kurowski A, et al. Randomized trial of the chest compressions effectiveness comparing 3 feedback CPR devices and standard basic life support by nurses. Am J Emerg Med. 2016; 34(3): 381–385, doi: 10.1016/j.ajem.2015.11.003, indexed in Pubmed: 26612703.
22. Majer J, Kaminska H, Wieczorek W, et al. Impact of a CPRmeter feedback device on chest compression quality performed by nurses — a randomized crossover study. Disaster Emerg Med J. 2018; 3(1): 36–37, doi: 10.5603/demj.2018.0008.
23. Kurowski A, Czyżewski L, Bogdański L, et al. Quality of chest compression with CardioPump CPR compared to single rescuer standard BLS. Am J Emerg Med. 2015; 33(1): 114–115, doi: 10.1016/j.ajem.2014.10.027, indexed in Pubmed: 25455057.
24. Abelairas-Gómez C, Barcala-Furelos R, Szarpak Ł, et al. The effect of strength training on quality of prolonged basic cardiopulmonary resuscitation. Kardiol Pol. 2017; 75(1): 21–27, doi: 10.5603/KP.a2016.0165, indexed in Pubmed: 27878801.
25. Jäntti H, Silfvast T, Turpeinen A, et al. Influence of chest compression rate guidance on the quality of cardiopulmonary resuscitation performed on manikins. Resuscitation. 2009; 80(4): 453–457, doi: 10.1016/j.resuscitation.2009.01.001, indexed in Pubmed: 19203821.
26. Szarpak Ł, Truszewski Z, Smereka J, et al. Does the use of a chest compression system in children improve the effectiveness of chest compressions? A randomised crossover simulation pilot study. Kardiol Pol. 2016; 74(12): 1499–1504, doi: 10.5603/KP.a2016.0107, indexed in Pubmed: 27391911.
27. Smereka J, Kasiński M, Smereka A, et al. The quality of a newly developed infant chest compression method applied by paramedics: a randomised crossover manikin trial. Kardiol Pol. 2017; 75(6): 589––595, doi: 10.5603/KP.a2017.0015, indexed in Pubmed: 28150278.
28. Solevåg AL, Schmölzer GM. Optimal Chest Compression Rate and Compression to Ventilation Ratio in Delivery Room Resuscitation: Evidence from Newborn Piglets and Neonatal Manikins. Front Pediatr. 2017; 5: 3, doi: 10.3389/fped.2017.00003, indexed in Pubmed: 28168185.
29. Zou Y, Shi W, Zhu Y, et al. Rate at 120/min provides qualified chest compression during cardiopulmonary resuscitation. Am J Emerg Med. 2015; 33(4): 535–538, doi: 10.1016/j.ajem.2015.01.024, indexed in Pubmed: 25662803.
30. Lee SH, Ryu JiHo, Min MKi, et al. Optimal chest compression rate in cardiopulmonary resuscitation: a prospective, randomized crossover study using a manikin model. Eur J Emerg Med. 2016; 23(4): 253–257, doi: 10.1097/MEJ.0000000000000249, indexed in Pubmed: 25710082.
31. Idris AH, Guffey D, Aufderheide TP, et al. Resuscitation Outcomes Consortium (ROC) Investigators. Relationship between chest compression rates and outcomes from cardiac arrest. Circulation. 2012; 125(24): 3004–3012, doi: 10.1161/CIRCULATIONAHA.111.059535, indexed in Pubmed: 22623717.
32. Dosman CF, Jones RL. High-frequency chest compression: a summary of the literature. Can Respir J. 2005; 12(1): 37–41, doi: 10.1155/2005/525813, indexed in Pubmed: 15776126.
33. Austin AL, Spalding CN, Landa KN, et al. A Randomized Control Trial of Cardiopulmonary Feedback Devices and Their Impact on Infant Chest Compression Quality: A Simulation Study. Pediatr Emerg Care. 2017 [Epub ahead of print], doi: 10.1097/PEC.0000000000001312, indexed in Pubmed: 29084067.
34. Smereka J, Szarpak L, Smereka A, et al. Evaluation of new two-thumb chest compression technique for infant CPR performed by novice physicians. A randomized, crossover, manikin trial. Am J Emerg Med. 2017; 35(4): 604–609, doi: 10.1016/j.ajem.2016.12.045, indexed in Pubmed: 28040386.

VIA MEDICA

ORIGINAL ARTICLE

Cardiology Journal
2021, Vol. 28, No. 3, 446–452
DOI: 10.5603/CJ.a2019.0108

ISSN 1897–5593
eISSN 1898–018X

Acute effects of difference in glucose intake on arterial stiffness in healthy subjects

Ryota Kobayashi[1], Kaori Sato[2], Miki Sakazaki[3], Yukie Nagai[3], Soichiro Iwanuma[4], Nobuyuki Ohashi[4], Takeo Hashiguchi[4]

[1]Center for Fundamental Education, Teikyo University of Science: 2-2-1 Senju, Sakuragi, Adachi-ku, Tokyo, Japan
[2]College of Liberal Arts, International Christian University: 3-10-2, Osawa, Mitaka Shi, Tokyo To, Japan
[3]Research and Development Division, Mitsui Sugar Co., Ltd: 36-2 Nihonbashihakozakicho, Chuo City, Tokyo, Japan
[4]Department of School Education, Teikyo University of Science: 2-2-1 Senju, Sakuragi, Adachi-ku, Tokyo, Japan

Abstract

Background: *Post-prandial hyperglycemia is associated with higher cardiovascular risk, which causes arterial stiffening and impaired function. Although post-prandial increases in blood glucose are proportional to the level of intake, the acute effects of different glucose intakes on arterial stiffness have not been fully characterized. The present study aimed to determine the acute effects of differences in glucose intake on arterial stiffness.*

Methods: *Six healthy middle-aged and elderly individuals (mean age, 60.0 ± 12.1 years) were orally administered 15, 20, and 25 g of glucose on separate days in a randomized, controlled, cross-over fashion. Brachial-ankle pulse wave velocity, heart-brachial pulse wave velocity, cardio-ankle vascular index, brachial and ankle blood pressure, heart rate, and blood glucose and serum insulin concentrations before and 30, 60, and 90 min after glucose ingestion were measured.*

Results: *Compared to baseline, brachial-ankle pulse wave velocity was higher at 30, 60 and 90 min after ingestion of 25 g glucose, and higher at 90 min after ingestion of 20 g glucose, but at no time points after ingestion of 15 g. Cardio-ankle vascular index was higher at 60 min than at baseline after ingestion of 25 g glucose, but not after ingestion of 15 or 20 g.*

Conclusions: *These results suggest that brachial-ankle pulse wave velocity and cardio-ankle vascular index is affected by the quantity of glucose ingested. Proposed presently is that glucose intake should be reduced at each meal to avoid increases in brachial-ankle pulse wave velocity and cardio-ankle vascular index during acute hyperglycemia.* (Cardiol J 2021; 28, 3: 446–452)

Key words: arterial stiffness, brachial-ankle pulse wave velocity, cardio-ankle vascular index, quantity of glucose ingestion, healthy subjects

Introduction

High central (aortic), peripheral (leg) and systemic pulse wave velocity (PWV) and cardio--ankle vascular index (CAVI) are indices of arterial stiffness and are used as important determinants and indices of cardiovascular risk [1, 2]. Moreover, high ankle systolic blood pressure (SBP) has been proposed as an independent risk factor for the development of cardiovascular disease [3]. Wohlfahrt et al. [4] reported that arterial stiffness correlates with ankle SBP. Inhibition of any increases in arte-

Address for correspondence: Ryota Kobayashi, PhD, Center for Fundamental Education, Teikyo University of Science: 2-2-1 Senju, Sakuragi, Adachi-ku, Tokyo 120-0045, Japan, tel: +81 80 9193 3605, fax: 03-6910-3800, e-mail: rkobayashi@ntu.ac.jp

Received: 7.05.2019 Accepted: 29.09.2019

rial stiffness and ankle SBP might thus be beneficial for health.

Arterial stiffness and ankle SBP acutely increase after glucose ingestion [5, 6], and higher post-prandial hyperglycemia is associated with cardiovascular risk, which causes arterial stiffening and impaired functioning [7]. Furthermore, a new World Health Organization (WHO) guideline recommends that adults and children reduce the daily intake of free sugars to < 25 g [8]. Although post-prandial increases in blood glucose (BG) are known to be proportional to the level of intake [9], whether arterial stiffness and SBP will increase after ingesting < 25 g of glucose remains unclear.

The present study aimed to investigate the acute effects of differences in glucose intake on arterial stiffness and SBP. Hypothesized herein is that differences in glucose intake would affect changes in arterial stiffness and SBP after glucose ingestion in older adults.

Methods

Subjects

In this study there are 6 healthy subjects (mean age, 60 ± 12 years). All lived a sedentary lifestyle (≥ 2 years without regular exercise as assessed by the international physical activity questionnaire) and were normotensive (< 140/90 mmHg), normoglycemia (< 109 mg/dL), non-smokers, without symptoms or history of overt chronic disease (Table 1). All participants were fully informed about the experimental procedures as well as the purpose of the study before providing written, informed consent to participate. The Ethics Committee at Teikyo University of Science approved this study, which proceeded in accordance with the guidelines for human experimentation published by the documented institutional review board (approval no. 18034). This study also conformed to the principles of the Declaration of Helsinki.

Study design

Each participant completed 3 trials in random order: orally administered 15, 20, and 25 g glucose (in 200 mL of water, consumed within 5 min) on separate days. All subjects then rested for at least 10 min in a supine position to establish a stable baseline. Each volunteer waited about 2–3 days after completion of one trial before crossing over to the next trial. Brachial-ankle PWV was measured, (baPWV indicative of systemic arterial stiffness), heart-brachial PWV (hbPWV, indicative of proximal aortic arterial stiffness), brachial and ankle SBP, diastolic blood pressure (DBP), pulse pressure (PP), heart rate (HR), CAVI (indicative of systemic arterial stiffness), and BG and serum insulin concentrations, before (baseline) and 30, 60, and 90 min after glucose ingestion. All these measurements, including baPWV, hbPWV, CAVI, and fasting BG, were evaluated after 12 h of fasting (Fig. 1).

Anthropometrics

Height and weight were measured to the nearest 0.5 cm using a stadiometer, and body composi-

Table 1. Characteristics of study participants.

Parameters	Value
Age [years]	60 ± 12
Height [cm]	165 ± 11
Weight [kg]	62 ± 14
Body fat [%]	24 ± 4
BMI [kg/m^2]	22 ± 2
Brachial SBP [mmHg]	120 ± 20
Ankle SBP [mmHg]	141 ± 11
BG [mg/dL]	94 ± 9
Insulin [mg/dL]	5 ± 3
HDL-C [mg/dL]	58 ± 7
Triglycerides [mg/dL]	97 ± 25

Values represent mean ± standard deviation; BMI — body mass index; BG — blood glucose; HDL-C — high-density lipoprotein cholesterol; SBP — systolic blood pressure

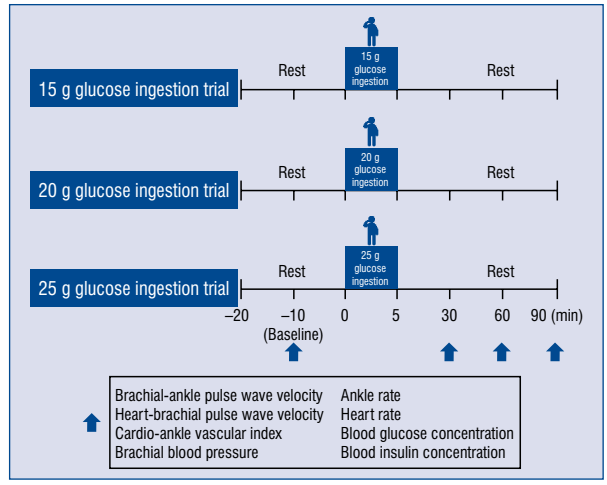

Figure 1. Study design. After 10 min of supine rest, pulse wave velocity, cardio-ankle vascular index, brachial and ankle blood pressure, heart rate, blood glucose level and blood insulin level were measured before (baseline) and at 30, 60 and 90 min after glucose ingestion (15, 20 and 25 g).

tion was determined using a body composition analyzer (WB-150 PMA; TANITA Co., Tokyo, Japan).

Arterial stiffness

baPWV, hbPWV, BP, and HR was measured using a form PWV/ABI vascular testing device [10] (Fukuda-Colin Co., Tokyo, Japan) and CAVI using a VaSera VS-1500® vascular testing device [11] (Fukuda Denshi Co., Tokyo, Japan). baPWV is an index that reflects systemic arterial stiffness and hbPWV reflects proximal aortic stiffness. The CAVI is an index that reflects systemic arterial stiffness is theoretically adjusted by blood pressure.

Blood pressure and heart rate

Brachial and ankle SBP, mean BP (MBP) and DBP, PP and HR while in supine resting were measured in triplicate using an automated oscillometric-form PWV/ABI device (Form PWV/ /ABI; Fukuda-Colin Co., Tokyo, Japan) over the brachial and ankle arteries. Carotid SBP, which has been proposed as an indicator of the magnitude of wave reflections, was also obtained from pressure waveforms [12].

Blood glucose and insulin levels

Venous blood was withdrawn from participants via catheter in the right or left arm before, and at 30, 60 and 90 min after ingestion of 15, 20 or 25 g glucose. Levels of BG and insulin were assayed using the ultraviolet-hexokinase method and chemiluminescent enzyme immunoassay, respectively.

Oral glucose ingestion

15, 20, and 25 g of glucose were orally administered to each participant (in 200 mL of water, consumed within 5 min) on separate days using a cross-over design in the morning after an overnight (12 h) fast. The glucose beverage (200 mL) was within the standard for adult humans and was consumed within 5 min [13].

Sample size

A power analysis was performed with G*Power 3 to determine the appropriate sample size. Effect size for arterial stiffness at the laboratory was 0.5. To detect differences with 60% power and a one-tailed α of 5% in the laboratory using analysis of variance, it was calculated that each intervention would require 6 individuals.

Statistical analyses

All data are presented as mean ± standard deviation (SD). The normal distribution of all data was confirmed using the Kolmogorov-Smirnov test. Data were analyzed using repeated-measures two-way analysis of variance, with variables of group and time. Significant differences between mean values were identified using the Bonferroni post-test. Data were analyzed using SPSS version 25 (IBM, Armonk, NY), with statistical significance being accepted at the level of $p < 0.05$.

Results

Baseline baPWV, hbPWV, and CAVI did not differ between trials ($p > 0.05$, Fig. 2). The baPWV was higher at 30, 60 and 90 min than at baseline after ingestion of 25 g glucose trial ($p < 0.05$, Fig. 2A), and significantly higher at 90 min than at baseline after ingestion of 20 g glucose trial ($p < 0.05$, Fig. 2A), but no significant changes were seen after ingestion of 15 g glucose trial ($p > 0.05$, Fig. 2A). The hbPWV was no different at 30, 60, or 90 min than at baseline after ingestion of any quantity of glucose ($p > 0.05$, Fig. 2B). CAVI was significantly higher at 60 min than at baseline after ingestion of 25 g glucose trial ($p < 0.05$, Fig. 2C), but no significant differences were seen following the 15 or 20 g trial ($p > 0.05$, Fig. 2C).

Brachial SBP, DBP and PP and ankle DBP did not differ significantly according to glucose dose ($p > 0.05$ each, Table 2). Brachial SBP, DBP and PP and ankle DBP were not significantly different at 30, 60 or 90 min than at baseline after ingesting any quantity of glucose ($p > 0.05$ each, Table 2). Ankle SBP was significantly higher at 30, 60 and 90 min than at baseline after ingestion of 25 g glucose trial ($p < 0.05$, Table 2), and at 60 and 90 min after ingestion of 20 g glucose trial ($p < 0.05$, Table 2), but no significant differences were seen following the ingestion of 15 g glucose trial ($p > 0.05$, Table 2). Ankle PP was significantly higher at 60 and 90 min than at baseline after ingestion of 20 and 25 g glucose trial ($p < 0.05$, Table 2), but no significant differences were seen following ingestion of 15 g glucose trial ($p > 0.05$, Table 2).

Blood glucose was significantly higher at 60 min after the ingestion in the ingestion of 20 or 25 g glucose compared with the ingestion of 15 g glucose trial ($p < 0.05$, Table 3). Compared to baseline, BG was significantly higher at 30 min after ingestion of 15 g glucose trial ($p < 0.05$, Table 3), at 30 and 60 min after ingestion of 20 g glucose trial ($p < 0.05$, Table 3), and at 30, 60, and 90 min after ingestion of 25 g ($p < 0.05$, Table 3). Compared to baseline, serum insulin was significantly higher at

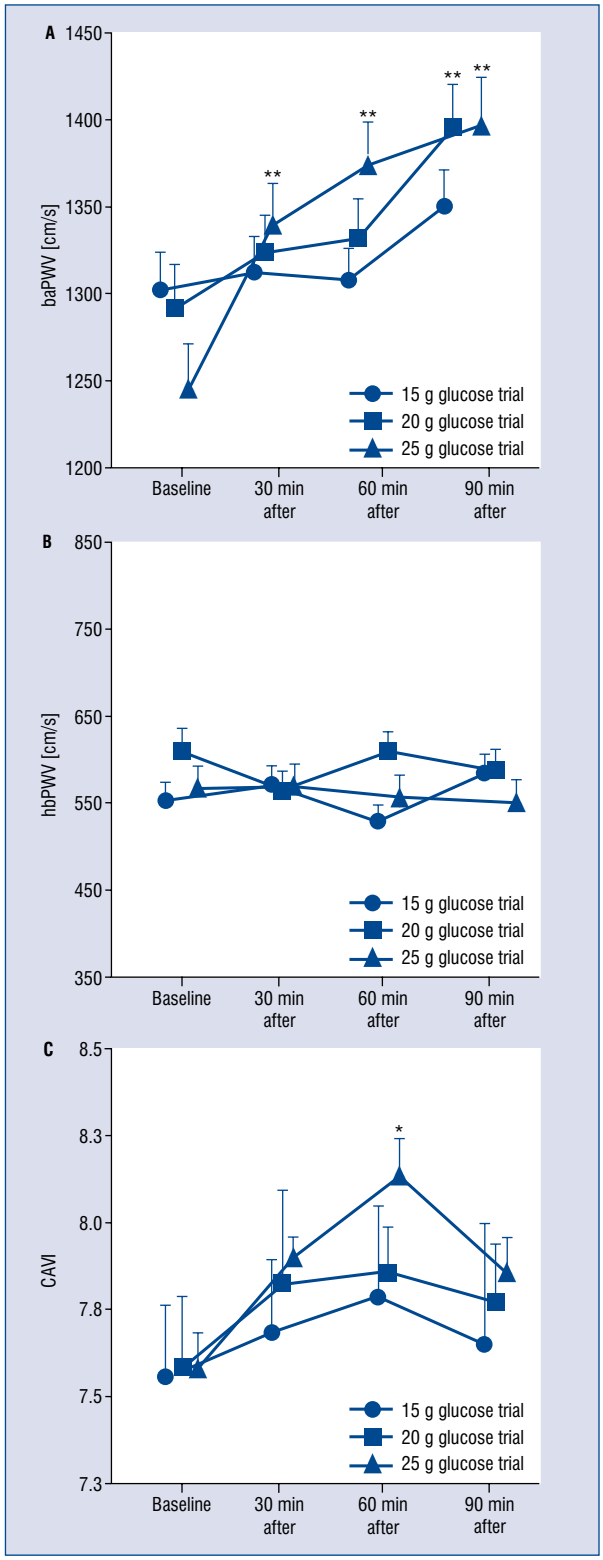

Figure 2. Changes in pulse wave velocity and cardio-ankle vascular index (CAVI) before (baseline) and after glucose ingestion. Values represent mean ± standard deviation; baPWV — brachial-ankle pulse wave velocity; hbPWV — heart-brachial pulse wave velocity; *p < 0.05 vs. baseline; **p < 0.01 vs. baseline.

30 min after ingestion of 15 g glucose trial ($p < 0.05$, Table 3), at 60 and 90 min after 20 g ($p < 0.05$, Table 3), and at 30, 60, and 90 min than at baseline after 25 g glucose trial ($p < 0.05$, Table 3).

Discussion

The novel finding of this study was that baPWV and CAVI were significantly increased after ingestion of 25 g glucose, and baPWV was significantly increased after ingestion of 20 g glucose, but not after ingestion of 15 g. These results suggest that baPWV and CAVI only increase after larger doses of glucose. It was therefore proposed that glucose intake in a single meal should be reduced to prevent significant post-prandial increases in arterial stiffness.

Arterial stiffness acutely increases following high-carbohydrate meals. Indeed, Grassi et al. [14] and Gomez-Sanchez et al. [15] reported that systemic and peripheral arterial stiffness increased after glucose ingestion in healthy volunteers. Higher cardiovascular risk is associated with post-prandial hyperglycemia, which causes arterial stiffening [7]. The current WHO guideline recommends that adults and children reduce the daily intake of free sugars to < 25 g [8]. It was shown that baPWV was significantly higher at 30, 60 and 90 min than at baseline after ingestion of 25 g glucose, and was significantly higher at 90 min than at baseline after ingestion of 20 g glucose, whereas no significant change was seen after ingestion of 15 g. Thus, consuming drinks and meals with lower sugar content might be effective in reducing the amount of glucose ingested at a single sitting, and thus suppress the increase in arterial stiffness that follows glucose ingestion. In addition, future research should use a method that does not increase arterial stiffness because of high-dose glucose ingestion, such as by changing from the use of glucose to palatinose.

Aortic arterial stiffness increases after glucose ingestion in obese individuals and those with metabolic syndrome [16]. It was previously reported that leg PWV increases acutely, whereas aortic PWV does not change, after oral ingestion of 75 g glucose in healthy individuals [5, 17]. Current findings indicate that both baPWV and CAVI significantly increase after ingestion of 25 g glucose, and baPWV significantly increases after ingestion of 20 g of glucose, whereas hbPWV (an indicator of proximal aortic stiffness) is unaffected by ingestion of 15–25 g glucose in healthy older individuals.

Table 2. Changes in cardiovascular indices before and after glucose ingestion.

	Baseline	After 30 min	After 60 min	After 90 min
Brachial systolic blood pressure [mmHg]				
15 g glucose ingestion	120 ± 20	118 ± 12	120 ± 16	122 ± 17
20 g glucose ingestion	118 ± 16	119 ± 15	123 ± 14	125 ± 20
25 g glucose ingestion	119 ± 17	120 ± 15	123 ± 14	121 ± 17
Brachial diastolic blood pressure [mmHg]				
15 g glucose ingestion	76 ± 15	75 ± 10	76 ± 10	78 ± 9
20 g glucose ingestion	75 ± 14	75 ± 11	79 ± 10	80 ± 13
25 g glucose ingestion	75 ± 15	78 ± 11	76 ± 11	77 ± 12
Brachial pulse pressure [mmHg]				
15 g glucose ingestion	44 ± 6	42 ± 4	43 ± 8	44 ± 10
20 g glucose ingestion	42 ± 4	44 ± 7	43 ± 5	45 ± 8
25 g glucose ingestion	44 ± 4	42 ± 8	46 ± 5	43 ± 5
Ankle systolic blood pressure [mmHg]				
15 g glucose ingestion	141 ± 11	141 ± 9	141 ± 9	146 ± 9
20 g glucose ingestion	140 ± 10	144 ± 10	152 ± 11**	151 ± 12**
25 g glucose ingestion	139 ± 11	147 ± 9*	153 ± 10**	151 ± 10**
Ankle diastolic blood pressure [mmHg]				
15 g glucose ingestion	76 ± 15	75 ± 10	76 ± 11	77 ± 9
20 g glucose ingestion	76 ± 11	76 ± 13	80 ± 11	80 ± 13
25 g glucose ingestion	76 ± 12	78 ± 12	78 ± 10	78 ± 15
Ankle pulse pressure [mmHg]				
15 g glucose ingestion	65 ± 13	65 ± 12	64 ± 15	68 ± 15
20 g glucose ingestion	64 ± 14	68 ± 16	71 ± 17*	71 ± 17*
25 g glucose ingestion	62 ± 16	68 ± 12	74 ± 16**	72 ± 11**
Heart rate [beats/min]				
15 g glucose ingestion	62 ± 9	60 ± 8	59 ± 8	62 ± 10
20 g glucose ingestion	63 ± 9	59 ± 7	60 ± 7	58 ± 7
25 g glucose ingestion	62 ± 9	60 ± 10	62 ± 9	59 ± 8

Values are mean ± standard deviation. *p < 0.05 vs. baseline; **p < 0.01 vs. baseline

Table 3. Changes in blood glucose and insulin levels before and after glucose ingestion.

	Baseline	After 30 min	After 60 min	After 90 min
Blood glucose [mg/dL]				
15 g glucose ingestion	94 ± 9	130 ± 28**	108 ± 17	94 ± 17
20 g glucose ingestion	98 ± 5	139 ± 21**	137 ± 26**,†	110 ± 20
25 g glucose ingestion	93 ± 12	142 ± 21**	137 ± 26**,†	107 ± 20**
Insulin [mg/dL]				
15 g glucose ingestion	5 ± 3	11 ± 9*	9 ± 5	6 ± 5
20 g glucose ingestion	5 ± 2	10 ± 4	15 ± 8**	9 ± 2**
25 g glucose ingestion	5 ± 2	13 ± 8*	13 ± 5**	9 ± 2**

Values represent mean ± standard deviation. *p < 0.05 vs. baseline; **p < 0.01 vs. baseline; †p < 0.05 vs. 15 g glucose ingestion

The increase in arterial stiffness after ingestion of glucose might thus be stronger in the lower limb artery than in the aorta. However, changes in aortic PWV after glucose ingestion might occur in obese older individuals (those with high insulin resistance).

Greater arterial stiffness after meals is associated with increases in SBP [5, 18]. It was shown herein, that hbPWV and brachial SBP were not significantly changed after ingestion of glucose. The present study shows that baPWV and ankle SBP increased after ingestion of glucose. It was previously reported that leg PWV and ankle SBP increased acutely, whereas aortic PWV and aortic SBP did not change significantly, after oral ingestion of 75 g glucose in healthy individuals [5, 18]. This rise in ankle SBP may be indicative of an increase in baPWV (the main is leg PWV) after ingestion of 20 and 25 g glucose. However, this was not directly assessed, representing an important limitation of this study. Importantly, it was shown that CAVI increased significantly after ingestion of 25 g glucose. CAVI is independent of blood pressure variations during measurement [19]. The level of oxidative stress, as determined by measuring thiobarbituric acid reactive substances (TBARS), acutely increases after a 75-g oral glucose tolerance test [20], and Kawano et al. [20] have shown that TBARS after glucose ingestion correlates with BG. Tso et al. [21] have shown that TBARS correlates with arterial stiffness. Thus, the increase in CAVI after ingesting 25 g glucose might be associated with oxidative stress induced by hyperglycemia. However, levels of oxidative stress were not assessed, representing another limitation of the present study.

From the above context, it was considered that increased arterial stiffness after ingesting 20 g of glucose was mainly related to elevated SBP. Moreover, increased arterial stiffness after ingesting 25 g of glucose might be associated with decreased vascular endothelial function due to increased oxidative stress and a rise in SBP. Studying the mechanisms underlying increases in arterial stiffness due to differences in glucose intake will be important in future research.

Limitations of the study

Some other limitations must be addressed when considering the present findings. The participants were healthy subjects, which precludes the generalization of our findings to younger individuals. In addition, the sample size was very small (n = 6), although the effects of glucose dose on arterial stiffness differed sufficiently in detecting significant differences and the differences identified were similar to those identified in previous studies (n = 6) of acute changes in arterial stiffness [21]. There was also no control group. A further limitation is the lack of carotid-femoral PWV which is the gold standard technique for the assessment of arterial stiffness. Finally, this study was not designed to determine the possible mechanisms underlying the acute effects of glucose intake on PWV and CAVI.

Conclusions

Significant increases in baPWV and CAVI were identified after ingestion of 25 g glucose, and baPWV significantly increased after ingestion of 20 g glucose, but neither increased after 15 g of glucose. This suggests that arterial stiffness is only acutely affected by the ingestion of larger quantities of glucose. It was therefore proposed that glucose intake should be reduced at each meal to avoid increases in arterial stiffness during acute hyperglycemia.

Acknowledgements

This work was supported by a research funding from Mitsui Sugar Co., Ltd.

Conflict of interest: None declared

References

1. Yamashina A, Tomiyama H, Arai T, et al. Nomogram of the relation of brachial-ankle pulse wave velocity with blood pressure. Hypertens Res. 2003; 26(10): 801–806, doi: 10.1291/hypres.26.801, indexed in Pubmed: 14621183.
2. van Sloten TT, Schram MT, van den Hurk K, et al. Local stiffness of the carotid and femoral artery is associated with incident cardiovascular events and all-cause mortality: the Hoorn study. J Am Coll Cardiol. 2014; 63(17): 1739–1747, doi: 10.1016/j.jacc.2013.12.041, indexed in Pubmed: 24583306.
3. Tsuchikura S, Shoji T, Kimoto E, et al. Central versus peripheral arterial stiffness in association with coronary, cerebral and peripheral arterial disease. Atherosclerosis. 2010; 211(2): 480–485, doi: 10.1016/j.atherosclerosis.2010.03.037, indexed in Pubmed: 20430390.
4. Wohlfahrt P, Krajčoviechová A, Seidlerová J, et al. Lower-extremity arterial stiffness vs. aortic stiffness in the general population. Hypertens Res. 2013; 36(8): 718–724, doi: 10.1038/hr.2013.21, indexed in Pubmed: 23575382.
5. Kobayashi R, Yoshida S, Okamoto T. Arterial stiffness after glucose ingestion in exercise-trained versus untrained men. Appl Physiol Nutr Metab. 2015; 40(11): 1151–1156, doi: 10.1139/apnm-2015-0131, indexed in Pubmed: 26444929.
6. Kobayashi R, Yoshida S, Okamoto T. Effects of acute aerobic exercise on arterial stiffness before and after glucose ingestion. Int J Sports Med. 2017; 38(1): 12–18, doi: 10.1055/s-0042-115019, indexed in Pubmed: 27813047.
7. Jacome-Sosa M, Parks EJ, Bruno RS, et al. Postprandial metabolism of macronutrients and cardiometabolic risk: recent developments, emerging concepts, and future directions. Adv Nutr. 2016; 7(2): 364–374, doi: 10.3945/an.115.010397, indexed in Pubmed: 26980820.

8. WHO Guidelines Approved by the Guidelines Review Committee. Guideline: sugars intake for adults and children. World Health Organization. Geneva 2015.
9. Jenkins DJ, Wolever TM, Taylor RH, et al. Glycemic index of foods: a physiological basis for carbohydrate exchange. Am J Clin Nutr. 1981; 34(3): 362–366, doi: 10.1093/ajcn/34.3.362, indexed in Pubmed: 6259925.
10. Sugawara J, Tomoto T, Tanaka H. Heart-to-Brachium pulse wave velocity as a measure of proximal aortic stiffness: MRI and longitudinal studies. Am J Hypertens. 2019; 32(2): 146–154, doi: 10.1093/ajh/hpy166, indexed in Pubmed: 30445561.
11. Nishiwaki M, Takahara K, Matsumoto N. Arterial stiffness in young adult swimmers. Eur J Appl Physiol. 2017; 117(1): 131–138, doi: 10.1007/s00421-016-3505-9, indexed in Pubmed: 27873019.
12. Okamoto T, Sakamaki MS, Min SK, et al. Repeated cessation and resumption of resistance training attenuates increases in arterial stiffness. Int J Sports Med. 2015; 36(6): 440–445, doi: 10.1055/s-0034-1398584, indexed in Pubmed: 25734911.
13. Seino Y, Nanjo K, Tajima N, et al. Report of the committee on the classification and diagnostic criteria of diabetes mellitus. J Diabetes Investig. 2010; 1(5): 212–228, doi: 10.1111/j.2040-1124.2010.00074.x, indexed in Pubmed: 24843435.
14. Grassi D, Desideri G, Necozione S, et al. Protective effects of flavanol-rich dark chocolate on endothelial function and wave reflection during acute hyperglycemia. Hypertension. 2012; 60(3): 827–832, doi: 10.1161/HYPERTENSIONAHA.112.193995, indexed in Pubmed: 22851734.
15. Gomez-Sanchez L, Garcia-Ortiz L, Patino-Alonso MC, et al. MARK Group. Glycemic markers and relation with arterial stiffness in Caucasian subjects of the MARK study. PLoS One. 2017; 12(4): e0175982, doi: 10.1371/journal.pone.0175982, indexed in Pubmed: 28414819.
16. Baynard T, Carhart RL, Weinstock RS, et al. Short-term exercise training improves aerobic capacity with no change in arterial function in obesity. Eur J Appl Physiol. 2009; 107(3): 299–308, doi: 10.1007/s00421-009-1126-2, indexed in Pubmed: 19609554.
17. Kobayashi R, Hashimoto Y, Hatakeyama H, et al. Acute effects of aerobic exercise intensity on arterial stiffness after glucose ingestion in young men. Clin Physiol Funct Imaging. 2018; 38(1): 138–144, doi: 10.1111/cpf.12395, indexed in Pubmed: 27758064.
18. Blendea MC, Bard M, Sowers JR, et al. High-fat meal impairs vascular compliance in a subgroup of young healthy subjects. Metabolism. 2005; 54(10): 1337–1344, doi: 10.1016/j.metabol.2005.04.023, indexed in Pubmed: 16154433.
19. Shirai K, Utino J, Otsuka K, et al. A novel blood pressure-independent arterial wall stiffness parameter; cardio-ankle vascular index (CAVI). J Atheroscler Thromb. 2006; 13(2): 101–107, doi: 10.5551/jat.13.101, indexed in Pubmed: 16733298.
20. Kawano H, Motoyama T, Hirashima O, et al. Hyperglycemia rapidly suppresses flow-mediated endothelium-dependent vasodilation of brachial artery. J Am Coll Cardiol. 1999; 34(1): 146–154, doi: 10.1016/s0735-1097(99)00168-0.
21. Tso TK, Huang WN, Huang HY, et al. Association of brachial-ankle pulse wave velocity with cardiovascular risk factors in systemic lupus erythematosus. Lupus. 2005; 14(11): 878–883, doi: 10.1191/0961203305lu2234oa, indexed in Pubmed: 16335579.

VIA MEDICA

ORIGINAL ARTICLE

Cardiology Journal
2021, Vol. 28, No. 3, 453–459
DOI: 10.5603/CJ.a2020.0074

ISSN 1897–5593
eISSN 1898–018X

Elevated circulating level of P2X7 receptor is related to severity of coronary artery stenosis and prognosis of acute myocardial infarction

Xiang-Xiang Shi, Kang-Chun Zheng, Pei-Ren Shan, Lei Zhang, Sheng-Jie Wu, Zhou-Qing Huang

Cardiac Center, Department of Cardiology, The Key Lab of Cardiovascular Disease of Wenzhou, The First Affiliated Hospital of Wenzhou Medical University, Wenzhou, Zhejiang, People's Republic of China

Abstract

Background: *Acute myocardial infarction (AMI) is a severely life-threatening cardiovascular disease. Previous research has identified an association between the P2X7 receptor (P2X7R) and the development of atherosclerosis. However, the correlation of its expression with the clinical prognosis of patients with AMI remains unclear. The present study aimed to investigate the potential role of P2X7R in Chinese patients with AMI.*

Methods: *Seventy-nine patients with AMI and 48 controls were consecutively enrolled in this prospective observational study. Circulating P2X7R mRNA expression levels and other clinical variables were determined upon admission to the hospital. Patients were followed up for 360 days, and the end-point was considered as the occurrence of major adverse cardiovascular events (MACE).*

Results: *Circulating P2X7R mRNA expression level in peripheral blood mononuclear cells of patients with AMI were significantly higher than those in controls and had promising diagnostic ability of AMI with an area under the curve of 0.928. Furthermore, P2X7R was demonstrated to be correlated positively with the severity of coronary artery stenosis. Additionally, this is the first study to indicate that higher P2X7R mRNA expression is associated with a higher rate of MACE within 360 days after AMI.*

Conclusions: *The present study showed that the circulating level of P2X7R was elevated in AMI patients and was closely associated with the severity of coronary artery stenosis and prognosis of AMI.*
(Cardiol J 2021; 28, 3: 453–459)

Key words: P2X7R, acute myocardial infarction, coronary artery stenosis, prognosis

Introduction

Myocardial infarction, a cardiovascular disease that severely threatens human health, is primarily caused by atherosclerosis of the coronary artery. Pathogenesis of atherosclerosis involves the accumulation of lipids and leukocytes in the intima of blood vessel walls leading to plaque, inflammation, and alteration of innate and adaptive immunities [1, 2]. Rupture of the vulnerable plaque, characterized by a thin fibrous cap and lipid-rich core is the main cause of coronary thrombosis at the site of plaque, leading to acute myocardial infarction (AMI) [3].

Purinergic receptor P2X7 (P2X7R) is a ligand-gated cation channel that is significantly expressed in original immune cells. P2X7R is the most compelling member of the purinergic receptor family owing to its unique phenotype and is involved in the production and activation of inflammatory cytokine interleukin-1 beta for the modulation of inflammatory responses [4]. Research has demonstrated that P2X7R is highly expressed in endothelial cells and macrophages infiltrating the atherosclerotic plaques in human carotid arteries [5]. Peng et al. [6] reported that P2X7R plays a crucial role in the development of atherosclerosis through the regu-

Address for correspondence: Zhou-Qing Huang, MD, PhD, Department of Cardiology, the First Affiliated Hospital of Wenzhou Medical University, Zhejiang, 325000, China, e-mail: susiehzq@126.com

Received: 11.11.2019 Accepted: 6.05.2020

Table 1. Characteristics of patients with acute myocardial infarction (AMI) and controls.

	AMI (n = 79)	Controls (n = 48)	P
Age [years]	62.9 ± 12.9	64.8 ± 10.3	0.393
Male	65 (79.5%)	26 (54.2%)	0.001*
Hypertension	44 (55.6%)	33 (68.8%)	0.144
Diabetes	19 (24.1%)	11 (22.9%)	0.884
Smoking	42 (53.2%)	13 (27.1%)	0.004*
Laboratory parameters:			
TC [mmol/L]	4.91 ± 1.1	4.27 ± 0.9	0.001*
TG [mmol/L]	1.40 ± 1.3	1.57 ± 0.7	0.435
LDL [mmol/L]	3.09 ± 0.9	2.58 ± 0.9	0.004*
HDL [mmol/L]	1.07 ± 0.2	1.12 ± 0.3	0.385
WBC [$\times 10^9$/L]	8.97 ± 3.0	6.56 ± 1.8	0.000*
Thyroxine [nmol/L]	97.49 ± 27.1	104.16 ± 23.4	0.163
RDW [%]	13.47 ± 1.0	13.03 ± 0.8	0.008*
CRP [mg/L]	23.61 ± 19.5	5.15 ± 7.3	0.000*
sUA [μmol/L]	366.5 ± 103.6	362.3 ± 91.4	0.820

Data presented as mean ± standard deviation for variables; TC — total cholesterol; TG — triglycerides; LDL — low–density lipoprotein; HDL — high–density lipoprotein; WBC — white blood count; RDW — red–cell distribution width; CRP — C–reactive protein; sUA — serum uric acid; *$p < 0.05$ AMI vs. control

lation of NLRP3 inflammasome activation. Interestingly, rheumatoid arthritis is coupled with increased incidence of myocardial infarction, and the severity of arthritis has been proven to be reduced in P2X7 receptor knockout mice [7].

This accumulating evidence suggests the possibility of an association between P2X7R and the development of atherosclerosis; however, the significance of its expression in clinical patients with AMI remains unclear. The present study was conducted to investigate the potential role of P2X7R in AMI.

Methods

Study subjects

Seventy-nine patients with AMI (ICD-9 codes 410), undergoing coronary angiography in the cardiac care unit of the First Affiliated Hospital of Wenzhou Medical College (China), were consecutively recruited for the present study (Table 1). AMI, including ST-segment elevation myocardial infarction (STEMI) and non-ST-segment elevation myocardial infarction (NSTEMI), was diagnosed based on the presence of two of the following criteria: prolonged chest pain; typical electrocardiogram changes; and increased troponin I level (> 0.15 μg/L). The control group comprised 48 patients recruited from the cardiology department. These patients presented chest discomfort and certain risk factors for coronary disease, but their coronary angiography results were normal. Exclusion criteria included patients with ischemic stroke history, peripheral vascular disease, hematological diseases, acute or chronic inflammation, liver dysfunction (2 times higher than the upper limit of the reference range of AST/ALT), severe renal dysfunction (chronic kidney disease stage: G4–5), autoimmune disease, and cancer.

Patients in both AMI and control groups were treated with dual antiplatelet therapy and statin as per standard protocol after hospitalization. Gensini scores were used to evaluate the severity of coronary stenotic lesions and was calculated by two technicians based on imaging results taken at different angles of the angiocardiography.

Written informed consent was obtained from all subjects before enrollment into this study. The study was approved by the Medical Ethics Committee of the First Affiliated Hospital of Wenzhou Medical College (No. 2017-145) and was performed in accordance with the Declaration of Helsinki.

All patients underwent clinical follow-up for one complete year after discharge, to determine the end point based on the findings at the last visit or last telephone call. However, some patients were lost during follow-up for various reasons. The composite end point was major adverse cardiovascular events (MACE), which included all-cause death, myocardial infarction, target lesion

revascularization, heart failure, and recurrent angina, which were identified through phone-calls or hospitalization.

Sample collection

In the AMI group, emergency coronary angiography or percutaneous coronary intervention was performed within 12 h of symptom onset, and blood samples were collected immediately after the procedure. In the control group, blood samples were obtained immediately after coronary angiography following their admission. Peripheral venous blood was drawn from the antecubital vein while the patients were in a fasting state. Blood was collected with EDTA as an anticoagulant. Peripheral blood mononuclear cells (PBMCs) were immediately isolated from peripheral venous blood using Ficoll density gradient centrifugation.

Quantitative real-time PCR

RNA extraction from PBMCs was performed according to manufacturer protocol (using TRIzol, Invitrogen). Synthesis of cDNAs was performed by reverse transcription with 2 μg of total RNA using a cDNA Transcription kit (Thermo Fisher Scientific), as described by the manufacturer. Real-time polymerase chain reactions (PCR) were performed by SYBR Premix Ex Taq Kit (TaKaRa, Japan) according to manufacturer instructions. The PCR reactions were evaluated by the ABI-7500 Sequence Detection System. The primer sequences used in the study were as follows: P2X7R (NM_002562.5), forward: 5'-GAACAATATCGACTTCCCCGG-3', reverse: 5'-TTATCGCCTGTTTCTCGGAAG-3'; GAPDH (NM_001256799.2), forward: 5'-CAGGAGGCATTGCTGATGAT-3', reverse: 5'-GAAGGCTGGGGCTCATTT-3'. Values were normalized to that of the housekeeping gene GAPDH. According to manufacturer guidelines, the $^{\Delta\Delta}$Ct method was used to determine relative expression levels. Statistical analyses were performed using $^{\Delta\Delta}$Ct values.

Statistical analysis

Statistical analysis was performed using SPSS v.20 software (SPSS Inc., Chicago, IL). All clinical data were represented as mean ± standard deviation for continuous variables, and as number (%) for incidence rates. Independent-samples T test or the Wilcoxon Rank Sum Test was used for comparison of the two groups of individuals. Chi-square test was used to compare proportions. The association between relative levels of P2X7R and follow-up endpoints was ascertained by the Kaplan-Meier analysis. Receiver operating characteristic (ROC) curve analysis was performed to assess P2X7R as a predictor for distinguishing AMI from non-AMI. Correlations between variables were determined with the Spearman test. The univariate and multivariate cox regression analysis was performed to assess P2X7R expression levels and risk of MACE after myocardial infarction. In all tests, a value of $p < 0.05$ was considered statistically significant.

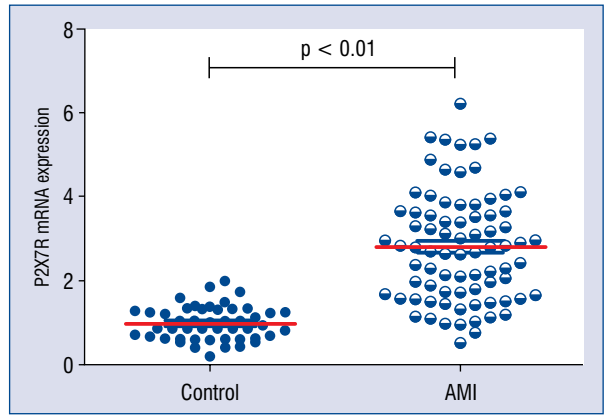

Figure 1. Circulating P2X7R mRNA expression levels in the acute myocardial infarction (AMI) and control groups. Data are presented as the mean ± standard error of the mean; $p < 0.01$ compared to the control.

Results

Baseline characteristics of patients

The baseline characteristics of patients are shown in Table 1. There were 73 cases of STEMI and 6 cases of NSTEMI in the AMI group. Among them, 76 cases were treated with emergency PCI and 3 cases were treated with elective CABG after coronary angiography. No statistical difference in age, hypertension, diabetes, triglycerides, high-density lipoprotein, thyroxine, and uric acid was observed between the two groups. The AMI group had higher values of male-to-female ratio, proportion of smoking, total cholesterol, low-density lipoprotein (LDL), white blood count, red cell distribution width, and C-reactive protein (CRP) ($p < 0.01$) than the control group.

P2X7R mRNA expression levels

The P2X7R mRNA expression in PBMCs of 127 blood samples, determined by quantitative real-time PCR, is shown in Figure 1. The AMI group had 2.85-fold higher P2X7R mRNA expression than the control group (2.81 ± 0.15 vs. 0.99 ± ± 0.06, $p < 0.01$, Fig. 1).

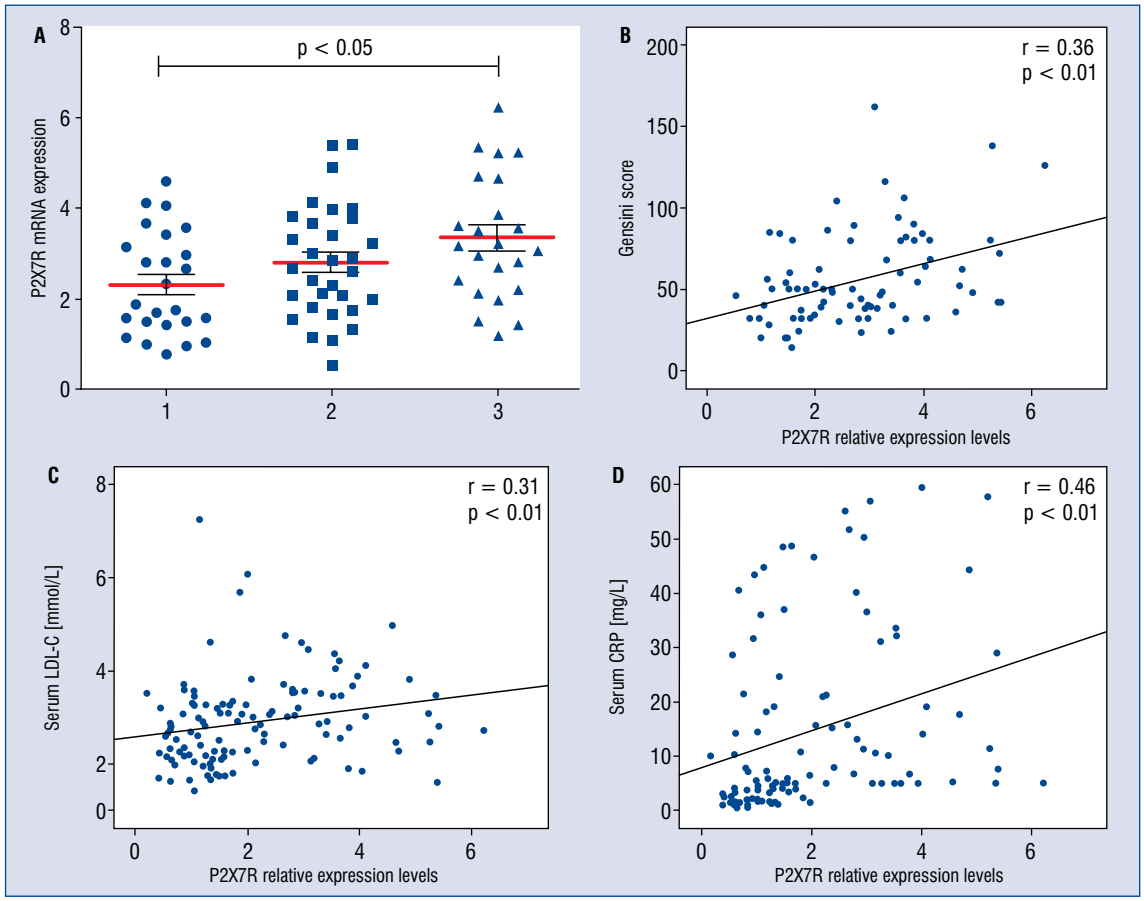

Figure 2. Pattern of circulating P2X7R expression levels in patients with acute myocardial infarction (AMI); **A.** Relative P2X7R levels in patients with 1, 2, or 3 affected branches (n = 1, 2, and 3); red lines represent the mean values; **B.** Correlations between plasma P2X7R levels and coronary Gensini scores in patients with AMI (r = 0.36, p < 0.01); **C.** Correlations between plasma P2X7R levels and serum low-density lipoprotein cholesterol (LDL-C); **D.** Correlations between plasma P2X7R levels and serum C-reactive protein (CRP).

P2X7R mRNA levels and stenosis

As shown in Figure 2A, significantly higher P2X7R mRNA expression was detected in patients with AMI with three-vessel lesions than in patients with single-vessel lesions ($p < 0.05$). A significant Spearman correlation coefficient was noted between angiographic Gensini scores and circulating P2X7R mRNA expression levels ($r = 0.36$, $p < 0.01$, Fig. 2B). Additionally, P2X7R mRNA expression levels were found to be positively correlated with serum LDL and CRP values ($r = 0.31$ and 0.46, $p < 0.05$; Fig. 2C, D).

The diagnostic ability of P2X7R in AMI

ROC analysis was performed to determine the diagnostic ability of P2X7R in AMI. The ROC curves of P2X7R mRNA expression levels in PBMCs could distinguish between the AMI and control groups with an area under the curve (AUC) of 0.928 (95% confidence interval [CI] 0.885–0.971, $p < 0.01$, Fig. 3). The ROC curves revealed that the cut-off value of P2X7R mRNA expression in PBMCs differentiating patients with AMI from control subjects was 1.418.

P2X7R mRNA and MACE

Patients enrolled in this study were followed up for 360 days. Fourteen patients were lost to follow-up. All subjects were divided into two groups according to fold changes of P2X7R mRNA by dichotomization: the lower level (0.52–2.68-fold changes) and the higher level (2.69–5.42-fold changes). The end point incidence significantly differed according to P2X7R expression levels, as analyzed using the Kaplan–Meier curve ($\chi^2 = 5.29$, $p = 0.021$; Fig. 4). The univariate and multivariate Cox regression analysis revealed that P2X7R expression levels significantly increased the risk

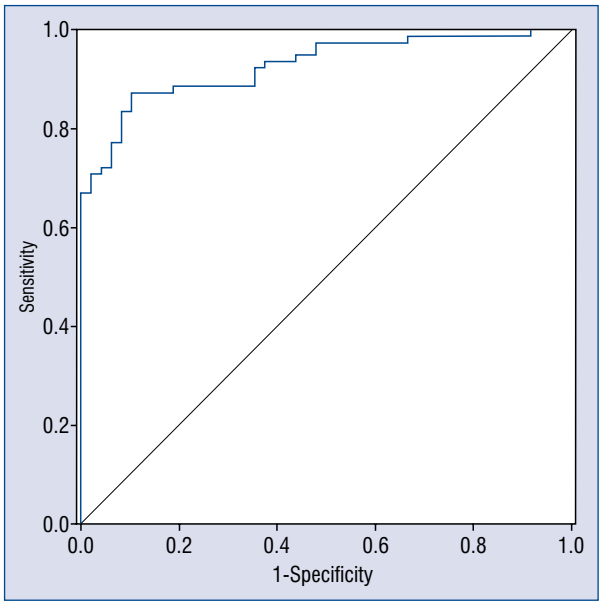

Figure 3. Receiver operating characteristic curve analysis of P2X7R expression level in peripheral blood mononuclear cells to predict acute myocardial infarction.

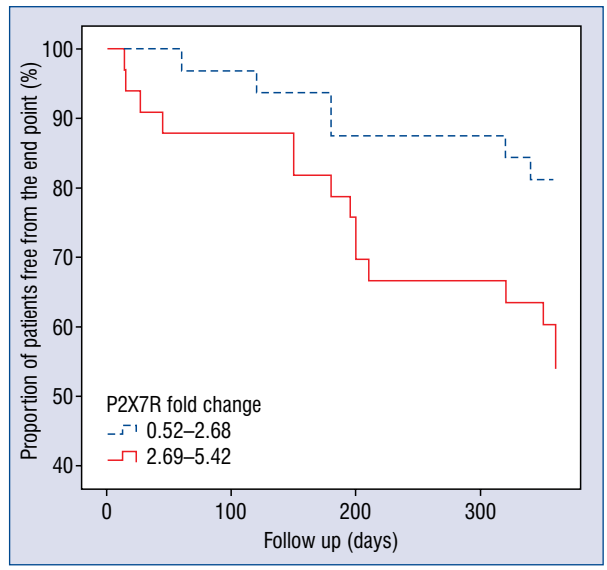

Figure 4. Kaplan–Meier curve analysis of patients free of end point after acute myocardial infarction, according to P2X7R mRNA expression level. The end point was defined as all-cause death, myocardial infarction, target lesion revascularization, heart failure, and recurrent angina.

Table 2. The correlations of the P2X7R mRNA expression level with major adverse cardiovascular events after acute myocardial infarction using the uni and multivariate Cox analysis.

Factors	Univariate Cox		Multivariate Cox	
	HR (95% CI)	P	HR (95% CI)	P
Age	1.01 (0.98–1.04)	0.640	1.00 (0.96–1.05)	0.860
Sex	0.43 (0.25–1.83)	0.669	0.46 (0.11–1.96)	0.294
Hypertension	5.09(1.50–17.32)	0.009	3.60 (1.02–12.74)	0.047
Diabetes	2.39 (1.01–5.69)	0.049	1.26 (0.46–3.41)	0.652
Smoking	1.30 (0.55–3.10)	0.547	1.68 (0.53–5.29)	0.380
Total cholesterol	0.91 (0.61–1.35)	0.632	1.04 (0.36–3.01)	0.942
LDL-C	0.83 (0.50–1.37)	0.465	0.74 (0.20–2.75)	0.652
Higher P2X7R level	2.87 (1.11–7.42)	0.029*	3.28 (1.12–9.65)	0.031*

*Patients with a lower level of P2X7R mRNA expression (0.52–2.68-fold changes) were set as the reference group. CI — confidence interval; HR — hazard ratio; LDL-C — low-density lipoprotein; higher P2X7R level, 2.69–5.42-fold changes of P2X7R mRNA expression level

of MACE after myocardial infarction (hazard ratio [HR] 2.87, 95% CI 1.11–7.42 and HR 3.28, 95% CI 1.12–9.65; Table 2).

Discussion

Atherosclerosis is thought to be the primary cause of AMI. Initiation, progression, and complications of atherosclerotic plaque are considered to be a result of the complex phenomena involving the interplay of lipoproteins, vascular wall components, blood cells, and the immune system. Multiple levels of evidence support a close relationship between inflammation and atherosclerosis.

P2X7R is considered to play dual roles in several inflammatory pathological conditions [8]. P2X7R functions as a second signal during NLRP3 inflammasome activation and interleukin (IL)-1β release. It contributes to activation of effector T cells, favors polarization of T cells into Th17 cells, and reduces suppressive activity and viability of Tregs. On the other hand, P2X7R can induce an

excessive production and release of inflammatory mediators coupled to a high incidence of apoptotic and necrotic cell death due the release of large amounts of ATP, which causes a self-sustained pro-inflammatory deleterious cycle.

In the present study, it was found that P2X7R mRNA expression levels were elevated in PBMCs of patients with AMI, and evaluated the diagnostic ability of P2X7R using ROC analyses. The AUC for P2X7R was 0.928 (95% CI 0.885–0.971) for differentiating between patients with AMI from control subjects. Furthermore, the indicated P2X7R was positively correlated with severity of coronary artery stenosis, and was linearly correlated with serum LDL and CRP. Based on a current understanding, P2X7R clearly plays a key role in cardiovascular physiology and pathophysiology. It shows deleterious effects in cardiovascular diseases by promoting inflammation, thrombosis, and endothelial dysfunction [9]. Its activation promotes the assembly of NLRP3 inflammasome and an unconventional release of pro-inflammatory leaderless cytokines IL-1β and IL-18 [10]. A previous study illustrated that inhibition of P2X7R may be able to suppress the AMPK/MAPK signaling pathway and consequently downregulate both EMMPRIN and MMP-9 expression in monocyte-derived macrophages, which correlated with advanced atherosclerotic lesions, followed by plaque rupture and myocardial infarction [11]. Furthermore, Stachon et al. [12] found that P2X7 receptor is highly expressed in murine atherosclerotic lesions, particularly in lesioned macrophages, and P2X7-deficient mice showed smaller atherosclerotic lesions than P2X7-competent mice after 16 weeks of a high cholesterol diet. All of these effects together suggest that P2X7R, indeed participates in the development of atherosclerosis.

However, data on the relationship between P2X7R and MACE after AMI remains insufficient. The inhibition of P2X7 receptor attenuated sympathetic nerve sprouting after myocardial infarction via the NLRP3/IL-1β pathway, which contributes to neural and cardiac remodeling [13]. Microglial P2X7R in rat hypothalamic paraventricular nuclei regulate the sympathoexcitatory responses in AMI [14]. NONRATT021972 siRNA decreases the upregulation of P2X7R and improves cardiac function after myocardial ischemia [15]. According to available research, this is the first report to propose that a higher expression of P2X7R mRNA is independently associated with higher rate of MACE within 360 days of AMI. Although inflammatory markers, such as hs-CRP, have been shown to identify patients with increased risk for incident coronary heart disease [16], but there were no significant associations between hs-CRP levels after AMI and their symptoms, function and quality of life after adjusting for prior health status [17]. Giuliani et al. [18] found correlation of P2X7R and CRP was widely different depending on the disease and best correlation was found in patients suffering of ischemia. So P2X7R measurement might complement that of CRP in a differential diagnosis of inflammatory conditions of different etiology.

Limitations of the study

Nevertheless, this study did have several limitations. Firstly, it was a single-center study with a relatively small study population; changes in long-term clinical outcomes may need to be confirmed by increasing both the total number of patients and the duration of follow-up. Secondly, this study lacked cardiac remodeling data during the follow-up period; therefore, further studies are warranted. Thirdly, measurement of P2X7 protein was lacking which should be required in further study.

Conclusions

The present study identified that the purinergic receptor P2X7R was elevated in AMI patients and was closely associated with the severity of coronary artery stenosis and prognosis of AMI.

Funding

This study was supported by the Bureau of traditional Chinese Medicine of Zhejiang Province (No. 2016ZA137 and No. LQ15H020005), the National Natural Science Foundation of China (No. 81670224).

Conflict of interest: None declared

References

1. Packard R, Lichtman A, Libby P. Innate and adaptive immunity in atherosclerosis. Sem Immunopathol. 2009; 31(1): 5–22, doi: 10.1007/s00281-009-0153-8.
2. Hansson GK. Inflammation, atherosclerosis, and coronary artery disease. N Engl J Med. 2005; 352(16): 1685–1695, doi: 10.1056/NEJMra043430, indexed in Pubmed: 15843671.
3. Newby AC, George SJ, Ismail Y, et al. Vulnerable atherosclerotic plaque metalloproteinases and foam cell phenotypes. Thromb Haemost. 2009; 101(6): 1006–1011, indexed in Pubmed: 19492140.
4. Baroja-Mazo A, Pelegrín P. Modulating P2X7 receptor signaling during rheumatoid arthritis: new therapeutic approaches for bisphosphonates. J Osteoporos. 2012; 2012: 408242, doi: 10.1155/2012/408242, indexed in Pubmed: 22830074.

5. Piscopiello M, Sessa M, Anzalone N, et al. P2X7 receptor is expressed in human vessels and might play a role in atherosclerosis. Int J Cardiol. 2013; 168(3): 2863–2866, doi: 10.1016/j.ijcard.2013.03.084, indexed in Pubmed: 23602287.
6. Peng K, Liu L, Wei D, et al. P2X7R is involved in the progression of atherosclerosis by promoting NLRP3 inflammasome activation. Int J Mol Med. 2015; 35(5): 1179–1188, doi: 10.3892/ijmm.2015.2129, indexed in Pubmed: 25761252.
7. Labasi JM, Petrushova N, Donovan C, et al. Absence of the P2X7 receptor alters leukocyte function and attenuates an inflammatory response. J Immunol. 2002; 168(12): 6436–6445, doi: 10.4049/jimmunol.168.12.6436, indexed in Pubmed: 12055263.
8. Savio L, Mello P, Silva C, et al. The P2X7 receptor in inflammatory diseases: angel or demon? Front Pharmacol. 2018; 9, doi: 10.3389/fphar.2018.00052.
9. Burnstock G. Purinergic signaling in the cardiovascular system. Circulation Research. 2017; 120(1): 207–228, doi: 10.1161/circresaha.116.309726.
10. Mariathasan S, Weiss DS, Newton K, et al. Cryopyrin activates the inflammasome in response to toxins and ATP. Nature. 2006; 440(7081): 228–232, doi: 10.1038/nature04515, indexed in Pubmed: 16407890.
11. Lin Lu, Huang S, Zhu Z, et al. P2X7 receptor regulates EMMPRIN and MMP9 expression through AMPK/MAPK signaling in PMA induced macrophages. Mol Med Rep. 2018; 18(3): 3027–3033, doi: 10.3892/mmr.2018.9282, indexed in Pubmed: 30015874.
12. Stachon P, Heidenreich A, Merz J, et al. P2X deficiency blocks lesional inflammasome activity and ameliorates atherosclerosis in mice. Circulation. 2017; 135(25): 2524–2533, doi: 10.1161/CIRCULATIONAHA.117.027400, indexed in Pubmed: 28377486.
13. Yin J, Wang Yu, Hu H, et al. P2X receptor inhibition attenuated sympathetic nerve sprouting after myocardial infarction via the NLRP3/IL-1β pathway. J Cell Mol Med. 2017; 21(11): 2695–2710, doi: 10.1111/jcmm.13185, indexed in Pubmed: 28470940.
14. Du D, Jiang M, Liu M, et al. Microglial P2X receptor in the hypothalamic paraventricular nuclei contributes to sympathoexcitatory responses in acute myocardial infarction rat. Neurosci Lett. 2015; 587: 22–28, doi: 10.1016/j.neulet.2014.12.026, indexed in Pubmed: 25524407.
15. Tu G, Zou L, Liu S, et al. Long noncoding NONRATT021972 siRNA normalized abnormal sympathetic activity mediated by the upregulation of P2X7 receptor in superior cervical ganglia after myocardial ischemia. Purinergic Signal. 2016; 12(3): 521–535, doi: 10.1007/s11302-016-9518-3, indexed in Pubmed: 27215605.
16. Kaptoge S, Di Angelantonio E, Lowe G, et al. C-reactive protein concentration and risk of coronary heart disease, stroke, and mortality: an individual participant meta-analysis. Lancet. 2010; 375(9709): 132–140, doi: 10.1016/S0140-6736(09)61717-7, indexed in Pubmed: 20031199.
17. Pokharel Y, Sharma PP, Qintar M, et al. High-sensitivity C-reactive protein levels and health status outcomes after myocardial infarction. Atherosclerosis. 2017; 266: 16–23, doi: 10.1016/j.atherosclerosis.2017.09.019, indexed in Pubmed: 28946036.
18. Giuliani AL, Berchan M, Sanz JM, et al. The P2X7 receptor is shed into circulation: correlation with C-reactive protein levels. Front Immunol. 2019; 10: 793, doi: 10.3389/fimmu.2019.00793, indexed in Pubmed: 31031771.

VIA MEDICA

REVIEW ARTICLE

Cardiology Journal
2021, Vol. 28, No. 3, 460–472
DOI: 10.5603/CJ.a2020.0093

ISSN 1897–5593
eISSN 1898–018X

Clinical applications of artificial intelligence in cardiology on the verge of the decade

Konrad Pieszko[1, 2], Jarosław Hiczkiewicz[1, 2], Jan Budzianowski[1, 2], Bogdan Musielak[1, 2], Dariusz Hiczkiewicz[1, 2], Wojciech Faron[1], Janusz Rzeźniczak[3], Paweł Burchardt[3, 4]

[1]Clinical Department of Cardiology, Nowa Sol Multidisciplinary Hospital, Nowa Sol, Poland
[2]University of Zielona Gora, Poland
[3]Cardiology Clinic, Jozef Strus Hospital, Poznan, Poland
[4]Department of Biology and Environmental Protection, Poznan University of Medical Sciences, Poznan, Poland

Abstract

Artificial intelligence (AI) has been hailed as the fourth industrial revolution and its influence on people's lives is increasing. The research on AI applications in medicine is progressing rapidly. This revolution shows promise for more precise diagnoses, streamlined workflows, increased accessibility to healthcare services and new insights into ever-growing population-wide datasets. While some applications have already found their way into contemporary patient care, we are still in the early days of the AI-era in medicine.

Despite the popularity of these new technologies, many practitioners lack an understanding of AI methods, their benefits, and pitfalls. This review aims to provide information about the general concepts of machine learning (ML) with special focus on the applications of such techniques in cardiovascular medicine. It also sets out the current trends in research related to medical applications of AI.

Along with new possibilities, new threats arise — acknowledging and understanding them is as important as understanding the ML methodology itself. Therefore, attention is also paid to the current opinions and guidelines regarding the validation and safety of AI-powered tools. (Cardiol J 2021; 28, 3: 460–472)

Key words: machine learning, artificial intelligence, cardiology

Introduction

Medical practitioners build their clinical experience when treating thousands of patients during their lifetime. However, nobody lives long enough to experience all possible variants and cases personally. Moreover, the perception and decision making of physicians may vary over time depending on different factors e.g. fatigue, which was reported to affect a physicians' performance in many studies [1]. Constantly dealing with large amounts of data in different modalities is the norm. This is where machines offer their computational advantage as they can easily digest enormous quantities of data. Machine learning (ML) can be understood as a fundamental technology required to meaningfully process data that exceeds the capacity and comprehensive abilities of a human brain [2].

Artificial intelligence (AI) is often described as software allowing computer systems to perform tasks that are believed to require human intelligence. This is an umbrella term for many computational methods, some of which are recently attracting a lot of attention from the medical community. The advantages of a computerized approach over medical data analysis include lowered cost,

Address for correspondence: Konrad Pieszko, MD, Clinical Department of Cardiology, Nowa Sol Multidisciplinary Hospital, ul. Chałubińskiego 7, 67–100 Nowa Sól, Poland, tel: +48 728 358 082, e-mail: konrad.pieszko@gmail.com

Received: 18.02.2020 Accepted: 25.05.2020

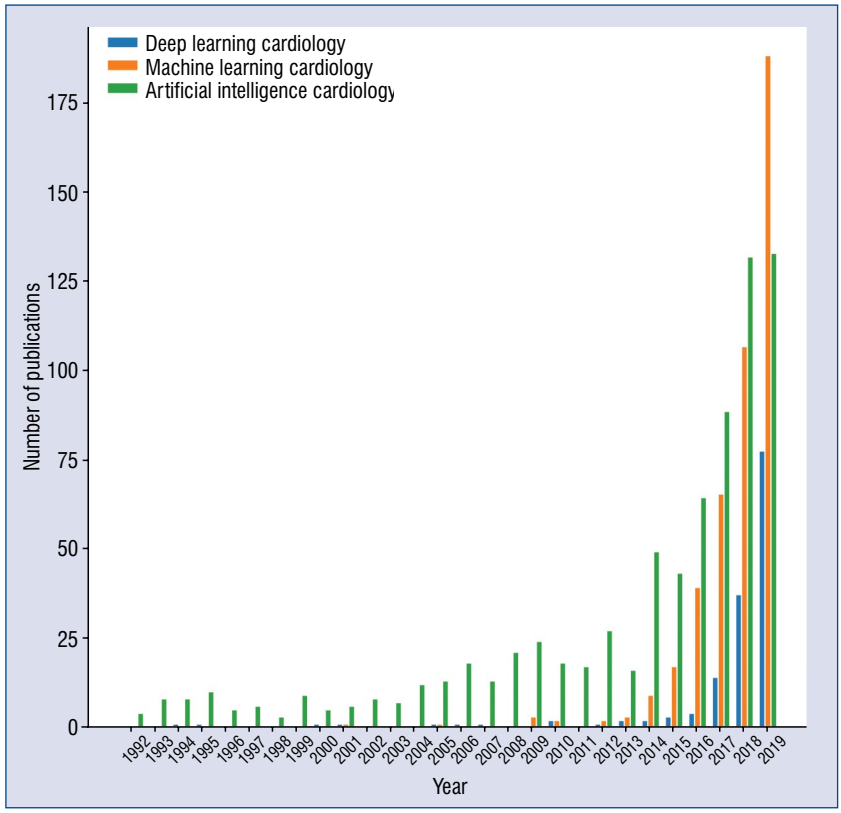

Figure 1. The number of publications related to artificial medicine over the last 15 years. Each series represents the number of results found in PubMed matching the given phrase by the year of publication.

increased speed and accessibility. In this review, some of the most prominent and promising practical applications of ML techniques in the field of cardiology are described. Also discussed are the potential safety issues related to the use of AI in clinical practice.

Recent years have triggered a rapid growth in ML-related publications in all fields of medicine. The growth in interest in this area has been exponential as illustrated in Figure 1. Although the greatest progress in the field of AI happened over the last 10 years, the onset of AI can be traced back much earlier. The historical aspect of AI is discussed in more detail by Benjamins et al. [3].

Owing to the popularity of this topic, many reviews have been published with the aim of familiarizing the reader with the relatively new concepts in AI methods [2, 4]. The specific applications of AI in cardiology have also been reviewed [3, 5–8]. Some of these papers focused on general usage scenarios of ML in cardiology [9] while others provided deeper insights into specific applications e.g. image analysis [10–12]. Some reviews covered technical aspects of various ML methods in greater detail [5]. Although many reviews have already been published, the field of medical AI is progressing very rapidly, and new research is published almost every day. This paper aims to present some of the most recent applications of AI in cardiology and discusses many safety concerns, which have recently received a lot of attention from the scientific community.

Overview of artificial intelligence and machine learning

The most commonly used terms "artificial intelligence" (AI) and "machine learning" (ML) are interrelated and are sometimes used in a similar context. However, they do require some disambiguation. Figure 2 presents how the most common techniques relate to each other.

Artificial intelligence is often described as human-like intelligence demonstrated by a machine. This is a broad term that applies to systems based on ML as well as to expert systems and robotics. ML, by contrast, is a group of algorithms that allow a computer to learn to perform a specific task based on several examples.

Machine learning algorithms are rooted in so-called traditional statistics. The simplest ML model

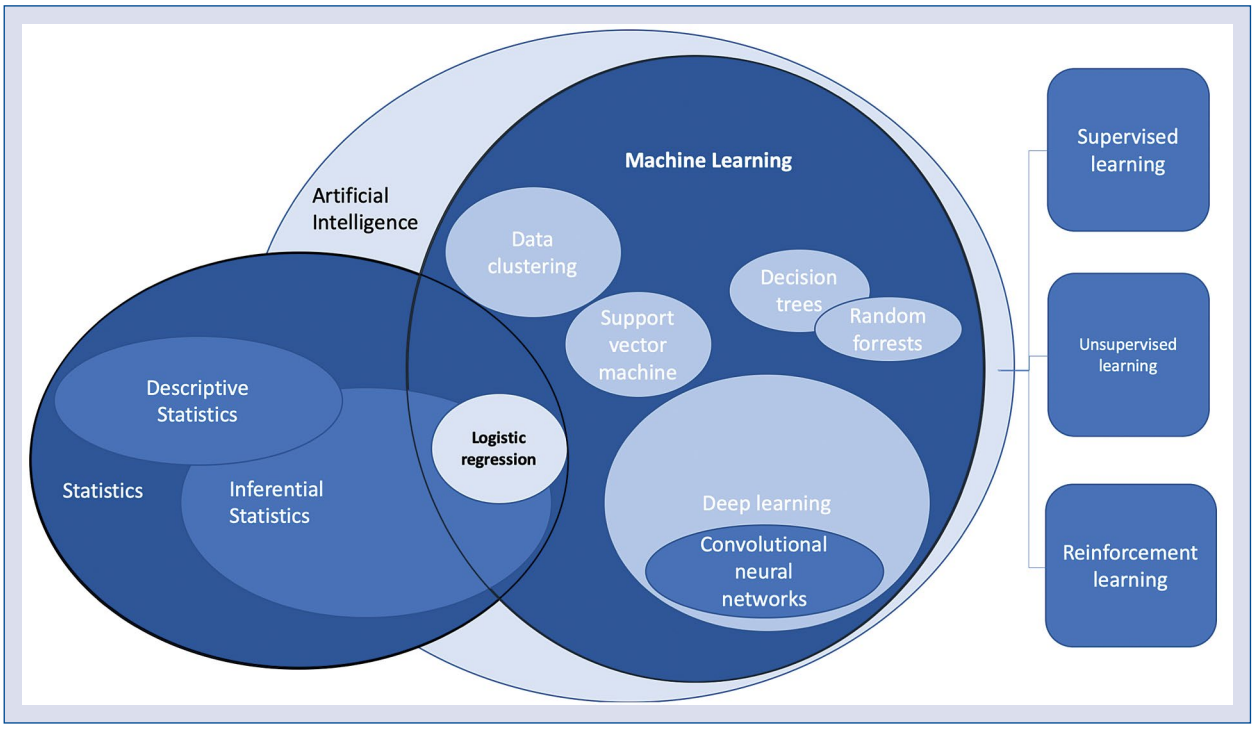

Figure 2. The machine learning and statistical methods and their relation to each other. On the right: three most common machine learning paradigms.

can be based on logistic regression. However, more sophisticated methods including decision trees, support vector machines, random forests or neural networks that have the advantage of handling complex and non-linear relationships within the data while avoiding 'improper dichotomization' [5]. The most recently developed techniques include deep neural networks, also called deep learning. These algorithms allow for the rapid progress of image recognition, natural language processing, speech recognition and are widely used in the latest medical research [2, 13].

Machine learning workflow

There are three standard ways in which any machine-learning model can be trained: supervised, unsupervised and reinforced (so called reinforcement learning). The first paradigm takes advantage of a set of labeled data — examples of input data along with correct answers. The dataset is divided into training, validation and test sets at an early stage of data manipulation. The training set is used to create the model — this is the data the algorithm learns from. To assess the process of learning, the validation set is used. During the process of training, the performance of the model is assessed multiple times on the validation set and the model improves gradually. In some cases, samples from the training and validation sets are shuffled in a process called cross-validation. The test set is used when the training process is finished to assess model performance on unseen data. The choice of sizes of these sets is based on available resources and depends on several factors. Generally, the more cases there are in the training set, the better the model performs. However, at some point, the model performance reaches a plateau and does not improve significantly despite adding new cases. In a cornerstone study by Gulshan et al. [14], such a plateau was observed when using 60,000 or more training images. On the other hand, the more cases that are held out in the test/ /validation sets, the narrower are the confidence intervals of a classifiers' performance measures. When comparing two classifiers, the absolute number of cases needed in the test set can be estimated using statistical test power calculations [15]. Figure 3 illustrates the typical workflow for the application of AI in a prediction task.

Interestingly, through unsupervised learning, it is possible to find patterns in the data without explicitly specifying what we are looking for. Various algorithms including hierarchical clustering, k-means clustering, neural networks, and many others can allow for the self-organization of the

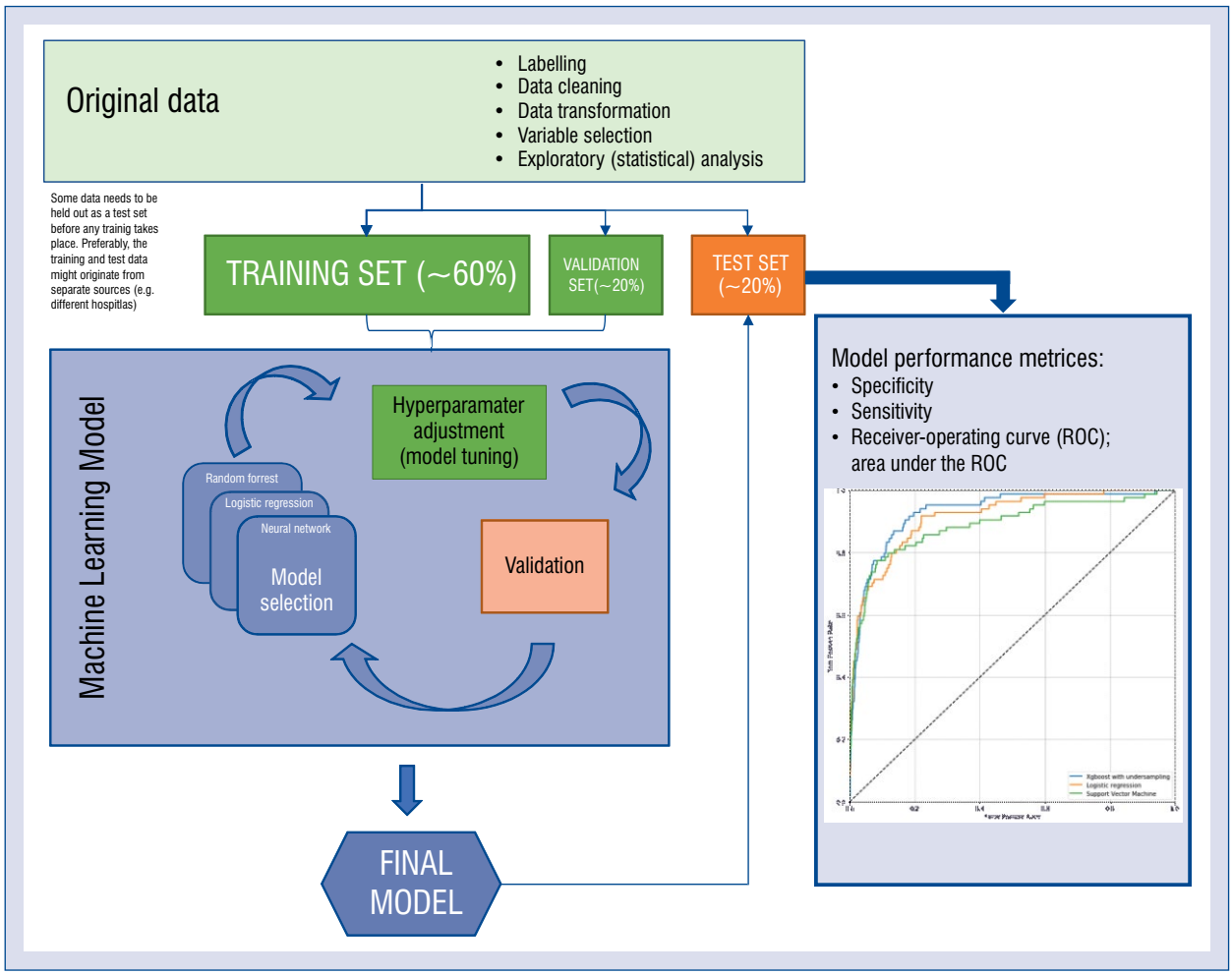

Figure 3. The workflow for a typical task for medical artificial intelligence — supervised learning.

data. This is usually a starting point for analyses using conventional statistical methods. Unsupervised learning imitates human intelligence and the ability to draw conclusions based on the data alone.

In the last paradigm, reinforcement learning, the learning process is continuous — the system works and learns from its own mistakes. These kinds of models are very successful in various applications (a program based on reinforcement learning [AlphaGo] beat the world champion in the game of 'Go' in 2017 — a task believed to be impossible for a machine) [16]. Despite being a great area of research, reinforcement learning has not been widely adopted in medical applications yet. As the model can modify its behavior over time, it has not been well established on how to ensure its clinical safety.

Deep learning

Deep neural networks, often referred to as deep learning allowed for a great leap forward in image recognition and natural language processing including automatic translation, voice recognition, and many other breakthroughs [17]. The image recognition techniques proved to be very useful in the analysis of medical images and physiological signals like electrocardiogram (ECG). The core concept lies in mimicking the way the human visual cortex works.

Bizopoulos and Koutsouries [18] in their systematic review provided a detailed overview of the applications of deep learning in the field of cardiology with insights into the various methodologies and architectures used. They also made a listing of publicly available datasets that can be used for developing and benchmarking ML models.

In this review, working principles and detailed properties of various ML algorithms are not discussed. Anyone interested in acquiring more detailed knowledge can refer to the article by Johnson et al. [5] where they describe the working principles of a number of ML methods along with their advantages and disadvantages.

How can artificial intelligence contribute to the area of cardiology?

In many usage scenarios AI is designed to mimic actions typically performed by a doctor — it recognizes a disease in images or classifies some other signals to provide an answer that a trained specialist would base on the same data. However, one of the most inspiring applications of AI is where it can provide insights into the data that were not anticipated by finding patterns in high-dimensional data. A canonical example is the study of diabetic retinopathy images — the algorithm was designed to determine a patient's cardiovascular risk based on an eye fundus image alone [19]. It turned out that the model was not only able to predict the total risk but also could determine the individual risk factors (sex, age, systolic blood pressure) to a degree of precision not reported before. Such results not only have a great potential for practical application but can also guide basic research given that sex differences in eye fundus are not yet fully understood.

Another example of an ML model analyzes data in a different way than doctors are used to doing was presented by researchers from the Mayo Clinic [20]. Using a deep neural network trained on over 600,000 ECGs, they showed that it was possible to identify the 'electrocardiographic signature' of paroxysmal atrial fibrillation in a standard 12-lead 10-second ECG taken during sinus rhythm. They achieved an area under the receiver-operating curve of 0.9, proving this method could be potentially useful for population-wide atrial fibrillation screening.

Soon the same team went even further and developed a model able to predict the presence of asymptomatic left ventricular dysfunction using the digital data from resting ECGs and trans-thoracic echocardiograms of 97,827 subjects [21]. Then, they validated it prospectively [22]. Currently, they are running a randomized clinical trial to investigate the usefulness of the proposed approach for screening for asymptomatic left ventricular dysfunction in primary care settings [23].

Unsupervised learning can be of great value when it comes to discovering new patterns and structures in data. In this technique, data is fed to an algorithm without labels and then becomes self-organized into multiple subgroups based on similarities between data points. This allows for the identification of new, unknown features and can drive further research. Shah et al. [24] used this approach to prospectively study patients with diagnosed heart failure with preserved ejection fraction. By applying an unsupervised ML method called hierarchical cluster analysis, they were able to classify the subjects into three distinctive phenogroups that differed significantly in terms of outcomes. Another study [25] used a similar methodology to identify groups with a potential substrate for heart failure among hypertensive patients. These are good examples of how unsupervised learning techniques can provide a starting point for further analyses using supervised methods and inferential statistics. Such an approach may lead to the development of more specific treatment strategies according to the paradigm of precision medicine [26]. Very recently, Wang et al. [27] used an unsupervised autoencoder based on a deep learning algorithm to represent data from electronic health records and compared the classification based on these learned features with more conventional approaches.

Table 1 presents a non-exhaustive list of AI research examples in the field of cardiology [20–22, 28–56]. This list is intended to give a general overview of possible areas of application and demonstrates how AI can improve various aspects of patient care in cardiology. The studies are grouped by the type of input data used (imaging data, ECG signal, clinical data). A brief description of the methodology is provided for each example.

AI — hype or hope?

Artificial intelligence has brought as much hope as fear even long before it became a reality. It is even argued that there is little evidence that it improves patient outcomes [57]. This section aims to illustrate some of the potential threats and difficulties that need to be overcome to ensure that medical AI benefits us all.

AI safety

What if a machine makes the wrong diagnosis? There are indeed safety concerns regarding the use of automated decision support systems. One of the issues that can affect the practical safety of an AI-based classification tool is the 'hidden stratification' of the dataset. This term was coined by researchers from the University of Adelaide and Stanford University [58] and describes a situation in supervised learning when, due to the coarse labeling of the data (for example normal vs. abnormal), there are some unrecognized subgroups within each label. Obviously, the machine cannot learn a class if it was not labeled specifically. The system can learn to recognize the more general label quite well while underperforming on some

Table 1. Examples of artificial intelligence applications in cardiology.

Diagnostic modality/type of data used	Application	Study methodology	Reference(s)
Echocardiography	Identification of echocardiographic views	A convolutional neural network was used to distinguish between 15 standard echocardiographic views with an accuracy of 97.8%	Madani et al. 2018 [28]
	Differentiating CP from RCM	The model was based on an associative memory classifier algorithm. Echocardiograms of 50 patients with CP, 44 with RCM and 47 controls were used to train the model	Sengupta et al. 2016 [29]
	Fully automated echocardiogram interpretation and detection of selected clinical conditions	A convolutional neural network was trained on 14,035 echocardiograms to identify views, perform the segmentation of heart chambers, determine ejection fraction and other measurements and finally to detect a number of clinical conditions (cardiomyopathy, cardiac amyloidosis and pulmonary arterial hypertension with the C statistics of 0.93, 0.87, and 0.85, respectively)	Zhang et al. 2018 [30]
CT	Calculating CS based on CT-angiography scans. (May obviate the need for a separate CS scan; thus, reducing the radiation dose)	The authors designed a convolutional neural network that processes each of the three axes (axial, saggital, coronal) separately. The model was trained using a total of 250 hand-annotated exams	Wolterink et al. 2016 [31]
	Calculating FFR values based on cardiac CT	The models created using convolutional neural networks have some advantages (including shorter computation times) over the clinically validated approach based on computational fluid dynamics while maintaining a non-inferior performance	Coenen et al. 2018 [32] Tesche et al. 2018 [33]
	Predicting all--cause mortality based on cardiac CT and clinical variables	25 clinical and 44 CT-derived variables of over 10,000 patients were used to train the iterative Logit Boost algorithm. The resulting model could predict a 5-year mortality rate with the c-statistic of 0.79	Motwani et al. 2017 [34]
	CT scan denoising — improving readability of acquired images while also reducing the necessary radiation exposure	The authors obtained scans using 20% and 100% of the clinical radiation dose. The model based on generative adversarial network architecture was trained to generate full-quality images based on the images acquired with a low radiation dose	Wolterink et al. 2017 [35]
	Detecting significant coronary lesions based on the motion of the LV myocardium	The complex model consisted of a convolutional neural network (for the myocardium segmentation), an unsupervised convolutional autoencoder (for the extraction of the myocardium characteristics) and a support vector classifier	Zreik et al. 2018 [36]
	Predicting cardiac death after myocardial perfusion SPECT imaging	A total of 122 features (both the clinical data and variables derived from SPECT scans) of over 8,000 patients were used to train the multiple ML models. A model based on SVM outperformed baseline logistic regression as well as random forests	Haro Alonso et al. 2019 [37]
	Detecting the presence and location of significant coronary artery stenosis based on SPECT images	In these multicenter studies, all patients underwent myocardial perfusion imaging and coronary angiography within 6 months. A deep neural network was trained to predict obstructive coronary disease based on SPECT myocardial perfusion images	Betancur et al. 2018, 2019 [38, 39]

→

Table 1 (cont.). Examples of artificial intelligence applications in cardiology.

Diagnostic modality/type of data used	Application	Study methodology	Reference(s)
	Predicting MACE using a combination of clinical data and myocardial perfusion SPECT images	28 clinical variables, 17 stress test variables, and 25 imaging variables of 2,619 patients were analyzed. The ML model was based on the Logit Boost algorithm	Betancur et al. 2018 [40]
MRI	Segmentation of heart structures, automatic measurement of the LV end-diastolic volume and other values	A fully convolutional neural network was trained using pixel-annotated MRI images from 4,875 patients. The model was able to perform highly accurate automatic measurements and delineation of heart structures	Bai et al. 2018 [41]
	Detecting abnormalities of aortic valve	The authors developed a novel strategy for training medical ML models using unlabeled imaging data. They created a weakly-supervised model capable of diagnosing aortic valve abnormalities in MRI scans	Fries et al. 2019 [42]
	Objective assessment of atrial scarring for patients with AF	The authors developed a complete pipeline for atrial scarring segmentation. A classification algorithm based on SVM was used	Yang et al. 2018 [43]
	Diagnosing pulmonary hypertension based on cardiovascular MRI	The model was trained using 220 MRI scans of patients who had also underwent right heart catheterization	Swift et al. 2020 [44]
Coronary angiography	Segmentation of coronary vessels from angiograms	The model was based on a U-Net architecture (a type of a deep neural network). 3,302 still images of coronary arteries were used to train the model	Yang et al. 2019 [45]
ECG signal	Diagnosing ALVD using ECG only	The ECG signals and echocardiographic data of 97,829 patients were used (the time between ECG and echocardiography was less than 2 weeks). A model based on a neural network could predict ALVD with a sensitivity and specificity of 86%. The initial study laid the groundwork for a prospective evaluation and the ongoing clinical trial	Attia et al. 2019 [21,22]
	Detecting paroxysmal AF based on contemporary 12-lead ECG taken on SR	The authors have shown that it is possible to identify an 'electrocardiographic signature' of paroxysmal AF in a routine 10-second 12-lead ECG. The use of a convolutional neural network allowed the detection of signals invisible to the human eye	Attia et al. 2019 [20]
	Predicting the development of moderate to severe MR based on 12-lead ECG using a deep neural network	The AUROC in external validation of 10,865 cases was 0.877. Positively diagnosed patients also had a higher chance of developing MR in the future. Additionally, the authors used visualization techniques that helped understand which parts of an ECG influence the decisions of their algorithm	Kwon et al. 2020 [46]
EHR	Predicting cardiovascular risk based on records from primary care	30 variables identified within the primary health records of 378,256 patients were analyzed. The authors used a number of ML algorithms including logistic regression, random forests and neural networks	Weng et al. 2017 [47]

→

Table 1 (cont.). Examples of artificial intelligence applications in cardiology.

Diagnostic modality/type of data used	Application	Study methodology	Reference(s)
	Predicting the in-hospital mortality rate, readmission and a prolonged length of stay based on raw electronic health records	Multi-year medical histories stored in EHRs linked to 216,221 hospitalizations were converted into over 46 billion data points, each representing a result, clinical event, physician's note etc. An ensemble of three types of neural networks was trained to predict various clinical endpoints with high accuracy	Rajkomar et al. 2018 [48]
	Predicting the probability of in-hospital death at the time of admission	The model was crated based on retrospective data but validated prospectively and externally in 3 different hospitals. A total number of over 75,000 admissions were used to create and validate the model. The AUROC was 0.86 in an external validation	Brajer et al. 2020 [49]
Clinical data	Predicting readmission of patients with heart failure	An EHR-wide feature selection (over 4,000 variables were considered) and a model based on logistic regression was developed to predict the 30-day readmission rates	Shameer et al. 2017 [50]
	Predicting long- and short-term mortality after ACS	In these papers various 'classical' ML models (support vector machines, random forests, xgboost) were developed to predict mortality after acute coronary syndromes using clinical data	Shouval et al. 2017 [51] Wallert et al. 2017 [52] Pieszko et al. 2018, 2019 [53, 54]
	Predicting the risk of MACE and bleeding after ACS	The data on over 24,000 patients with ACSs were pooled from 4 randomized controlled trials. The ML algorithm demonstrated superiority over traditional risk scores	Gibson et al. 2020 [55]
	Selecting the right patients for CRT	Classical ML algorithms were applied to predict survival after CRT implantation. The model based on random forest showed the best performance	Kalscheur et al. 2018 [56]

ACS — acute coronary syndrome; AF — atrial fibrillation; ALVD — asymptomatic left ventricular dysfunction; CP — constrictive pericarditis; CRT — cardiac resynchronization therapy; CS — Calcium Score; CT — computed tomography; EHR — electronic health records; ECG — electrocardiogram; FFR — fractional flow reserve; LV — left ventricle; MACE — major adverse cardiac events; ML — machine learning; MR — mitral regurgitation; MRI — magnetic resonance imaging; RCM — restrictive cardiomyopathy; SR — sinus rhythm; SVM — support vector machines; SPECT — single-photon emission computed tomography

specific subtype that was not given a separate label despite different clinical characteristics (Fig. 4). As a result, the reported performance measures can be good, albeit do not reflect the actual clinical usefulness of the model. If the 'hidden' subtype is a more dangerous one, it is clear that the consequences could be serious. This leads to a situation contrary to the common sense of a doctor, who intuitively tries to exclude the most dangerous diagnoses first (even if they are not common). Simply phrased, AI trained by means of an improperly labeled dataset may seem to make few mistakes but may still fail in very important cases, while a doctor could still make mistakes in less important cases. The difference between a computer and a human being lies in the fact that humans understand the consequences of their decisions and try to do their best when they know that the stakes are high.

Oakden-Rayner et al. [58] recognize the underlying mechanisms that cause these types of errors and they propose several methods to address this issue. The main reason why hidden stratification can occur is the improper labeling of the data (oversimplified labels). One method proposed to prevent the hidden stratification is the use of exhaustive prospective data labeling in a tree-like fashion that includes classes and finer subclasses, which may be additionally weighted given their clinical significance. Such a predefined schema could even be standardized by an external authority and serve for benchmarking the models designed for a similar task. One of the studies that

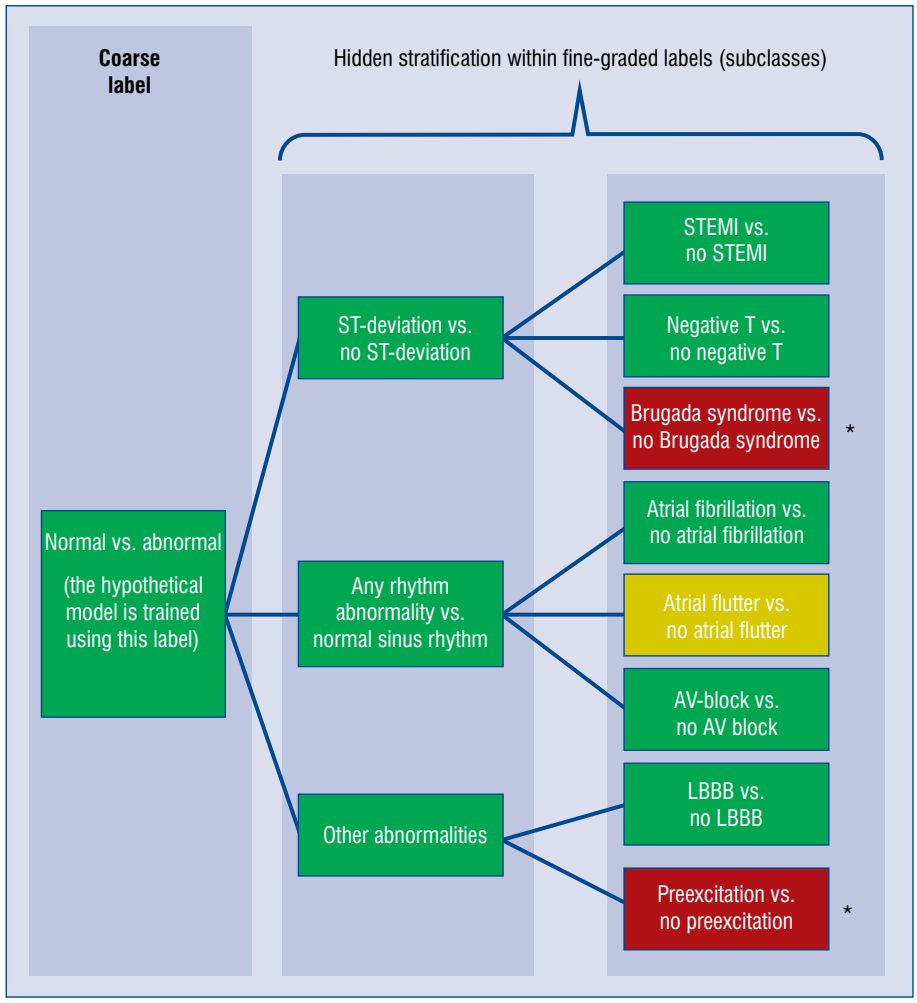

Figure 4. Hidden stratification explained using a hypothetical model for electrocardiogram (ECG) abnormality prediction. The model is trained to detect any abnormality in ECG and it works very well, having high specificity and sensitivity. However, the errors are not equally distributed across possible abnormal conditions. Some of the errors are detected very well while others are ignored by the algorithm. Such cases are rare so the fact that the model does not recognize these abnormal conditions does not significantly affect the overall performance in detecting any ECG abnormality; AV — atrioventricular; LBBB — left bundle branch block; NSTEMI — non-ST-segment elevation myocardial infarction; STEMI — ST-segment elevation myocardial infarction; *rare conditions; predictive performance: green background of a box means good; yellow — moderate; red — poor.

used such a well-defined label structure, including coarse classes and more fine-graded subclasses, was used in the classification of skin lesion images [59].

Explainable AI

Although often perceived as a black-box, there are various methods to provide insights into how ML methods generate their predictions. In contrast to traditional, regression-based statistical inference, more complex methods can model real-world relationships in a better way. In such cases, ML methods can even be used as a source of analytical insights into the data by providing information on how each variable affects the outcome.

The explanatory features of AI also have their legal aspects. The General Data Protection Regulation, which was introduced in the European Union in 2016, imposes constraints on how personal data can be used in automated decision systems and so-called 'profiling', including healthcare applications. These regulations form additional safety measures for the protection of privacy while also guaranteeing the 'right to explanation' [60]. They introduce several practical challenges for the design and practical deployment of machine-learning

algorithms. Providing explanatory features (i.e. a way in which the model can communicate what led to its final conclusion) can be seen as an additional safety measure. Such an explanation can be provided in a form of a graph illustrating the importance of features, a heatmap (in the case of images) or a full written report, similar to the one that a physician would write [61]. A very recent study proved that explanatory features increases a doctor's trust as a decision support tool and a willingness to follow its advice. However, there is no evidence that presenting a prediction alongside such an explanation leads to a better clinical outcome than showing the prediction alone. In fact, automation bias could theoretically even lead to worse clinical outcomes [62].

Is the AI biased?

As machine-learned models are finding their way into routine medical practice, concerns are raised regarding the potential statistical bias (that might be introduced into the model) as well as the automation bias (related to the use of AI tools by doctors).

The source of statistical bias lies in the data that was used to train the algorithm, either because it was not representative of the population or because it contained non-ignorable (not randomly distributed) missing values or additional data points (e.g. given that doctors are more likely to perform additional tests if the patient is in poor condition) [63–65]. This kind of bias is nothing new and has always been a concern for prediction models. The use of AI decision support tools can also introduce so-called 'automation bias' which relates to the behavioral aspects seen in automation systems used by humans. This topic was discussed in great detail in the paper by Parasuraman and Manzey [62].

Automation bias is caused by a natural human tendency to pay less attention to automated tasks when under pressure. This happens because the users tend to ascribe greater power and authority to automated aids than to other sources of advice. In other words, a 'human in the loop' is likely to follow the advice of AI, even if other available sources and his own knowledge contradict that.

Clinical trials — Are we there yet?

Despite the rapid development and growing interest in the applications of ML methods in medicine, the majority of up-to-date publications are based on experiments in laboratory settings. There have been very few studies which indicate that using AI-based tools improves patient outcomes.

The fact that a new drug works as expected in pre-clinical experiments does not prove its usefulness and safety. Similarly, studies have shown that achieving good results when testing a ML model in a controlled environment does not necessarily mean that it will improve patient outcomes [66] when used in standard practice. Various psychological factors affect a doctors' response to the suggestions of computer systems and it is known that the presence of such a system can sometimes decrease their vigilance resulting in lower sensitivity. This can be well illustrated by the adoption of computer-aided detection for mammography — a sort of AI algorithm developed in the 1990s in the United States, aimed to assist radiologists in assessing mammograms. The algorithm had been developed before the 'deep learning era' but it seemed to improve breast cancer diagnostics in laboratory settings. It was reimbursed by medical insurers who decided to pay more for assessing radiograms using computer-aided detection. However, in clinical setting it did not only fail to improve radiologists' performance but also decreased their sensitivity [67].

Up till now there have been very few clinical trials related to the use of AI-tools in medicine [68]. One such study proved that AI-assisted colonoscopy could help detect more malignant lesions but it also increased the number of unnecessary biopsies [69]. Another example is the EAGLE trial that was mentioned earlier [23]. A recent randomized control trial evaluated the application of an early warning system against hypotension during elective surgery [70]. Despite many studies conducted prospectively and on a large scale, we still know very little about how the actual application of AI in healthcare affects patients and doctors. Well-designed randomized clinical trials are needed to prove the safety and usefulness of medical AI in real-world settings.

Summary

Artificial intelligence is anticipated to shape the new decade and bring meaningful changes to society, the economy, healthcare and people's lifestyles. For these reasons, AI has been hailed as the fourth industrial revolution [71]. The 'technology of the future' is already here but converting this into an actual benefit for patients is a task that lies with clinicians.

Recent years have seen numerous studies that took advantage of various breeds of AI. In many cases algorithms were designed and

validated using the retrospective data only. We are now entering the phase in which ML models need to be tested prospectively and in clinical settings. Knowing how data-hungry ML models are, it is important to develop and adopt the standards of data acquisition that make it easier to cooperate on multi-center projects. On the other hand, we also need to standardize the tools used to monitor the performance of AI-based systems.

Acknowledgements

The authors would like to thank Dr. Paweł Budzianowski, PhD, for his helpful advice on the various technical issues described in this paper.

Conflict of interest: None declared

References

1. Gates M, Wingert A, Featherstone R, et al. Impact of fatigue and insufficient sleep on physician and patient outcomes: a systematic review. BMJ Open. 2018; 8(9): e021967, doi: 10.1136/bmjopen-2018-021967, indexed in Pubmed: 30244211.
2. Rajkomar A, Dean J, Kohane I, et al. Machine Learning in Medicine. N Engl J Med. 2019; 380(14): 1347–1358, doi: 10.1056/NEJMra1814259, indexed in Pubmed: 30943338.
3. Benjamins JW, Hendriks T, Knuuti J, et al. A primer in artificial intelligence in cardiovascular medicine. Neth Heart J. 2019; 27(9): 392–402, doi: 10.1007/s12471-019-1286-6, indexed in Pubmed: 31111458.
4. Liu Y, Chen PHC, Krause J, et al. How to read articles that use machine learning: users' guides to the medical literature. JAMA. 2019; 322(18): 1806–1816, doi: 10.1001/jama.2019.16489, indexed in Pubmed: 31714992.
5. Johnson KW, Torres Soto J, Glicksberg BS, et al. Artificial Intelligence in Cardiology. J Am Coll Cardiol. 2018; 71(23): 2668–2679, doi: 10.1016/j.jacc.2018.03.521, indexed in Pubmed: 29880128.
6. Shameer K, Johnson KW, Glicksberg BS, et al. Machine learning in cardiovascular medicine: are we there yet? Heart. 2018; 104(14): 1156–1164, doi: 10.1136/heartjnl-2017-311198, indexed in Pubmed: 29352006.
7. Mazzanti M, Shirka E, Gjergo H, et al. Imaging, health record, and artificial intelligence: hype or hope? Curr Cardiol Rep. 2018; 20(6): 48, doi: 10.1007/s11886-018-0990-y, indexed in Pubmed: 29749590.
8. Seetharam K, Shrestha S, Sengupta PP. Artificial Intelligence in Cardiovascular Medicine. Curr Treat Options Cardiovasc Med. 2019; 21(6): 25, doi: 10.1007/s11936-019-0728-1, indexed in Pubmed: 31089906.
9. Dorado-Díaz PI, Sampedro-Gómez J, Vicente-Palacios V, et al. Applications of artificial intelligence in cardiology. The future is already here. Rev Esp Cardiol (Engl Ed). 2019; 72(12): 1065–1075, doi: 10.1016/j.rec.2019.05.014, indexed in Pubmed: 31611150.
10. Dey D, Slomka PJ, Leeson P, et al. Artificial intelligence in cardiovascular imaging: JACC state-of-the-art review. J Am Coll Cardiol. 2019; 73(11): 1317–1335, doi: 10.1016/j.jacc.2018.12.054, indexed in Pubmed: 30898208.
11. Siegersma KR, Leiner T, Chew DP, et al. Artificial intelligence in cardiovascular imaging: state of the art and implications for the imaging cardiologist. Neth Heart J. 2019; 27(9): 403–413, doi: 10.1007/s12471-019-01311-1, indexed in Pubmed: 31399886.
12. Litjens G, Ciompi F, Wolterink JM, et al. State-of-the-Art Deep Learning in Cardiovascular Image Analysis. JACC Cardiovasc Imaging. 2019; 12(8 Pt 1): 1549–1565, doi: 10.1016/j.jcmg.2019.06.009, indexed in Pubmed: 31395244.
13. Litjens G, Ciompi F, Wolterink JM, et al. State-of-the-Art Deep Learning in Cardiovascular Image Analysis. JACC Cardiovasc Imaging. 2019; 12(8 Pt 1): 1549–1565, doi: 10.1016/j.jcmg.2019.06.009, indexed in Pubmed: 31395244.
14. Gulshan V, Peng L, Coram M, et al. Development and validation of a deep learning algorithm for detection of diabetic retinopathy in retinal fundus photographs. JAMA. 2016; 316(22): 2402–2410, doi: 10.1001/jama.2016.17216, indexed in Pubmed: 27898976.
15. Beleites C, Neugebauer U, Bocklitz T, et al. Sample size planning for classification models. Anal Chim Acta. 2013; 760: 25–33, doi: 10.1016/j.aca.2012.11.007, indexed in Pubmed: 23265730.
16. Silver D, Huang A, Maddison CJ, et al. Mastering the game of Go with deep neural networks and tree search. Nature. 2016; 529(7587): 484–489, doi: 10.1038/nature16961, indexed in Pubmed: 26819042.
17. LeCun Y, Bengio Y, Hinton G. Deep learning. Nature. 2015; 521(7553): 436–444, doi: 10.1038/nature14539, indexed in Pubmed: 26017442.
18. Bizopoulos P, Koutsouris D. Deep learning in cardiology. IEEE Rev Biomed Eng. 2019; 12: 168–193, doi: 10.1109/RBME.2018.2885714, indexed in Pubmed: 30530339.
19. Poplin R, Varadarajan AV, Blumer K, et al. Prediction of cardiovascular risk factors from retinal fundus photographs via deep learning. Nat Biomed Eng. 2018; 2(3): 158–164, doi: 10.1038/s41551-018-0195-0, indexed in Pubmed: 31015713.
20. Attia ZI, Noseworthy PA, Lopez-Jimenez F, et al. An artificial intelligence-enabled ECG algorithm for the identification of patients with atrial fibrillation during sinus rhythm: a retrospective analysis of outcome prediction. Lancet. 2019; 394(10201): 861–867, doi: 10.1016/S0140-6736(19)31721-0, indexed in Pubmed: 31378392.
21. Attia ZI, Kapa S, Lopez-Jimenez F, et al. Screening for cardiac contractile dysfunction using an artificial intelligence-enabled electrocardiogram. Nat Med. 2019; 25(1): 70–74, doi: 10.1038/s41591-018-0240-2, indexed in Pubmed: 30617318.
22. Attia ZI, Kapa S, Yao X, et al. Prospective validation of a deep learning electrocardiogram algorithm for the detection of left ventricular systolic dysfunction. J Cardiovasc Electrophysiol. 2019; 30(5): 668–674, doi: 10.1111/jce.13889, indexed in Pubmed: 30821035.
23. Yao X, McCoy RG, Friedman PA, et al. ECG AI-Guided Screening for Low Ejection Fraction (EAGLE): Rationale and design of a pragmatic cluster randomized trial. Am Heart J. 2020; 219: 31–36, doi: 10.1016/j.ahj.2019.10.007, indexed in Pubmed: 31710842.
24. Shah SJ, Katz DH, Selvaraj S, et al. Phenomapping for novel classification of heart failure with preserved ejection fraction. Circulation. 2015; 131(3): 269–279, doi: 10.1161/CIRCULATIONAHA.114.010637, indexed in Pubmed: 25398313.
25. Katz DH, Deo RC, Aguilar FG, et al. Phenomapping for the Identification of Hypertensive Patients with the Myocardial Substrate for Heart Failure with Preserved Ejection Fraction. J Cardiovasc Transl Res. 2017; 10(3): 275–284, doi: 10.1007/s12265-017-9739-z, indexed in Pubmed: 28258421.

26. Krittanawong C, Zhang H, Wang Z, et al. Artificial Intelligence in Precision Cardiovascular Medicine. J Am Coll Cardiol. 2017; 69(21): 2657–2664, doi: 10.1016/j.jacc.2017.03.571, indexed in Pubmed: 28545640.
27. Wang L, Tong L, Davis D, et al. The application of unsupervised deep learning in predictive models using electronic health records. BMC Med Res Methodol. 2020; 20(1): 37, doi: 10.1186/s12874-020-00923-1, indexed in Pubmed: 32101147.
28. Madani A, Arnaout R, Mofrad M, et al. Fast and accurate view classification of echocardiograms using deep learning. NPJ Digit Med. 2018; 1, doi: 10.1038/s41746-017-0013-1, indexed in Pubmed: 30828647.
29. Sengupta PP, Huang YM, Bansal M, et al. Cognitive Machine-Learning Algorithm for Cardiac Imaging: A Pilot Study for Differentiating Constrictive Pericarditis From Restrictive Cardiomyopathy. Circ Cardiovasc Imaging. 2016; 9(6), doi: 10.1161/CIRCIMAGING.115.004330, indexed in Pubmed: 27266599.
30. Zhang J, Gajjala S, Agrawal P, et al. Fully Automated Echocardiogram Interpretation in Clinical Practice. Circulation. 2018; 138(16): 1623–1635, doi: 10.1161/CIRCULATIONAHA.118.034338, indexed in Pubmed: 30354459.
31. Wolterink JM, Leiner T, de Vos BD, et al. Automatic coronary artery calcium scoring in cardiac CT angiography using paired convolutional neural networks. Med Image Anal. 2016; 34: 123–136, doi: 10.1016/j.media.2016.04.004, indexed in Pubmed: 27138584.
32. Coenen A, Kim YH, Kruk M, et al. Diagnostic accuracy of a machine-learning approach to coronary computed tomographic angiography-based fractional flow reserve: result from the MACHINE consortium. Circ Cardiovasc Imaging. 2018; 11(6): e007217, doi: 10.1161/CIRCIMAGING.117.007217, indexed in Pubmed: 29914866.
33. Tesche C, De Cecco CN, Baumann S, et al. Coronary CT angiography-derived fractional flow reserve: machine learning algorithm versus computational fluid dynamics modeling. Radiology. 2018; 288(1): 64–72, doi: 10.1148/radiol.2018171291, indexed in Pubmed: 29634438.
34. Motwani M, Dey D, Berman DS, et al. Machine learning for prediction of all-cause mortality in patients with suspected coronary artery disease: a 5-year multicentre prospective registry analysis. Eur Heart J. 2017; 38(7): 500–507, doi: 10.1093/eurheartj/ehw188, indexed in Pubmed: 27252451.
35. Wolterink JM, Leiner T, Viergever MA, et al. Generative adversarial networks for noise reduction in low-dose CT. IEEE Trans Med Imaging. 2017; 36(12): 2536–2545, doi: 10.1109/TMI.2017.2708987, indexed in Pubmed: 28574346.
36. Zreik M, Lessmann N, van Hamersvelt RW, et al. Deep learning analysis of the myocardium in coronary CT angiography for identification of patients with functionally significant coronary artery stenosis. Med Image Anal. 2018; 44: 72–85, doi: 10.1016/j.media.2017.11.008, indexed in Pubmed: 29197253.
37. Haro Alonso D, Wernick MN, Yang Y, et al. Prediction of cardiac death after adenosine myocardial perfusion SPECT based on machine learning. J Nucl Cardiol. 2019; 26(5): 1746–1754, doi: 10.1007/s12350-018-1250-7, indexed in Pubmed: 29542015.
38. Betancur J, Commandeur F, Motlagh M, et al. Deep learning for prediction of obstructive disease from fast myocardial perfusion SPECT: a multicenter study. JACC Cardiovasc Imaging. 2018; 11(11): 1654–1663, doi: 10.1016/j.jcmg.2018.01.020, indexed in Pubmed: 29550305.
39. Betancur J, Hu LH, Commandeur F, et al. Deep learning analysis of upright-supine high-efficiency SPECT myocardial perfusion imaging for prediction of obstructive coronary artery disease: a multicenter study. J Nucl Med. 2019; 60(5): 664–670, doi: 10.2967/jnumed.118.213538, indexed in Pubmed: 30262516.
40. Betancur J, Otaki Y, Motwani M, et al. Prognostic value of combined clinical and Myocardial perfusion imaging data using machine learning. JACC Cardiovasc Imaging. 2018; 11(7): 1000–1009, doi: 10.1016/j.jcmg.2017.07.024, indexed in Pubmed: 29055639.
41. Bai W, Sinclair M, Tarroni G, et al. Automated cardiovascular magnetic resonance image analysis with fully convolutional networks. J Cardiovasc Magn Reson. 2018; 20(1): 65, doi: 10.1186/s12968-018-0471-x, indexed in Pubmed: 30217194.
42. Fries JA, Varma P, Chen VS, et al. Weakly supervised classification of aortic valve malformations using unlabeled cardiac MRI sequences. Nat Commun. 2019; 10(1): 3111, doi: 10.1038/s41467-019-11012-3, indexed in Pubmed: 31308376.
43. Yang G, Zhuang X, Khan H, et al. Fully automatic segmentation and objective assessment of atrial scars for long-standing persistent atrial fibrillation patients using late gadolinium-enhanced MRI. Med Phys. 2018; 45(4): 1562–1576, doi: 10.1002/mp.12832, indexed in Pubmed: 29480931.
44. Swift AJ, Lu H, Uthoff J, et al. A machine learning cardiac magnetic resonance approach to extract disease features and automate pulmonary arterial hypertension diagnosis. Eur Heart J Cardiovasc Imaging. 2020 [Epub ahead of print], doi: 10.1093/ehjci/jeaa001, indexed in Pubmed: 31998956.
45. Yang Su, Kweon J, Roh JH, et al. Deep learning segmentation of major vessels in X-ray coronary angiography. Sci Rep. 2019; 9(1): 16897, doi: 10.1038/s41598-019-53254-7, indexed in Pubmed: 31729445.
46. Kwon JM, Kim KH, Akkus Z, et al. Artificial intelligence for detecting mitral regurgitation using electrocardiography. J Electrocardiol. 2020; 59: 151–157, doi: 10.1016/j.jelectrocard.2020.02.008, indexed in Pubmed: 32146201.
47. Weng SF, Reps J, Kai J, et al. Can machine-learning improve cardiovascular risk prediction using routine clinical data? PLoS One. 2017; 12(4): e0174944, doi: 10.1371/journal.pone.0174944, indexed in Pubmed: 28376093.
48. Rajkomar A, Oren E, Chen K, et al. Scalable and accurate deep learning with electronic health records. NPJ Digit Med. 2018; 1: 18, doi: 10.1038/s41746-018-0029-1, indexed in Pubmed: 31304302.
49. Brajer N, Cozzi B, Gao M, et al. Prospective and External Evaluation of a Machine Learning Model to Predict In-Hospital Mortality of Adults at Time of Admission. JAMA Netw Open. 2020; 3(2): e1920733, doi: 10.1001/jamanetworkopen.2019.20733, indexed in Pubmed: 32031645.
50. Shameer K, Johnson KW, Yahi A, et al. Predictive modeling of hospital readmission rates using electronic medical record-wide machine learning: a case-study using mount sinai heart failure cohort. Pac Symp Biocomput. 2017; 22: 276–287, doi: 10.1142/9789813207813_0027, indexed in Pubmed: 27896982.
51. Shouval R, Hadanny A, Shlomo N, et al. Machine learning for prediction of 30-day mortality after ST elevation myocardial infraction: an acute coronary syndrome israeli survey data mining study. Int J Cardiol. 2017; 246: 7–13, doi: 10.1016/j.ijcard.2017.05.067, indexed in Pubmed: 28867023.
52. Wallert J, Tomasoni M, Madison G, et al. Predicting two-year survival versus non-survival after first myocardial infarction using machine learning and Swedish national register data. BMC Med Inform Decis Mak. 2017; 17(1): 99, doi: 10.1186/s12911-017-0500-y, indexed in Pubmed: 28679442.

53. Pieszko K, Hiczkiewicz J, Budzianowski P, et al. Predicting long-term mortality after acute coronary syndrome using machine learning techniques and hematological markers. Dis Markers. 2019; 2019: 9056402, doi: 10.1155/2019/9056402, indexed in Pubmed: 30838085.
54. Pieszko K, Hiczkiewicz J, Budzianowski P, et al. Machine-learned models using hematological inflammation markers in the prediction of short-term acute coronary syndrome outcomes. J Transl Med. 2018; 16(1): 334, doi: 10.1186/s12967-018-1702-5, indexed in Pubmed: 30509300.
55. Gibson WJ, Nafee T, Travis R, et al. Machine learning versus traditional risk stratification methods in acute coronary syndrome: a pooled randomized clinical trial analysis. J Thromb Thrombolysis. 2020; 49(1): 1–9, doi: 10.1007/s11239-019-01940-8, indexed in Pubmed: 31535314.
56. Kalscheur MM, Kipp RT, Tattersall MC, et al. Machine learning algorithm predicts cardiac resynchronization therapy outcomes: lessons from the COMPANION trial. Circ Arrhythm Electrophysiol. 2018; 11(1): e005499, doi: 10.1161/CIRCEP.117.005499, indexed in Pubmed: 29326129.
57. Panch T, Mattie H, Celi L. The "inconvenient truth" about AI in healthcare. npj Digital Medicine. 2019; 2(1), doi: 10.1038/s41746-019-0155-4, indexed in Pubmed: 31453372.
58. Oakden-Rayner L, Dunnmon J, Carneiro G, et al. Hidden stratification causes clinically meaningful failures in machine learning for medical imaging. Proceedings of the ACM Conference on Health, Inference, and Learning. 2020, doi: 10.1145/3368555.3384468.
59. Esteva A, Kuprel B, Novoa RA, et al. Dermatologist-level classification of skin cancer with deep neural networks. Nature. 2017; 542(7639): 115–118, doi: 10.1038/nature21056, indexed in Pubmed: 28117445.
60. Goodman B, Flaxman S. European Union Regulations on Algorithmic Decision-Making and a "Right to Explanation". AI Magazine. 2017; 38(3): 50–57, doi: 10.1609/aimag.v38i3.2741.
61. Gale W, Oakden-Rayner L, Carneiro G, et al. Producing radiologist-quality reports for interpretable deep learning. 2019 IEEE 16th International Symposium on Biomedical Imaging (ISBI 2019). 2019, doi: 10.1109/isbi.2019.8759236.
62. Parasuraman R, Manzey DH. Complacency and bias in human use of automation: an attentional integration. Hum Factors. 2010; 52(3): 381–410, doi: 10.1177/0018720810376055, indexed in Pubmed: 21077562.
63. Hripcsak G, Knirsch C, Zhou Li, et al. Bias associated with mining electronic health records. J Biomed Discov Collab. 2011; 6: 48–52, doi: 10.5210/disco.v6i0.3581, indexed in Pubmed: 21647858.
64. Gianfrancesco MA, Tamang S, Yazdany J, et al. Potential biases in machine learning algorithms using electronic health record data. JAMA Intern Med. 2018; 178(11): 1544–1547, doi: 10.1001/jamainternmed.2018.3763, indexed in Pubmed: 30128552.
65. Parikh RB, Teeple S, Navathe AS. Addressing bias in artificial intelligence in health care. JAMA. 2019 [Epub ahead of print], doi: 10.1001/jama.2019.18058, indexed in Pubmed: 31755905.
66. Gur D, Bandos A, Cohen C, et al. The "laboratory" effect: comparing radiologists' performance and variability during prospective clinical and laboratory mammography interpretations. Radiology. 2008; 249(1): 47–53, doi: 10.1148/radiol.2491072025, indexed in Pubmed: 18682584.
67. Lehman CD, Wellman RD, Buist DSM, et al. Breast Cancer Surveillance Consortium. Diagnostic accuracy of digital screening mammography with and without computer-aided detection. JAMA Intern Med. 2015; 175(11): 1828–1837, doi: 10.1001/jamainternmed.2015.5231, indexed in Pubmed: 26414882.
68. Angus DC. Randomized clinical trials of artificial intelligence. JAMA. 2020 [Epub ahead of print], doi: 10.1001/jama.2020.1039, indexed in Pubmed: 32065828.
69. Wang Pu, Berzin TM, Glissen Brown JR, et al. Real-time automatic detection system increases colonoscopic polyp and adenoma detection rates: a prospective randomised controlled study. Gut. 2019; 68(10): 1813–1819, doi: 10.1136/gutjnl-2018-317500, indexed in Pubmed: 30814121.
70. Wijnberge M, Geerts BF, Hol L, et al. Effect of a machine learning-derived early warning system for intraoperative hypotension vs standard care on depth and duration of intraoperative hypotension during elective noncardiac surgery: the HYPE randomized clinical trial. JAMA. 2020 [Epub ahead of print], doi: 10.1001/jama.2020.0592, indexed in Pubmed: 32065827.
71. Schwab K. The fourth industrial revolution. Currency. 2017: 192.

VIA MEDICA

REVIEW ARTICLE

Cardiology Journal
2021, Vol. 28, No. 3, 473–482
DOI: 10.5603/CJ.a2020.0061

ISSN 1897–5593
eISSN 1898–018X

Role of extracellular signal-regulated kinase 1/2 signaling underlying cardiac hypertrophy

Zhi-Peng Yan[1, 2], Jie-Ting Li[2], Ni Zeng[2], Guo-Xin Ni[1]

[1]School of Sport Medicine and Rehabilitation, Beijing Sport University, China
[2]Department of Rehabilitation Medicine, The First Affiliated Hospital of Fujian Medical University, China

Abstract

Cardiac hypertrophy is the result of increased myocardial cell size responding to an increased workload and developmental signals. These extrinsic and intrinsic stimuli as key drivers of cardiac hypertrophy have spurred efforts to target their associated signaling pathways. The extracellular signal-regulated kinases 1/2 (ERK1/2), as an essential member of mitogen-activated protein kinases (MAPKs), has been widely recognized for promoting cardiac growth. Several modified transgenic mouse models have been generated through either affecting the upstream kinase to change ERK1/2 activity, manipulating the direct role of ERK1/2 in the heart, or targeting phosphatases or MAPK scaffold proteins to alter total ERK1/2 activity in response to an increased workload. Using these models, both regulation of the upstream events and modulation of each isoform and indirect effector could provide important insights into how ERK1/2 modulates cardiomyocyte biology. Furthermore, a plethora of compounds, inhibitors, and regulators have emerged in consideration of ERK, or its MAPK kinases, are possible therapeutic targets against cardiac hypertrophic diseases. Herein, is a review of the available evidence regarding the exact role of ERK1/2 in regulating cardiac hypertrophy and a discussion of pharmacological strategy for treatment of cardiac hypertrophy. (Cardiol J 2021; 28, 3: 473–482)

Key words: ERK1/2, cardiac hypertrophy, cardiomyocyte, genetic approaches, pharmacological strategy

Introduction

The mammalian heart is a muscular pump that circulates blood throughout the body to maintain perfusion of peripheral organs, which meets their demand during both regular and stressful conditions. In response to an increased workload, enlargement of the heart occurs and is defined as an increase in heart size without changes in myocyte number. Physiological hypertrophy observed in normal growth or trained athletes is considered an adaptive and compensatory response to maintain cardiac function and improved cardiac contractility. By contrast, cardiac hypertrophy under pathological conditions, such as ischemic heart disease, hypertension, and heart failure, is referred to as pathological hypertrophy. This type of hypertrophy is associated with the production of high levels of hemodynamic overload, interstitial fibrosis, and myocardial cell damage and loss [1, 2]. Because cardiac hypertrophy plays a central role in cardiac remodeling and is an independent risk factor for cardiac events, understanding the molecular mechanisms is vital.

Previous studies have shown that a group of medical genetic syndromes referred to as RASopathie are caused by germline mutations in genes that encode components or regulators of the RAS-RAF-MEK-ERK pathway, which include neurofibromatosis type 1, Noonan syndrome, Costello syndrome, and cardio-facio-cutaneous syndrome [3]. These patients suffered from cardiomyopathies suggesting that the RAS/MAPK pathway is critical to normal heart development. Moreover, before mouse genetics entered the mainstream of experiments, studies were conducted mainly on

Address for correspondence: Prof. Guo-Xin Ni, School of Sports Medicine and Rehabilitation, Beijing Sport University, tel: +(86)-10-62989780, fax:+(86)-10-62989670, e-mail: niguoxin@bsu.edu.cn

Received: 11.12.2019 Accepted: 12.04.2020

cultured neonatal rat cardiomyocytes or inadequate "myocyte-like" cell lines which discovered the activation of the extracellular signal-regulated kinases 1/2 (ERK1/2) pathway under the hormone and mechanical stretch in the heart, suggesting a direct causation between ERK1/2 signaling and the hypertrophic response [4, 5]. To support this hypothesis, the use of dominant negative MEK1, antisense oligonucleotides against ERK1/2, dephosphorylation of ERK1/2, and pharmacologic inhibitors of MEK1/2 provided convincing data, indicating that MEK1-ERK1/2 is both necessary and sufficient for cardiac hypertrophy [6–10]. Autophosphorylation of ERK1/2 on Thr188 was also observed in isolated cardiomyocytes induced by hypertrophic stimulus [11]. Although considerable evidence elucidates that the activated MEK1/2-ERK1/2 can regulate cardiac hypertrophy in vitro, the results of other similarly designed culture-based studies are quite different [12, 13]; one study even suggested that ERK1/2 activation is anti-hypertrophic [14]. In addition to traditional two-dimensional (2D) in vitro systems, three-dimensional (3D) tissue models have also offered new tools in the study of cardiovascular disease recently [15]. In response to 3D conditions, the activation of ERK1/2 was observed during cardiomyogenesis, and the phosphorylation of ERK1/2 was higher compared to cells on 2D films, which provides insight into ERK1/2 pathways driving heart development [16, 17]. With regard to the whole organ phenomenon in a dynamically changing neuroendocrine environment under cardiac hypertrophy and heart failure, culture-based or tissue-engineering approaches have only provided some basic physiological parameters within a largely 2D or 3D environment [18]. However, these approaches will always be necessary because of the simplified process established in a largely isolated system and temporal relationships. More recently, a new method, known as mathematical optimization framework, also analyzed the complex ERK1/2 cascade in cardiomyocytes to find efficient adjustment screws for this cascade that is important for cardiomyocyte survival and maladaptive heart muscle growth [19].

In this review, the focus was on the main thread of the RAS-RAF-MEK-ERK pathway and summarize the more recent knowledge about the functional activity of ERK pathway in the cardiac organ to reveal the exact role of ERK1/2 in regulating cardiac hypertrophy. Also, the latest scientific results of addressing ERK signaling as a therapeutic target for the treatment of cardiac hypertrophy is discussed.

Components and regulation of the ERK cascade

As ERK1 and ERK2 are 83% identical in sequence and share most of the same signaling activities, they are usually referred to as ERK1/2 [20]. However, these two proteins are not entirely functionally redundant. For instance, ERK1 knockout animals appear normal and are viable, while ERK2 deletion results in embryonic lethality [21]. In cardiomyocytes, the canonical ERK1/2 signal cascade is initiated by the activation of the small G protein rat sarcoma (RAS) in the cell membrane, which leads to the recruitment and activation of RAF-1 (MAP3K), which further phosphorylates the dual-specificity protein kinases MEK1/2 (MAP2K); eventually, MEK1/2 characteristically activate ERK1/2 (MAPK) by phosphorylating the threonine-glutamate-tyrosine (TEY) motif in the phosphorylation loop. Active ERK is then released from the MEK and phosphorylates a wide array of cytoplasmic substrates. Alternatively, activation of ERK is translocated to the nucleus and phosphorylates numerous transcription factors, which result in the induction of growth and proliferation and in the prevention of cell death [22]. Furthermore, the specificity of ERK biological effects is influenced by many factors, including (i) duration and strength of the signals, (ii) interaction with various scaffold proteins, (iii) subcellular localization, (iv) extensive cross-talk and interplay between the ERK cascade and other intracellular signaling pathways, and (v) presence of several similar isoforms at each tier of the cascade [23]. Although many of these mechanisms could independently determine signaling specificity and magnitude of the signaling outcome, they often work in coordination with each other to ensure proper downstream effects. Additionally, the pro-hypertrophic, pro-survival and pro-death effects of ERK1/2 converge on mitochondria upon their crucial roles in metabolism of cardiomyocyte. In response to types of stimuli, ERK1/2 can modulate mitochondria-mediated cardiomyocyte function directly through the interaction with mitochondria [24], or indirectly, by activation/inhibition of ERK-dependent downstream signaling molecules or mediators [25–28]. Finally, the inactivation of ERKs is regulated by various phosphatases, including dual-specificity MAPK phosphatases (MKPs), protein serine/threonine phosphatases (PPs), and protein tyrosine phosphatases (PTP) [29, 30].

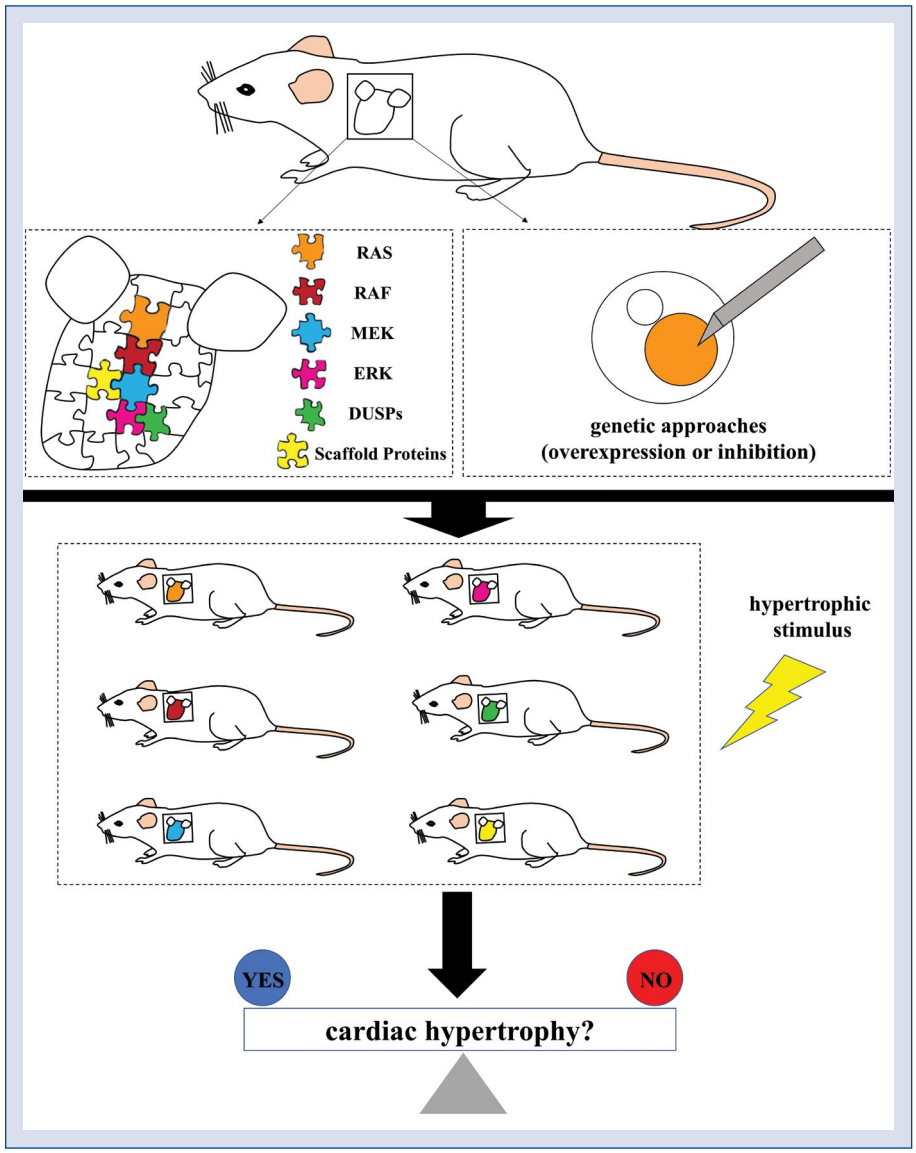

Figure 1. Schematic diagram of extracellular signal-regulated kinases (ERK) pathway and mitogen-activated protein kinase (MAPK)-associated genetic mouse models. In cardiomyocytes, the canonical ERK1/2 signal cascade is initiated by the activation of the small G protein rat sarcoma (RAS) in the cell membrane, which leads to the recruitment and activation of RAF-1, which further phosphorylates the dual-specificity protein kinases MEK1/2; eventually, MEK1/2 characteristically activate ERK1/2. In response to growth factors, hormones, and mechanical stress, the RAS-RAF--MEK-ERK pathway, dual-specificity phosphatases (DUSPs) and scaffold proteins were overexpressed or inhibited in the mouse to change ERK1/2 activity, which examines the connection between ERK activation and cardiac hypertrophy; RAF — rapidly accelerated fibrosarcoma; MEK — MAPK/ERK kinase.

ERK1/2 and cardiac hypertrophy

Studying the role of the RAS-RAF-MEK-ERK pathway in the heart, did not, herein, satisfy a detailed understanding of the physiological function of the cascade, which revealed that cardiomyocytes are isolated from their physiological environment, the present investigation focuses on the emergence of genetic approaches in mice using gained or lost functional mutants (Fig. 1).

Targeting upstream kinase

The previously published H-Ras-V12 transgenic model with overstimulating of the RAS hinted at the trend of decompensation and dilatation of the heart and developed a chain of events that contrib-

uted to the pathogenesis of cardiovascular disease [31–33]. Subsequently, Wei et al. [34] demonstrated that discontinuing overactivation of this pathway after the onset of cardiomyopathy could lead to improved survival and cardiomyopathy lesion scores, suggesting the reversibility of early pathogenic hypertrophy. More recently, the possible anti-hypertrophic effect of RAS inhibition in the setting of pressure-overload cardiac hypertrophy in rats was examined [35]. After pressure-overload induction and Ras-mutant gene transfer, the hypertrophic degrees of the heart in both Ras mutants were similar. However, the Ras-Val12 mutant increases left ventricular systolic diameter and reduces left ventricular fractional shortening compared to control and dominant negative mutant N17-DN-Ras (DN-Ras). Moreover, DN-Ras exhibited some similarities with physiologic hypertrophy, especially the lower expression of markers of pathologic cardiac hypertrophy. Although these studies used different promoters to drive RAS expression, the same constitutively activated RAS mutants were generated, indicating that the inactivation of Ras is cardioprotective rather than anti-hypertrophic. Ras directly activates Raf-1, which may subsequently lead to MEK1-ERK1/2 activation. It also activates other intracellular signaling pathways. Importantly, its activation is involved in pathological changes in sarcoplasmic reticulum calcium handling [36, 37].

Activating mutations in the serine-threonine kinase Raf cause cardiac hypertrophy and contribute to Noonan syndrome in humans. Heterozygous Raf1L613V mice were generated and exhibited eccentric cardiac hypertrophy, aberrant cardiac fetal gene expression, and decompensation following pressure overload, but treatment of these mice with MEK inhibitors (PD0325901) or constitutive deletion of ERK effector (RSK3) rescued Raf-mediated cardiac hypertrophy and other phenotypic abnormalities [38, 39]. In addition, a dominant negative form of Raf-1 animals had obvious resistance to the development of cardiac hypertrophy and hypertrophic gene induction in response to pressure overload [40]. Both groups found that, while Raf-1 kinase activity was essential for cardiac hypertrophy, enhanced MEK-ERK activity was critical for causing RAF1-mutant phenotypes. However, recently, Yin et al. [41] showed that left ventricular hypertrophy was due to the interplay of cardiac cell types. Using inducible Raf1L613V expression, mutant RAF1 expression in cardiomyocytes enhanced Ca2+ sensitivity and cardiac contractility rather than hypertrophy. By contrast, endothelial/endocardial (EC)-restricted mutant expression does not affect contractility, but evokes hypertrophy. Moreover, aberrant RAF1 activity in cardiomyocytes or cardiac fibroblasts, but not ECs, contributes to pressure overload-induced fibrosis in Noonan syndrome cardiomyopathy. These results support a paradigm shift away from the myocyte-centric view of cardiac development and disease.

Even though RAS transgenic mice exhibited cardiac hypertrophy associated with cardiomyopathy, MEK1 transgenic mice showed a stable concentric hypertrophy without any signal of decompensation up to 12 months of age [42]. Furthermore, these mice expressing activated MEK1 showed a dramatic increase in cardiac function measured by echocardiography and isolated working heart preparation, and there was activation of ERK1/2, but not p38 or JNK. In addition, MEK1 transgenic mice showed resistance to ischemia/reperfusion-induced apoptosis. These outcomes suggest that MEK-ERK not only sufficiently induces normally hypertrophic response, but that it also has a bearing on partial resistance to apoptosis.

Taken together, these results support that the RAS-RAF-MEK-ERK pathway is generally regarded as pro-hypertrophic and suggest that sustained cascade activation also plays a cardioprotective role in the heart. Furthermore, the closer the upstream kinase is to ERK, the stronger the correlation with hypertrophic process. This may be because the initial upstream kinase is more susceptible to interference from other factors.

Targeting ERK1/2

In view that evidence of non-redundancy is apparent from isoform-specific ERK targeted mice, overexpression of intrinsically active ERK1 and ERK2 in the heart were generated to further test the effects of ERK1/2. A recent study reported transgenic mice expressing activated ERK1 under the transcriptional control of the α-MHC promoter — which, similar to the observations in hypertrophy, is phosphorylated on both the TEY and the Thr207 motifs and is overexpressed at pathophysiological levels — developed a modest adaptive hypertrophy with increased contractile function and without fibrosis [43]. Nevertheless, another recent study demonstrated that volume overload-induced eccentric hypertrophy is associated with reduced cardiac ERK1/2 activation while phosphorylation of other MAPKs was unaffected in vivo. However, transgenic mice with cardiomyocyte-specific ERK2 overexpression did not alter left ventricular dilation and hypertrophy [44]. Importantly, Molkentin et al.

[18] found that high levels of ERK2 overexpression in the heart from two independent transgenic lines with the same α-MHC promoter did not induce hypertrophy. However, MEK1 transgenic mice crossed with ERK2 transgenic mice showed synergistic hypertrophy. Although ERK2 seems to be dominant in the results of the knockout experiment, the single overexpression of these two kinds of MAPK appears inconsistent, and the relationship between MEK1/2 and ERK2 is likely to be close. These results indicate that ERK1 may induce the hypertrophic effect after the inhibition of MEK1/2. Further, a novel ERK2 autophosphorylation site, other than TEY phosphorylation, was found on Thr188 after stimulation with pressure overload and in failing human hearts [11]. The equivalent phosphorylation was also discovered on EKR1 at Thr207 [45, 46]. The authors generated several lines of transgenic mice overexpressing ERK2 with mutations at Thr188. Compared with baseline wild type mice, no hypertrophy was observed in these mice [11]. After pressure overload, the ERK2T188D (gain-of-function ERK) mice showed more striking hypertrophy, not the ERK2T188A or ERK2T188S (phosphorylation-deficient ERK) mice. This mechanism depends on upstream signals — specifically, activation of Gq-coupled receptors, which release G$\beta\gamma$; activation of the entire Raf-MEK-ERK cascade; subsequent phosphorylation of ERK1/2 within the TEY motif; and ERK dimerization. The integration of these signaling events leads to autophosphorylation of ERK2 at Thr188. In addition, the phosphorylation of Thr188 is related to the pathological morphology of hypertrophy [47]. It is generally believed that the specific role of Thr188 phosphorylation of ERK1/2 in vivo was to transform adaptive ERK signals into maladaptive signals. However, this notion is based on a study of mice overexpressing ERK2 Thr188 mutants, which may eliminate catalytic activity of ERK.

Contrary to the gain of function of ERK1/2, some reports on ERK knockout mice suggested that ERK1/2 signaling may not be necessary to mediate cardiac growth in vivo. ERK1 null (–/–) and ERK2 null (+/–) mice showed no reduction in cardiac hypertrophy response to pathologic stimulus--induced by transverse aortic constriction (TAC) or to physiologic stimulus-induced by swimming [48]. Moreover, mice lacking all ERK1/2 protein in the heart (ERK1–/– ERK2fl/fl-Cre) were generated. After eliminating both isoforms, the heart still increased in weight with both aging and pathological stress stimulation, where the heart showed spontaneous dilatation and the cardiomyocytes showed spontaneous lengthening [49]. Another study examined the cardiomyocyte-specific deletion of the ERK2 gene (ERK2cko mice). Following short-term pathological hypertrophic stresses, the mutant mice showed attenuated hypertrophic remodeling characterized by a blunted increase in the cross--sectional area of individual myocytes. However, the absence of ERK2 did not affect physiological hypertrophy induced by exercise [50].

Above all, these results suggest that either ERK1/2 are not critical for mediating cardiac hypertrophy under pathophysiologic stress or the remaining ERK1/2 activity in each gene-targeted mouse model was sufficient to mediate the signaling events required to drive the hypertrophic response. This outcome places ERK at the crossroads of cardiac hypertrophic signaling pathways and raises the possibility that different isoforms of ERK may play different roles in regulating the growth of cardiac myocytes.

Targeting phosphatases and MAPK scaffold proteins

Due to the high embryonic lethality, it was difficult to generate ERK1–/– ERK2+/– mice (3 of 4 alleles deleted) to address the necessity of ERK1/2 signaling in mediating cardiac hypertrophy. Therefore, other approaches are desirable to more effectively alter total ERK1/2 activity within the heart. Dual-specificity phosphatases (DUSPs), the largest family of MAPK-selective phosphatases, act to dephosphorylate both the p-Ser/Thr and -Tyr residues that are essential for cytosolic and/ /or nuclear MAPK activity. A precedent for these phosphatases appeared with the description of DUSP6–/– mice [51]. An increase in basal ERK1/2 phosphorylation in the absence of DUSP6 was identified, but no effect was observed on other MAPKs after stimulation. DUSP6–/– mice with larger hearts was not due to hypertrophy, but rather to hypercellularity of the myocytes. A recent study confirmed a similar finding in the zebrafish heart by suppressing the Dusp6 function, which showed that DUSP6 attenuated Ras/MAPK signaling during regeneration, and inactivation of DUSP6 could enhance cardiac repair [52]. Opposite to the activation of ERK1/2, multiple lines of DUSP6 contained in the mouse heart were specifically generated [48]. Similar to ERK1 null (–/–) and ERK2 null (+/–) mice, low-, medium-, and high-Dusp6 Tg mice showed no reduction in hypertrophy after pressure overload stimulation, neuroendocrine agonist infusion, or physiologic exercise stimulation, though

the activation of all cardiac ERK1/2 at baseline were nearly eliminated. Notably, a phosphatase known as DUSP8 has drawn attention recently. DUSP8–/– mice increased ERK1/2 phosphorylation and were mildly hypercontractile at baseline with the concentric remodeling of the heart, which provided prolonged protection from progressing towards heart failure in two surgery-induced disease models [53]. While cardiac-specific overexpression of DUSP8 produced spontaneous eccentric remodeling with heart failure, overexpression of DUSP8 in the heart caused dephosphorylation of all three major MAPK terminal effectors. Overall, although these studies suggest that ERK1/2 manipulated by DUSP6 and DUSP8 are not required for mediating hypertrophy per se, one critical point to consider is that other DUSPs such as DUSP2, -4, -5, -7, and -9 also dephosphorylate ERK1/2 [54]. While 13 DUSP proteins are dedicated to regulating and recycling the MAPKs, each appears to have a highly specialized regulatory role.

Given that MAPK scaffolding proteins enable the formation of specific signaling complexes and subcellular localization in the activation of an MAPK cascade, many studies of genetic mouse models, specifically MAPK scaffolding proteins, have further reinforced a direct role for ERK1/2 pathway in stress-induced cardiac hypertrophy. Scaffold proteins tether MAPK/ERK signaling at the sarcomere and plasma membrane in the cardiac muscle and regulate ERK signaling strength and duration [55]. As such, ANKRD1, which conducts the components of the sarcomere-associated biomechanical sensors, can be markedly induced by various hypertrophic stimuli and in distinct animal models of hypertrophy. ANKRD1-overexpressing transgenic mice developed less hypertrophy, and no differences were evident in heart function compared to wild-type mice in TAC- and isoproterenol-induced models [56], which were mediated by the inhibition of ERK1/2 and TGF-β pathways. Conversely, striking cardiac hypertrophy with reactivation of the cardiac fetal gene program induced by chronic phenylephrine infusion in wild-type mice was completely eliminated in ANKRD1 null mice via ANKRD1-ERK-GATA4 complex to regulate hypertrophic responses [57]. This phenomenon may be caused by different hypertrophic stimuli. Respectively, IQGAP1, which bind to the plasma membrane, played a part in the maintenance of cardiomyocyte physiology and the induction of adaptive hypertrophy. IQGAP1-null mice initially developed compensatory hypertrophy and unaltered basal heart function in response to pressure overload, but with a prolonged stimulus, they showed acceleration towards the development of maladaptive hypertrophy resulting in a decrease of cardiac contractility [58]. These results emphasize that different scaffold proteins may mediate the spatial regulation of ERK1/2 activation, which in turn determines the substrate specificity of pathological states associated with cardiac hypertrophy. Additionally, MAPK scaffolds, such as MP1 [59] and DYRK1A [60], have been characterized in the heart, but their role in cardiac remodeling has not yet been addressed. By extension, readers can see several excellent recent reviews on this issue [61, 62].

Pharmacological strategy for the treatment of cardiac hypertrophy

Despite substantial advances, there is still a major demand for finding novel therapeutic strategies to use in the hypertrophic process of cardiac remodeling and cardiac events. Although ERK activation events need to be investigated further and refined in detail, ERK or its MAPK kinases, is a possible therapeutic target for a pharmacological strategy against cardiac hypertrophic diseases. If the intrinsic manipulation of ERK is insufficient to reliably achieve complete remission, an obvious alternative strategy is to target extrinsically potential compounds, inhibitors, or regulators.

Compounds

Recent works are underway to discover compounds that inhibit this pathway and thus provide a potential therapeutic agent that could attenuate cardiac growth. Traditional Chinese medicine has been reported to be effective for the treatment of cardiac hypertrophy in animal models, such as Baicalein and Bu-Shen-Jiang-Ya [63] decoction (BSJYD). Baicalein, known for its antibacterial, antiviral, and anti-inflammatory effects, protects against cardiac hypertrophy and fibrosis in response to chronic pressure overload by regulating the MEK-ERK1/2 signaling pathway [63]. Additionally, BSJYD treatment decreases systolic blood pressure and heart rate efficiently and suppresses the hypertension-induced cardiac hypertrophy associated with the suppressive effect of BSJYD on the EKR signaling pathway [64]. Other compounds were also reported to target the ERK pathway. Sun et al. [65] showed that gentisic acid attenuates pressure overload-induced cardiac hypertrophy and fibrosis in mice through inhibition of the ERK1/2 pathway. Additionally, Li et al. [66] demonstrated

that selumetinib could attenuate pathological and physiological cardiac hypertrophy in vivo caused by pressure overload and swimming. In short, these preclinical studies encourage the emergence of more effective compounds to target cardiac hypertrophy with aberrant ERK activation.

Inhibitors

Developed for the treatment of various cancers, kinase inhibitors are also used to reduce excessive signal activation in cardiac hypertrophy. One study that explored the effects of the MEK inhibitor of Pimasertib on cardiac hypertrophy and heart failure showed a reversible effect of Pimasertib on a transgenic model expressing an activated MET receptor, which was attributed to the inhibition of ERK1/2 pathway [67]. Several in vitro studies have also explored the effects of MEK inhibitor effects on cultured cardiomyocytes. Two of the most commonly utilized are PD98059 and U0126. PD98059 reversed leukemia inhibitory factor-induced cardiomyocyte hypertrophy [68]. Similarly, U0126 blocked cardiomyocyte growth induced by endothelin-1 and phenylephrine [69]. As available MEK inhibitors for the ERK signaling pathway, these agents target regions distinct from the ATP pocket. However, these two inhibitors inhibit all MEKs upstream of the ERKs, including MEK1, MEK2, and MEK5. More recently, a newly potent and selective MEK inhibitor called TAK733 was confirmed to suppress norepinephrine or phenylepinephrine-induced cardiomyocyte hypertrophy through the depression of MEK-ERK signaling [70]. These studies support the role of MEK-ERK cascade in promoting hypertrophy, but the inherent non-selectivity of some inhibitors should not be ignored because of their effects on MEK5.

Regulators

It is common knowledge that MAPK pathways are largely associated with G protein-coupled receptor (GPCRs)-mediated signaling. Belonging to cell membrane receptors, GPCRs interact with G proteins to activate multiple downstream intracellular cascades and in turn modulate subsets of effector proteins [71]. Regulators of G protein signaling (RGS) proteins are negative regulators of G protein mediated signaling that serve as GTPase activating protein for heterotrimeric G proteins. Recently, accumulating studies have demonstrated that RGS proteins can regulate cardiac hypertrophy independent of GTPase-activating protein activity. Among them, RGS3 [72], RGS5 [73], RGS10 [74], RGS12 [75], and RGS14 [76] protect against pressure overload-induced hypertrophic response and improve cardiac function by inhibiting MEK–ERK1/2 signaling. Notably, unlike most overexpression approaches leading to beneficial effects on the heart, RGS12-defcient hearts showed a decreased cardiomyocyte cross area without predisposing the heart to adverse remodeling and failure. Although RGS10, RGS12 and RGS14 belong to the R12/D subfamily, the reason for such opposing responses is not completely understood. Considering the anti-hypertrophic effect attributed to some RGS proteins through MEK–ERK1/2 signaling, their potential as targets for therapeutic intervention warrants further examination.

Conclusions

In summary, although the ERK cascade is a major signaling component and regulates many distinct cellular processes, the functional role of the ERK1/2 in the heart still presents a potential dilemma. As this review shows, many current approaches are based solely on opposite ways to dissect the cardiac disease states, such as cell culture versus mouse genetics, direct versus indirect manipulation of ERK1/2, and gain versus loss of function. However, the ERK cascade is mainly regulated at several levels by different phosphatases and scaffold proteins, other signaling pathways, subcellular localization, and even different isoforms per se. Many of these mechanisms can work together to determine the final specificity of the cascade. While uncontrolled activation of RAS-RAF-MEK-ERK signaling may lead to cardiac hypertrophy, inhibiting the pathway may also make the heart more susceptible to stress induced cardiomyocyte death. Therefore, to unravel the ERK1/2 mechanisms, more sophisticated model systems are required, which will help us to make sure the critical role of ERK1/2 and the ensuing effects in the heart. In light of the lack of uniform results in ERK biology in cardiac hypertrophy, translation of the knowledge about pro-hypertrophic signaling pathways may lead to both exciting and challenging clinical insights.

Acknowledgements

This work was supported by National Natural Science Foundation of China (81871848).

Conflict of interest: None declared

References

1. Shimizu I, Minamino T. Physiological and pathological cardiac hypertrophy. J Mol Cell Cardiol. 2016; 97: 245–262, doi: 10.1016/j.yjmcc.2016.06.001, indexed in Pubmed: 27262674.
2. Nakamura M, Sadoshima J. Mechanisms of physiological and pathological cardiac hypertrophy. Nat Rev Cardiol. 2018; 15(7): 387–407, doi: 10.1038/s41569-018-0007-y, indexed in Pubmed: 29674714.
3. Rauen KA. The RASopathies. Annu Rev Genomics Hum Genet. 2013; 14: 355–369, doi: 10.1146/annurev-genom-091212-153523, indexed in Pubmed: 23875798.
4. Post GR, Goldstein D, Thuerauf DJ, et al. Dissociation of p44 and p42 mitogen-activated protein kinase activation from receptor-induced hypertrophy in neonatal rat ventricular myocytes. J Biol Chem. 1996; 271(14): 8452–8457, doi: 10.1074/jbc.271.14.8452, indexed in Pubmed: 8626545.
5. Yamazaki T, Tobe K, Hoh E, et al. Mechanical loading activates mitogen-activated protein kinase and S6 peptide kinase in cultured rat cardiac myocytes. J Biol Chem. 1993; 268(16): 12069–12076, indexed in Pubmed: 7685031.
6. Ueyama T, Kawashima S, Sakoda T, et al. Requirement of activation of the extracellular signal-regulated kinase cascade in myocardial cell hypertrophy. J Mol Cell Cardiol. 2000; 32(6): 947–960, doi: 10.1006/jmcc.2000.1135, indexed in Pubmed: 10888249.
7. Liang F, Lu S, Gardner DG. Endothelin-dependent and -independent components of strain-activated brain natriuretic peptide gene transcription require extracellular signal regulated kinase and p38 mitogen-activated protein kinase. Hypertension. 2000; 35(1 Pt 2): 188–192, doi: 10.1161/01.hyp.35.1.188, indexed in Pubmed: 10642296.
8. Liang Q, Wiese RJ, Bueno OF, et al. The transcription factor GATA4 is activated by extracellular signal-regulated kinase 1- and 2-mediated phosphorylation of serine 105 in cardiomyocytes. Mol Cell Biol. 2001; 21(21): 7460–7469, doi: 10.1128/MCB.21.21.7460-7469.2001, indexed in Pubmed: 11585926.
9. Glennon PE, Kaddoura S, Sale EM, et al. Depletion of mitogen-activated protein kinase using an antisense oligodeoxynucleotide approach downregulates the phenylephrine-induced hypertrophic response in rat cardiac myocytes. Circ Res. 1996; 78(6): 954–961, doi: 10.1161/01.res.78.6.954, indexed in Pubmed: 8635245.
10. Ferguson BS, Harrison BC, Jeong MY, et al. Signal-dependent repression of DUSP5 by class I HDACs controls nuclear ERK activity and cardiomyocyte hypertrophy. Proc Natl Acad Sci U S A. 2013; 110(24): 9806–9811, doi: 10.1073/pnas.1301509110, indexed in Pubmed: 23720316.
11. Lorenz K, Schmitt JP, Schmitteckert EM, et al. A new type of ERK1/2 autophosphorylation causes cardiac hypertrophy. Nat Med. 2009; 15(1): 75–83, doi: 10.1038/nm.1893, indexed in Pubmed: 19060905.
12. Thorburn J, Frost JA, Thorburn A. Mitogen-activated protein kinases mediate changes in gene expression, but not cytoskeletal organization associated with cardiac muscle cell hypertrophy. J Cell Biol. 1994; 126(6): 1565–1572, doi: 10.1083/jcb.126.6.1565, indexed in Pubmed: 8089186.
13. Thorburn J, McMahon M, Thorburn A. Raf-1 kinase activity is necessary and sufficient for gene expression changes but not sufficient for cellular morphology changes associated with cardiac myocyte hypertrophy. J Biol Chem. 1994; 269(48): 30580–30586, indexed in Pubmed: 7982977.
14. Silberbach M, Gorenc T, Hershberger RE, et al. Extracellular signal-regulated protein kinase activation is required for the anti-hypertrophic effect of atrial natriuretic factor in neonatal rat ventricular myocytes. J Biol Chem. 1999; 274(35): 24858–24864, doi: 10.1074/jbc.274.35.24858, indexed in Pubmed: 10455158.
15. Mathur A, Ma Z, Loskill P, et al. In vitro cardiac tissue models: Current status and future prospects. Adv Drug Deliv Rev. 2016; 96: 203–213, doi: 10.1016/j.addr.2015.09.011, indexed in Pubmed: 26428618.
16. Vozzi F, Logrand F, Cabiati M, et al. Biomimetic engineering of the cardiac tissue through processing, functionalization, and biological characterization of polyester urethanes. Biomed Mater. 2018; 13(5): 055006, doi: 10.1088/1748-605X/aaca5b, indexed in Pubmed: 29869614.
17. Ghosh LD, Jain A, Sundaresan NR, et al. Elucidating molecular events underlying topography mediated cardiomyogenesis of stem cells on 3D nanofibrous scaffolds. Mater Sci Eng C Mater Biol Appl. 2018; 88: 104–114, doi: 10.1016/j.msec.2018.03.012, indexed in Pubmed: 29636125.
18. Molkentin JD, Robbins J. With great power comes great responsibility: using mouse genetics to study cardiac hypertrophy and failure. J Mol Cell Cardiol. 2009; 46(2): 130–136, doi: 10.1016/j.yjmcc.2008.09.002, indexed in Pubmed: 18845155.
19. Breitenbach T, Lorenz K, Dandekar T. How to steer and control ERK and the ERK signaling cascade exemplified by looking at cardiac insufficiency. Int J Mol Sci. 2019; 20(9), doi: 10.3390/ijms20092179, indexed in Pubmed: 31052520.
20. Lloyd AC. Distinct functions for ERKs? J Biol. 2006; 5(5): 13, doi: 10.1186/jbiol46, indexed in Pubmed: 16879721.
21. Gerits N, Kostenko S, Moens U. In vivo functions of mitogen-activated protein kinases: conclusions from knock-in and knock-out mice. Transgenic Res. 2007; 16(3): 281–314, doi: 10.1007/s11248-006-9052-0, indexed in Pubmed: 17219248.
22. Wang Y. Mitogen-activated protein kinases in heart development and diseases. Circulation. 2007; 116(12): 1413–1423, doi: 10.1161//CIRCULATIONAHA.106.679589, indexed in Pubmed: 17875982.
23. Shaul YD, Seger R. The MEK/ERK cascade: from signaling specificity to diverse functions. Biochim Biophys Acta. 2007; 1773(8): 1213–1226, doi: 10.1016/j.bbamcr.2006.10.005, indexed in Pubmed: 17112607.
24. García-Niño WR, Correa F, Rodríguez-Barrena JI, et al. Cardioprotective kinase signaling to subsarcolemmal and interfibrillar mitochondria is mediated by caveolar structures. Basic Res Cardiol. 2017; 112(2): 15, doi: 10.1007/s00395-017-0607-4, indexed in Pubmed: 28160133.
25. Nomura S, Satoh M, Fujita T, et al. Cardiomyocyte gene programs encoding morphological and functional signatures in cardiac hypertrophy and failure. Nat Commun. 2018; 9(1): 4435, doi: 10.1038/s41467-018-06639-7, indexed in Pubmed: 30375404.
26. Lu YT, Li LZ, Yang YL, et al. Succinate induces aberrant mitochondrial fission in cardiomyocytes through GPR91 signaling. Cell Death Dis. 2018; 9(6): 672, doi: 10.1038/s41419-018-0708-5, indexed in Pubmed: 29867110.
27. Huang CY, Chen JY, Kuo CH, et al. Mitochondrial ROS-induced ERK1/2 activation and HSF2-mediated AT R upregulation are required for doxorubicin-induced cardiotoxicity. J Cell Physiol. 2018; 233(1): 463–475, doi: 10.1002/jcp.25905, indexed in Pubmed: 28295305.
28. Gartz M, Darlington A, Afzal MZ, et al. Exosomes exert cardioprotection in dystrophin-deficient cardiomyocytes via ERK1/2-

p38/MAPK signaling. Sci Rep. 2018; 8(1): 16519, doi: 10.1038/s41598-018-34879-6, indexed in Pubmed: 30410044.
29. Liu R, Molkentin JD. Regulation of cardiac hypertrophy and remodeling through the dual-specificity MAPK phosphatases (DUSPs). J Mol Cell Cardiol. 2016; 101: 44–49, doi: 10.1016/j.yjmcc.2016.08.018, indexed in Pubmed: 27575022.
30. Junttila MR, Li SP, Westermarck J. Phosphatase-mediated crosstalk between MAPK signaling pathways in the regulation of cell survival. FASEB J. 2008; 22(4): 954–965, doi: 10.1096/fj.06-7859rev, indexed in Pubmed: 18039929.
31. Hunter JJ, Tanaka N, Rockman HA, et al. Ventricular expression of a MLC-2v-ras fusion gene induces cardiac hypertrophy and selective diastolic dysfunction in transgenic mice. J Biol Chem. 1995; 270(39): 23173–23178, doi: 10.1074/jbc.270.39.23173, indexed in Pubmed: 7559464.
32. Zheng M, Dilly K, Dos Santos Cruz J, et al. Sarcoplasmic reticulum calcium defect in Ras-induced hypertrophic cardiomyopathy heart. Am J Physiol Heart Circ Physiol. 2004; 286(1): H424–H433, doi: 10.1152/ajpheart.00110.2003, indexed in Pubmed: 12969887.
33. Mitchell S, Ota A, Foster W, et al. Distinct gene expression profiles in adult mouse heart following targeted MAP kinase activation. Physiol Genomics. 2006; 25(1): 50–59, doi: 10.1152/physiolgenomics.00224.2005, indexed in Pubmed: 16368875.
34. Wei BR, Martin PL, Hoover SB, et al. Capacity for resolution of Ras-MAPK-initiated early pathogenic myocardial hypertrophy modeled in mice. Comp Med. 2011; 61(2): 109–118, indexed in Pubmed: 21535921.
35. Ramos-Kuri M, Rapti K, Mehel H, et al. Dominant negative Ras attenuates pathological ventricular remodeling in pressure overload cardiac hypertrophy. Biochim Biophys Acta. 2015; 1853(11 Pt A): 2870–2884, doi: 10.1016/j.bbamcr.2015.08.006, indexed in Pubmed: 26260012.
36. Ho PD, Zechner DK, He H, et al. The Raf-MEK-ERK cascade represents a common pathway for alteration of intracellular calcium by Ras and protein kinase C in cardiac myocytes. J Biol Chem. 1998; 273(34): 21730–21735, doi: 10.1074/jbc.273.34.21730, indexed in Pubmed: 9705309.
37. Rose BA, Force T, Wang Y. Mitogen-activated protein kinase signaling in the heart: angels versus demons in a heart-breaking tale. Physiol Rev. 2010; 90(4): 1507–1546, doi: 10.1152/physrev.00054.2009, indexed in Pubmed: 20959622.
38. Wu X, Simpson J, Hong JH, et al. MEK-ERK pathway modulation ameliorates disease phenotypes in a mouse model of Noonan syndrome associated with the Raf1(L613V) mutation. J Clin Invest. 2011; 121(3): 1009–1025, doi: 10.1172/JCI44929, indexed in Pubmed: 21339642.
39. Passariello CL, Martinez EC, Thakur H, et al. RSK3 is required for concentric myocyte hypertrophy in an activated Raf1 model for Noonan syndrome. J Mol Cell Cardiol. 2016; 93: 98–105, doi: 10.1016/j.yjmcc.2016.02.020, indexed in Pubmed: 26940993.
40. Harris IS, Zhang S, Treskov I, et al. Raf-1 kinase is required for cardiac hypertrophy and cardiomyocyte survival in response to pressure overload. Circulation. 2004; 110(6): 718–723, doi: 10.1161/01.CIR.0000138190.50127.6A, indexed in Pubmed: 15289381.
41. Yin JC, Platt MJ, Tian X, et al. Cellular interplay via cytokine hierarchy causes pathological cardiac hypertrophy in RAF1-mutant Noonan syndrome. Nat Commun. 2017; 8: 15518, doi: 10.1038/ncomms15518, indexed in Pubmed: 28548091.
42. Bueno OF, De Windt LJ, Tymitz KM, et al. The MEK1-ERK1/2 signaling pathway promotes compensated cardiac hypertrophy in transgenic mice. EMBO J. 2000; 19(23): 6341–6350, doi: 10.1093/emboj/19.23.6341, indexed in Pubmed: 11101507.
43. Mutlak M, Schlesinger-Laufer M, Haas T, et al. Extracellular signal-regulated kinase (ERK) activation preserves cardiac function in pressure overload induced hypertrophy. Int J Cardiol. 2018; 270: 204–213, doi: 10.1016/j.ijcard.2018.05.068, indexed in Pubmed: 29857938.
44. Jochmann S, Elkenani M, Mohamed BA, et al. Assessing the role of extracellular signal-regulated kinases 1 and 2 in volume overload-induced cardiac remodelling. ESC Heart Fail. 2019; 6(5): 1015–1026, doi: 10.1002/ehf2.12497, indexed in Pubmed: 31322843.
45. Smorodinsky-Atias K, Goshen-Lago T, Goldberg-Carp A, et al. Intrinsically active variants of Erk oncogenically transform cells and disclose unexpected autophosphorylation capability that is independent of TEY phosphorylation. Mol Biol Cell. 2016; 27(6): 1026–1039, doi: 10.1091/mbc.E15-07-0521, indexed in Pubmed: 26658610.
46. Lai S, Pelech S. Regulatory roles of conserved phosphorylation sites in the activation T-loop of the MAP kinase ERK1. Mol Biol Cell. 2016; 27(6): 1040–1050, doi: 10.1091/mbc.E15-07-0527, indexed in Pubmed: 26823016.
47. Ruppert C, Deiss K, Herrmann S, et al. Interference with ERK(Thr188) phosphorylation impairs pathological but not physiological cardiac hypertrophy. Proc Natl Acad Sci USA. 2013; 110(18): 7440–7445, doi: 10.1073/pnas.1221999110, indexed in Pubmed: 23589880.
48. Purcell NH, Wilkins BJ, York A, et al. Genetic inhibition of cardiac ERK1/2 promotes stress-induced apoptosis and heart failure but has no effect on hypertrophy in vivo. Proc Natl Acad Sci USA. 2007; 104(35): 14074–14079, doi: 10.1073/pnas.0610906104, indexed in Pubmed: 17709754.
49. Kehat I, Davis J, Tiburcy M, et al. Extracellular signal-regulated kinases 1 and 2 regulate the balance between eccentric and concentric cardiac growth. Circ Res. 2011; 108(2): 176–183, doi: 10.1161/CIRCRESAHA.110.231514, indexed in Pubmed: 21127295.
50. Ulm S, Liu W, Zi M, et al. Targeted deletion of ERK2 in cardiomyocytes attenuates hypertrophic response but provokes pathological stress induced cardiac dysfunction. J Mol Cell Cardiol. 2014; 72: 104–116, doi: 10.1016/j.yjmcc.2014.03.002, indexed in Pubmed: 24631771.
51. Maillet M, Purcell NH, Sargent MA, et al. DUSP6 (MKP3) null mice show enhanced ERK1/2 phosphorylation at baseline and increased myocyte proliferation in the heart affecting disease susceptibility. J Biol Chem. 2008; 283(45): 31246–31255, doi: 10.1074/jbc.M806085200, indexed in Pubmed: 18753132.
52. Missinato MA, Saydmohammed M, Zuppo DA, et al. Dusp6 attenuates Ras/MAPK signaling to limit zebrafish heart regeneration. Development. 2018; 145(5), doi: 10.1242/dev.157206, indexed in Pubmed: 29444893.
53. Liu R, van Berlo JH, York AJ, et al. DUSP8 regulates cardiac ventricular remodeling by altering ERK1/2 signaling. Circ Res. 2016; 119(2): 249–260, doi: 10.1161/CIRCRESAHA.115.308238, indexed in Pubmed: 27225478.
54. Owens DM, Keyse SM. Differential regulation of MAP kinase signalling by dual-specificity protein phosphatases. Oncogene. 2007; 26(22): 3203–3213, doi: 10.1038/sj.onc.1210412, indexed in Pubmed: 17496916.

55. Casar B, Crespo P. ERK signals: scaffolding scaffolds? Front Cell Dev Biol. 2016; 4: 49, doi: 10.3389/fcell.2016.00049, indexed in Pubmed: 27303664.
56. Song Y, Xu J, Li Y, et al. Cardiac ankyrin repeat protein attenuates cardiac hypertrophy by inhibition of ERK1/2 and TGF-β signaling pathways. PLoS One. 2012; 7(12): e50436, doi: 10.1371/journal.pone.0050436, indexed in Pubmed: 23227174.
57. Zhong L, Chiusa M, Cadar AG, et al. Targeted inhibition of ANKRD1 disrupts sarcomeric ERK-GATA4 signal transduction and abrogates phenylephrine-induced cardiomyocyte hypertrophy. Cardiovasc Res. 2015; 106(2): 261–271, doi: 10.1093/cvr/cvv108, indexed in Pubmed: 25770146.
58. Sbroggiò M, Carnevale D, Bertero A, et al. IQGAP1 regulates ERK1/2 and AKT signalling in the heart and sustains functional remodelling upon pressure overload. Cardiovasc Res. 2011; 91(3): 456–464, doi: 10.1093/cvr/cvr103, indexed in Pubmed: 21493702.
59. Kolch W. Coordinating ERK/MAPK signalling through scaffolds and inhibitors. Nat Rev Mol Cell Biol. 2005; 6(11): 827–837, doi: 10.1038/nrm1743, indexed in Pubmed: 16227978.
60. Himpel S, Tegge W, Frank R, et al. Specificity determinants of substrate recognition by the protein kinase DYRK1A. J Biol Chem. 2000; 275(4): 2431–2438, doi: 10.1074/jbc.275.4.2431, indexed in Pubmed: 10644696.
61. Liang Y, Sheikh F. Scaffold proteins regulating extracellular regulated kinase function in cardiac hypertrophy and disease. Front Pharmacol. 2016; 7: 37, doi: 10.3389/fphar.2016.00037, indexed in Pubmed: 26973524.
62. Tarone G, Sbroggiò M, Brancaccio M. Key role of ERK1/2 molecular scaffolds in heart pathology. Cell Mol Life Sci. 2013; 70(21): 4047–4054, doi: 10.1007/s00018-013-1321-5, indexed in Pubmed: 23532408.
63. Zong J, Zhang Dp, Zhou H, et al. Baicalein protects against cardiac hypertrophy through blocking MEK-ERK1/2 signaling. J Cell Biochem. 2013; 114(5): 1058–1065, doi: 10.1002/jcb.24445, indexed in Pubmed: 23225340.
64. Xiong X, Yang X, Duan L, et al. Traditional Chinese medicine suppresses left ventricular hypertrophy by targeting extracellular signal-regulated kinases signaling pathway in spontaneously hypertensive rats. Sci Rep. 2017; 7: 42965, doi: 10.1038/srep42965, indexed in Pubmed: 28225023.
65. Sun S, Kee HJ, Jin Li, et al. Gentisic acid attenuates pressure overload-induced cardiac hypertrophy and fibrosis in mice through inhibition of the ERK1/2 pathway. J Cell Mol Med. 2018; 22(12): 5964–5977, doi: 10.1111/jcmm.13869, indexed in Pubmed: 30256522.
66. Li C, Chen Z, Yang H, et al. Selumetinib, an Oral Anti-Neoplastic Drug, May Attenuate Cardiac Hypertrophy via Targeting the ERK Pathway. PLoS One. 2016; 11(7): e0159079, doi: 10.1371/journal.pone.0159079, indexed in Pubmed: 27438013.
67. Sala V, Gallo S, Gatti S, et al. Cardiac concentric hypertrophy promoted by activated Met receptor is mitigated in vivo by inhibition of Erk1,2 signalling with Pimasertib. J Mol Cell Cardiol. 2016; 93: 84–97, doi: 10.1016/j.yjmcc.2016.02.017, indexed in Pubmed: 26924269.
68. Kodama H, Fukuda K, Pan J, et al. Significance of ERK cascade compared with JAK/STAT and PI3-K pathway in gp130-mediated cardiac hypertrophy. Am J Physiol Heart Circ Physiol. 2000; 279(4): H1635–H1644, doi: 10.1152/ajpheart.2000.279.4.H1635, indexed in Pubmed: 11009450.
69. Yue TL, Gu JL, Wang C, et al. Extracellular signal-regulated kinase plays an essential role in hypertrophic agonists, endothelin-1 and phenylephrine-induced cardiomyocyte hypertrophy. J Biol Chem. 2000; 275(48): 37895–37901, doi: 10.1074/jbc.M007037200, indexed in Pubmed: 10984495.
70. Lee CY, Lee J, Seo HH, et al. TAK733 attenuates adrenergic receptor-mediated cardiomyocyte hypertrophy via inhibiting Erk-Thr188 phosphorylation. Clin Hemorheol Microcirc. 2019; 72(2): 179–187, doi: 10.3233/CH-180476, indexed in Pubmed: 30714951.
71. Woodard GE, Jardín I, Berna-Erro A, et al. Regulators of G-protein-signaling proteins: negative modulators of G-protein-coupled receptor signaling. Int Rev Cell Mol Biol. 2015; 317: 97–183, doi: 10.1016/bs.ircmb.2015.02.001, indexed in Pubmed: 26008785.
72. Liu Yu, Huang He, Zhang Y, et al. Regulator of G protein signaling 3 protects against cardiac hypertrophy in mice. J Cell Biochem. 2014; 115(5): 977–986, doi: 10.1002/jcb.24741, indexed in Pubmed: 24375609.
73. Li H, He C, Feng J, et al. Regulator of G protein signaling 5 protects against cardiac hypertrophy and fibrosis during biomechanical stress of pressure overload. Proc Natl Acad Sci USA. 2010; 107(31): 13818–13823, doi: 10.1073/pnas.1008397107, indexed in Pubmed: 20643937.
74. Miao R, Lu Y, Xing X, et al. Regulator of G-protein signaling 10 negatively regulates cardiac remodeling by blocking mitogen-activated protein kinase-extracellular signal-regulated protein kinase 1/2 signaling. Hypertension. 2016; 67(1): 86–98, doi: 10.1161/HYPERTENSIONAHA.115.05957, indexed in Pubmed: 26573707.
75. Huang J, Chen L, Yao Y, et al. Pivotal role of regulator of G-protein signaling 12 in pathological cardiac hypertrophy. Hypertension. 2016; 67(6): 1228–1236, doi: 10.1161/HYPERTENSIONAHA.115.06877, indexed in Pubmed: 27091895.
76. Li Y, Tang XH, Li XH, et al. Regulator of G protein signalling 14 attenuates cardiac remodelling through the MEK-ERK1/2 signalling pathway. Basic Res Cardiol. 2016; 111(4): 47, doi: 10.1007/s00395-016-0566-1, indexed in Pubmed: 27298141.

VIA MEDICA

RESEARCH LETTER

Cardiology Journal
2021, Vol. 28, No. 3, 483–485
DOI: 10.5603/CJ.a2021.0033

ISSN 1897–5593
eISSN 1898–018X

Monitoring of QTc interval in patients with COVID-19. First experience with a portable ECG-recording device

María Abellas-Sequeiros[1], Cristina Lozano-Granero[1], Cristina García-Sebastián[1], Eduardo Franco-Díez[1], Antonio Hernández-Madrid[1], Javier Moreno-Planas[1], Jaime Masjuan-Vallejo[2], Marcelo Sanmartín-Fernández[1], Jose Luis Zamorano-Gómez[1]

[1]Cardiology Department, Hospital Ramón y Cajal, Madrid, Spain
[2]Neurology Deapartment, Hospital Ramón y Cajal, Madrid, Spain

This article is accompanied by the editorial on page 358

Treatment of coronavirus disease 2019 (COVID-19), as a new entity lacking sufficient evidence-based pharmacotherapy, was initially based in drugs with in-vitro activity against severe acute respiratory syndrome coronavirus 2 (SARS-CoV-2) such as hydroxychloroquine, azithromycin and lopinavir/ritonavir. Each of these drugs is known to prolong QT interval [1–3]. This phenomenon is of utmost importance, as it is associated with early after-depolarizations, which can generate short-coupled premature action potentials that lead to ventricular fibrillation and sudden cardiac death [4]. Therefore, it seems mandatory to implement monitoring systems, in a scenario where the use of portable electrocardiographic-recording devices could be useful.

This is an observational prospective study in a tertiary hospital. Patients hospitalized for confirmed SARS-CoV-2 pneumonia and receiving specific treatment with either hydroxychloroquine, azithromycin or lopinavir/ritonavir (or combination) were included. Patients were classified into three groups: group 1 received one drug, group 2 received a combination of two drugs and group 3 received a combination of three drugs. Patients in which the electrocardiogram (ECG) tracing obtained with the mobile ECG recording device was of poor quality were excluded from the study.

Clinical information and 12-lead ECG recordings were collected. Baseline QT interval was measured in limb leads using the admission-ECG. The patients received pharmacological treatment according to center-specific guidelines. Verbal informed consent was obtained from patients and approval from the ethics committee of our center was received. A Kardia-Mobile 6L® (AliveCor, Inc., Mountain View, California) was used for ECG monitoring. This device, approved by the Food and Drug Administration for QT interval monitoring, consists of a lightweight 3-electrode hardware capable of registering a 6-lead ECG and a smartphone software application. ECGs were recorded periodically with the physicians' criteria. A subset of patients at early discharge were offered one device to daily self-monitoring. Corrected QT (QTc) interval was calculated using the Bazett formula. Primary outcome was to describe the usefulness of telemonitoring in COVID-19 patients for management of QT-prolonging drugs by assessing the proportion of patients with significant ECG changes that imply a change in management. Secondary outcome was to evaluate the inter-observer reproducibility of QT interval quantification using this gadget.

The Shapiro-Wilk test was used to assess normality in continuous variables. Continuous variables were compared using the Wilcoxon or Kruskal-Wallis tests, as appropriate. The Wilcoxon signed-rank test was used for paired measurements. Bilateral p values < 0.05 were considered statistically significant. To test inter-observer vari-

Address for correspondence: Cristina Lozano-Granero, MD, Cardiology Department, Hospital Ramón y Cajal, Ctra, Colmenar Viejo, km 9100, 28034, Madrid, Spain, tel: +34 678-69-00-25, e-mail: cristina.lozano@hotmail.es

Received: 11.09.2020 Accepted: 2.12.2020

Table 1. Clinical characteristics and QTc interval evolution in the three treatment groups.

	Group 1 (one drug) N = 9 (13.0%)	Group 2 (two drugs) N = 37 (53.6%)	Group 3 (three drugs) N = 23 (33.3%)	P
Clinical characteristics				
Age [years]	55.0 ± 18.3	66.0 ± 16.2	58.0 ± 15.8	0.248
Male sex	6 (66.7%)	25 (67.6%)	18 (78.3%)	0.643
Dyslipidemia	5 (55.6%)	9 (24.3%)	7 (30.4%)	0.749
Diabetes	7 (77.8%)	4 (10.8%)	5 (21.7%)	0.525
Hypertension	3 (33.3%)	16 (43.2%)	8 (34.8%)	0.387
Previous cardiopathy	6 (66.7%)	11 (29.7%)	3 (13.0%)	0.305
COPD	7 (77.8%)	6 (16.2%)	1 (8.7%)	0.679
Atrial fibrillation	1 (11.1%)	3 (8.1%)	0	0.297
Mortality	0	4 (10.8%)	0	0.159
QTc interval				
QTc interval at admission [ms]	340.0 [320.0–350.0]	408.0 [377.2–423.5]	394.0 [373.0–422.5]	0.039
Maximal QTc interval [ms]	418.0 [384.5–460.5]	426.0 [412.0–450.0]	435.0 [405.0–450.0]	0.085
QTc > 450 ms	3 (33.3%)	9 (24.3%)	6 (26.1%)	0.859
ΔQTc > 60 ms	1 (11.1%)	4 (15.4%)	3 (9.7%)	0.818

Qualitative variables are shown as number (percentage); quantitative variables are shown as mean ± standard deviation or median [interquartile range], as appropriate; COPD — chronic obstructive pulmonary disease

ability of QTc measurements, 120 random ECGs were analysed by two independent cardiologists. Intraclass correlation coefficient was obtained (two-way random, average measures, absolute agreement). Statistical analysis was performed using SPSS (IBM Inc., Armonk, NY).

A total of 70 patients fulfilled criteria. Tracings obtained with the portable device were of sufficient quality to provide an accurate QT interval measurement in 69 of them (98.6%). Mean follow-up was 6.2 ± 8.4 days. Characteristics of the different groups are shown in Table 1. An increase in QTc interval was observed in all treatment groups, being non-significant in group 1 (group 1: 340 [320.0–350.0] vs. 418 [384.5–460.5], p = 0.109). Significance was reached in both group 2 (408 [377.2–423.5] vs. 426 [412.0–450.0], p = 0.002) and group 3 (394 [373.0–422.5] vs. 435 [405.0–450.0], p = 0.001). Eighteen (25.7%) patients developed a QTc interval > 450 ms. These patients were significantly older (67.5 ± 14.9 vs. 55.0 ± 16.0 years, p = 0.004) and were more likely diagnosed of chronic obstructive pulmonary disease (33.3% vs. 5.9%, p = 0.009) and previous cardiopathy (50% vs. 13.7%, p = 0.007). Taking into consideration the information given by the ECG monitoring devices, physicians adopted a different approach in the management of 12 (17.4%) patients. Treatment was modified in 9 (13%) patients because of prolongation of the QTc interval (1 of them also developed first degree atrioventricular block, with a PR interval up to 280 ms); 2 (2.9%) patients required monitoring intensification (1 of them because of first degree atrioventricular block and the other because of prolongation of the QTc interval) and anticoagulation was started in one patient because of atrial fibrillation diagnosis.

The subgroup of 16 patients who were given a recorder to continue daily monitoring experienced also significant prolongation of the QTc interval (381.0 [372.0–401.5] at admission vs. 424.0 [406.0–436.7] at peak, p = 0.002), with mean time to reach the maximum QTc: 2 ± 1.8 days). By the end of the monitoring phase, QTc intervals were shorter than those at admission (381.0 [372.0–401.5] vs. 350.0 [334.2–369.0]; p = 0.019).

Inter-observer intraclass correlation coefficient was 0.824, 95% confidence interval 0.733––0.882 (good agreement).

Herein, is presented one of the first series of patients both hospitalized [5, 6] and discharged with COVID-19 with electrocardiographic surveillance using a portable ECG recorder [7]. The device proved to be useful for ECG monitoring in these patients, detecting ECG anomalies of enough importance to promote a change in management in

17.4% of them. These anomalies consisted not only in QTc interval prolongation, but also in PR interval prolongation and atrial arrhythmias. These small, light gadgets allow physicians to quickly perform an ECG to a high number of patients, including the monitoring of outpatients. These characteristics were determinant to ensure safe management in the first wave of the COVID-19 pandemic, when an enormous number of patients overtook available resources.

The intraclass correlation coefficient points a good agreement in the measurements of QTc interval using these portable recorders, supporting the solidness of this handheld device. Once confirmed the value and the reliability of these devices, ECG portable recorders are called to be part of the workaday armamentarium in our hospitals.

Conflict of interest: None declared

References

1. Ray WA, Murray KT, Hall K, et al. Azithromycin and the risk of cardiovascular death. N Engl J Med. 2012; 366(20): 1881–1890, doi: 10.1056/NEJMoa1003833, indexed in Pubmed: 22591294.
2. Chen CY, Wang FL, Lin CC. Chronic hydroxychloroquine use associated with QT prolongation and refractory ventricular arrhythmia. Clin Toxicol (Phila). 2006; 44(2): 173–175, doi: 10.1080/15563650500514558, indexed in Pubmed: 16615675.
3. Anson B, Weaver J, Ackerman M, et al. Blockade of HERG channels by HIV protease inhibitors. Lancet. 2005; 365(9460): 682–686, doi: 10.1016/s0140-6736(05)70936-3.
4. Straus SM, Kors JA, De Bruin ML, et al. Prolonged QTc interval and risk of sudden cardiac death in a population of older adults. J Am Coll Cardiol. 2006; 47(2): 362–367, doi: 10.1016/j.jacc.2005.08.067, indexed in Pubmed: 16412861.
5. Chang D, Saleh M, Gabriels J, et al. Inpatient use of ambulatory telemetry monitors for COVID-19 patients treated with hydroxychloroquine and/or azithromycin. J Am Coll Cardiol. 2020; 75(23): 2992–2993, doi: 10.1016/j.jacc.2020.04.032, indexed in Pubmed: 32330546.
6. Guerrero LR, Ongay AG, Álvarez ÁC, et al. Protocolo de manejo hospitalario de alteraciones electrocardiográficas en pacientes con COVID-19 con un sistema portátil vinculado a smartphone. REC: CardioClinics. 2020; 55(3): 192–195, doi: 10.1016/j.rccl.2020.05.006.
7. Strik M, Caillol T, Ramirez FD, et al. Validating QT-interval measurement using the apple watch ECG to enable remote monitoring during the COVID-19 pandemic. Circulation. 2020; 142(4): 416–418, doi: 10.1161/CIRCULATIONAHA.120.048253, indexed in Pubmed: 32478565.

VIA MEDICA

RESEARCH LETTER

Cardiology Journal
2021, Vol. 28, No. 3, 486–488
DOI: 10.5603/CJ.a2020.0076

ISSN 1897–5593
eISSN 1898–018X

Assessment of anti-dislodgment capability for contemporary drug eluting stents

Yicong Ye*, Xiliang Zhao*, Yong Zeng

Beijing Institute of Heart, Lung and Blood Vessel Diseases, Beijing Anzhen Hospital, Capital Medical University, Beijing, China

Stent dislodgment is one catastrophic complication of percutaneous coronary intervention (PCI), especially in tortuous and calcified lesions. The anti-dislodgment capability of different stent platforms may be varied due to different designs. However, data on the anti-dislodgment capability of contemporary stent platforms are still unavailable. Thus, the aim herein, was to compare the anti-dislodgment capability of different stent platforms with a bench test.

Three types of stent platforms (n = 3 for each stent platform) were included in the bench test, including XIENCE Xpedition (3.0 × 23 mm, Abbott), Resolute Integrity (3.0 × 22 mm, Medtronic), Synergy (3.0 × 24 mm, Boston Scientific). The anti-dislodgment capability was assessed by Instron 5943 (Boston, US). Appropriate stent holder was determined according to the profile measurement of each stent (Inner diameter of stent holder = = measured stent profile – 2 × structs thickness). The force was recorded during the pullback process with the speed of 50.8 mm/min. Maximal dislodgement force was defined as the first peak value of the force record in 5 mm pullback. Operators were blinded to the brands of the stent platforms. Study design was in accordance with two standard guides from China (standard guide for measuring securement of balloon expandable vascular stent mounted on delivery system, YY/T 0807-2010, https://www.chinesestandard.net/China/Chinese.aspx/YYT0807-2010; Cardiovascular implants Endovascular devices. Part 2: Vascular stents, YY/T 0663.2-2016, https://www.chinesestandard.net/China/Chinese.aspx/YYT0663.2-2016). Data were presented as median [interquartile range]. Group comparisons were performed using the Kruskal-Wallis test with a post-hoc test. All statistical tests were performed using GraphPad Prism version 5.00 (GraphPad Software, San Diego California USA) in a two-sided manner. Values of $p < 0.05$ were considered statistically significant.

The recorded force of each stent during the pullback process was presented in Figure 1A–C. The median of maximal dislodgement force for 3 stent platforms was as follows: XIENCE Xpedition group: 10.31 N; Resolute Integrity group: 6.93 N; Synergy group: 6.19 N. There were significant differences among the three groups ($p = 0.027$). Group comparisons indicated that XIENCE Xpedition had higher maximal dislodgement forces than the Synergy group (10.31 [9.76–10.33] N vs. 6.19 [5.48-–6.50] N, $p = 0.022$), while there was no difference between the Resolute Integrity and Synergy groups (6.93 [6.64–7.00] N vs. 6.19 [5.48–6.50] N, $p = 0.539$), or between Resolute Integrity and XIENCE Xpedition (6.93 [6.64–7.00] N vs. 10.31 [9.76–10.33] N, $p = 0.539$) (Fig. 1D).

Stent dislodgment is an uncommon complication during PCI which is primarily due to calcification and tortuosity of the lesion. The prevalence of stent dislodgement was up to ~8% in the early 1990s [1]. Fortunately, the rate of stent dislodgement has significantly decreased which may be explained by the increased operator experience and advancement in stent technology [2]. Several parameters of stent platform including profile,

Address for correspondence: Dr. Yong Zeng, Beijing Institute of Heart, Lung and Blood Vessel Diseases, Beijing Anzhen Hospital, Capital Medical University, No. 2, Anzhen Road, Chaoyan District, 100029, Beijing, China, tel: 86-10-64456159, fax: 86-10-64456159, e-mail: anzhenzy@163.com

Received: 27.02.2020 Accepted: 16.05.2020

**Yicong Ye and Xiliang Zhao contributed equally to the study.*

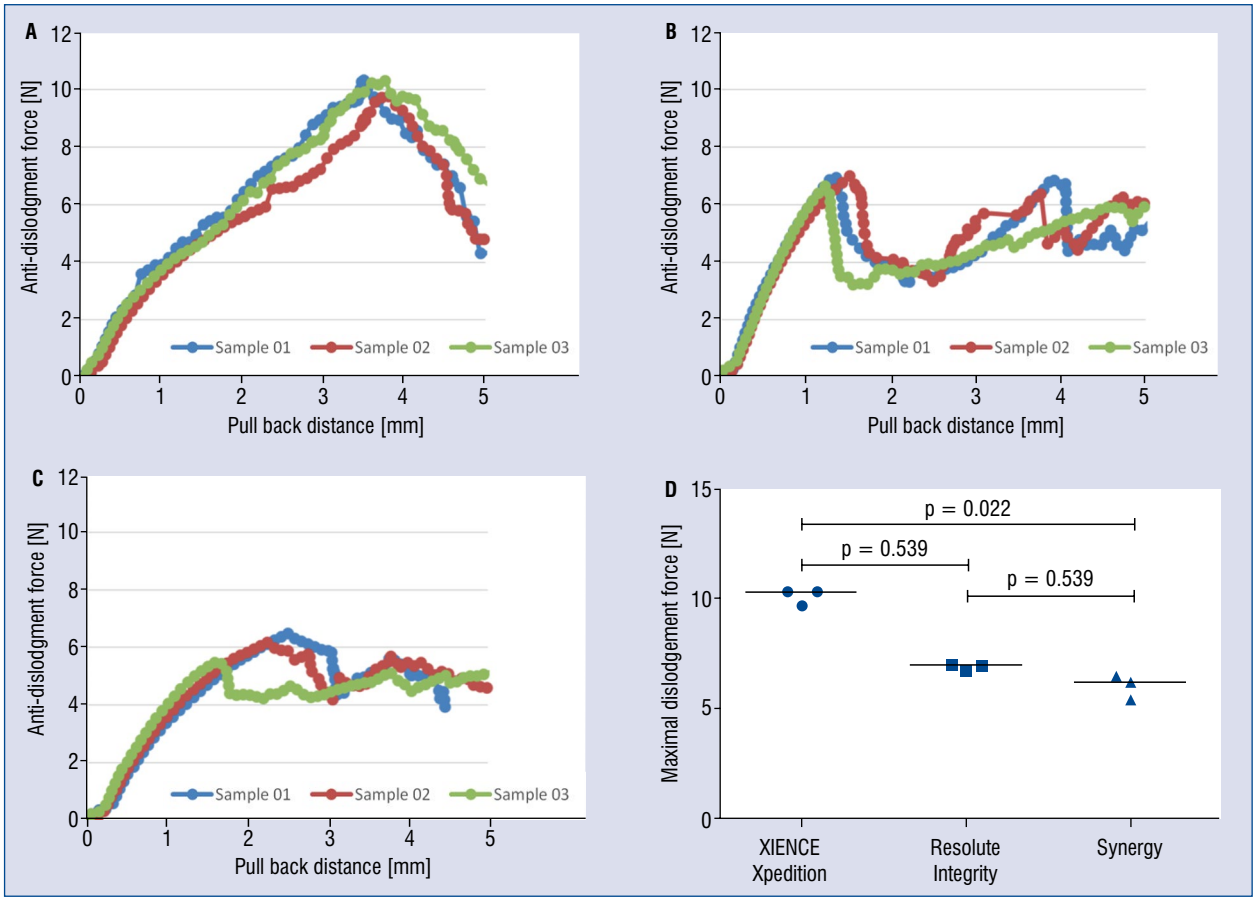

Figure 1. The values of force (N) during the pullback process for different drug eluting stents (with the speed of 50.8 mm/min). The force curves recorded in 5 mm pullback for XIENCE Xpedition (**A**), Resolute Integrity (**B**), and Synergy (**C**); **D.** Comparison of maximal dislodgement force among three drug eluting stents.

flexibility, and adhesion are associated with risk of stent dislodgment. Data on the profiles of commercial stents are available and some studies have provided a numerical approach to assess the stent flexibility [3]. However, so far there are no published data evaluating the adhesion of stent platforms. The present study is the first study to assess stent adhesion with numerical data, which is one of the major components of anti-dislodgment capability. There are some potential explanations for the difference in maximal dislodgment force among three types of drug eluting stents (DES). First, stent platforms vary among different DES. XIENCE Xpedition and Resolute integrity stents use a cobalt chromium platform with MULTI-LINK and continuous sinusoid designs, respectively. On the other hand, Synergy uses the platinum chromium platform with a different number of connectors (e.g. 4 connectors on proximal end and 2 connectors throughout body for 2.50–3.50 mm stents). Second, the stent crimping technique is a key determinant for maximal dislodgment force. However, stent crimping techniques for different DES are patented and are not available to the public. The current study has several limitations. First, the sample size was small. Second, an *in-vitro* study could not provide the same environment as in the coronary arteries. Finally, the latest generation of DES such as XIENCE Sierra or Resolute Onyx were not used.

Current bench test found that anti-dislodgment capability varied among the stent platforms and XIENCE Xpedition may be higher than Resolute Integrity and Synergy. Further study is needed to verify this preliminary result.

Acknowledgements

This study was supported by The National Key research and development Program (2018YFC1312801).

Conflict of interest: None declared

References

1. Schatz RA, Baim DS, Leon M, et al. Clinical experience with the Palmaz-Schatz coronary stent. Initial results of a multicenter study. Circulation. 1991; 83(1): 148–161, doi: 10.1161/01.cir.83.1.148, indexed in Pubmed: 1984878.
2. Kwan TW, Chaudhry M, Huang Y, et al. Approaches for dislo-dged stent retrieval during transradial percutaneous coronary interventions. Catheter Cardiovasc Interv. 2013; 81(6): E245–E249, doi: 10.1002/ccd.24483, indexed in Pubmed: 22581524.
3. Petrini L, Migliavacca F, Auricchio F, et al. Numerical investigation of the intravascular coronary stent flexibility. J Biomech. 2004; 37(4): 495–501, doi: 10.1016/j.jbiomech.2003.09.002, indexed in Pubmed: 14996561.

VIA MEDICA

RESEARCH LETTER

Cardiology Journal
2021, Vol. 28, No. 3, 489–491
DOI: 10.5603/CJ.a2021.0039

ISSN 1897–5593
eISSN 1898–018X

Conscious sedation and local anesthesia for transcarotid transcatheter aortic valve implantation: Why not?

Damian Hudziak[1], Radosław Gocoł[1], Konrad Mendrala[2], Wojciech Wojakowski[3], Grzegorz Smolka[3], Radosław Parma[3], Maciej Kaźmierski[3], Tomasz Darocha[2]

[1]Department of Cardiac Surgery, Medical University of Silesia, Katowice, Poland
[2]Department of Anesthesiology and Intensive Care, Medical University of Silesia, Katowice, Poland
[3]Division of Cardiology and Structural Heart Diseases, Medical University of Silesia, Katowice, Poland

Since Modine et al. [1] performed the first transcarotid (TC) transcatheter aortic valve implantation (TAVI) in 2009, it has become a safe and reproducible alternative for patients not suitable for transfemoral access (TF) [1, 2]. Both self-expandable and balloon-expandable transcatheter valves can be implanted through the common carotid artery. The majority of TC-TAVI are performed under general anesthesia [3], although a minimally invasive strategy (MIS) with local anesthesia and conscious sedation has also been reported [4]. Presented herein, are 2 cases of TC-TAVI implanted through the left common carotid artery (LCCA) under regional anesthesia at the Upper-Silesian Medical Center of the Medical University of Silesia in Katowice, Poland.

Patient 1. An 81-year-old female, who was not eligible for aortic valve surgery because of frailty syndrome and cachexia with low body mass index (19 kg/m^2). The patient presented with decompensated heart failure (New York heart Association [NYHA] class III). The perioperative risk was estimated at 4.6% and 5.7% (EuroSCORE and Society of Thoracic Surgeons [STS], respectively). Transthoracic echocardiography (TTE) revealed severe aortic stenosis with aortic valve area (AVA) 0.65 cm^2, Vmax 4.1 m/s, and mean gradient (PGmean) 40 mmHg. Left ventricular ejection fraction (LVEF) was 65%, and coronary angiography showed no significant stenosis. As multislice computed tomography (MSCT) imaging (Fig. 1A–C) revealed massive calcifications and critical stenosis of both iliac arteries, the patient was selected for TC-TAVI. The LCCA dimension was 6.1 mm, and there was no significant stenosis.

Patient 2. A 75-year-old male with severe aortic stenosis (AVA 0.7 cm^2, Vmax 3.1 m/s, PGmean 28 mmHg), reduced to 35% LVEF, heart failure (NYHA III) and numerous comorbidities (history of several myocardial infarctions, multiple percutaneous coronary intervention with stent implantation, atrial fibrillation, pacemaker, left internal carotid artery occlusion, critical right internal carotid artery stenosis, type II diabetes mellitus, renal failure, hypertension and history of abdominal aorta aneurysm excision) was scheduled for the TAVI procedure via the LCCA (diameter 6.7 mm). The decision was made by the Heart Team based on MSCT (Fig. 1D–F). The STS score was 11.8% and EuroSCORE 36.4%.

The MSCT images analysis, TC-TAVI surgery eligible criteria, intraoperative monitoring, and operation techniques did not differ from those reported in previous studies [5]. Both procedures were performed by a multidisciplinary specialist team in a hybrid operating room. No premedication was administered prior to the surgery. Basic parameters such as electrocardiogram, pulse oximetry, respiratory rate, invasive blood pressure monitoring were acquired with a Philips IntelliVue monitor. Oxygen was supplemented through a nasal cannula. Preemptive multimodal analgesia with intravenous oxycodone (2 mg), paracetamol (1 g) and metamizole (1 g) was administered before regional anesthesia. The large venous access was

Address for correspondence: Damian Hudziak, MD, PhD, Department of Cardiac Surgery, Medical University of Silesia, ul. Ziołowa 47, 40–635 Katowice, Poland, tel: +48 507037783, e-mail: damhud@gmail.com

Received: 29.10.2020 Accepted: 28.02.2021

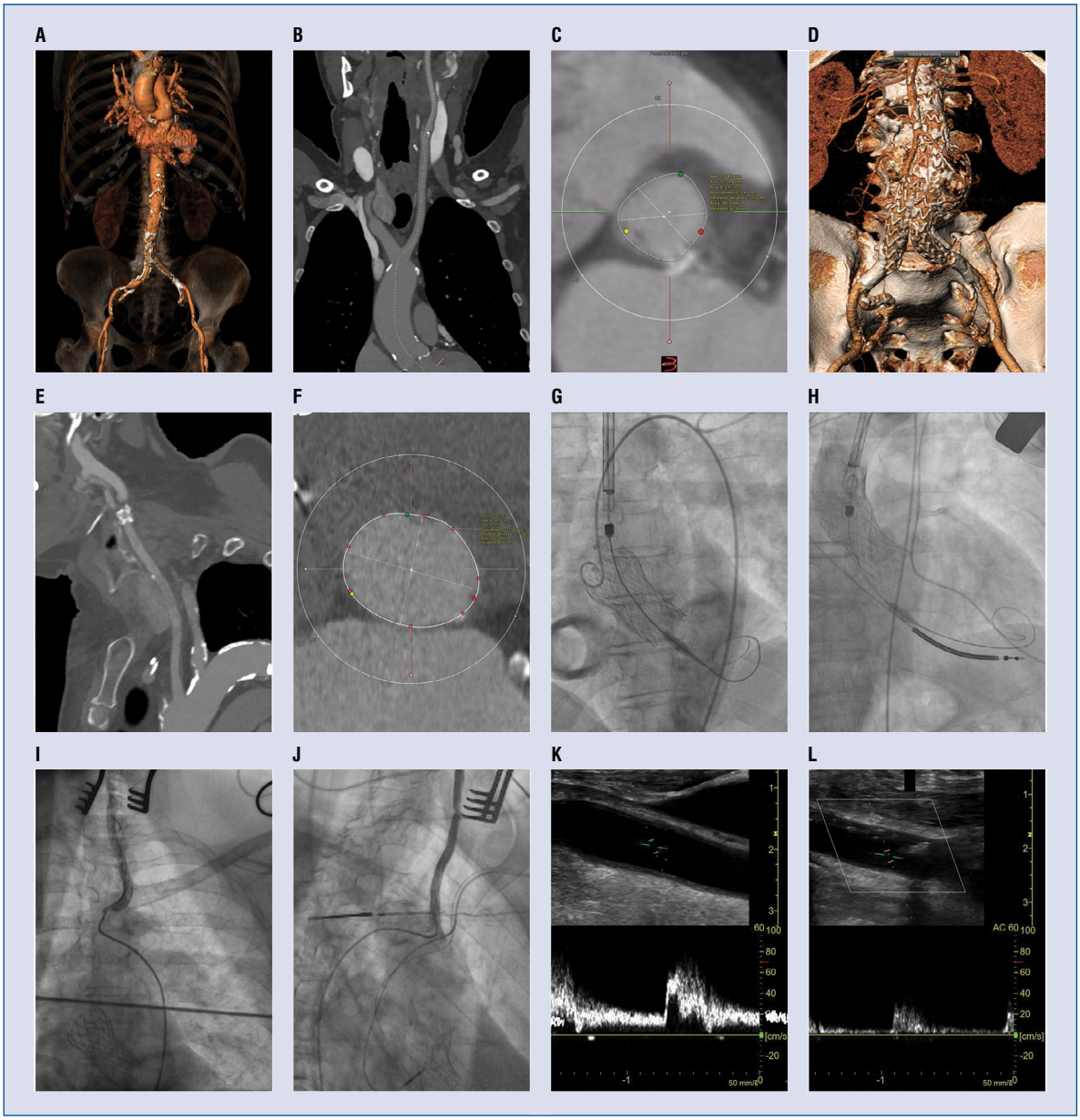

Figure 1. Periprocedural imaging. **A.** Three-dimensional (3D) reconstruction image of the multislice computed tomography (MSCT) of the iliofemoral arteries and abdominal aorta in Patient 1; **B.** Image of the MSCT of the left carotid artery and aortic arch in Patient 1; **C.** Image of the MSCT dimensions of the aortic annulus in Patient 1; **D.** 3D reconstruction image of the MSCT of the iliofemoral arteries and abdominal aorta in Patient 2; **E.** Image of the MSCT dimensions of the aortic annulus in Patient 2; **F.** Image of the MSCT of the left carotid artery and aortic arch in Patient 2; **G.** Implanted aortic valve prosthesis in Patient 1; **H.** Image of the implanted aortic valve prosthesis in Patient 2; **I.** Image of the control left common carotid artery (LCCA) arteriography in Patient 1; **J.** Image of the control arteriography of the LCCA in Patient 2; **K.** Image of the control Doppler ultrasonography of the LCCA in Patient 1; **L.** Image of the control Doppler ultrasonography of the LCCA in Patient 2.

obtained under the ultrasound guidance. A Pajunk SonoTAP needle was inserted under the posterior border of the sternocleidomastoid muscle targeting the superficial cervical plexus and 20 mL of 0.5% Ropivacaine. The quality of the block was evaluated with the pinprick sensation test.

Both procedures were successful, and no major complications occurred during the surgery. Self-expanding valves (Evolut R 26 and Evolut R 34; Medtronic, Inc., Minneapolis, Minnesota, USA) were implanted without pre- or post-dilatation. Both procedures' duration was similar (60 and

55 min, respectively) (Fig. 1G, H). No neurological incidents were observed in the perioperative period. The values of cerebral oximetry acquired during the MIS were comparable to those obtained during procedures under general anesthesia. Moreover, hemodynamic profiles of patients were stable, and no inotropic support was required. A control carotid angiography (Fig. 1I, J) showed normal flow in the LCCA of both patients. The postoperative renal function was preserved at normal levels (estimated glomerular filtration rate 78 and 59 mL/min/1.73 m^2, respectively). One patient had a postoperative complication unrelated to the carotid access. This concerned major bleeding per the Valve Academic Research Consortium-2 consensus from the femoral artery after the removal of the vascular sheath used for the pig-tail catheter [6]. The bleeding site was managed surgically, and the patient received two units of packed red blood cells. A TTE assessment confirmed the correct function of the implanted valves (PGmean 5.2 mmHg and 7 mmHg, Vmax 1.8 m/s and 1.9 m/s), no paravalvular leak and no LVEF reduction in both patients. A Doppler ultrasound (Fig. 1K, L) showed the normal flow through the LCCA (low values of maximum systolic velocity and end-diastolic velocity). The patients were discharged home after 8 and 6 days, respectively, with improved physical status (NYHA I and II, respectively).

To this day, at the documented hospital, the vast majority of TC-TAVI (37 of 39) have been performed under general anesthesia with endotracheal intubation. This seems to be comparable with the experience of other centers [3, 4]. In contrast to TF-TAVI, the TC-TAVI technique improves the implantation precision due to the short distance between the system insertion site and the aortic valve but requires the patient's immobility. Thus, while general anesthesia eliminates the patient's involuntary movements, it is the method of choice for uncooperative patients. The decision in the present cases to perform TC-TAVI under conscious sedation and local anesthesia was based on two reasons: in the cachectic Patient 1, there was a risk of the endotracheal tube misplacement in the trachea and making the LCCA difficult to be exposed. Additionally, in Patient 2 with diffuse carotid arteriosclerosis, MIS allowed for conscious cerebral function monitoring during the procedure.

There are no clear guidelines concerning the anesthesia to be used in TC-TAVI. According to Azmoun et al. [7], MIS reduces respiratory complications in older patients with frailty syndrome. In addition, although Debry et al. [4] showed a reduction of cerebrovascular incidents with MIS, this was not confirmed by the General Anesthesia versus Local Anesthesia for carotid surgery (GALA) study [8]. General anesthesia with low surgical impulsion can develop into hypotonia, increased demand for vasoactive agents, and consequently worsen kidney function, whilst patients under local anesthesia have an increased risk of hypoventilation and aspiration [9].

Our initial observations of TC-TAVI procedures performed under conscious sedation and local anesthesia confirm that it can be safely performed by a well-trained Heart Team and an experienced anesthesiologist.

Conflict of interest: None declared

References

1. Modine T, Sudre A, Delhaye C, et al. Transcutaneous aortic valve implantation using the left carotid access: feasibility and early clinical outcomes. Ann Thorac Surg. 2012; 93(5): 1489–1494, doi: 10.1016/j.athoracsur.2012.01.030, indexed in Pubmed: 22464036.
2. Watanabe M, Takahashi S, Yamaoka H, et al. Comparison of transcarotid vs. Transfemoral transcatheter aortic valve implantation. Circ J. 2018; 82(10): 2518–2522, doi: 10.1253/circj.CJ-18-0530, indexed in Pubmed: 30068794.
3. Wee IJ, Stonier T, Harrison M, et al. Transcarotid transcatheter aortic valve implantation: A systematic review. J Cardiol. 2018; 71(6): 525–533, doi: 10.1016/j.jjcc.2018.01.010, indexed in Pubmed: 29499894.
4. Debry N, Delhaye C, Azmoun A, et al. Transcarotid transcatheter aortic valve replacement: general or local anesthesia. JACC Cardiovasc Interv. 2016; 9(20): 2113–2120, doi: 10.1016/j.jcin.2016.08.013, indexed in Pubmed: 27765304.
5. Hudziak D, Nowak A, Gocoł R, et al. Prospective registry on cerebral oximetry-guided transcarotid TAVI in patients with moderate-high risk aortic stenosis. Minerva Cardioangiol. 2019; 67(1): 11–18, doi: 10.23736/S0026-4725.18.04799-0, indexed in Pubmed: 30226033.
6. Kappetein AP, Head SJ, Généreux P, et al. Updated standardized endpoint definitions for transcatheter aortic valve implantation: the Valve Academic Research Consortium-2 consensus document (VARC-2). Eur J Cardiothorac Surg. 2012; 42(5): S45–S60, doi: 10.1093/ejcts/ezs533, indexed in Pubmed: 23026738.
7. Azmoun A, Amabile N, Ramadan R, et al. Transcatheter aortic valve implantation through carotid artery access under local anaesthesia. Eur J Cardiothorac Surg. 2014; 46(4): 693–698, doi: 10.1093/ejcts/ezt619, indexed in Pubmed: 24431170.
8. General anaesthesia versus local anaesthesia for carotid surgery (GALA): a multicentre, randomised controlled trial. Lancet. 2008; 372(9656): 2132–2142, doi: 10.1016/s0140-6736(08)61699-2.
9. Mayr NP, Michel J, Bleiziffer S, et al. Sedation or general anesthesia for transcatheter aortic valve implantation (TAVI). J Thorac Dis. 2015; 7(9): 1518–1526, doi: 10.3978/j.issn.2072-1439.2015.08.21, indexed in Pubmed: 26543597.

VIA MEDICA

RESEARCH LETTER

Cardiology Journal
2021, Vol. 28, No. 3, 492–493
DOI: 10.5603/CJ.a2021.0037

ISSN 1897–5593
eISSN 1898–018X

Efficacy and safety of levosimendan and dobutamine in heart failure: A systematic review and meta-analysis

Milosz J. Jaguszewski[1], Aleksandra Gasecka[2, 3], Radoslaw Targonski[1, 4], Krzysztof J. Filipiak[2], Lukasz Szarpak[5, 6]

[1]1st Department of Cardiology, Medical University of Gdansk, Poland
[2]1st Chair and Department of Cardiology, Medical University of Warsaw, Poland
[3]Department of Cardiology, University Medical Center Utrecht, The Netherlands
[4]Department of Cardiac and Vascular Surgery, Medical University of Gdansk, Poland
[5]Maria Sklodowska-Curie Medical Academy in Warsaw, Poland
[6]Maria Sklodowska-Curie Białystok Oncology Center, Białystok, Poland

This paper was guest edited by Prof. Togay Evrin

Levosimendan is a new inodilator which has three main mechanisms of action: increases the calcium sensitivity of cardiomyocytes by binding to cardiac troponin C, acts as a vasodilator due to the opening of potassium channels, thus exerting cardioprotective effects [1]. Due to the unique mechanism of action, levosimendan has multifaceted cardioprotective effects, as demonstrated previously [2]. Levosimendan is indicated for inotropic support in acute decompensated heart failure (HF) in situations where conventional therapy is not sufficient, and in cases where inotropic support is considered appropriate (class IIb recommendation according to the European Society of Cardiology guidelines) [3]. In addition, levosimendan was showed to accelerate the recovery in patients with takotsubo cardiomyopathy [4]. Dobutamine, in turn, remains the most widely used therapy in patients with acute decompensated HF. Although dobutamine improves hemodynamics and symptoms in these patients, it has been associated with an increased risk of death and other cardiovascular events [5]. Hence, there is a greatly unmet need for agents that improve hemodynamics and relieve symptoms without adversely affecting survival. In contrast to dobutamine, levosimendan has a safe and predictable profile of action and does not induce tolerance, facilitating its administration in HF patients [6].

Because the results of previous clinical studies are inconclusive, herein was performed a systematic review and meta-analysis to verify the efficacy and safety of levosimendan and dobutamine in patients with acute HF. Two authors (L.S. and A.G.) independently searched PubMed, the Cochrane Library and the Google Scholar for articles written in English (last update January 7th, 2021). The key search words were: "levosimendan" AND "dobutamine" AND "heart failure" OR "HF". All statistical analyses were performed with Review Manager Software 5.4 (The Cochrane Collaboration, Oxford, Copenhagen, Denmark). All results are presented as mean difference (MD) or odds ratio (OR) with 95% confidence interval (CI). When the continuous outcome was reported in a study as median, range, and interquartile range, means and standard deviations were estimated using the formula described by Hozo et al. [7]. The random-effects model was used for $I^2 > 50\%$. Statistical testing was two-tailed. $P < 0.05$ was considered statistically significant.

Address for correspondence: Aleksandra Gąsecka, MD, PhD, 1st Chair and Department of Cardiology, Medical University of Warsaw, ul. Banacha 1a, 02–097 Warszawa, Poland, tel: +48 22 599 19 51, e-mail: aleksandra.gasecka@wum.edu.pl

Received: 26.02.2021 Accepted: 14.03.2021

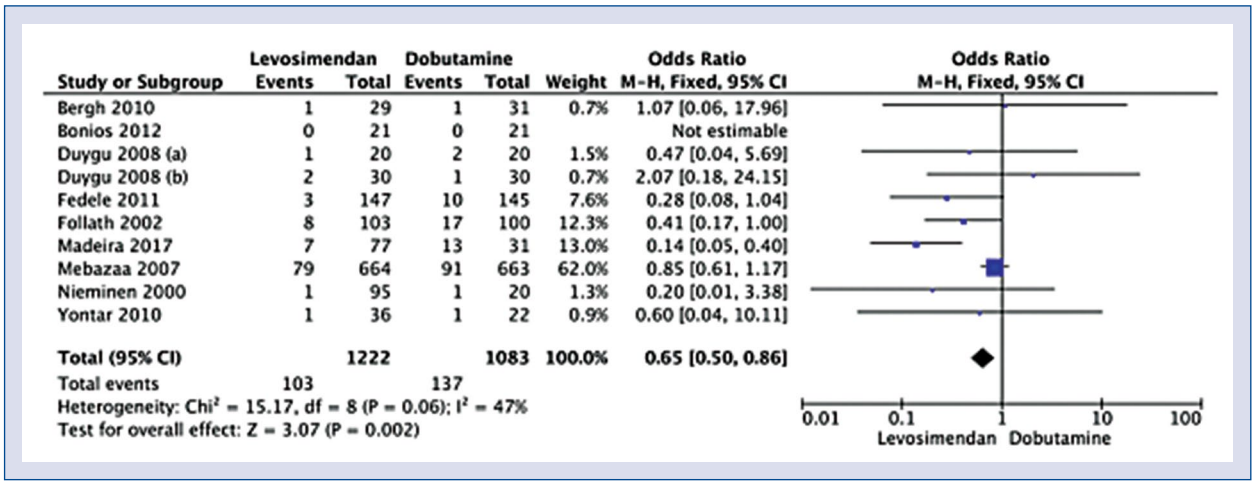

Figure 1. Forest plot of in-hospital mortality in the levosimendan versus the dobutamine group. The center of each square represents the weighted odds ratio for individual trials, and the corresponding horizontal line stands for 95% confidence interval (CI). The diamonds represent pooled results. Procedure time presented in seconds.

Ten studies including 2305 were eligible for quantitative analysis. The full list of the included publications is presented in **Supplementary Digital Content**. Characteristics of included studies was presented in **Supplementary Table S1**. In-hospital mortality (or 30-day mortality) group was reported in 10 studies and occurred in 8.4% patients treated with levosimendan and 12.7% patients treated with dobutamine (OR = 0.65; 95% CI: 0.50–0.86; p = 0.002; I^2 = 47%; Fig. 1). In contrast, 6-month mortality was reported in 3 studies and was 25.8% for levosimendan compared with 29.5% for dobutamine (OR = 0.84; 95% CI: 0.67–1.04; p = 0.11; I^2 = 36%; **Suppl. Fig. S1**).

The use of levosimendan compared to dobutamine was associated with a lower frequency of complications including acute decompensated cardiac failure (12.2% vs. 16.8%, respectively; OR = 69; 95% CI: 0.51–0.93; p = 0.02; I^2 = 0%), and a higher risk of atrial fibrillation (8.1% vs. 5.4%; OR = 1.56; 95% CI: 1.04–2.35; p = 0.03; I^2 = 0%). A detailed overview of adverse events is presented in **Supplementary Table S2**.

Length of hospital stay was 10.7 ± 7.0 days in the levosimendan group compared to 12.4 ± 6.6 days in the dobutamine group (MD = –1.92; 95% CI: –2.47 to –1.36; p < 0.001; I^2 = 0%; **Suppl. Fig. S2**).

In conclusion, the present study demonstrated that levosimendan decreased in-hospital (or 30--days) mortality and length of hospital stay, compared to dobutamine. In addition, there was a trend towards lower 6-month mortality on levosimendan. Taking into account the promising results of our meta-analysis and the cardioprotective effects of levosimendan demonstrated in multiple studies, there is a need for a well-designed multicenter randomized placebo-controlled study, including an adequately large group of outpatients with acute HF to ultimately determine the effect of levosimendan on long-term prognosis [8].

Conflict of interest: None declared

References

1. Pathak A, Lebrin M, Vaccaro A, et al. Pharmacology of levosimendan: inotropic, vasodilatory and cardioprotective effects. J Clin Pharm Ther. 2013; 38(5): 341–349, doi: 10.1111/jcpt.12067, indexed in Pubmed: 23594161.
2. Pollesello P, Papp Z. The cardioprotective effects of levosimendan: preclinical and clinical evidence. J Cardiovasc Pharmacol. 2007; 50(3): 257–263, doi: 10.1097/FJC.0b013e3180986230, indexed in Pubmed: 17878752.
3. Harjola VP, Giannakoulas G, von Lewinski D, et al. Use of levosimendan in acute heart failure. Eur Heart J Suppl. 2018; 20(Suppl I): I2–II10, doi: 10.1093/eurheartj/suy039, indexed in Pubmed: 30555279.
4. Yaman M, Arslan U, Kaya A, et al. Levosimendan accelerates recovery in patients with takotsubo cardiomyopathy. Cardiol J. 2016; 23(6): 610–615, doi: 10.5603/CJ.a2016.0100, indexed in Pubmed: 27910084.
5. Bayram M, De Luca L, Massie MB, et al. Reassessment of dobutamine, dopamine, and milrinone in the management of acute heart failure syndromes. Am J Cardiol. 2005; 96(6A): 47G–58G, doi: 10.1016/j.amjcard.2005.07.021, indexed in Pubmed: 16181823.
6. Slawsky MT, Colucci WS, Gottlieb SS, et al. Acute hemodynamic and clinical effects of levosimendan in patients with severe heart failure. Study Investigators. Circulation. 2000; 102(18): 2222–2227, doi: 10.1161/01.cir.102.18.2222, indexed in Pubmed: 11056096.
7. Hozo SP, Djulbegovic B, Hozo I. Estimating the mean and variance from the median, range, and the size of a sample. BMC Med Res Methodol. 2005; 5: 13, doi: 10.1186/1471-2288-5-13, indexed in Pubmed: 15840177.
8. Tycińska A, Gierlotka M, Bugajski J, et al. Levosimendan in the treatment of patients with acute cardiac conditions: an expert opinion of the Association of Intensive Cardiac Care of the Polish Cardiac Society. Kardiol Pol. 2020; 78(7-8): 825–834, doi: 10.33963/KP.15551, indexed in Pubmed: 32788567.

VIA MEDICA

IMAGE IN CARDIOVASCULAR MEDICINE

Cardiology Journal
2021, Vol. 28, No. 3, 494–495
DOI: 10.5603/CJ.2021.0049

ISSN 1897–5593
eISSN 1898–018X

Multivessel coronary thrombosis in a COVID-19 patient: Lungs are not always a culprit

Michał Kuzemczak[1, 2, 3]*, Charalampos Kavvouras[1]*, Mohammad Alkhalil[1], Jonah Himelfarb[1], Mark Osten[1]

[1]Peter Munk Cardiac Center, Division of Cardiology, Toronto General Hospital, University Health Network, Toronto, Canada
[2]Chair of Emergency Medicine, Department of Medical Rescue, Poznan University of Medical Sciences, Poznan, Poland
[3]Department of Invasive Cardiology, Central Clinical Hospital of the Ministry of Interior and Administration, Warsaw, Poland

A 54-year-old man, with no cardiovascular risk factors, was admitted with 2-hour chest pain. Five days earlier, he had been found to be coronavirus disease 2019 (COVID-19) positive, but his clinical condition had allowed him to be managed at home.

On admission, the patient was hemodynamically stable, afebrile, with no respiratory symptoms. His electrocardiogram was consistent with ST-segment elevation myocardial infarction. His complete blood count, international normalized ratio, activated partial thromboplastin time, and C-reactive protein were normal. D-dimer was 4400 μg/L, ferritin was 914 μg/L and high sensitivity troponin I > 50000 ng/L. Neither pulmonary embolism nor COVID-19 features was detected on computed tomography.

Coronary angiography revealed an acute occlusion of the proximal left anterior descending artery (LAD) (Fig. 1A) and non-occlusive thrombus in the proximal right coronary artery (RCA). The latter artery was occluded in the second and the third posterolateral branches (Fig. 1B, C). The flow in the LAD was restored with a drug-eluting stent (Fig. 1D, E). An attempt to retrieve the RCA thrombi with a thrombectomy catheter was unsuccessful (Fig. 1F) and a decision was made to treat the patient with a bolus and 18-hour infusion of eptifibatide and dual antiplatelet therapy (acetylsalicylic acid plus ticagrelor). The patient was transferred to our dedicated COVID-19 ward in stable condition. Further in-hospital stay was uneventful.

The presented case was unique as there was a lack of either cardiovascular factors or respiratory symptoms. Previous cases of COVID-19 patients have mainly reported on multivessel coronary thrombosis in the context of severe pneumonia or multiorgan failure. The present case implies a unique hypercoagulable state associated with COVID-19 irrespective of cardiovascular risk factors and lung involvement.

Conflict of interest: None declared

Address for correspondence: Michał Kuzemczak, MD, PhD, MSc, Toronto General Hospital, Division of Cardiology, 585 University Avenue, Toronto, Ontario, M5G 2C4 Canada, tel: +1 (647) 675 4669, e-mail: michal.kuzemczak@gmail.com

Received: 17.11.2020 Accepted: 28.02.2021

**Contributed equally*

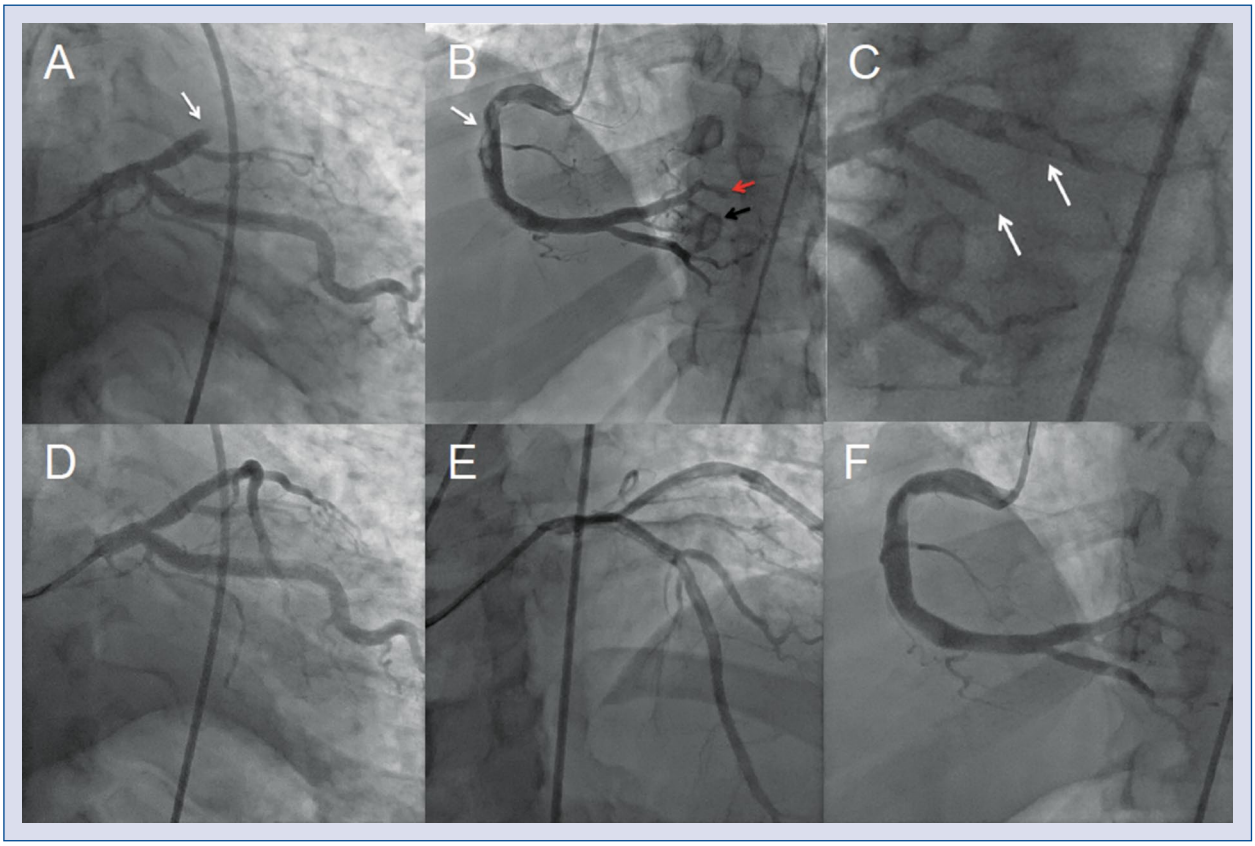

Figure 1. A. Acute occlusion of the left anterior descending artery (LAD; arrow); **B.** Thrombus (white arrow) in the proximal segment of the right coronary artery (RCA) and occlusion of the second (black arrow) and the third posterolateral branch (RPL; red arrow); **C.** Thrombus burden in the second and the third RPL (white arrows); **D, E.** Postprocedural left coronary angiography; **F.** Post-procedural right coronary angiography.

VIA MEDICA

IMAGE IN CARDIOVASCULAR MEDICINE

Cardiology Journal
2021, Vol. 28, No. 3, 496–497
DOI: 10.5603/CJ.2021.0050

ISSN 1897–5593
eISSN 1898–018X

Multimodality imaging of a hairpin-like coronary fistula between the right coronary artery and the coronary sinus

Yuan Peng[1, 2 #], Yali Yang[1, 2 #], Yuman Li[1, 2], Ziming Zhang[1, 2], Lin He[1, 2], Lingyun Fang[1, 2], Chao Guo[3], Nianguo Dong[3], Mingxing Xie[1, 2]

[1]Department of Ultrasound, Union Hospital, Tongji Medical College, Huazhong University of Science and Technology, Wuhan, China
[2]Hubei Province Key Laboratory of Molecular Imaging, Wuhan, China
[3]Department of Cardiovascular Surgery, Union Hospital, Tongji Medical College, Huazhong University of Science and Technology, Wuhan, China

A 37-year-old man was referred to our hospital with a 2-year history of chest pain. It frequently occurred during moderate exercise. Coronary computed tomography angiography (CTA) showed a dilated tortuous right coronary artery (RCA) (Fig. 1A–C). His clinician suspected that he might have suffered from Kawasaki disease in his childhood and arranged for an echocardiographic examination. Transthoracic echocardiography showed a dilated RCA and an enlarged coronary sinus (CS) with a bright flow (Fig. 1D). Continuous-wave Doppler revealed a continuous-wave flow at the coronary sinus (CS). Transesophageal echocardiography (TEE) demonstrated a tortuous coronary fistula from the distal RCA, which connected with the CS aneurysm through a 5 mm wide defect (Fig. 1E, F). The digital subtraction angiography confirmed the hairpin-like RCA–to–CS fistula, which was difficult to plug (Fig. 1G, **Suppl. Video 1**). The mean pulmonary arterial pressure was 30 mmHg, and the right ventricle was slightly enlarged. The patient was then taken for surgical treatment. The CS aneurysm was incised longitudinally adjacent to the great cardiac vein, allowing operative closure of the secluded fistula (Fig. 1H, I). The post-procedure TEE demonstrated no shunt. The patient made a rapid recovery after the operation, and had no chest pain during exercise at 3-month follow-up.

Coronary artery fistula (CAF) is a rare cardiac anomaly. CTA is recognized to be very accurate in order to diagnose CAF. The missed diagnosis resulted from the fact that this fistula came from the distal RCA and the defect was concealed in the CS. However, multi-modal imaging can provide anatomical and hemodynamic information of this rare RCA–to–CS fistula for choosing a reliable treatment.

Conflict of interest: None declared

Address for correspondence: Mingxing Xie, MD, PhD, 1277 Jiefang Avenue, Wuhan, China, tel: +86 (27) 85726430, fax: +86 (27) 85726386, e-mail: xiemx@hust.edu.cn; Nianguo Dong, MD, PhD, 1277 Jiefang Avenue, Wuhan, China, tel: +86 13971181551, fax: +86 (27) 85726386, e-mail: dongnianguo@hotmail.com

Received: 14.10.2020 Accepted: 7.12.2020

[#]Both authors contributed equally to this manuscript.

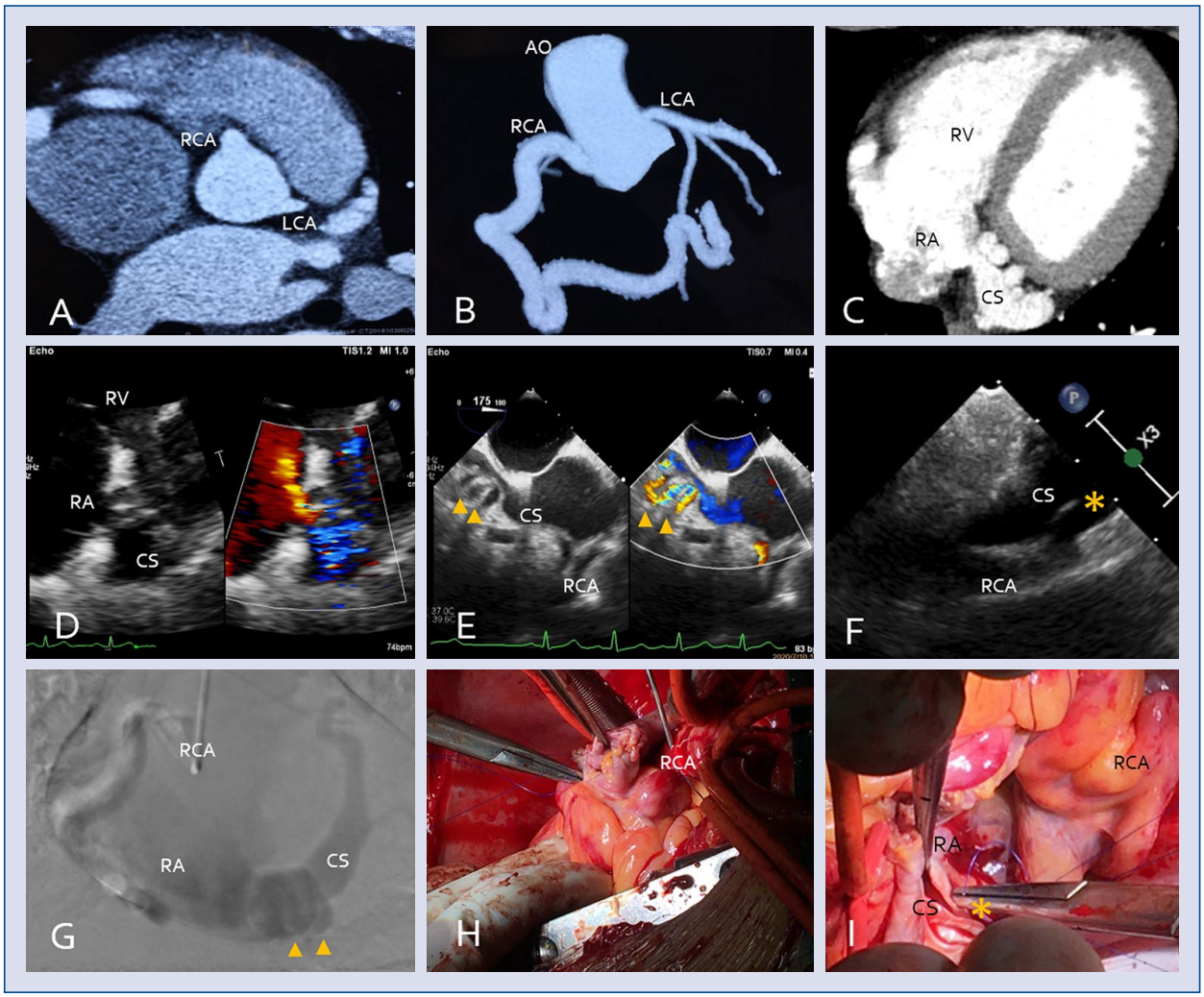

Figure 1. A–C. The coronary artery computed tomography angiography (CTA) showed the origin of a tortuous dilated right coronary artery (RCA), its course and a dilated coronary sinus (CS); **D.** Transthoracic echocardiography showed a bright flow from the dilated CS; **E, F.** Transesophageal echocardiography showed a hairpin-like coronary fistula and the defect between the distal RCA and the CS aneurysm (arrow, asterisk); **G.** The angiography demonstrated the termination of the RCA fistula (arrow); **H, I.** At surgery, the tortuous dilated RCA can be seen, while the defect was concealed in the CS (asterisk); LCA — left coronary artery; AO — aorta; RA — right atrium; RV — right ventricle.

VIA MEDICA

IMAGE IN CARDIOVASCULAR MEDICINE

Cardiology Journal
2021, Vol. 28, No. 3, 498–499
DOI: 10.5603/CJ.2021.0051

ISSN 1897–5593
eISSN 1898–018X

An unusual combination of large Eustachian valve in a young patient with Friedreich's ataxia cardiomyopathy

Stylianos A. Karvounaris[1], Georgios S. Papaetis[2, 3], Petros P. Mavrommatis[4]

[1]Department of Cardiology, Evangelismos Hospital, Paphos, Cyprus
[2]Internal Medicine and Diabetes Clinic, Paphos, Cyprus
[3]CDA College, Paphos, Cyprus
[4]Cardiac Care Center, Paphos, Cyprus

A 20-year-old male with Friedreich ataxia (FA) presented with dyspnoea and palpitations over the prior 2 days. Atrial fibrillation with rapid ventricular response and inverted T waves in leads III, aVF, V5, V6 were found on the electrocardiogram. The transthoracic echocardiogram, with the patient being in atrial fibrillation, showed concentric hypertrophy and left ventricular ejection fraction of approximately 50%. Surprisingly, an incomplete membrane into the right atrium was noted (Fig. 1A, B). The cardiac rhythm was restored to sinus rhythm after 24 hours. Further study with transesophageal and contrast echo clearly demonstrated the presence of an incomplete membrane dividing the right atrium into two chambers (Fig. 1C, D). Color and pulsed Doppler showed a turbulent eccentric flow across the two portions of the right atrium, without a significant gradient, expressing a large Eustachian valve or an incomplete cor triatriatum dextrum. Moreover, the presence of a patent foramen ovale noted and the left atrial appendage was free of thrombi. Agitated contrast saline infusion enhanced clarification of the anatomy. The turbulent and eccentric flow was crossing the 'hole' of the membrane and entering the proximal right atrium cavity, swirling in it, before moving through the distal right atrium cavity to the tricuspid valve relatively unconstructively (Fig. 1E, F). Cardiac magnetic resonance imaging was performed and documented the presence of large Eustachian valve in the presence of cardiomyopathy (FA-CM). The patient is under close echocardiographic follow-up. According to available research this is the first published description of a large Eustachian valve in a patient with FA-CM.

Conflict of interest: None declared

Address for correspondence: Georgios S. Papaetis, MD, PhD, Internal Medicine and Diabetes Clinic, Eleftherios Venizelos Avenue 62, Paphos, Cyprus, tel: 0035799273573, fax: 0035726220451, e-mail: gpapaetis@yahoo.gr

Received: 6.11.2020 Accepted: 6.12.2020

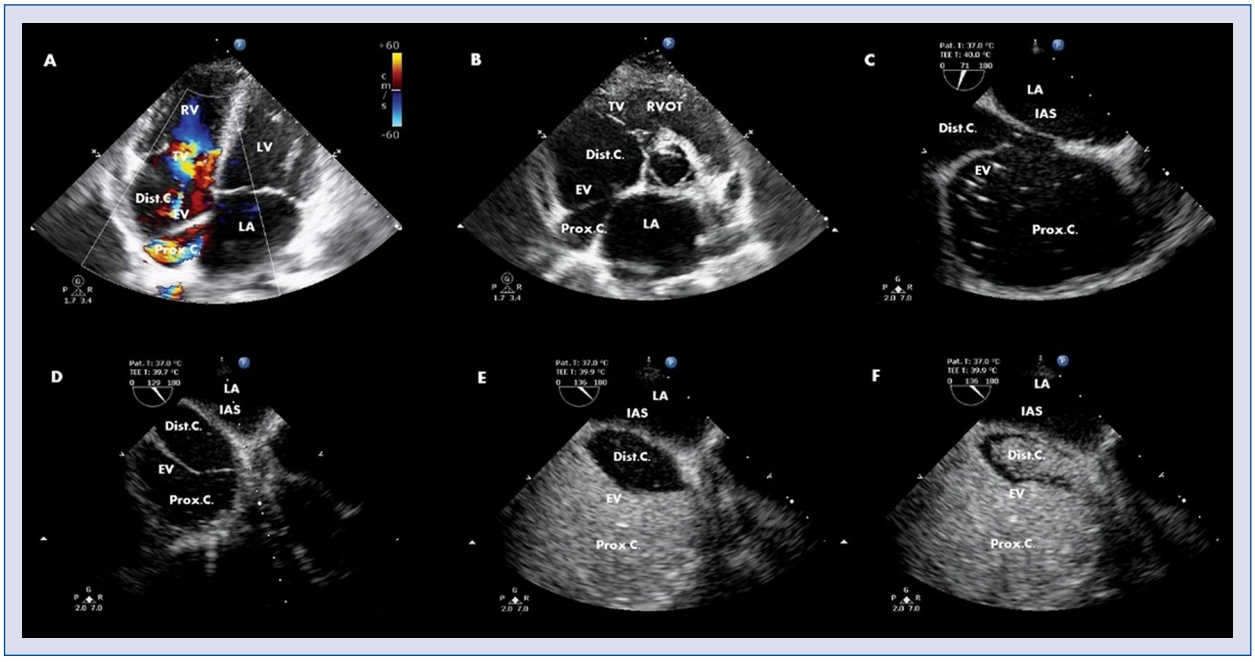

Figure 1. A. A large Eustachian valve divides the right atrium in two cavities (transthoracic echocardiogram [TTE] 4C); **B.** TTE SAX; **C.** Transesophageal echocardiogram (TEE) 70°; **D.** TEE 130°. Agitated contrast saline infusion initially fills the proximal right atrium (RA) cavity only; **E.** Later the contrast enters the distal RA cavity; **F.** Echo contrast free space between the two RA cavities represents the Eustachian valve (EV); LV — left ventricle; RV — right ventricle; LA — left atrium; Prox.C — proximal right atrium cavity; Dist.C — distal right atrium cavity; IAS — interatrium septum; TV — tricuspid valve.

VIA MEDICA

IMAGE IN CARDIOVASCULR MEDICINE

Cardiology Journal
2021, Vol. 28, No. 3, 500–501
DOI: 10.5603/CJ.2021.0052

ISSN 1897–5593
eISSN 1898–018X

Rare murmur in a patient with constrictive pericarditis

Yukio Abe, Toshio Saito, Takahiko Naruko

Department of Cardiology, Osaka City General Hospital, Osaka, Japan

An 80-year-old man was admitted with severe limb edema. A harsh sound at early diastole was audible by auscultation at the left sternal border. The computed tomography from a referral clinic revealed a thick pericardial layer with a severely calcified surface around the right ventricular free wall (Fig. 1A). He was diagnosed by echocardiography with right-sided heart failure due to constrictive pericarditis (CP) and mild to moderate pulmonary regurgitation (PR) at early diastole (Fig. 1B). A phonocardiogram showed a high-pitched regurgitant murmur at the left sternal border with a short duration during early diastole right after the pulmonary component of the second heart sound (Fig. 1C). The PR arising from the gradient with rapid deceleration between pulmonary artery pressure and the CP-induced dip of the right ventricular pressure was proven by right heart catheterization as the cause of the rare murmur (Fig. 1D, **Suppl. Video with sound**). He had a history of pulmonary tuberculosis. Consequently, tuberculous pericarditis was thought to be the cause of his CP, and a surgical pericardial dissection was performed. The intensity of the diastolic murmur became smaller, and the duration became longer after the surgery. Early diastolic PR with rapid deceleration of the gradient between the pulmonary artery pressure and the dip of the right ventricular pressure in patients with CP has been previously reported using Doppler echocardiography, whereas the corresponding murmur has not. According to available research, this is the first report of the dip-induced harsh PR murmur during early diastole in a patient with constrictive pericarditis.

Conflict of interest: None declared

Address for correspondence: Yukio Abe, MD, PhD, Department of Cardiology, Osaka City General Hospital, 2-13-22 Miyakojima-hondori, Miyakojima-ku, Osaka 534-0021, Japan, tel: +81-6-6929-1221, fax: +81-6-6929-1090, e-mail: abeyukio@aol.com

Received: 5.12.2020 Accepted: 28.02.2020

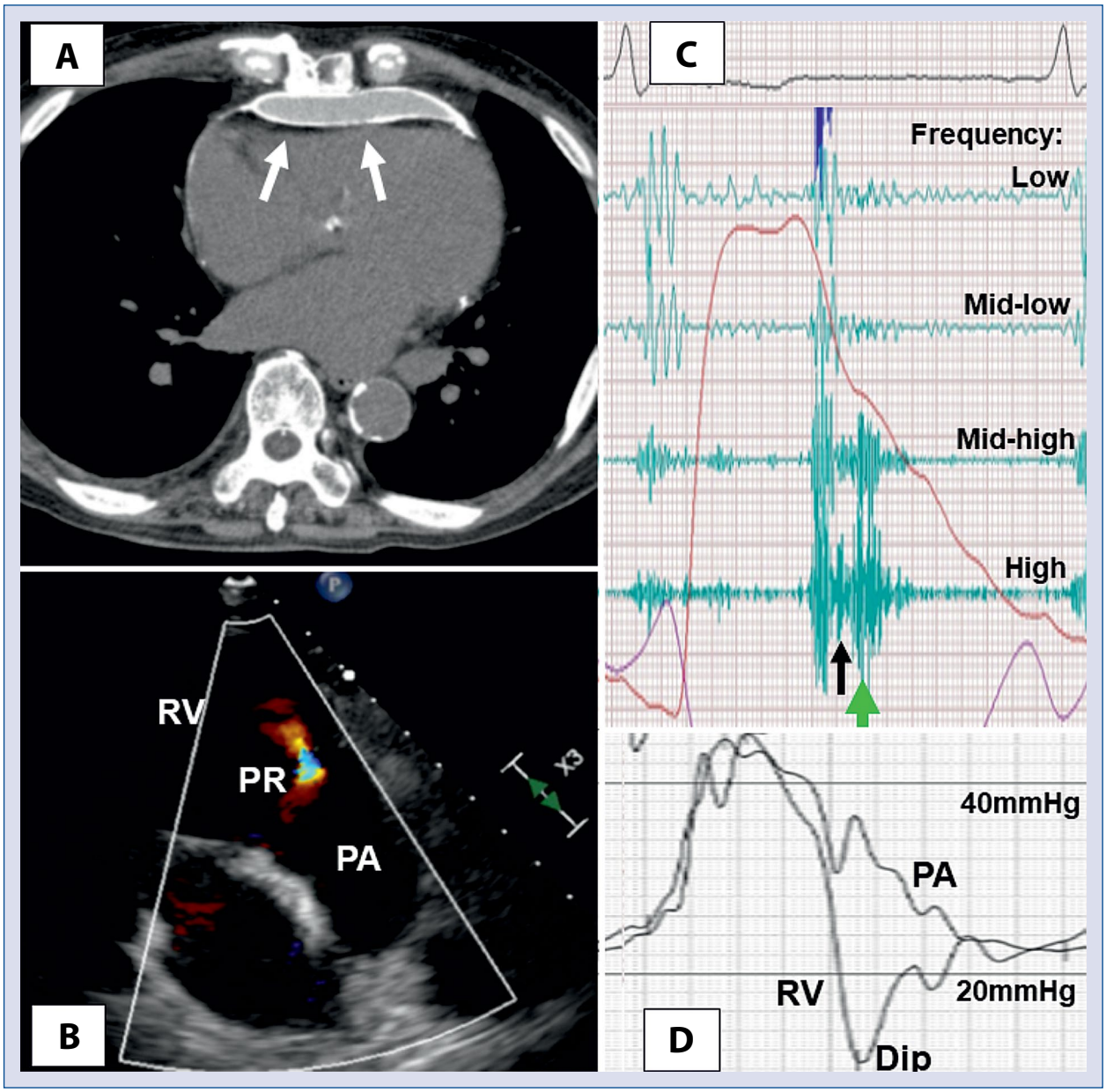

Figure 1. A. A calcified pericardial layer in the computed tomography (white arrows); **B.** Moderate pulmonary regurgitation (PR) in echocardiography; **C.** A high-pitched murmur (green arrow) during early diastole right after the pulmonary component (black arrow) of the second heart sound in a phonocardiogram recorded at the left sternal border; **D.** The gradient with rapid deceleration between pulmonary artery (PA) pressure and the dip of the right ventricular (RV) pressure recorded at catheterization.